

University of Alberta

Implementation and Evaluation of  
Spatiotemporal Prediction Algorithms  
and  
Prediction of Spatially Distributed  
Greenhouse Gas Inventories

by

James Rodway

A thesis submitted to the Faculty of Graduate Studies and Research in partial fulfillment  
of the requirements for the degree of

Master of Science

in

Software Engineering and Intelligent Systems

Department of Electrical and Computer Engineering

© James Rodway  
Fall 2011  
Edmonton, Alberta

Permission is hereby granted to the University of Alberta Libraries to reproduce single copies of this thesis and to lend or sell such copies for private, scholarly or scientific research purposes only.

Where the thesis is converted to, or otherwise made available in digital form, the University of Alberta will advise potential users of the thesis of these terms.

The author reserves all other publication and other rights in association with the copyright in the thesis and, except as herein before provided, neither the thesis nor any substantial portion thereof may be printed or otherwise reproduced in any material form whatsoever without the author's prior written permission.

## **Abstract**

Growing environmental concerns require monitoring and modelling of greenhouse gases. These modelling efforts require processing of massive datasets in a timely fashion. This, in turn, can lead to feasibility problems when estimating values of missing data points. This thesis examines and compares multiple methods for estimating values of missing data points, including their spatiotemporal extensions. Resulting predictions are compared from the perspective of accuracy and computational efficiency. The results show that kriging based methods generally outperform the others in terms of accuracy, but took longer to process. Hierarchical methods prove to be a more suitable choice, providing slightly less accurate results at much shorter times, especially for dense datasets.

The second part of the thesis explores a scheme for updating emission inventories using socioeconomic data. Random forest and extreme machine learning techniques applied for this task show poor performance on real-world data.

## **Acknowledgements**

This thesis represents the result of my time in the M.Sc. program at the University of Alberta and would not have been possible without the help of many people. I would like to thank my supervisor Dr. Petr Musilek, whose guidance and motivation was essential in my completion of this project. Data provided by Dr. Pavel Juruš was instrumental for computational experiments described in this document.

I also would like to thank my family, Art, Bobbi, Rose and John for their support and encouragement during this endeavour. Much appreciation goes to Kelly Robinson, whose love and patience has been a tremendous asset.

# Contents

<b>1</b>	<b>Introduction</b>	<b>1</b>
1.1	Motivation . . . . .	1
1.2	Thesis Objectives . . . . .	2
1.3	Organization . . . . .	2
<b>2</b>	<b>Background</b>	<b>4</b>
2.1	Missing Data . . . . .	4
2.2	Inventory Prediction . . . . .	7
<b>3</b>	<b>Missing Data</b>	<b>9</b>
3.1	Data Sources . . . . .	10
3.1.1	CarbonTracker Model Data . . . . .	10
3.1.2	WRF-CHEM Model Output Data . . . . .	10
3.1.3	Creation of Experimental Datasets for Prediction . . . . .	11
3.1.4	Characteristics of the Data Used . . . . .	11
3.2	Data Preprocessing . . . . .	12
3.2.1	Assignment to a Grid . . . . .	12
3.2.2	Calculation of Summary Statistics . . . . .	14
3.2.3	Variogram Modelling . . . . .	14
3.2.4	Trend Modelling and Removal . . . . .	16
3.3	Estimation Methods . . . . .	21
3.3.1	Nonstatistical Estimates . . . . .	21
3.3.2	Statistical Estimates . . . . .	23
3.4	Metrics for Comparison . . . . .	38

3.5	Results and Discussion . . . . .	39
3.5.1	Static Results . . . . .	39
3.5.2	Dynamic Results . . . . .	58
3.6	Summary . . . . .	63
<b>4</b>	<b>Inventory Prediction</b>	<b>65</b>
4.1	Data Sources . . . . .	65
4.2	Data Preprocessing . . . . .	66
4.3	Model Building . . . . .	67
4.3.1	Random Forests . . . . .	67
4.3.2	Extreme Machine Learning . . . . .	70
4.4	Results and Discussion . . . . .	72
4.5	Summary . . . . .	76
<b>5</b>	<b>Conclusions, Contributions, and Future Work</b>	<b>81</b>
5.1	Conclusions . . . . .	81
5.2	Thesis Contributions . . . . .	82
5.2.1	Missing Data . . . . .	82
5.2.2	Inventory Prediction . . . . .	83
5.3	Future Work . . . . .	83
5.3.1	Missing Data . . . . .	83
5.3.2	Inventory Prediction . . . . .	84
	<b>References</b>	<b>86</b>
<b>A</b>	<b>Missing Data Prediction Supplementary Material</b>	<b>92</b>
A.1	Complete Graphs . . . . .	92
A.1.1	Detrending . . . . .	92
A.1.2	Error Graphs . . . . .	99
A.2	Method Rankings . . . . .	136
A.3	MSPE and MAPE Values . . . . .	152
A.3.1	Grouped by Estimation Method . . . . .	152
A.3.2	Grouped by Detrending Method . . . . .	162

<b>B List of Socioeconomic Variables Used for Inventory Prediction</b>	<b>172</b>
B.1 Regular Variables . . . . .	172
B.2 Per Capita Variables . . . . .	173
<b>C Inventory Prediction Data Tables</b>	<b>175</b>

# List of Tables

3.1	CT RR, top methods as ranked by MSPE. . . . .	46
3.2	CT RR, top methods as ranked by MAPE . . . . .	47
3.3	MO RR, top methods as ranked by MSPE. . . . .	47
3.4	MO RR, top methods as ranked by MAPE. . . . .	48
3.5	CT MM, top methods as ranked by MSPE. . . . .	48
3.6	CT MM, top methods as ranked by MAPE. . . . .	49
3.7	MO MM, top methods as ranked by MSPE. . . . .	49
3.8	MO MM, top methods as ranked by MAPE. . . . .	50
3.9	MSPE values for non-hierarchical methods using randomly removed data. . .	58
3.10	MSPE values for static hierarchical methods using randomly removed data. .	58
3.11	MSPE values for dynamic hierarchical methods, MO RR data . . . . .	59
3.12	MSPE values for non-hierarchical methods using 3SG datasets. . . . .	60
3.13	MSPE values for static hierarchical methods using 3SG datasets. . . . .	61
3.14	MSPE values for dynamic hierarchical methods, MO1 3SG data . . . . .	62
3.15	MSPE values for dynamic hierarchical methods, MO2 3SG data . . . . .	63
3.16	MSPE values for dynamic hierarchical methods, CT 3SG data . . . . .	64
A.1	CT RR, methods ranked by MSPE, pt1. . . . .	136
A.2	CT RR, methods ranked by MSPE, pt2. . . . .	137
A.3	CT RR, methods ranked by MAPE, pt1. . . . .	138
A.4	CT RR, methods ranked by MAPE, pt2. . . . .	139
A.5	MO RR, methods ranked by MSPE, pt1. . . . .	140
A.6	MO RR, methods ranked by MSPE, pt2. . . . .	141
A.7	MO RR, methods ranked by MAPE, pt1. . . . .	142

A.8	MO RR, methods ranked by MAPE, pt2. . . . .	143
A.9	CT MM, methods ranked by MSPE, pt1. . . . .	144
A.10	CT MM, methods ranked by MSPE, pt2. . . . .	145
A.11	CT MM, methods ranked by MAPE, pt1. . . . .	146
A.12	CT MM, methods ranked by MAPE, pt2. . . . .	147
A.13	MO MM, methods ranked by MSPE, pt1. . . . .	148
A.14	MO MM, methods ranked by MSPE, pt2. . . . .	149
A.15	MO MM, methods ranked by MAPE, pt1. . . . .	150
A.16	MO MM, methods ranked by MAPE, pt2. . . . .	151
A.17	CT RR, MSPE grouped by estimation method. . . . .	152
A.18	CT RR, MAPE grouped by estimation method. . . . .	153
A.19	CT RR, time grouped by estimation method. . . . .	154
A.20	MO RR, MSPE grouped by estimation method. . . . .	155
A.21	MO RR, MAPE grouped by estimation method. . . . .	156
A.22	MO RR, time grouped by estimation method. . . . .	157
A.23	CT MM, MSPE grouped by estimation method. . . . .	158
A.24	CT MM, MAPE grouped by estimation method. . . . .	159
A.25	MO MM, MSPE grouped by estimation method. . . . .	160
A.26	MO MM, MAPE grouped by estimation method. . . . .	161
A.27	CT RR, MSPE grouped by detrending method. . . . .	162
A.28	CT RR, MAPE grouped by detrending method. . . . .	163
A.29	CT RR, time grouped by detrending method. . . . .	164
A.30	MO RR, MSPE grouped by detrending method. . . . .	165
A.31	MO RR, MAPE grouped by detrending method. . . . .	166
A.32	MO RR, time grouped by detrending method. . . . .	167
A.33	CT MM, MSPE grouped by detrending method. . . . .	168
A.34	CT MM, MAPE grouped by detrending method. . . . .	169
A.35	MO MM, MSPE grouped by detrending method. . . . .	170
A.36	MO MM, MAPE grouped by detrending method. . . . .	171
C.1	Summary statistics for reported data used with RF prediction. . . . .	175
C.2	Summary statistics for reported data used with ELM prediction. . . . .	175

C.3	Summary statistics for predictions made with RF. . . . .	176
C.4	Summary statistics for predictions made with ELM. . . . .	176
C.5	Summary statistics for absolute error from RF predictions. . . . .	176
C.6	Summary statistics for absolute error from ELM predictions. . . . .	177
C.7	Summary statistics for RF percentage error. . . . .	177
C.8	Summary statistics for ELM percentage error. . . . .	177

# List of Figures

3.1	Summary of procedure for estimation of missing data. . . . .	9
3.2	Histograms for static datasets. . . . .	13
3.3	Basis function for FRS ( $\eta = 0.5$ ). . . . .	21
3.4	Determining which points to use for LSK. . . . .	25
3.5	Uptree predictions. . . . .	28
3.6	Downtree predictions. . . . .	29
3.7	Dynamic weightings. . . . .	31
3.8	Variograms across time. . . . .	34
3.9	Neural network activation function for hidden and output neurons. . . . .	36
3.10	Neural network used for inclusion of dynamics. . . . .	37
3.11	Histogram of raw data values for CT data . . . . .	41
3.12	Histogram of raw data values for MO data . . . . .	41
3.13	Effect of 3rd level ATPS detrending on CT data . . . . .	42
3.14	Effect of 3rd level ATPS detrending on MO data . . . . .	43
3.15	MO data, simple mean removal, MPV . . . . .	52
3.16	MO data, 3rd level ATPS detrending, MPV . . . . .	53
3.17	CT data, 3rd level ATPS detrending, MPV . . . . .	53
3.18	Processing time comparisons (RR data). . . . .	57
4.1	Mean reported value comparison. . . . .	69
4.2	MAPE Comparison . . . . .	75
4.3	MAPE over mean reported value comparison. . . . .	76
4.4	MPE comparison . . . . .	78
4.5	Total percentage difference comparison. . . . .	79

A.1	Effect of 1st order GLS detrending on CT data . . . . .	93
A.2	Effect of 3rd order GLS detrending on CT data. . . . .	94
A.3	Effect of 1st order GLS detrending on MO data . . . . .	95
A.4	Effect of 3rd order GLS detrending on MO data. . . . .	96
A.5	Effect of 3rd level FRS detrending on CT data. . . . .	97
A.6	Effect of 3rd level FRS detrending on MO data. . . . .	98
A.7	MSPE comparisons for different detrending methods applied to CT data. . .	101
A.8	MAPE comparisons for different detrending methods applied to RR CT data.	104
A.9	MSPE comparison for different detrending methods applied to RR MO data.	107
A.10	MAPE comparison for different detrending methods applied to RR MO data.	110
A.11	MPV comparisons for different detrending methods applied to RR CT data. .	112
A.12	MPV comparison for different detrending methods applied to RR MO data. .	114
A.13	Processing time comparisons (RR data). . . . .	117
A.14	MSPE comparisons for different detrending methods applied to MM CT data.	120
A.15	MAPE comparisons for different detrending methods applied to MM CT data.	123
A.16	MSPE comparison for different detrending methods applied to MM MO data.	126
A.17	MAPE comparison for different detrending methods applied to MM MO data.	129
A.18	MPV comparisons for different detrending methods applied to MM CT data.	132
A.19	MPV comparison for different detrending methods applied to MM MO data.	135

# Symbols and Abbreviations

$\alpha$	Variogram nugget effect parameter
$\beta$	Variogram sill parameter
$z$	Vector of observed values
$\chi$	Smoothing parameter
$\Lambda$	Variogram range/frequency parameter
$\phi$	Longitude of a point
$\theta$	Latitude of a point
$h$	Lag distance between grid cells
$N$	Total number of predictions made
$n$	Total number of observed values
2ES	Double Exponential Smoothing
3ES	Triple Exponential Smoothing
3SG	3rd step good dataset configuration
ATPS	Aggregated Thin Plate Splines
CT	CarbonTracker
DMM	Dynamic multiresolution spatial model
DMURS	Dynamic multiresolution spatial predictor
FA	Flat Average

FNN	Forecasting Neural Network
FRS	Fixed Rank Smoothing
GLS	Generalised least squares
IDW	Inverse distance weighted prediction
KBF	Kriging Based Forecast
LSK	Local simple kriging
LVA	Locally Varying Anisotropy
MAE	Mean absolute error
MAPE	Mean absolute prediction error
MM	Missing Middle
MO	Model Output
MPV	Mean Prediction Variance
MRSM	Multiresolution spatial model
MSPE	Mean squared prediction error
MURS	Multiresolution spatial predictor
NIR	Near Infrared
NN	Nearest neighbour interpolation
OK	Ordinary Kriging
SK	Simple kriging
SM	Simple Mean Removal
TS	Trend Surface

# Chapter 1

## Introduction

### 1.1 Motivation

Human activities have always affected the planet. However, a steady population increase is precipitating effects that cannot be ignored: for instance, the plethora of different gases released into the atmosphere by increasing human activity affects climate, ocean acidification and plant growth.

Carbon dioxide is of particular interest as this gas is linked to all of these phenomena. which has been linked to all of these phenomena. Carbon dioxide ( $\text{CO}_2$ ) does not absorb energy from the sun, but it absorbs some of the energy released from the earth: that is,  $\text{CO}_2$  lets the energy in, but does not let all of it out, resulting in global warming [1].  $\text{CO}_2$  is also linked to a recent decrease in oceanic pH because of the chemical changes that take place when it is dissolved in water [2].  $\text{CO}_2$  is an integral in photosynthesis, so changes in  $\text{CO}_2$  concentration affect the growth behaviour of plants [3, 4].

Atmospheric concentrations of carbon dioxide have increased about 100 ppm since preindustrial times [5, p.137], and this increase has highlighted the role carbon dioxide plays in these different systems. Models are usually built to help us understand the relation of different gases to earthly systems. Two discussed here concern the remote sensing of atmospheric component concentrations and the accounting of various anthropogenic emissions, each presenting challenges to the investigator. This thesis explores possible solutions to the problem of missing data in sets acquired by remote sensing: different methods of spatial and

spatiotemporal inference are implemented and compared. For the problem of out-of-date emission inventories, two possible methods of predicting updated values are examined.

## 1.2 Thesis Objectives

This thesis contributes to the areas of computer modelling of greenhouse gas emissions in the following ways:

- Methods of spatial interpolation are compared, including nearest neighbour interpolation, inverse distance weighting interpolation, simple kriging, localised simple kriging, ordinary kriging, multiresolution spatial models, and multiresolution spatial predictors.
- Different spatial trend removal techniques are compared, including general least squares, thin plate splines, and fixed rank smoothing.
- The extension of the hierarchical methods to include dynamic information in spatial prediction is explored. Four relatively simple dynamic models were implemented, namely double exponential smoothing, triple exponential smoothing, a simple forecasting neural network, and a kriging style forecasting technique.
- Different implemented methods were assessed using experimental data sets with a variety of different missing data configurations.
- An updated spatially distributed greenhouse gas emissions inventory was created using random forest and extreme learning machine techniques.

## 1.3 Organization

The thesis comprises five chapters. Background information is presented in chapter 2. Chapter 3 discusses the work done on the estimation of missing data. Section 3.1 outlines the different sources of data that were used for this work, as well as the steps taken to generate experimental datasets with missing data from complete data sources. The necessary preprocessing steps performed prior to the application of different estimation algorithms, including

variogram modelling and trend removal, are discussed in section 3.2. In section 3.3, nonstatistical estimation methods (section 3.3.1) and statistical estimation methods (section 3.3.2) are compared. Results of the different runs are discussed in section 3.5.

Chapter 4 contains work related to the prediction of greenhouse gas inventories. Short descriptions of the data used and the preprocessing performed are given in sections 4.1 and 4.2, respectively. The two methods used are described in section 4.3: random forest regression (section 4.3.1) and extreme machine learning (section 4.3.2). Results of the inventory predictions are discussed in section 4.4.

A summary of the work done and the conclusions reached are presented in chapter 5. The limitations to this work are considered and potential improvements to the field are suggested.

# Chapter 2

## Background

### 2.1 Missing Data

Increasing interest in global atmospheric processes has resulted in placement of a rising number of Earth-observing satellites. With their global coverage and continuous measurements, these satellites have become indispensable tools for studying phenomena such as land use, ocean surface temperature, and concentration of atmospheric gases. However, because of the number of measurements it is possible to take, the spatial and temporal sizes of these datasets can be very large, and this may lead to difficulties during processing. The estimation of missing values is an example of a problem that may be encountered in such a dataset.

Missing data points are frequently encountered in remotely sensed greenhouse gas measurements. Several satellites have been launched with instruments capable of measuring total or averaged column quantities of carbon dioxide ( $\text{CO}_2$ ) and methane ( $\text{CH}_4$ ), two important greenhouse gases. Some of the instruments used to take these measurements make use of the near infrared (NIR) spectrum of light, the wavelengths of which can be absorbed by  $\text{CH}_4$ ,  $\text{CO}_2$ , and nitrous oxide ( $\text{N}_2\text{O}$ ) [6]. Light from the sun contains components in the NIR region, as does the blackbody radiation emitted from the Earth. As NIR radiation passes through the atmosphere, it is absorbed by  $\text{CH}_4$ ,  $\text{CO}_2$ , and  $\text{N}_2\text{O}$ , causing characteristic absorption bands, which can be measured by the satellite's instruments. Analysis of the light's spectrum provides an estimate of the quantity of different gases present.

Atmospheric aerosols and clouds can have negative effects on the reliability of these measurements [7], and measurements are usually rendered unusable when such interference is present. Cloud cover over the Earth at any given time can reach 75% [8], so atmospheric interference can result in a large amount of missing data. As water absorbs in the NIR region, measurements over large bodies of water are prone to water interference. Data are further depleted when measurements are taken in swaths due to the sun-synchronous orbits of many observing satellites. Thus, collected atmospheric data can be spatially and temporally sparse, depending on the scale being considered.

Completing datasets with estimates of missing data is a useful preprocessing step for inputs to climate, circulation, and other models that make use of greenhouse gas measurements at high spatial and temporal resolutions. However, due to the growing size of the datasets, some of the traditional methods of missing point estimation have now become computationally infeasible.

The problem of missing data, common to many fields, is managed with spatial statistics. The kriging technique makes use of the spatial correlation present in the data in order to make the best linear unbiased predictions [9]. Variance in these predictions is defined and calculable. However, kriging involves the inversion of a covariance matrix, the size of which depends on the number of values collected; thus, for large datasets, kriging is computationally infeasible. Various properties of the spatial correlation of a dataset can be leveraged to reduce the size of the covariance matrix, and make such a prediction computationally feasible [10], but the results can be worse with regard to prediction and variance [11, p.130-134].

There are a number of different variations of kriging, many of which apply additional constraints on the solution in order to relax some of the assumptions made for the simple case. Where the simple case assumes a constant known mean everywhere in the spatial domain, ordinary kriging assumes a constant unknown mean and predicts it. Universal kriging goes further and assumes that the mean is a spatially varying, linear combination of known functions and estimates the weights used in the linear combination [11, p.151]. With kriging methods such as these, it can be beneficial to restrict the kriging neighbourhood, as this allows the trend surfaces predicted to be applied only to more localised areas where they may be more representative [12].

A number of simple methods are available that have much lower computational require-

ments, lending themselves well to dense datasets. For example, nearest neighbour and inverse distance weighting [13] enable processing of large amounts of spatial data relatively quickly. However, these methods do not factor in information about the spatial variability of the data, and will usually have higher error. Additionally, these methods do not provide an estimate of the variance associated with the prediction.

More recently, newer statistical techniques have been developed to predict missing data from large spatial datasets: multiresolution spatial models [14], multiresolution spatial predictors [15], fixed rank filtering [16], and fixed rank kriging [17] are defined here.

Multiresolution models make use of a hierarchical tree structure which aggregates the data to a ‘root’ node, then smooths it back down to the ‘leaves,’ filling in all the missing points during the process. Multiresolution predictors make use of a number of multiresolution spatial models, each slightly shifted. These shifted models give slightly different values for the predicted points, which are then overlaid and combined to create the final prediction. This operation improves the performance by making the predicted field less ‘blocky.’ These hierarchical methods also enjoy a ‘root’ node which is a convenient place to incorporate dynamic information without incurring a large performance penalty, while further improving prediction performance [18].

Fixed rank filtering and kriging improve on computation time by making use of non-stationary covariance basis functions, the number of which is fixed. This fixed number is usually chosen to be small in comparison to the large number of data points available in order to reduce computational cost. This is justified through some assumptions regarding the covariance structure of the data. The methods greatly speed up the time required while allowing only slight losses in prediction performance. These methods were not implemented in this thesis because the emphasis was on potential improvements garnered from the incorporation of historical information, which is more easily implemented using hierarchical models.

A usual part of spatial interpolation is trend detection and removal, which may present its own problems in regard to computational feasibility. Detrending may be done to allow for better estimates of covariance structure and to allow the necessary assumptions to be made for the estimation methods [19, p.177]. Many of the methods appropriate for spatial data utilise the matrix inversion that causes kriging computations to be unmanageable, for

example, generalised least squares regression. Other methods, not as statistically correct, such as thin plate splines or simple mean removal, may fail to satisfy the different assumptions required by the estimation algorithms. More recent developments in this area include fixed rank smoothing [20].

## 2.2 Inventory Prediction

Emission modelling usually requires an accounting of anthropogenic emissions, or an emissions inventory. This inventory contains the amounts of various gases that have been released in certain areas at certain times. However, due to the effort required to compile the data, inventories are usually compiled for large political areas (e.g., countries) and for relatively long periods of time (e.g., years).

In order to be useful for some types of emissions modelling (e.g., inversion modelling), these inventories must be spatially and temporally disaggregated in order to reach the spatial and temporal resolutions of interest. While this can be accomplished to some degree using software tools, inventories where disaggregation has already been performed to some degree are available. For example, EDGAR inventories are provided at a spatial resolution of 0.1 degree and are broken down into emissions from various sectors (e.g., industrial, residential, etc.) [21].

The creation of an inventory like this takes a substantial amount of time and effort and as a result the most recently created inventories may be years behind the time period of interest. Even regional inventories that do not have to be spatially allocated can be 16 months behind the period for which they are created [22]. Emission modellers would benefit from spatially distributed emissions inventories that are predicted based on frequently available values.

Current approaches to updating emissions inventories focus on estimations of country wide emissions. These estimations are usually based on energy-use statistics [23] or macroeconomic indicators [22]. Most often, the purpose of performing inventory updating is for country-wide policy, so spatial disaggregation is not necessary. Emission forecasting methods that focus on smaller spatial and temporal scales tend to have the goals of forecasting very specific emissions, such as emissions from a certain power plant [24, 25]. These forecasting methods may have much available information, including exact fuel sources used

and detailed information about facility uptime. These methods are unsuitable for updating spatially distributed inventories, since the data required is not available, and forecasting methods would likely be infeasible on this scale.

## Chapter 3

# Missing Data

A number of spatial interpolation techniques were applied to experimental data sets created from modelled concentrations of atmospheric carbon dioxide. The interpolation methods examined include nearest neighbour (NN), inverse distance weighting (IDW), simple kriging (SK), local simple kriging (LSK), ordinary kriging (OK), multiresolution spatial models (MRSM), and multiresolution spatial predictors (MURS). Simple models were used to incorporate dynamic information into MRSM and MURS, creating a dynamic multiresolution model (DMM) and a dynamic multiresolution spatial predictor (DMURS). As part of data preprocessing, a few simple detrending methods were implemented including general least squares (GLS), thin plate splines (TPS), and a more recently developed technique, fixed rank smoothing (FRS).

Figure 3.1 shows the process used in this thesis to estimate missing data points.

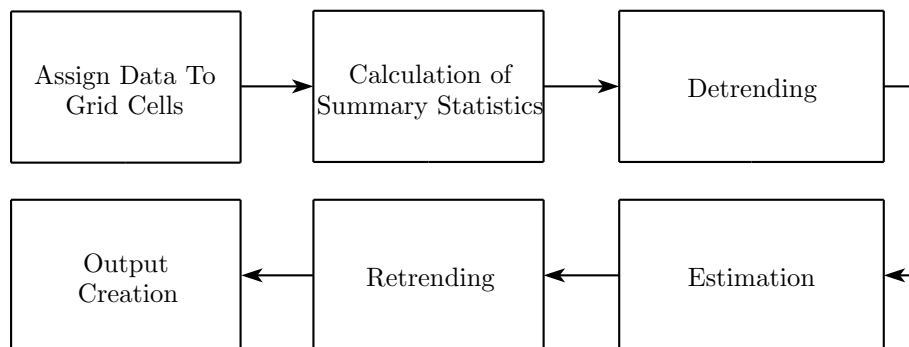


Figure 3.1: Summary of procedure for estimation of missing data.

## 3.1 Data Sources

To test the relative effectiveness and computational performance of different estimation methods as applied to greenhouse gas data, a complete dataset that reflects the spatial variability found with this type of data was employed. Two different sources of data considered in this thesis are described below.

### 3.1.1 CarbonTracker Model Data

CarbonTracker (CT) is a data assimilation system used for carbon dioxide [26]. The primary goal of the CT project is to estimate the carbon exchange between the atmosphere and the biosphere. A variety of different data sources have been used in the creation of CT model data, including satellite, aircraft and flux tower observations. Meteorological forecasts and atmospheric transport models are also used to get realistic estimates of CO<sub>2</sub> fluxes and concentrations. The model is run at a global scale with two nested regions covering North America and the United States at increasing resolutions.

For this work, the middle resolution was selected, which covers part of North America, including the United States and most of Canada. It has a time resolution of three hours, and is distributed on a  $40 \times 66$  cell grid, which covers an area from  $20^\circ$  to  $64^\circ$  latitude and  $-132^\circ$  to  $-60^\circ$  longitude. Thirty-four different vertical levels are provided, but only the lowest level was used in this work. CT data are publicly available in the netCDF format file [27].

### 3.1.2 WRF-CHEM Model Output Data

Compared to the CT data source, the WRF-CHEM model output (MO) data covers a much smaller spatial domain, but at a much higher resolution [28]. This dataset demonstrates the large changes in spatial variability that can occur in carbon dioxide concentrations over time, especially in areas of human activity. The domain encompasses northern Alberta and the data sources (EDGAR, [21]) used for its creation were modified to take time varying power generation into account. The time resolution for this data is 1 hour. The data is distributed on a  $99 \times 99$  cell grid, which roughly covers an area between  $52.3^\circ$  to  $61.5^\circ$  latitude and  $-121.5^\circ$  to  $-102.8^\circ$  longitude. While the CT data source uses grids defined regularly in

regards to latitude and longitude, the model output data are defined on a regular grid in regard to linear distances.

### **3.1.3 Creation of Experimental Datasets for Prediction**

In order to test the accuracy of estimates made using different estimation techniques, the model data previously discussed was used. These data sources have complete spatial coverage and reflect realistic spatial variability and concentration change of carbon dioxide over time. The complete model outputs were transformed into different datasets with different amounts of data removed in different spatial configurations. The missing data points were then predicted based on the existing points, and after estimates had been made, the inferred dataset was compared with the original dataset in order to calculate prediction errors. For the static case, data were both randomly removed (RR) based on a uniform random variable, and randomly removed with the additional removal of the center third (missing middle, MM). The dynamic case datasets had configurations of randomly removed data, and a time series in which only every third time step after the first 48 steps was well informed and the remainder had much more missing data (3rd step good, 3SG). These different missing data configurations were chosen to test potential scenarios, such as missing swaths, orbital patterns and measurement obstructions, that may arise when processing data coming from Earth-observing satellites.

### **3.1.4 Characteristics of the Data Used**

The following data were used to compare estimation methods:

- CT data from March 13, 2008 at 01:30,
- Static MO data from May 28, 2007 at 08:00,
- Dynamic MO data for a period of 250 hours starting from May 28, 2007 at 00:00 (hourly),
- Dynamic CT data for a period of 864 hours starting from September 6, 2007 at 08:00 (reported ever 3 hours).

After the grid assignment and calculation of summary statistics (section 3.2.1 and section 3.2.2), the static CT dataset was found to have a mean of 393.883 ppm and a variance of 23.771 ppm<sup>2</sup>, while the static MO dataset had a mean of 562.724 ppm and a variance of 198.778 ppm<sup>2</sup>. Values for the MO dataset are much higher than values for CT data because MO outputs were provided as ppm by mass, rather than by volume. As the main purpose for the use of these experimental datasets was to have a realistic spatial structure, this difference was not expected to affect the outcome.

Histograms of the MO and CT complete static data sets are shown in Figure 3.2a and Figure 3.2b, respectively.

## 3.2 Data Preprocessing

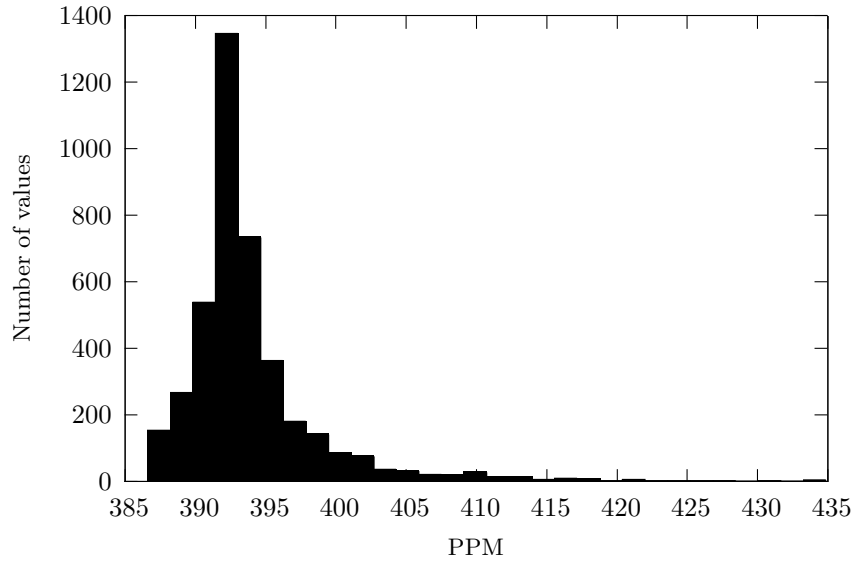
### 3.2.1 Assignment to a Grid

The data were first mapped to a regular latitude/longitude grid. The implementation of hierarchical algorithms limited the grid to sizes that are powers of two, since this allows for the entire hierarchical structure to form a perfect quad-tree resulting in a single root node. While this is not necessarily a requirement of the hierarchical algorithms, the generalisation to arbitrary hierarchical aggregation was not pursued in this work.

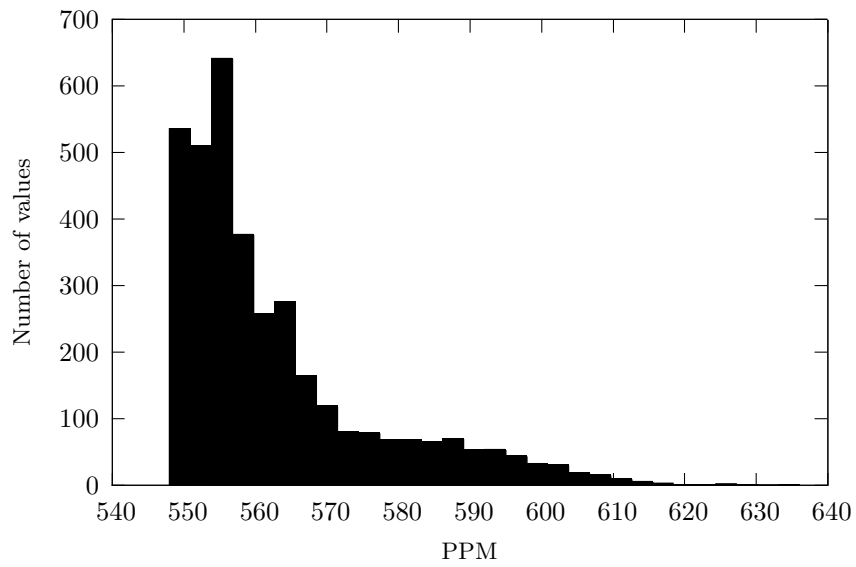
The assignment to the grid first involved the calculation of all the target grid intersection points. Data points are then overlaid on this created grid, and data values are assigned based on the weighted averages of the data points overlapping with the individual grid cells [29]. The weights were based on rough estimates of the amount of overlap between the data and the grid by first assigning each real value a number of inner points, and then counting the number of real value points in each of the grid cells. With this scheme the estimate of the grid cell value,  $\hat{z}$  is given as

$$\hat{z} = \frac{1}{N} \sum_{i=1}^N f(x_i),$$

where  $N$  is the number of real value points falling inside the grid cell,  $x_i$  is their location, and  $f(x_i)$  is the real value at that location. Recognising the similarity of this scheme to Monte Carlo integration [30], estimates of the variance for the target cells are calculated



(a) CT dataset.



(b) MO dataset.

Figure 3.2: Histograms for static datasets.

using

$$\sigma_z^2 = \frac{1}{N} \sum_{i=1}^N f(x_i)^2 - \hat{z}^2.$$

### 3.2.2 Calculation of Summary Statistics

In order to guide some of the following steps, certain statistics are calculated, including sample mean, sample variance, and percentage of grid cells that are uninformed. As it is a required value for many subsequent steps, distances between grid cells are also calculated.

The mean value of the observed points was calculated with

$$\hat{\mu} = \frac{1}{n} \sum_{i=1}^n x_i, \quad (3.1)$$

where  $n$  is the number of observed data points, and  $x_i$  is their value. The sample variance was calculated using

$$\hat{\sigma} = \frac{1}{n-1} \sum_{i=1}^n (x_i - \hat{\mu})^2,$$

where  $n$ ,  $x_i$ , and  $\hat{\mu}$  are as previously defined.

The distance between two points of latitude and longitude are calculated using the formula

$$d = R * \arccos(\sin(\theta_1) \sin(\theta_2) + \cos(\theta_1) \cos(\theta_2) \cos(\phi_1 - \phi_2)), \quad (3.2)$$

where  $R$  is the average radius of the Earth, taken to be 6372.797 km, and  $\theta_1$  and  $\theta_2$  are the latitudes of the first and second points, respectively; similarly  $\phi_1$  and  $\phi_2$  are the longitudes.

### 3.2.3 Variogram Modelling

Spatial variation is estimated using a variogram model. Before this model can be fit, the experimental variogram must be estimated. The classical variogram estimator is given by

$$\gamma(h) = \frac{1}{N(h)} \sum_{N(h)} (z_i - z_j)^2, \quad (3.3)$$

where  $N(h)$  is the number of pairs of data points separated by distance  $h$ , and  $z_i$  and  $z_j$  are data values of these points. While other variogram estimators exist, for example the weighted least squares estimator introduced in [31], comparisons show that the choice of estimator may depend on estimates of spatial dependence [32]. However, the same study also concludes that the simpler estimators should be acceptable for most purposes. Additionally, kriging shows a degree of robustness to small changes in variogram parameters, helping to make the case for the use of a simpler model [33].

The variogram model is fit to the points calculated using Eqn. 3.3. This exponential model [14] is defined as:

$$\hat{\gamma}(h) = \alpha + \beta(1 - e^{-\Lambda h}), \quad (3.4)$$

where  $\alpha$ ,  $\beta$ , and  $\Lambda$  correspond to the nugget, sill, and range of the variogram model, respectively, and  $h$  is the distance between grid cell centers. For simplicity, the variogram is currently modelled omnidirectionally and is fit using a rudimentary genetic algorithm. The modelling of an omnidirectional variogram implies the assumption of data isotropy, which may not always be the case. However, the locally varying anisotropy that may be necessary to properly model the directional variation is beyond the scope of the work presented here.

The rudimentary genetic algorithm that is used to fit the variogram model to the data is first provided with an estimate of the upper bound for the sill value, which was arbitrarily taken to be 125% of the calculated sample variance. An upper bound for the nugget value is also assigned and is given a value of 10% of the calculated sample variance. The fitness function used is the least squares error between the fit curves and the variogram points, with the addition of the squared value of the nugget. The addition of this last term causes lower nugget values to be selected, which corrects for a problem in previous versions where unbelievably large values would be selected, in part due to a few data point pairs with small spatial lags.

The use of automatic fitting techniques for variograms has been frowned upon because of the ability of those experienced with the type of data in question (atmospheric concentrations in this case) to better use it to meet the end goal of the analysis (point estimation here) [34, p.232]. Unfortunately, due to the number of variograms that would need to be estimated to

use this system operationally, manual fitting is likely not feasible. Methods of automatically fitting variograms do exist (see [35], for example), however it is hoped that the genetic algorithm method used here is more versatile and will allow for easier incorporation of expert information through simple changes in the fitness function.

### 3.2.4 Trend Modelling and Removal

In general, the statistical methods of estimation are based on the assumptions made, including stationarity, about the data being processed, and of the data distribution. For example, optimality of simple kriging is dependant the data being a Gaussian distribution, and can be sensitive to data with distributions that do not reflect this [11, p.144]. Considering the distributions of the data used here (Figure 3.2), this requirement for optimality is definitely not met. Additionally, the assumption of stationarity, meaning that the mean and variance are the same everywhere in the spatial field, is also generally not met. These problems can be mitigated by the removal of large scale trends [36, 37].

Here, a trend is first modelled using one of the methods outlined below. The trend surface is then subtracted from the observed values, creating residuals. The estimation methods then operate on these residuals, predicting values for the uninformed points. After this is completed, the trend surface is added back to complete the process.

#### 3.2.4.1 Simple Mean Removal

The simplest method of creating a zero mean dataset is to remove the arithmetic average from all of the observed values. While this can be performed quickly, it does not remove any large scale trend and simply shifts the data values down to around zero. In this thesis, this method has been called simple mean removal (SM).

#### 3.2.4.2 Generalised Least Squares

For smaller datasets, it may be computationally feasible and acceptable to model a large scale trend surface using generalised least squares (GLS) [19, p.176]. Starting with regular least squares, it is first assumed that

$$Y(s) = \mathbf{x}^T(s)\boldsymbol{\xi} + \epsilon(s),$$

where  $Y(s)$  is the data value,  $\mathbf{x}(s)$  is a row vector based on the order of the trend surface being fit,  $\boldsymbol{\xi}$  is a vector of weights estimated by fitting the trend,  $\epsilon(s)$  represents deviation from the trend, in this case this is the local variation, and  $s$  specifies the location of the point. The estimate for  $\boldsymbol{\xi}$  is found using

$$\boldsymbol{\xi} = (\mathbf{X}^T \mathbf{X})^{-1} \mathbf{X}^T \mathbf{z},$$

where the variance of the estimated  $\boldsymbol{\xi}$  is found using

$$VAR(\boldsymbol{\xi}) = \sigma^2 (\mathbf{X}^T \mathbf{X})^{-1},$$

where  $\mathbf{X}$  is a matrix based on the order of the trend surface and the locations of the measured data points, and  $\mathbf{z}$  is a vector of the observed data values. Since the data are spatially distributed, it may make more sense to fit the trend surface taking more of the spatial structure into account. By first estimating the variogram of the data and creating the covariance matrix  $\mathbf{C}$ , the following estimates for  $\boldsymbol{\xi}$  may instead be used

$$\boldsymbol{\xi} = (\mathbf{X}^T \mathbf{C}^{-1} \mathbf{X})^{-1} \mathbf{X}^T \mathbf{C}^{-1} \mathbf{z},$$

with a variance similar to the previous variance,

$$VAR(\boldsymbol{\xi}) = (\mathbf{X}^T \mathbf{C}^{-1} \mathbf{X})^{-1}.$$

Unfortunately, since estimations of variogram and trend are linked, in order to perfectly remove the trend, iterations between removal of the trend and estimation of the variogram may be required, although it is expected that many iterations will not be worth the effort. The requirement of the inversion of the matrix  $\mathbf{C}$ , which can be potentially very large, can make this a time consuming/computationally infeasible method of detrending.

### 3.2.4.3 Spline Trend Surfaces

For larger spatial areas and datasets, it may be both computationally infeasible and unrealistic to attempt trend surface modelling via generalised least squares. When dealing with larger areas and datasets, such as the entire globe, some sort of spline detrending is often

used.

**Thin Plate Splines** Thin plate splines are the two dimensional analog of the one dimensional splines, and can therefore be used for the interpolation of missing data points [38].

First, the function for ‘bending energy’ is defined as

$$E(h_{ij}) = \begin{cases} h_{ij}^2 \log(h_{ij}^2) & h_{ij} > 0 \\ 0 & h_{ij} = 0 \end{cases},$$

where  $h_{ij}$  is the distance between points  $i$  and  $j$ . This formula is used to populate the  $\mathbf{A}$  matrix such that

$$\mathbf{z} = \mathbf{A}\mathbf{a} + \mathbf{B}\mathbf{b},$$

where  $\mathbf{z}$  is the vector of  $n$  data values,  $\mathbf{A}$  is a  $n \times n$  matrix with entries of  $E(r_{ij})$ ,  $\mathbf{a}$  is a vector of weights,  $\mathbf{B}$  is a  $n \times 3$  matrix with rows of  $[1, x, y]$ , where  $x$  and  $y$  are the coordinates of the corresponding data value row in  $\mathbf{z}$ , and  $\mathbf{b}$  is a vector of weights corresponding to the coordinates. Vector  $\mathbf{b}$  is calculated using

$$\mathbf{b} = (\mathbf{B}^T \mathbf{A}^{-1} \mathbf{B})^{-1} \mathbf{B}^T \mathbf{A}^{-1} \mathbf{z},$$

followed by the calculation of vector  $\mathbf{a}$ ,

$$\mathbf{a} = \mathbf{A}^{-1}(\mathbf{z} - \mathbf{B}\mathbf{b}).$$

After vectors  $\mathbf{a}$  and  $\mathbf{b}$  have been calculated, values for unknown points may be interpolated using

$$z_i = b_0 + b_1 x_i + b_2 y_i + \sum_{j=1}^n E_{ij} a_j.$$

The above implementation of thin plate smoothing fits the surface exactly through each of the data points. To reduce the requirement for the surface to pass exactly through each point, the smoothing factor  $\chi$  is introduced,

$$\mathbf{z} = (\mathbf{A} + \chi\mathbf{I})\mathbf{a} + \mathbf{B}\mathbf{b},$$

and the calculations of vectors  $\mathbf{a}$  and  $\mathbf{b}$  are performed as before as before, with the substitution of  $(\mathbf{A} + \chi\mathbf{I})$  for  $\mathbf{A}$ . Selection of a suitable value for  $\chi$  is discussed in [39].

For the use of thin plate splines as a trend surface, implementation of the algorithm as described does not lend itself well to large datasets: since the  $\mathbf{A}$  matrix is always dense, a large number of data points makes its inversion infeasible.

**Thin plate splines with aggregation** In order to easily capture large scale effects and to reduce the amount of computation required to fit a trend, values can be aggregated up to a coarser resolution before fitting the surface [14], thus changing thin plate splines into aggregated thin plate splines (ATPS). Since the values are aggregated it is assured that the trend fit will be large scale, provided that a coarse enough resolution has been chosen. Also, the number of data points can fall drastically with aggregation, improving the likelihood of the problem being computationally feasible.

#### 3.2.4.4 Fixed Rank Smoothing

Fixed rank smoothing is a method of trend removal involving the use of a basis function matrix which has a much smaller size than the number of data points [20]. Two basis functions are selected:  $\psi(\bullet)$  is used to populate matrix  $\mathbf{T}$  and  $\zeta(\bullet)$  populates matrix  $\mathbf{S}$ .

Vectors for the locations of the knots and the data points are first defined as the vector  $[\cos(\theta)\cos(\phi), \cos(\theta)\sin(\phi), \sin(\theta)]$ , where  $\theta$  and  $\phi$  are the latitude and longitude of the points, respectively.

For this implementation, hierarchical aggregation was used to determine the locations of the knots. The aggregation level was passed in, and the knot locations were taken to be the centers of the cells at that resolution level.

In order to perform trend estimation, the following vectors must be estimated [20],

$$\hat{\boldsymbol{\alpha}} = (\mathbf{T}^T\boldsymbol{\Sigma}^{-1}\mathbf{T})^{-1}\mathbf{T}^T\boldsymbol{\Sigma}^{-1}\mathbf{z},$$

and

$$\hat{\boldsymbol{\gamma}} = \lambda^{-1} \mathbf{K}^{-1} \mathbf{S}^T \boldsymbol{\Sigma}^{-1} (\mathbf{z} - \mathbf{T} \hat{\boldsymbol{\alpha}}),$$

where  $\mathbf{z}$  is a vector of the observed values,  $\mathbf{K}$  is a diagonal penalty matrix,  $\mathbf{T}$  is a matrix of basis functions  $\psi(\bullet)$  evaluated between every knot and observed location,  $\mathbf{S}$  is a similarly defined matrix of  $\zeta(\bullet)$  basis functions, and  $\boldsymbol{\Sigma}^{-1}$  is defined as

$$\boldsymbol{\Sigma}^{-1} = (\chi^{-1} \mathbf{S} \mathbf{K}^{-1} \mathbf{S}^T + \mathbf{W})^{-1},$$

where  $\chi$  is a smoothing parameter and  $\mathbf{W}$  is a diagonal matrix containing values of measurement errors for the observed values.

After the necessary vectors are estimated, the trend surface may be evaluated for all locations using

$$f(\hat{s}_i) = \mathbf{T}_{s_i} \hat{\boldsymbol{\alpha}} + \mathbf{S}_{s_i} \hat{\boldsymbol{\gamma}}, \quad (3.5)$$

where  $f(\hat{s}_i)$  is the value of the estimated trend at location  $s_i$ ,  $\hat{\boldsymbol{\alpha}}$  and  $\hat{\boldsymbol{\gamma}}$  are vectors previously estimated, and  $\mathbf{T}_{s_i}$  and  $\mathbf{S}_{s_i}$  are vectors of the basis functions used in  $\mathbf{T}$  and  $\mathbf{S}$  evaluated for at location  $s_i$  for each knot location.

In the implementation used here, the basis function  $\psi(\bullet)$  is always equal to 1, and one knot was used for this basis. Thus  $\mathbf{T}_{s_i} \boldsymbol{\alpha}$  in Eqn. 3.5 is a constant bias over the domain, with spatial variation coming only from the  $\mathbf{S}_{s_i} \boldsymbol{\gamma}$  term.

The basis function used for  $\zeta(\bullet)$  is [40]

$$a = \frac{1 - \eta^2}{(1 - 2x\eta + \eta^2)^{1.5}},$$

where  $\eta$  is a bandwidth parameter between 0 and 1, and  $x$  is the cosine of the angles between the two vectors, computed using the dot product. A plot of the basis function is shown in Figure 3.3.

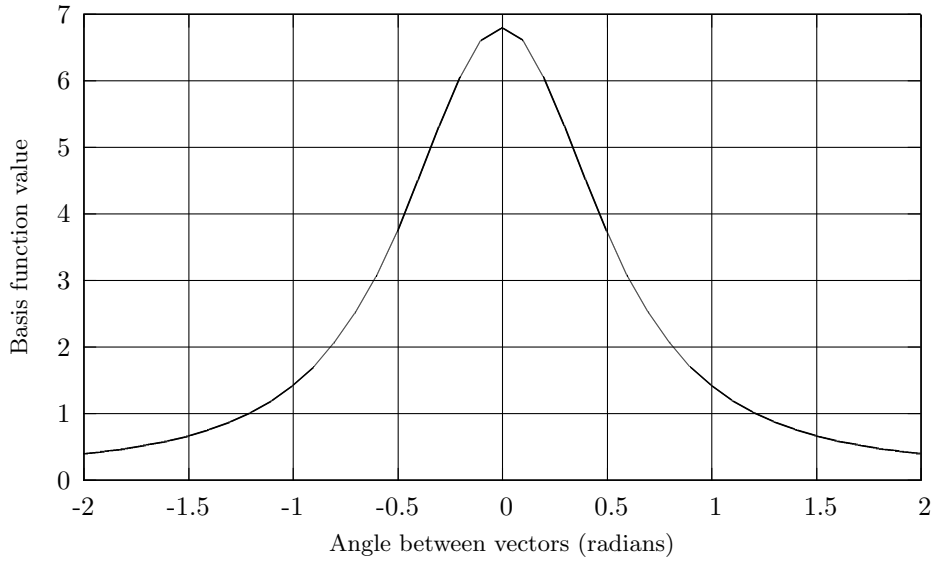


Figure 3.3: Basis function for FRS ( $\eta = 0.5$ ).

### 3.3 Estimation Methods

#### 3.3.1 Nonstatistical Estimates

Nonstatistical methods of estimation provide an estimate of the missing data value, but are not capable of providing a variance with that estimate. Generally, these methods are more computationally feasible since they are simpler, and do not rely on the variable's covariance matrix or any other similarly sized matrix. This increased feasibility and processing speed can come at the cost of a lower prediction accuracy.

##### 3.3.1.1 Arithmetic Average

The most basic method, an arithmetic average, was calculated for the different sets of data and then used as an estimated value for cells where no data were measured. Here, this estimation method is labelled as the flat average (FA). This is the only estimation method that was not applied to the detrended data as, ideally the mean of the detrended data will be zero and the result will be the same as the result for the trend surface (described below).

### 3.3.1.2 Trend Surface

The trend surface (TS) method relies in a calculated trend surface to fill in the missing data points. The trend surface was modelled as with every other estimation method, but instead of removing it for estimation, it is used to assign values to uninformed points. The different trend surfaces that were fit to the data and used for estimation are discussed in section 3.2.4.

### 3.3.1.3 Nearest Neighbour Interpolation

Nearest neighbour (NN) interpolation is a very simple method of estimation where the values of missing data points are assigned based on the value of the nearest observed point. Due to its simplicity, computation is very fast, but the predictions are blocky and, in areas of sparse data, large regions will be predicted based on a single point. More formally, the estimate of an unobserved point is given as

$$\hat{z}_i = z_j | (h_{ij} = (\min(h_{ij}) \forall j)),$$

where  $\hat{z}_i$  is the point being estimated,  $z_j$  is the value of the informed (observed) point, and  $h_{ij}$  is the distance between observed and unobserved points.

### 3.3.1.4 Inverse Distance Weighting

Inverse distance weighting (IDW) is another simple method of interpolation. Predictions are made by averaging measured data points, weighted by the inverse of the distance from the point being estimated [13]. Due to the relatively small spatial size of the datasets that have been used for testing, all measured points were used in the calculation of the estimate, as opposed points in a local neighbourhood. The estimate of an unmeasured location used here is give by

$$\hat{z}_i = \frac{\sum_{j=1}^n \frac{1}{h_{ij}^2} \times z_j}{\sum_{j=1}^n \frac{1}{h_{ij}^2}},$$

where  $n$  is the number of data points being considered,  $z_j$  is the value of the informed point, and  $h_{ij}$  is the distance between observed and unobserved points.

### 3.3.2 Statistical Estimates

Statistical methods treat data as random variables with some distribution. The estimates made for missing data points consist of a mean and a variance.

#### 3.3.2.1 Simple Kriging

Kriging, a statistical method of estimation, is discussed at length in [11]. Simple kriging (SK) is one of the variations of kriging used here. In SK, an assumption is made that the mean of the data is a constant value of zero everywhere. Kriging involves the calculation and modeling of an experimental variogram which is then used to create a covariance matrix  $\mathbf{C}$  using

$$\mathbf{C}(h) = \sigma^2 - \gamma(h),$$

where  $h$  is the distance between two measured points and  $\sigma^2$  is the experimental variance. This matrix needs to be created only once for each dataset, and is used in its inverted form, which also only needs to be computed once.

For each point being estimated, the vector  $\mathbf{c}$  is created, which is a vector of covariance between the point being estimated and all of the measured points that are being considered. Using  $\mathbf{C}$  and  $\mathbf{c}$ , a vector of kriging weights  $\boldsymbol{\lambda}$  is calculated as

$$\boldsymbol{\lambda} = \mathbf{C}^{-1}\mathbf{c}.$$

Using the calculated vector of weights  $\boldsymbol{\lambda}$  the prediction is calculated by vector multiplication with a vector of the observed data points  $\mathbf{z}$ . The estimated value is given by

$$\mu_{sk} = \mathbf{z}\boldsymbol{\lambda}, \tag{3.6}$$

and the variance of this estimate is calculated similarly, using

$$\sigma_{sk}^2 = \sigma^2 - \mathbf{c}^T\boldsymbol{\lambda}.$$

For these experiments, an omnidirectional variogram was used, as opposed to a direc-

tional one. This variogram was created using the variogram model described in section 3.2.3 (Eqn. 3.4).

In this series of tests, SK was implemented using the EIGEN library [41] and the UMF-PACK solver [42] for sparse matrix calculations. By trying to leverage situations where the range of the variogram is short, the hope is that the use of sparse matrix techniques will speed up the computation [10].

### 3.3.2.2 Local Simple Kriging

In practice, some programs that make use of kriging for missing data estimation will do so by considering only a local neighbourhood of points. While this method does not make sense for all types of data ([11, p.130-134]), in some cases it allows the prediction accuracy of kriging to be attained in a fraction of the computation time. The use of a smaller area is associated with ‘quasi-stationarity’ [34, pg.33-34], which is the idea that assumptions about stationarity may be made if a suitably sized neighbourhood surrounding the estimated point is chosen.

In this implementation of local simple kriging (LSK), only the points measured within the distance equal to the variogram range were considered when estimating an uninformed location. Also, in this implementation the screen effect is assumed to be an important factor. All data points ‘screened’ by closer points are removed from the prediction.

**Determining Screened Data Points** In order to determine the points to use in the estimation of a point using LSK, first the rough size of a neighbourhood surrounding the data point is estimated using the estimated value of the range from the variogram fitting process where this distance is given by

$$d_n = \frac{1}{\Lambda},$$

where, as previously,  $\Lambda$  is the variogram range parameter. A simplifying assumption is made by drawing a bounding box around this distance range. Only the points within this distance of the unknown point are considered for use in its estimation. The points are further filtered by determining if, for any point in this neighbourhood, there exists another point blocking the ‘line of sight’ between it and the unmeasured point. If such a point is found, the point

is discarded from the set used for prediction of the missing point.

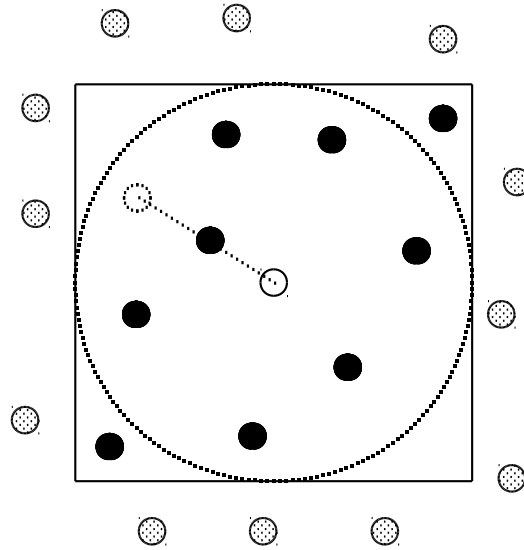


Figure 3.4: Determining which points to use for LSK.

In Figure 3.4, the actual distance  $d_n$  is shown by the dashed circle surrounding the unknown point, shown as a solid white circle. The solid bounding box is shown with a solid line. Data points (filled circles) within this box are further filtered with the ‘line of sight’ test, even if they are outside of the circular distance. The point shown as a small dashed circle is excluded from the prediction because there is not a clear path between it and the point to be estimated, and it is therefore assumed to have been screened.

### 3.3.2.3 Ordinary Kriging

Another variant of kriging assumes a constant mean, but not one that it is known; consequently, it also needs to be predicted. This kriging method is equivalent to a case of simple kriging where the mean is first removed, the residual is predicted, and the mean is added back, except that now the mean estimation occurs during the prediction rather than beforehand [19, p.192]. Ordinary kriging is procedurally similar to the simple kriging described in section 3.3.2.1, except that now there is an additional constraint placed on the kriging weights, namely, they must now sum to one. The equations for this type of prediction then become:

$$\begin{bmatrix} \boldsymbol{\lambda} \\ \nu \end{bmatrix} = \begin{bmatrix} \mathbf{C} & \begin{array}{c} 1 \\ \cdot \\ 1 \end{array} \\ \hline 1 & \dots & 1 & 0 \end{bmatrix}^{-1} \begin{bmatrix} \mathbf{c} \\ 1 \end{bmatrix},$$

where  $\mathbf{C}$ ,  $\mathbf{c}$ , and  $\boldsymbol{\lambda}$  are the same as the variables defined for simple kriging. The  $\nu$  parameter is a Lagrange multiplier used to minimise the kriging error subject to the constraint on the weights.

After this calculation, the prediction is then made using Eqn. 3.6. The variance is calculated using

$$\sigma_{ok}^2 = \begin{bmatrix} \mathbf{c} \\ 1 \end{bmatrix}^T \begin{bmatrix} \boldsymbol{\lambda} \\ \nu \end{bmatrix}.$$

### 3.3.2.4 Multiresolution Spatial Models

The multiresolution spatial model (MRSM) [15] involves the partitioning of a spatial area in progressively larger areas, that is moving from a resolution of  $j = J$  down to the coarser resolution of  $j = 1$  in a hierarchical fashion. After computation moving up the hierarchical structure is finished, computations are also performed moving back down the structure, toward the original resolution. This method does not involve inversions of large matrices as is required with the full kriging method. Additionally, modifications can be made to the process that will result in a ‘mass balance’ between the different resolutions [14]. This constraint ensures that there are no statistical inconsistencies between the resolutions, meaning that the predictions for all resolutions will be valid, rather than just the predictions made for the finest resolutions, which may be desirable for some applications. This was not implemented in this work, as the primary focus was comparison with nonhierarchical methods.

**Parameter Estimation** After the fitting of the variogram model, hierarchical methods require an additional parameter estimation step. Resolution specific variances are estimated using a method taken from [43]. To define  $\Theta = \{\sigma_1^2, \sigma_2^2 \dots \sigma_J^2\}$ , another rudimentary genetic algorithm is used to estimate a solution to the equation,

$$\hat{\Theta} = \arg \min_{\Theta} \sum_{h=1}^U \frac{N(h)}{\gamma(h, \Theta)} (\hat{\gamma}(h) - \gamma(h, \Theta))^2, \quad (3.7)$$

where  $\gamma(h, \Theta)$  is defined as

$$\gamma(h, \Theta) = \sigma^2 - \sum_{i=1}^J \tau_i \left(1 - \frac{h_i}{l_{ij}}\right) \sigma_i^2, \quad (3.8)$$

and where  $\tau_i$  is given by

$$\tau_i(x) = \begin{cases} 1 & \text{if } x \geq 0 \\ 0 & \text{if } x < 0 \end{cases}. \quad (3.9)$$

The algorithm for the estimation of  $\Theta$  splits the variogram sill value into different variances for different resolutions. Since the sill value is constant, the sum of the  $\sigma_n^2$  values must remain constant. In order to keep the sum the same, crossover is not used. The method of generating new solutions is that two  $\sigma_n^2$  values are selected at random from a given  $\Theta$ . A small randomly generated number is then added to one and subtracted from the other. The new values are then checked for negatives and values that are too large and, if these conditions are found, the changes are undone and  $\Theta$  is returned to the population. The algorithm continues until the maximum number of iterations is reached. The resulting  $\Theta$  is then used in the following two equations, the results of which are used in the actual estimation procedure:

$$\hat{\Sigma}_j = \sum_{i=1}^j \hat{\sigma}_i^2, \quad (3.10)$$

$$B_j = \hat{\Sigma}_{j-1} \hat{\Sigma}_j^{-1}, \quad (3.11)$$

where Eqn. 3.10 estimates the amount of total variance that can be assigned to each different resolution, and Eqn. 3.11 is used to provide estimates in the relative change in variance seen when moving between different resolutions.

**Uptree Prediction** Uptree prediction begins at the finest resolution and works up to the coarsest resolution. The initial step is the estimation of the high resolution ‘leaf’ mean and

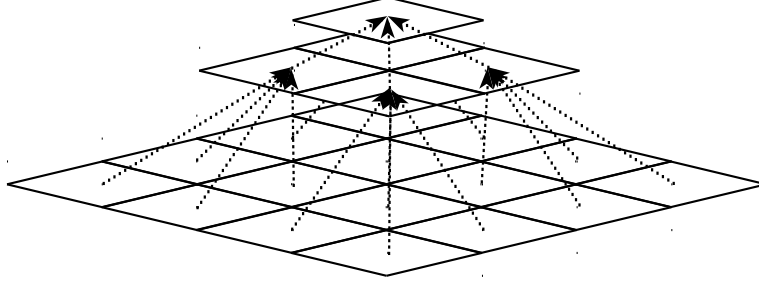


Figure 3.5: Uptree predictions.

variance values. The leaf mean is given by

$$\hat{y}_{J,k|J,k} = \delta(k)\hat{\Sigma}_J(\hat{\Sigma}_J + \alpha^2)^{-1}z_k,$$

where  $\delta(k)$  is a binary flag indicating if the cell had a measured value associated with it,  $\hat{\Sigma}_J$  is given by Eqn. 3.10,  $\alpha$  is the nugget effect value from Eqn. 3.4, and  $z_k$  is the data value of the cell. The leaf variance is given by

$$\Gamma_{J,k|J,k} = \hat{\Sigma}_J - \delta_k\hat{\Sigma}_J^2(\hat{\Sigma}_J + \alpha^2)^{-1},$$

where  $\delta(k)$ ,  $\hat{\Sigma}_J$ , and  $\alpha$  are the same as defined previously. After the initial estimation of the leaf cell values, the next step is to predict the value of the parent cell based on each of the child cells using

$$\hat{y}_{j,k|ch(j,k,i)} = B_{j+1}\hat{y}_{ch(j,k,i)|ch(j,k,i)} \quad (3.12)$$

where  $B_{j+1}$  is found using Eqn. 3.11. Similarly, the variance for each parent is predicted based on each of its child cells using,

$$\Gamma_{j,k|ch(j,k,i)} = B_{j+1}^2\Gamma_{ch(j,k,i)|ch(j,k,i)} + (1 - B_{j+1})\hat{\Sigma}_j. \quad (3.13)$$

To complete the uptree prediction for each of the parent cells, the predictions that were made using Eqn. 3.12 and Eqn. 3.13 are combined. The aggregation of the child variances is given by

$$\Gamma_{j,k|j,k} = (\hat{\Sigma}_j^{-1} + \sum_{i=1}^{n_{j1}n_{j2}} (\Gamma_{j,k|ch(j,k,i)}^{-1} - \hat{\Sigma}_j^{-1}))^{-1},$$

where  $\Gamma_{j,k|ch(j,k,i)}$  represents the variance that was calculated with Eqn. 3.13. The calculated value  $\Gamma_{j,k|j,k}$  is then used in the prediction of the parent mean using

$$\hat{y}_{j,k} = \Gamma_{j,k|j,k} \left( \sum_{i=1}^{n_{j1}n_{j2}} \Gamma_{j,k|ch(j,k,i)}^{-1} \hat{y}_{j,k|ch(j,k,i)} \right),$$

where  $\hat{y}_{j,k|ch(j,k,i)}$  for all the child cells has been previously calculated using Eqn. 3.12.

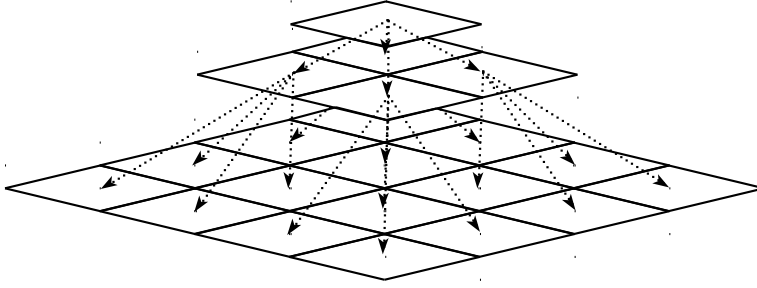


Figure 3.6: Downtree predictions.

**Downtree Prediction** Working back down the tree structure, downtree predictions are made based on the downtree predictions of cells at coarser resolutions and on uptree predictions of the cell being predicted. This process starts with the initial downtree prediction of the coarsest resolution mean using

$$\hat{y}_{1,k}^* = \hat{y}_{1,k},$$

and coarsest resolution variance

$$\Gamma_{1,k}^* = \Gamma_{1,k}.$$

The rest of the travel down the tree structure predicts the downtree mean of the cells with

$$\hat{y}_{j,k}^* = \hat{y}_{j,k|j,k} + B_j \Gamma_{j-1,k|ch(j-1,k,i)}^{-1} (\hat{y}_{j-1,k}^* - \hat{y}_{j-1,k|ch(j-1,k,i)}),$$

and the dntree variance,

$$\Gamma_{j,k}^* = \Gamma_{j,k|j,k} + \Gamma_{j,k|j,k}^2 B_j^2 \Gamma_{j-1,k|ch(j-1,k,i)}^{-2} (\Gamma_{j-1,k}^* - \Gamma_{j-1,k|ch(j-1,k,i)}).$$

**Final Steps** After completion of the dntree prediction, the leaf grid cells are predicted by taking into account all of the data originally present. Any splitting of the original domain that has taken place is now reversed, and the trend that had been previously removed is now added back in. The resulting predictions may appear blocky due to the hierarchical nature of the algorithm.

### 3.3.2.5 Multiresolution Spatial Predictor

An extension of the MRSM prediction method, the multiresolution spatial predictor (MURS) algorithm, seeks to gain smoother and more accurate predictions through multiple applications of the MRSM method [15]. The MURS algorithm begins with the parameter estimation used in MRSM, but the uptree/dntree prediction phase is performed multiple times, each using a spatially shifted version of the original leaf grid. In this implementation, 81 shifts were used, four grid cells in every direction along with the unshifted version. The results of these shifted predictions were collected in another tree structure and then averaged.

Since most of effort needed to perform MRSM estimation comes from parameter estimation, MURS does not add a significant amount of computation time, as this method only requires the variogram and resolution specific variances to be estimated once.

### 3.3.2.6 Dynamic Extensions

Through the inclusion of historical data, such as general measurements, summary statistics, and trends, it may be possible to correct estimations in areas with very few actual measurements. Historical data may even be used in place of measured data in areas where there is none [18]. By carrying information from the past forward for use in current estimations, less computationally intense methods can reach prediction accuracies usually found with more demanding methods. The addition of dynamic information to the multiresolution spatial model and multiresolution spatial predictor creates the dynamic multiresolution spatial model (DMM) and the dynamic multiresolution spatial predictor (DMURS), respec-

tively. Inclusion of the dynamics takes place at the coarsest resolution, which is one of the drawbacks of these methods [16].

In this work, different dynamic models were used. However the results of these models are incorporated into the hierarchical process the same way. The output of the dynamic model is combined with the current hierarchical values at the coarsest resolution in a weighted average. The weights for this average come from the percentage of the domain that is informed. If the entire domain is informed, the dynamic model output is disregarded. In cases where the domain is not as well informed, the dynamic model is increasingly relied upon. It was assumed that spatial information would always be more important to predicting current values than a temporal forecast, so nonlinear weights for the forecast and spatial values were used, as shown in Figure 3.7.

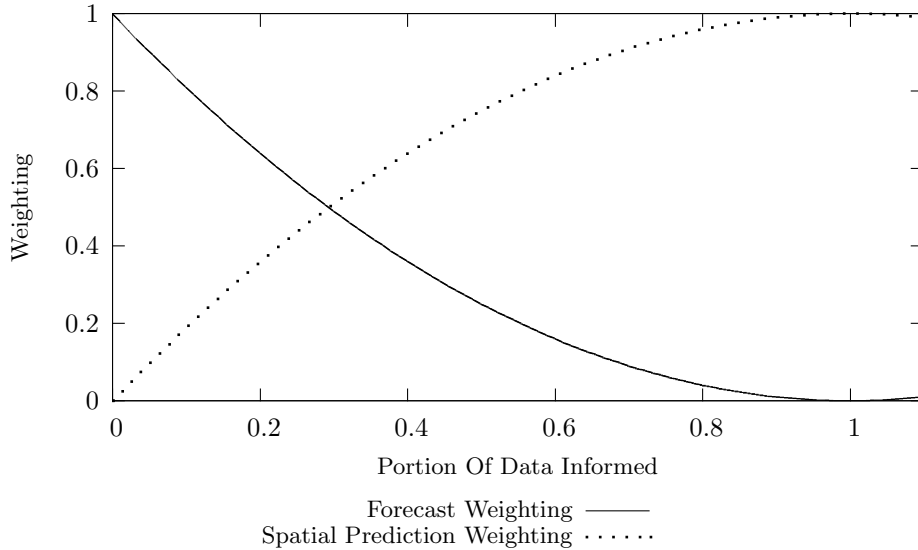


Figure 3.7: Dynamic weightings.

The average squared differences between values at different temporal separations is shown for the MO data at the original resolution after mapping (Figure 3.8a) and top level aggregation (Figure 3.8b). This shows the strong periodicity in the average squared difference, which occurs because of the changing electricity generation needs, as well as the different weather patterns that occur during different times of day. This may allow for past information to be used to increase prediction accuracy, as there are lower differences between values with a certain temporal separation, in this case, 24 hours. Similarly, the equivalent

graphs for the CT data are shown in Figure 3.8c and Figure 3.8d. In this case the period is 8 time steps, which translates to 24 hours because of the 3 hour temporal resolution of this data. The extremely low values present in the coarse resolution illustrate the lower variance of this dataset.

**Double Exponential Smoothing** Double exponential smoothing (2ES) is a method of smoothing a time series capable of handling a trend, as opposed to single exponential smoothing (no trend) and triple exponential smoothing (trend and periodic components) [44].

After the first time step has passed, the following values are calculated:

$$S_t = py_t + (1 - p)(S_{t-1} + b_{t-1}), \text{ and}$$

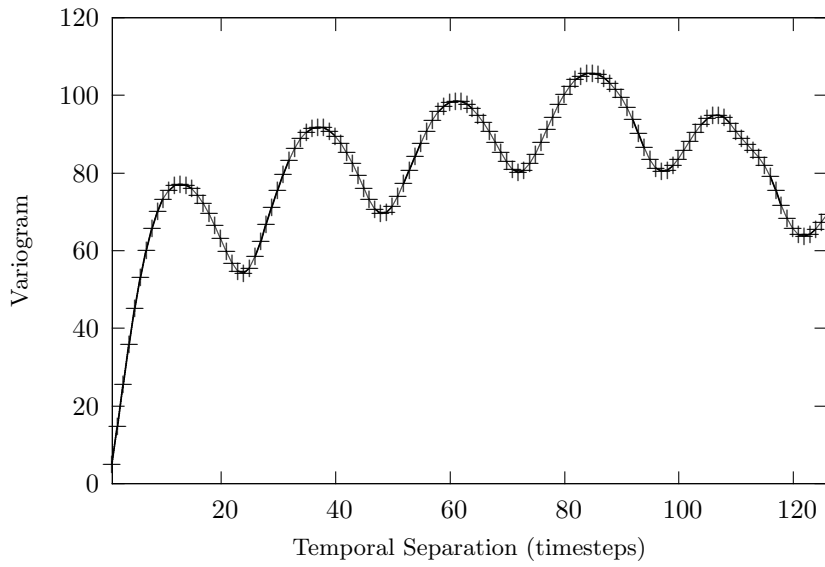
$$b_t = q(S_t - S_{t-1}) + (1 - q)b_{t-1},$$

where  $p$  and  $q$  are arbitrarily chosen constants between zero and one. The first values for  $S_{t-1}$  and  $b_{t-1}$  must be estimated. For each time step, future points can be forecast using

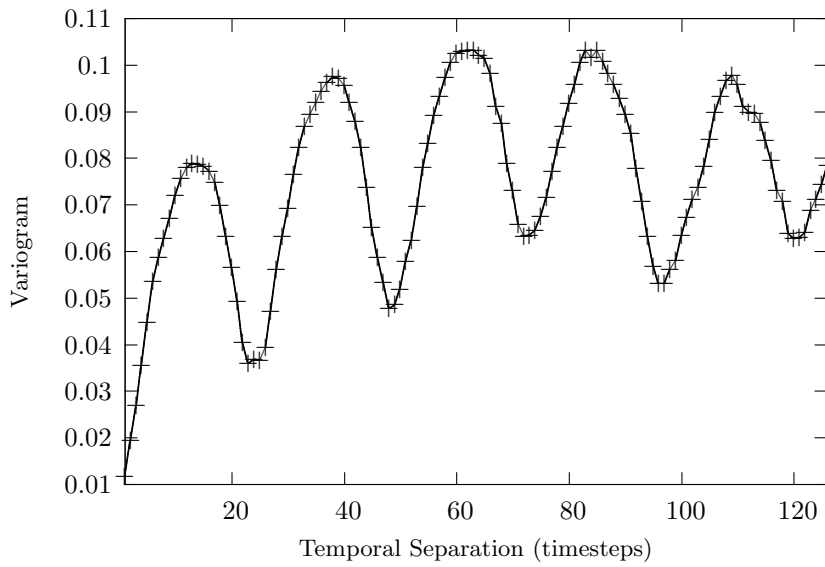
$$F_{t+1} = S_t + b_t.$$

In the current implementation, this forecast is carried forward to the next time step. Here, the forecast and the values from the current time step are combined using a weighted average, where the weights come from the proportion of the area that is informed. For example, in the area where the forecast is being carried forward, if the area is completely informed, then the forecast is effectively ignored. Similarly, if the area is completely uninformed, the forecast is completely relied upon. When the area is partially informed, the forecast and measurements are combined. With this method, scenarios where the area is completely uninformed or sparsely informed are expected to provide the largest gain in prediction performance over similar static methods.

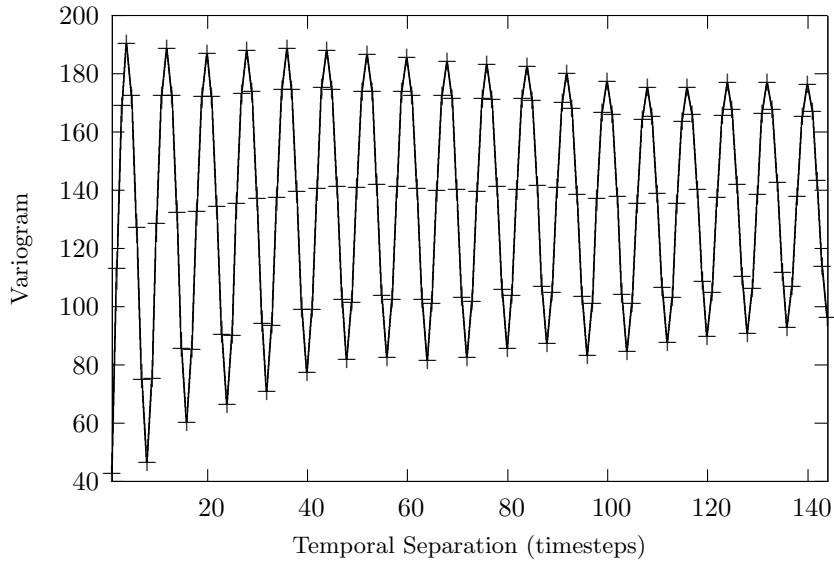
**Triple Exponential Smoothing** In the event that the time series has an element of periodicity, as can be the case when examining domains in which power generation plays a major role in carbon dioxide emissions, triple exponential smoothing (3ES) can be used [44].



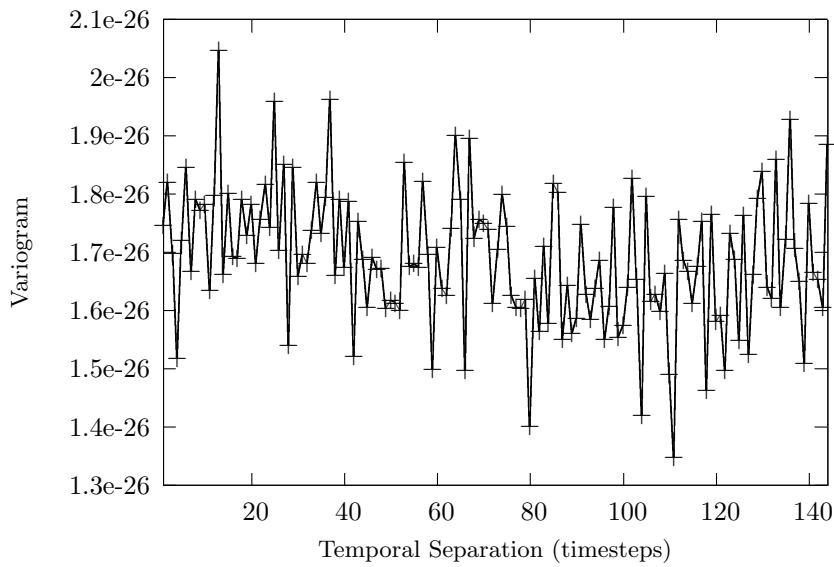
(a) Finest resolution (MO data).



(b) Coarsest resolution (MO data).



(c) Finest resolution (CT data).



(d) Coarsest resolution (CT data).

Figure 3.8: Variograms across time.

Smoothed observations can be calculated using

$$S_t = p \frac{y_t}{I_{t-L}} + (1-p)(S_{t-1} + b_{t-1}),$$

where  $y$  is the measured value,  $S$  is the smoothed observation,  $b$  is the trend factor,  $I$  is the seasonal index, and  $t$  is the time index.  $L$  is the number of periods contained in a complete season;  $b$  and  $I$  are calculated using

$$b_t = q(S_t - S_{t-1}) + (1-q)b_{t-1}, \text{ and}$$

$$I_t = r \frac{y_t}{S_t} + (1-r)I_{t-L},$$

where  $r$  is an arbitrary constant between 0 and 1. Forecasts for future values based on the current smoothed values are given by

$$F_{t+m} = (S_t + mb_t)I_{t-L+m},$$

where  $m$  is the number of time steps into the future for which the forecast is being made.

**Neural Network Based Forecast** A simple feed-forward backpropagation neural network was implemented in order to attempt forecasting of values when large amounts of data are missing, labelled a forecasting neural network (FNN). The network consisted of input nodes equalling the expected period of the input data (e.g., if the data were provided on an hourly basis and expected to be periodic over the day, the number of input neurons would be 24). Five hidden nodes and one output node were used. Prediction of top level mean and variance values were carried out independently.

The activation function used for all neurons, except for input neurons, with a linear activations, was

$$a = \frac{30}{1 + e^{(-x)}} - 15,$$

where  $x$  is the weighted sum of the inputs, and  $a$  is the activation function value, as shown in Figure 3.9. The sigmoidal activation function was scaled this way to accommodate the

expected top-level mean and variance values from the model output data.

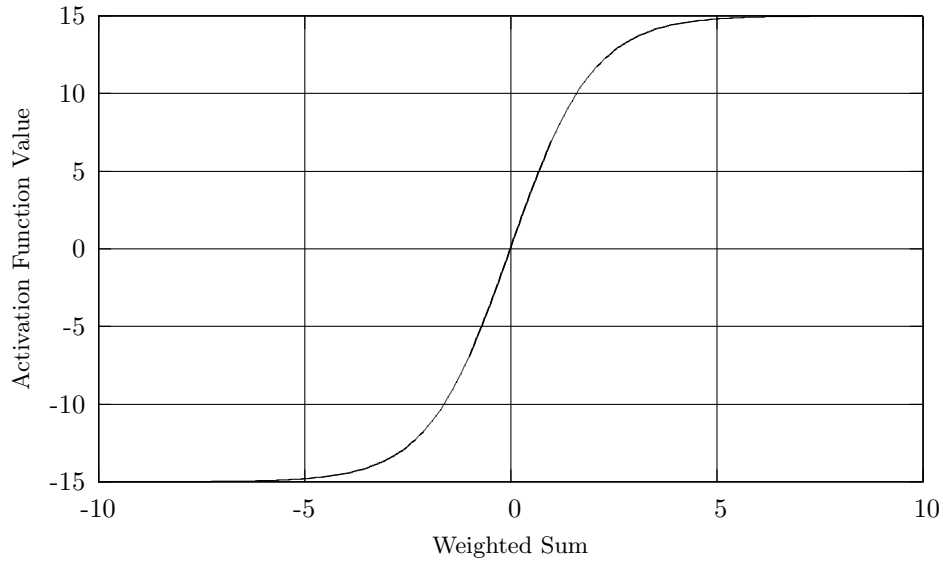


Figure 3.9: Neural network activation function for hidden and output neurons.

In order to keep the process as ‘online’ as possible, training occurs during prediction runs. If a relatively high amount of data is present, the run is used to train the network, and the network output is not used in any sort of forecasting. When relatively little data are present, the network is used to provide a prediction for the value, which is then in a weighted average calculation with the measured value. The weights are taken to be the proportion of informed/uninformed cells in the area being predicted. This weighted average is used as the top-level value.

**Kriging Based Forecast** Using the variograms calculated in Figure 3.8, forecasts were attempted using a kriging based technique, labelled as a kriging based forecast here (KBF) [11, p.124]. Due to the periodicity present in the experimental variograms, a different type of variogram model had to be used. The wave, or hole, model is given by,

$$\gamma(h) = \begin{cases} 0 & h = 0 \\ \alpha + \beta(1 - \Lambda \frac{\sin(\frac{h}{\Lambda})}{h}) & h > 0 \end{cases},$$

where  $\alpha$  and  $\beta$  are defined similarly to the variogram model that was fit for the pure spatial case (Eqn. 3.4). However, in this case,  $\Lambda$  is now the parameter controlling the period and

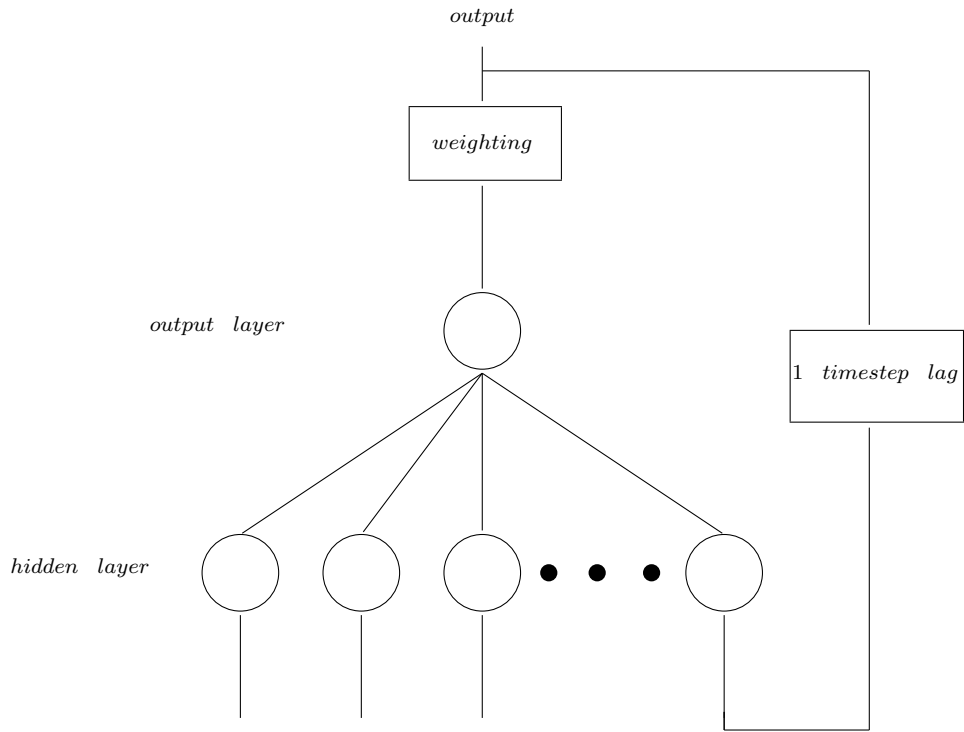


Figure 3.10: Neural network used for inclusion of dynamics.

magnitude of the oscillating component.

The forecast of a time series point takes place much like the spatial estimation method discussed in section 3.3.2.3, except, in this case, the spatial points are replaced with values at previous time steps. The number of previous time steps used in the forecast calculation can be capped to a given value to reduce computations required, and because of the increasing mismatch between experimental and modelled variograms for larger temporal separations.

Additionally, a low number of time steps were used for the forecasting here, since ordinary kriging was used for these forecasts. Since these forecasts amount to an extrapolation, the number of time steps was kept low in order to better fit the constant value trend that would be fit by the OK algorithm [12]. With the implemented OK algorithm, allowing too many previous values led to an error that increases with each time step, ultimately resulting in extremely high values.

The alternative would be to implement the more complex universal kriging algorithm, which would fit a polynomial trend and allow for the use of more time steps. However this would also increase the computational power required to keep track of more previous values and to actually perform the forecast.

### 3.4 Metrics for Comparison

**Mean Squared Prediction Error** Mean squared prediction error (MSPE) provides a measurement where large errors have much more influence than small errors. It is calculated as follows:

$$MSPE = \frac{1}{N} \sum_{i=1}^N (\hat{z}_i - z_i)^2,$$

where  $\hat{z}_i$  represents the  $i$ th prediction,  $z_i$  is the  $i$ th known value, and  $N$  is the total number of predictions made. For the experiments performed on a time series of spatial data, MSPE was calculated using every prediction made during the experiment, resulting in single value results. These results are used as the primary method of comparison for the dynamic methods.

**Mean Absolute Prediction Error** Unlike MSPE, the mean absolute prediction error (MAPE) provides an error measurement where all errors have influence linearly proportional to their magnitude; it is given by

$$MAPE = \frac{1}{N} \sum_{i=1}^N |(\hat{z}_i - z_i)|,$$

where  $\hat{z}_i$  represents the  $i$ th prediction,  $z_i$  is the  $i$ th known value, and  $N$  is the total number of predictions made.

**Mean Prediction Variance** Four of the estimation methods provide a variance associated with each prediction (SK, LSK, MRSM and MURS). Ideally, these variances are as small as possible, meaning that the confidence in the prediction is high. In order to compare the variances of these different estimation methods, a mean prediction variance (MPV) was calculated:

$$MPV = \frac{1}{N} \sum_{i=1}^N \sigma_i^2,$$

where  $N$  is the total number of predictions made and  $\sigma_i^2$  represents the variance associated with the  $i$ th prediction.

## 3.5 Results and Discussion

### 3.5.1 Static Results

The values for the speed and error comparisons shown here resulted from the averaging of 10 runs, each consisting of 11 predictions with an increasing amount of missing data. For each of these runs, the locations of the missing data were randomised. As the amount of missing data was increased, data points previously missing remained so. A second trial was also done, increasing the amount of missing data by removing points in the middle third of the spatial area (MM). This was done to investigate the behaviour of the different estimation methods when presented with larger continuous areas of missing data, bounded on either side by regions with randomly missing data as may occur when using real remotely sensed data.

### 3.5.1.1 Effect of Detrending on Distributions and Variograms

The goal of the detrending step is to remove any large scale trend present in the data in order to make more accurate predictions by more closely meeting the assumptions of the estimation methods. By performing trend removal and carrying out estimation using the resultant residuals, the distribution presented to the estimation method is changed, bringing it closer to the ideal case. In addition to the change in distribution, the use of residuals in variogram modelling causes the range and sill of the variogram to also change. As mentioned previously, since the variogram and modelled trend are linked (at least in the case of generalised least squares), it would be possible to iterate between variogram modelling and trend removal until a convergence was reached [19, p.177]. Here, however, a single pass was done, that is, the variogram was first modelled, then the trend was modelled and removed, and the variogram was estimated again.

To qualitatively examine the effect of the different implemented detrending methods on experimental datasets, sample datasets with randomly removed missing data were used to perform different types of detrending. Histograms for CT and MO data samples are shown in Figure 3.11 and Figure 3.12, respectively.

While all detrending methods affected the distribution and fit of variograms to some degree, the ATPS detrending method was the most effective qualitatively on distributions and variogram parameters. The ATPS detrending method was aggregated to the 3rd hierarchical level in this case. Histograms and fit variograms for ATPS detrended datasets are shown in Figures 3.13 and 3.14 for CT and MO data, respectively. Compared to the GLS detrending methods, the distributions appear more normal, especially with regard to the MO data. Fit variograms for both sets of data also show a large reduction in both range and sill variogram parameters. The histograms and before/after variograms for 1st and 3rd order GLS detrending, as well as FRS detrending can be found in Appendix A (section A.1.1).

Histograms of GLS detrended CT data did not noticeably change the overall shape of the distribution, other than to shift the mean of the data down to zero. However, the small changes that were made caused a lowering of the variogram parameters of sill and range, especially in the case of the 3rd order GLS. On the other hand, GLS detrended MO data were apparently affected more than CT data, likely due to the increased spatial variance of

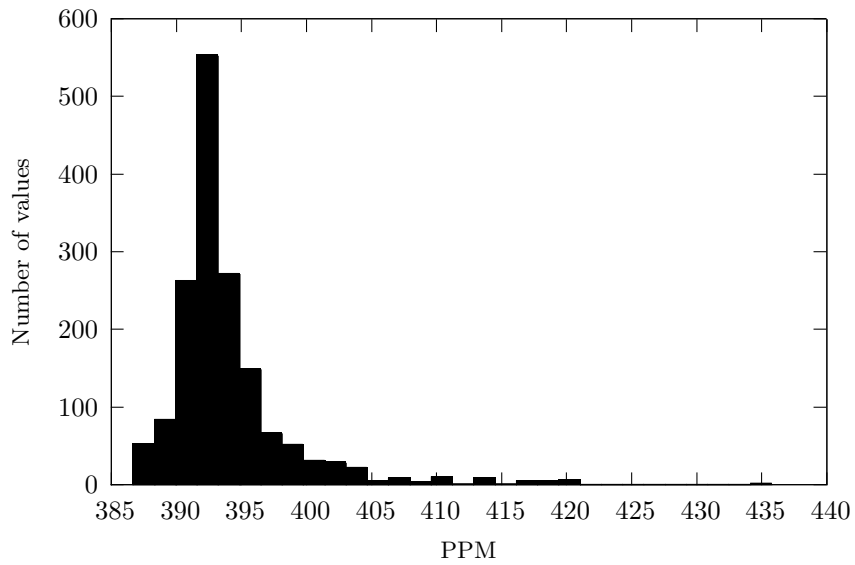


Figure 3.11: Histogram of raw data values for CT data, 60% of data values randomly removed.

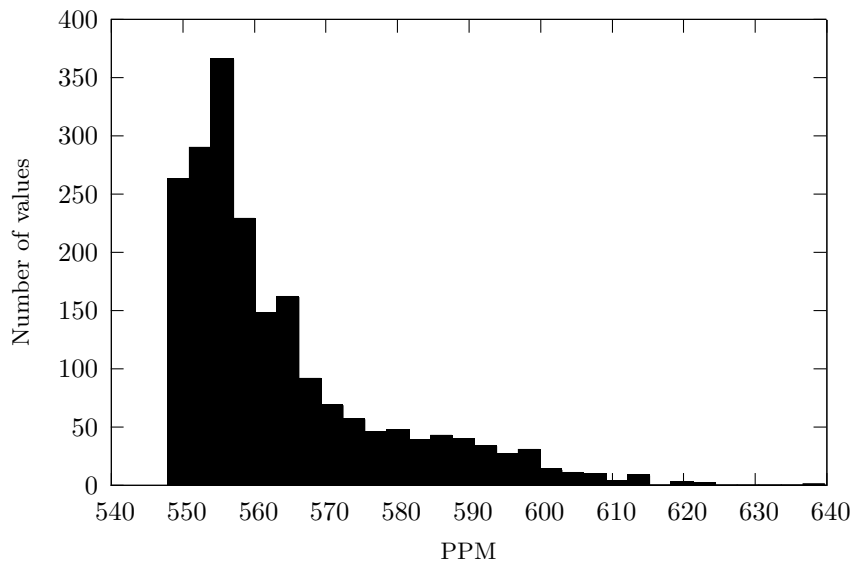
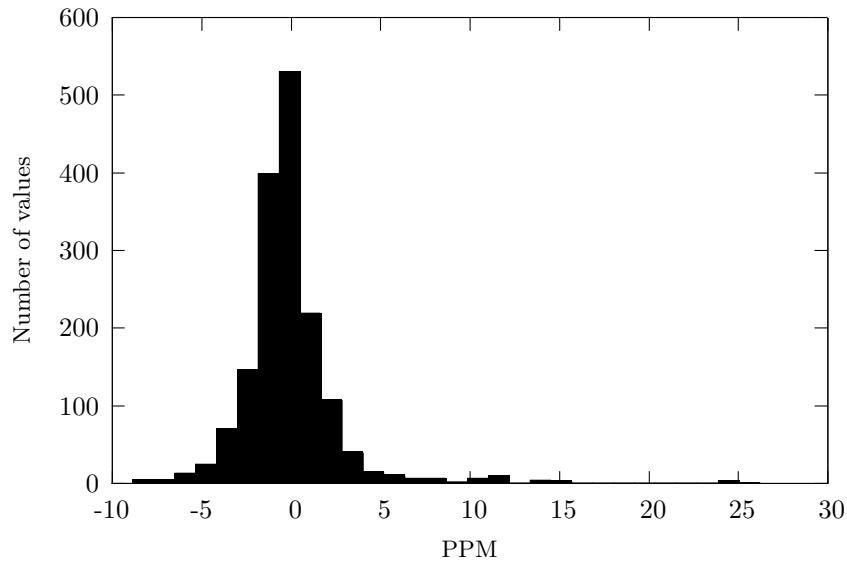
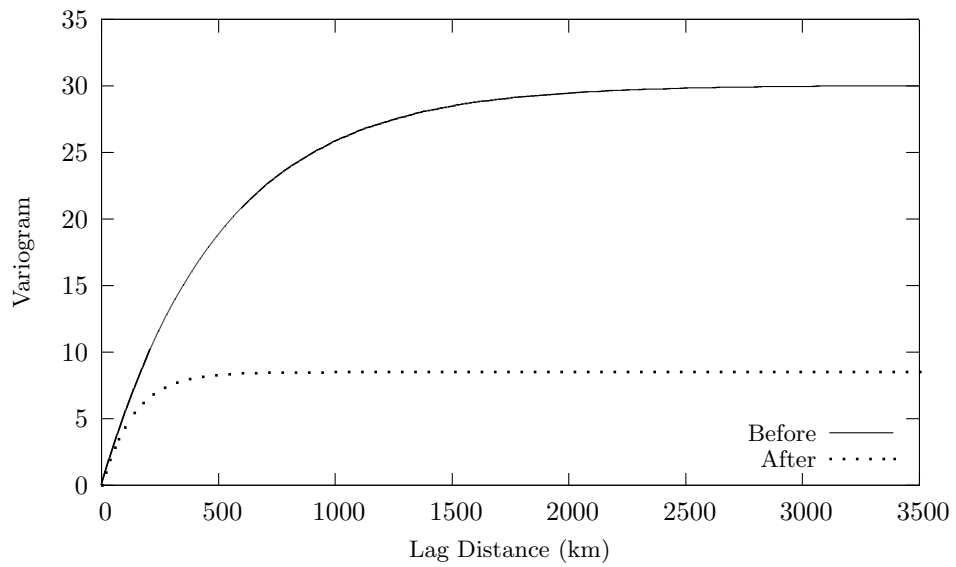


Figure 3.12: Histogram of raw data values for MO data, 50% of data values randomly removed.

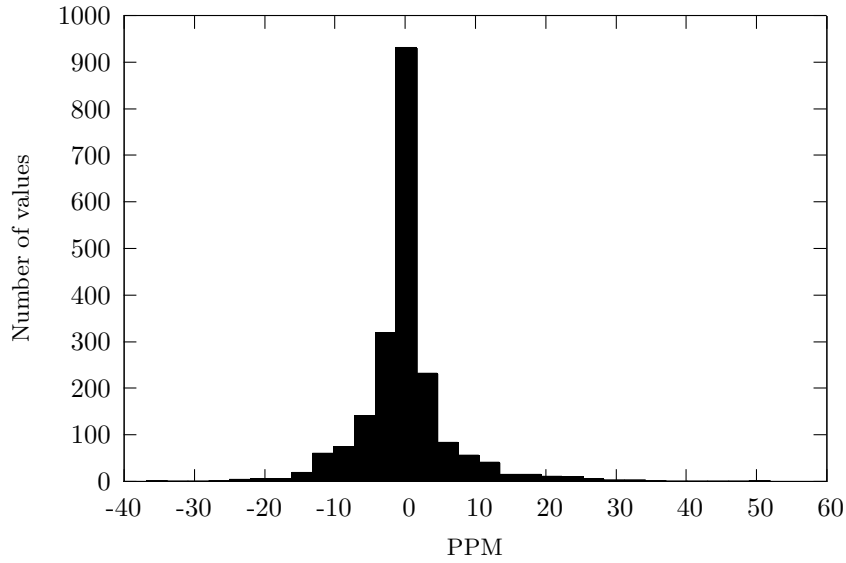


(a) Histogram of residual values after detrending.

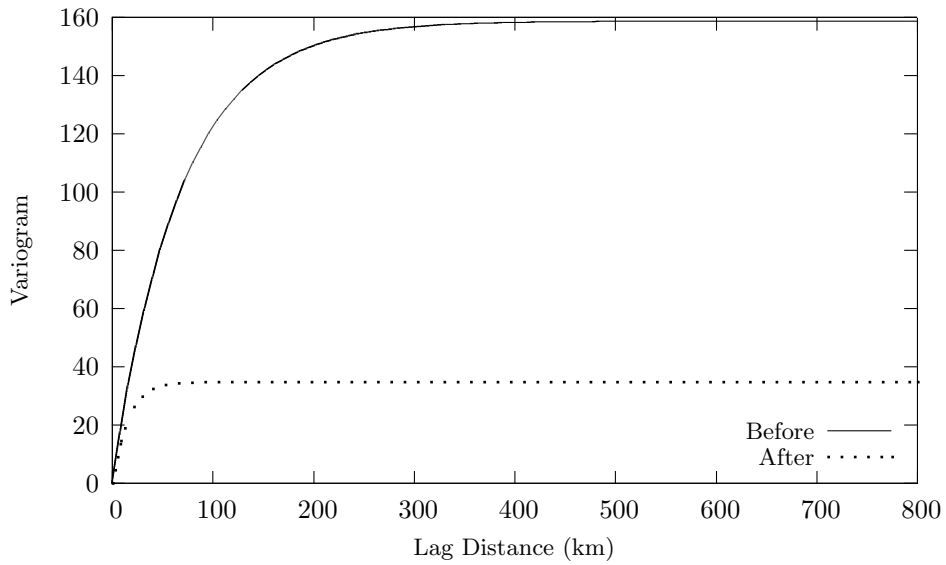


(b) Fit variograms before and after detrending.

Figure 3.13: Effect of 3rd level ATPS detrending on CT data



(a) Histogram of residual values after detrending.



(b) Fit variograms before and after detrending.

Figure 3.14: Effect of 3rd level ATPS detrending on MO data

the MO data. These distributions appear more normal than the original, as they now have a longer tail on the negative side where a sharp stop previously existed. The variogram parameters have also been affected more with this dataset and show a larger decrease in estimated sill value.

This difference between the changes in the GLS detrending and the ATPS detrending comes from both the aggregation up to the 3rd hierarchical level (meaning that some small scale variation is lost for detrending) and the number of points used to fit the trend surface. The aggregated cell centers were used to fit the ATPS trend surface. In this case there were 64 points, leading to a much rougher trend when compared with the 3rd order GLS method.

In order to reduce processing time, and to facilitate the fitting of a larger scale trend, the data were aggregated up to a coarser resolution before a thin plate spline surface was fit. While it may be possible to use the relaxation factor discussed in section 3.2.4.3 to solve this problem, the selection of a suitable value for  $\chi$  may require prior knowledge that is not available in practice. A few trial and error runs were done, resulting in a value of  $\chi = 0.1$  being used.

FRS detrending, as with ATPS detrending, gives histograms that appear more normally distributed than the originals, but the variogram sill and range parameters have not been reduced to the same degree as seen with ATPS detrending. This could be due to unsuitable selection of the basis functions and their locations.

### 3.5.1.2 Error Comparisons

In order to determine if any combination of estimation and detrending methods consistently performed better than others, the MSPE and MAPE values were ranked. Shorter forms of the tables are shown here, while the complete tables are located in Appendix A. Top rankings of randomly removed CT data by MSPE and MAPE are shown in Tables 3.1 and 3.2, respectively. Tables 3.5 and 3.6 show MSPE and MAPE rankings for CT MM data. Similarly, Tables 3.3 and 3.4 show rankings for randomly removed MO data, while Tables 3.7 and 3.8 show rankings for missing middle MO data.

For randomly removed CT data ranked by MSPE, the lowest amount of missing data is dominated by MURS estimation, followed by LSK. As the amount of missing data increases, kriging based methods, led by LSK, outperform all others. As the amount of missing data

increases further, nonstatistical methods begin to provide better estimates, occasionally outperforming some of the statistical methods. With respect to MAPE, the top methods are dominated by kriging based methods for most of the range of missing data. Other methods appear to be effective only at very high amounts of missing data. The detrending types here are primarily GLS detrending methods, with a higher incidence of SM than is seen when considering the MSPE rankings for this dataset.

With regard to randomly removed MO data, the best performers for all amounts of missing data for this dataset, when considering the MSPE ranking, were MURS and MRSM, both using a 3ATPS detrending surface. For most of the range of missing data, the kriging based methods are the next best performers. Here again, high amounts of missing data increase the performance of the nonstatistical methods; in this case, IDW outperforms some of the kriging based methods. Considering this same dataset with regard to MAPE, most of the missing data range is best served by kriging based methods. As with other nonstatistical methods, high amounts of missing data allows for better relative performance.

With MM CT data, the best performers are exclusively kriging based until around 70 percent of missing data where MURS takes over. MURS remains in the top list of performers, and is consistently paired with 3ATPS detrending except for very high amounts of missing data, which seems to favour the 3GLS detrending method for nearly all of the top performers.

Looking at MAPE, the top performers are consistently kriging based methods, again with the exception of very high amounts of missing data. However, in this case, the MURS estimation method paired with the 3ATPS detrending method appears among the top performers and remains there until a very high amount of missing data is reached.

Something interesting about the MM MO dataset is that one of the nonstatistical methods, namely IDW, appears in the top performers across the whole range of missing data. Kriging based methods make up the bulk of the top performers for most of the missing data range, with very few appearances by the hierarchical methods.

For this data set, the nonstatistical IDW method does not show up as consistently when the results are ranked using MAPE, instead, it is replaced with more kriging based estimations.

Unsurprisingly, there was less consistency in detrending methods than in estimation methods. However, the SM detrending method appears in the top performers with less

frequency than the other methods, and is rarely paired with a nonstatistical method; it is usually paired with a kriging based method. This demonstrates that, at least with these datasets, all the estimation methods benefit strongly from the removal of large scale trends, including the nonstatistical estimation methods, which do not have to make assumptions about the distribution or stationarity of the data.

Interestingly, nonstatistical methods performed relatively better in the presence of very high amounts of missing data. As they are the most computationally feasible for massive datasets, these methods would likely not be considered for datasets in which there are very few points. However, since in these tests all facets of estimation were performed with no prior knowledge, the lack of data means that there is difficulty in estimating and fitting a proper variogram model. With the inclusion of historical information and/or expert knowledge, it is possible that the statistical methods could be improved to levels better than those seen with the nonstatistical methods.

Table 3.1: CT RR, top methods as ranked by MSPE.

Percentage Data Removed											
19.26		30.88		41.33		50.98		60.21			
MURS	3GLS	LSK	3FRS	LSK	3FRS	LSK	3GLS	LSK	3ATPS	LSK	3ATPS
MURS	1GLS	SK	3FRS	LSK	3GLS	LSK	3ATPS	LSK	3GLS	LSK	3GLS
MURS	SM	MURS	3FRS	LSK	1GLS	LSK	1GLS	SK	3ATPS	SK	3ATPS
MURS	3FRS	OK	3FRS	LSK	SM	LSK	SM	LSK	1GLS	LSK	1GLS
MURS	3ATPS	LSK	3GLS	LSK	3ATPS	SK	3ATPS	OK	3ATPS	OK	3ATPS
LSK	3FRS	LSK	1GLS	SK	3FRS	LSK	3FRS	LSK	SM	LSK	SM
LSK	3ATPS	LSK	SM	OK	3FRS	OK	3ATPS	OK	3ATPS	LSK	3FRS
LSK	3GLS	MURS	3GLS	SK	3GLS	SK	3GLS	SK	3GLS	SK	3GLS
LSK	1GLS	LSK	3ATPS	OK	3GLS	OK	3GLS	OK	3GLS	OK	3GLS
LSK	SM	SK	3ATPS	OK	1GLS	OK	1GLS	OK	1GLS	SK	1GLS

Percentage Data Removed											
70.12		77.44		85.67		93.24		96.26		98.46	
LSK	3ATPS	MURS	3ATPS	IDW	3ATPS	SK	1GLS	SK	1GLS	LSK	3FRS
MURS	3ATPS	IDW	3ATPS	LSK	3ATPS	SK	SM	OK	SM	NN	3FRS
OK	3ATPS	LSK	3ATPS	SK	3ATPS	OK	3GLS	SK	SM	IDW	3FRS
SK	3ATPS	SK	3ATPS	SK	1GLS	OK	SM	OK	1GLS	SK	3FRS
IDW	3ATPS	OK	3ATPS	OK	1GLS	SK	3GLS	OK	3GLS	MURS	3FRS
MRSM	3ATPS	MRSM	3ATPS	OK	SM	OK	1GLS	SK	3GLS	OK	3FRS
LSK	3FRS	OK	3GLS	LSK	1GLS	LSK	1GLS	LSK	SM	TS	3FRS
LSK	3GLS	LSK	SM	SK	SM	OK	3FRS	MURS	3GLS	MRSM	3FRS
LSK	1GLS	SK	3GLS	MURS	3ATPS	LSK	SM	LSK	3GLS	NN	3GLS
SK	3FRS	SK	3FRS	SK	3GLS	SK	3FRS	OK	3FRS	IDW	3ATPS

Generally, for these tests, FA estimates are the worst performers, usually followed by TS predictions. The other non-statistical methods are more variable in their performance, meaning that between the two datasets they do not consistently perform better or worse than the statistical methods. This is likely due to the larger spatial variance present in the

Table 3.2: CT RR, top methods as ranked by MAPE

Percentage Data Removed											
19.26		30.88		41.33		50.98		60.21			
LSK	3GLS	LSK	3GLS	LSK	3GLS	SK	3GLS	LSK	1GLS		
LSK	1GLS	LSK	1GLS	LSK	1GLS	OK	3GLS	LSK	3GLS		
LSK	SM	LSK	SM	LSK	SM	OK	1GLS	SK	1GLS		
LSK	3FRS	SK	3GLS	OK	3GLS	SK	1GLS	OK	1GLS		
OK	1GLS	OK	3GLS	SK	3GLS	LSK	3GLS	SK	3GLS		
SK	1GLS	SK	1GLS	SK	1GLS	LSK	1GLS	OK	3GLS		
SK	3GLS	OK	1GLS	OK	1GLS	OK	SM	LSK	SM		
SK	SM	OK	SM	LSK	3FRS	SK	SM	SK	SM		
OK	3GLS	SK	SM	SK	SM	LSK	SM	OK	SM		
OK	SM	OK	3FRS	OK	SM	SK	3ATPS	OK	3ATPS		

Percentage Data Removed											
70.12		77.44		85.67		93.24		96.26		98.46	
LSK	1GLS	OK	3GLS	SK	1GLS	SK	1GLS	OK	SM	IDW	3GLS
LSK	3GLS	SK	1GLS	OK	1GLS	SK	SM	SK	1GLS	SK	3GLS
OK	1GLS	SK	3GLS	LSK	1GLS	OK	1GLS	SK	SM	IDW	3ATPS
LSK	SM	LSK	SM	SK	SM	OK	3GLS	OK	1GLS	OK	3GLS
SK	1GLS	LSK	1GLS	OK	SM	LSK	1GLS	LSK	SM	NN	3ATPS
OK	3GLS	LSK	3GLS	OK	3GLS	OK	SM	IDW	SM	OK	3ATPS
SK	3GLS	OK	1GLS	SK	3GLS	SK	3GLS	OK	3GLS	NN	3GLS
SK	SM	OK	SM	LSK	3GLS	LSK	3GLS	MURS	SM	SK	3ATPS
OK	SM	LSK	3ATPS	LSK	SM	LSK	SM	IDW	1GLS	MURS	3GLS
SK	3ATPS	SK	SM	SK	3ATPS	OK	3FRS	SK	3GLS	MURS	3ATPS

Table 3.3: MO RR, top methods as ranked by MSPE.

Percentage Data Removed											
19.53		26.20		33.79		41.77		50.24		60.91	
MURS	3ATPS	MURS	3ATPS	MURS	3ATPS	MURS	3ATPS	MURS	3ATPS	MURS	3ATPS
MRS	3ATPS	MRS	3ATPS	MRS	3ATPS	MRS	3ATPS	MRS	3ATPS	MRS	3ATPS
OK	1GLS	SK	1GLS	SK	SM	SK	SM	OK	SM	OK	1GLS
OK	SM	OK	SM	SK	1GLS	OK	SM	OK	1GLS	SK	1GLS
SK	1GLS	OK	1GLS	SK	3FRS	LSK	1GLS	OK	3FRS	OK	SM
LSK	SM	OK	3FRS	OK	SM	OK	3FRS	SK	3FRS	SK	3FRS
SK	3GLS	LSK	3GLS	OK	1GLS	LSK	3GLS	SK	SM	SK	SM
SK	SM	SK	3FRS	LSK	1GLS	LSK	3FRS	SK	3GLS	LSK	3FRS
OK	3GLS	LSK	3FRS	SK	3GLS	LSK	SM	LSK	SM	SK	3GLS
LSK	3FRS	SK	SM	LSK	SM	OK	1GLS	SK	1GLS	OK	3FRS

Percentage Data Removed											
68.48		79.59		90.26		94.90		97.44			
MURS	3ATPS	MURS	3ATPS	MURS	3ATPS	MURS	3ATPS	MURS	3ATPS		
MRS	3ATPS	MRS	3ATPS	MRS	3ATPS	MRS	3ATPS	MRS	3ATPS		
SK	3FRS	OK	1GLS	LSK	3GLS	LSK	1GLS	IDW	3GLS		
LSK	1GLS	LSK	3FRS	OK	3ATPS	SK	3ATPS	IDW	3ATPS		
LSK	SM	OK	SM	LSK	1GLS	SK	3FRS	IDW	3FRS		
OK	1GLS	SK	1GLS	LSK	3ATPS	IDW	3GLS	SK	3ATPS		
SK	3GLS	LSK	1GLS	OK	1GLS	IDW	3FRS	IDW	1GLS		
SK	1GLS	SK	3GLS	IDW	3ATPS	OK	1GLS	OK	3ATPS		
LSK	3FRS	OK	3FRS	SK	3ATPS	IDW	3ATPS	LSK	3ATPS		
SK	SM	OK	3ATPS	LSK	3FRS	LSK	3ATPS	IDW	SM		

Table 3.4: MO RR, top methods as ranked by MAPE.

Percentage Data Removed											
19.53		26.20		33.79		41.77		50.24		60.91	
OK	1GLS	SK	1GLS	SK	1GLS	SK	SM	OK	SM	OK	1GLS
OK	SM	LSK	3GLS	SK	SM	OK	SM	OK	1GLS	SK	1GLS
SK	1GLS	OK	SM	SK	3FRS	LSK	1GLS	OK	3FRS	OK	SM
SK	3GLS	OK	1GLS	OK	SM	LSK	3GLS	SK	3FRS	SK	3FRS
LSK	SM	OK	3FRS	OK	1GLS	OK	3FRS	SK	SM	SK	SM
OK	3GLS	LSK	3FRS	LSK	1GLS	LSK	3FRS	SK	3GLS	LSK	3FRS
LSK	3FRS	SK	3FRS	SK	3GLS	LSK	SM	LSK	SM	OK	3FRS
SK	SM	LSK	SM	LSK	SM	OK	1GLS	SK	1GLS	SK	3GLS
SK	3FRS	SK	SM	OK	3FRS	SK	1GLS	OK	3GLS	SK	3ATPS
LSK	3GLS	LSK	1GLS	OK	3GLS	SK	3GLS	LSK	1GLS	MURS	3ATPS

Percentage Data Removed									
68.48		79.59		90.26		94.90		97.44	
SK	3FRS	OK	1GLS	LSK	3GLS	SK	3ATPS	IDW	3ATPS
LSK	1GLS	LSK	3FRS	LSK	1GLS	LSK	1GLS	SK	3ATPS
LSK	SM	SK	1GLS	OK	3ATPS	IDW	3ATPS	MURS	3ATPS
OK	1GLS	OK	SM	OK	1GLS	LSK	3ATPS	OK	3ATPS
SK	3GLS	LSK	1GLS	SK	3ATPS	MURS	3ATPS	MRSRM	3ATPS
SK	1GLS	OK	3ATPS	LSK	3ATPS	MRSRM	3ATPS	LSK	3ATPS
LSK	3FRS	SK	3GLS	IDW	3ATPS	OK	3ATPS	IDW	3GLS
OK	3ATPS	OK	3FRS	SK	1GLS	NN	SM	TS	3ATPS
SK	3ATPS	SK	3ATPS	LSK	SM	OK	1GLS	IDW	3FRS
MURS	3ATPS	MURS	3ATPS	NN	3ATPS	IDW	3GLS	IDW	1GLS

Table 3.5: CT MM, top methods as ranked by MSPE.

Percentage Data Removed									
54.30		62.21		69.21		74.27		79.27	
SK	SM	SK	SM	SK	1GLS	SK	1GLS	OK	SM
OK	SM	OK	SM	SK	SM	OK	SM	SK	1GLS
SK	3ATPS	OK	1GLS	OK	1GLS	SK	SM	OK	1GLS
SK	3GLS	LSK	SM	OK	SM	OK	1GLS	SK	SM
OK	3ATPS	OK	3ATPS	LSK	SM	LSK	SM	MURS	3ATPS
OK	3GLS	OK	3GLS	MURS	3ATPS	LSK	1GLS	LSK	SM
SK	1GLS	SK	3ATPS	LSK	1GLS	MURS	3ATPS	LSK	1GLS
LSK	SM	SK	3GLS	SK	3ATPS	OK	3ATPS	MURS	1GLS
OK	1GLS	SK	1GLS	SK	3GLS	OK	3GLS	MURS	SM
LSK	3GLS	LSK	3GLS	OK	3ATPS	SK	3ATPS	IDW	1GLS

Percentage Data Removed											
85.11		88.57		93.26		96.75		98.27		99.24	
SK	1GLS	OK	1GLS	SK	SM	OK	1GLS	OK	1GLS	LSK	3ATPS
OK	1GLS	OK	SM	OK	1GLS	OK	SM	SK	1GLS	MRSRM	3GLS
OK	SM	SK	SM	SK	1GLS	OK	3ATPS	OK	3ATPS	OK	3GLS
SK	SM	SK	1GLS	LSK	3ATPS	SK	1GLS	LSK	3ATPS	LSK	3GLS
MURS	3ATPS	MURS	3ATPS	OK	SM	MURS	3ATPS	OK	SM	TS	3GLS
LSK	1GLS	OK	3ATPS	OK	3ATPS	SK	SM	OK	3GLS	SK	3ATPS
OK	3ATPS	LSK	SM	LSK	1GLS	MURS	SM	LSK	3GLS	SK	3GLS
OK	3GLS	LSK	1GLS	MURS	3ATPS	LSK	3ATPS	IDW	3GLS	IDW	3GLS
SK	3ATPS	MURS	1GLS	SK	3ATPS	IDW	SM	MURS	3ATPS	MURS	3GLS
SK	3GLS	MURS	SM	SK	3GLS	IDW	1GLS	SK	3ATPS	NN	3GLS

Table 3.6: CT MM, top methods as ranked by MAPE.

Percentage Data Removed											
54.30		62.21		69.21		74.27		79.27			
SK	SM	OK	1GLS	SK	1GLS	OK	1GLS	OK	SM	IDW	3ATPS
OK	SM	SK	SM	OK	1GLS	SK	1GLS	SK	1GLS	NN	3ATPS
SK	1GLS	OK	SM	SK	SM	SK	SM	LSK	1GLS	TS	3ATPS
OK	1GLS	SK	1GLS	OK	SM	OK	SM	OK	1GLS	LSK	3ATPS
LSK	SM	LSK	SM	LSK	SM	LSK	SM	LSK	SM	IDW	3GLS
MURS	3ATPS	LSK	1GLS	LSK	1GLS	LSK	1GLS	LSK	1GLS	SK	3ATPS
SK	3ATPS	MURS	3ATPS	MURS	3ATPS	MURS	3ATPS	MURS	3ATPS	MURS	1GLS
OK	3ATPS	SK	3ATPS	SK	3ATPS	SK	3ATPS	SK	3ATPS	MURS	1GLS
LSK	1GLS	OK	3ATPS	MURS	1GLS	OK	3ATPS	OK	3ATPS	LSK	3ATPS
IDW	SM	MURS	1GLS	OK	3ATPS	MURS	1GLS	MURS	1GLS	MURS	SM

Percentage Data Removed											
85.11		88.57		93.26		96.75		98.27		99.24	
SK	1GLS	SK	1GLS	OK	SM	OK	1GLS	OK	SM	IDW	3ATPS
OK	SM	OK	1GLS	OK	1GLS	OK	SM	OK	1GLS	NN	3ATPS
OK	1GLS	SK	SM	SK	1GLS	SK	1GLS	SK	1GLS	TS	3ATPS
SK	SM	OK	SM	SK	SM	OK	3ATPS	SK	SM	LSK	3ATPS
MURS	3ATPS	MURS	3ATPS	LSK	1GLS	SK	SM	MURS	3ATPS	IDW	3GLS
LSK	1GLS	OK	3ATPS	OK	3ATPS	LSK	1GLS	OK	3ATPS	TS	3GLS
LSK	SM	LSK	1GLS	MURS	3ATPS	IDW	SM	IDW	1GLS	SK	3ATPS
OK	3ATPS	LSK	SM	LSK	SM	MURS	3ATPS	IDW	SM	NN	3GLS
MURS	1GLS	MURS	1GLS	LSK	3ATPS	MURS	SM	MURS	SM	IDW	SM
MURS	SM	MURS	SM	MURS	SM	IDW	1GLS	MURS	1GLS	NN	SM

Table 3.7: MO MM, top methods as ranked by MSPE.

Percentage Data Removed											
48.97		53.13		58.06		63.28		68.80		75.6	
SK	3FRS	SK	3FRS	SK	3ATPS	SK	SM	OK	1GLS	OK	1GLS
LSK	3FRS	OK	1GLS	OK	3FRS	OK	3FRS	SK	3FRS	SK	3FRS
OK	3FRS	OK	3ATPS	SK	3GLS	OK	1GLS	OK	3FRS	OK	3FRS
SK	1GLS	SK	3ATPS	OK	SM	SK	3GLS	LSK	1GLS	SK	3GLS
OK	1GLS	OK	3FRS	OK	3ATPS	LSK	3FRS	OK	3GLS	SK	1GLS
IDW	1GLS	SK	1GLS	IDW	3ATPS	SK	1GLS	SK	1GLS	OK	3GLS
IDW	3FRS	LSK	3ATPS	LSK	3FRS	OK	3GLS	SK	3GLS	OK	3ATPS
SK	3GLS	LSK	3FRS	SK	1GLS	IDW	3ATPS	SK	3ATPS	LSK	3GLS
SK	3ATPS	LSK	3GLS	OK	3GLS	SK	3FRS	LSK	3FRS	SK	3ATPS
MURS	3ATPS	IDW	1GLS	MURS	3ATPS	IDW	3FRS	IDW	3FRS	IDW	3ATPS

Percentage Data Removed											
80.54		87.21		93.95		96.97		98.51			
OK	1GLS	SK	3ATPS	SK	3GLS	IDW	3GLS	IDW	3GLS	IDW	3GLS
SK	3FRS	MURS	3ATPS	IDW	3GLS	IDW	3FRS	IDW	3FRS	IDW	3FRS
LSK	3FRS	OK	3GLS	MURS	3ATPS	OK	3GLS	OK	3GLS	IDW	1GLS
OK	3FRS	SK	3GLS	OK	3ATPS	IDW	1GLS	OK	3GLS	IDW	1GLS
OK	3ATPS	MRS	3ATPS	OK	3GLS	SK	3FRS	LSK	3GLS	SK	3GLS
SK	1GLS	LSK	3GLS	SK	3ATPS	SK	3GLS	IDW	3ATPS	IDW	3ATPS
IDW	3ATPS	SK	3FRS	LSK	3GLS	OK	3FRS	SK	3GLS	SK	3GLS
OK	SM	OK	3ATPS	LSK	3FRS	NN	3GLS	TS	3GLS	TS	3GLS
SK	3GLS	IDW	3GLS	OK	3FRS	SK	1GLS	NN	1GLS	NN	1GLS
LSK	3GLS	IDW	3FRS	OK	1GLS	NN	1GLS	NN	SM	NN	SM

Table 3.8: MO MM, top methods as ranked by MAPE.

Percentage Data Removed											
48.97		53.13		58.06		63.28		68.80		75.6	
SK	1GLS	OK	1GLS	SK	1GLS	SK	SM	OK	1GLS	OK	1GLS
OK	1GLS	SK	1GLS	OK	1GLS	OK	1GLS	LSK	1GLS	SK	1GLS
SK	3FRS	LSK	1GLS	LSK	1GLS	SK	1GLS	SK	1GLS	SK	3FRS
LSK	3FRS	SK	3FRS	SK	3FRS	OK	3FRS	OK	3FRS	OK	3FRS
OK	3FRS	OK	3FRS	OK	SM	LSK	1GLS	SK	3FRS	LSK	1GLS
LSK	1GLS	LSK	3FRS	OK	3FRS	LSK	3FRS	SK	SM	SK	3ATPS
IDW	1GLS	IDW	1GLS	LSK	3FRS	OK	SM	SK	3ATPS	OK	3ATPS
IDW	3FRS	OK	3ATPS	SK	3ATPS	SK	3GLS	LSK	3FRS	SK	3GLS
MURS	1GLS	SK	3ATPS	OK	3ATPS	OK	3ATPS	OK	3GLS	MURS	3ATPS
SK	3ATPS	LSK	3ATPS	MURS	3ATPS	SK	3FRS	MURS	3ATPS	IDW	3ATPS

Percentage Data Removed											
80.54		87.21		93.95		96.97		98.51			
OK	1GLS	SK	3FRS	OK	1GLS	NN	1GLS	IDW	3FRS		
SK	1GLS	SK	3ATPS	LSK	3FRS	IDW	1GLS	IDW	3GLS		
LSK	3FRS	SK	1GLS	SK	1GLS	NN	SM	IDW	3ATPS		
SK	3FRS	MURS	3ATPS	OK	3FRS	SK	3FRS	IDW	1GLS		
OK	SM	OK	3ATPS	OK	3ATPS	IDW	3FRS	NN	1GLS		
OK	3FRS	MRS	3ATPS	SK	3ATPS	NN	3FRS	OK	3ATPS		
OK	3ATPS	OK	1GLS	SK	3GLS	NN	3GLS	NN	SM		
SK	SM	LSK	3ATPS	LSK	3ATPS	IDW	3GLS	TS	3ATPS		
IDW	3ATPS	SK	3GLS	MURS	3ATPS	SK	1GLS	LSK	3ATPS		
MURS	3ATPS	LSK	3FRS	IDW	3ATPS	OK	3FRS	SK	3ATPS		

MO dataset.

For CT data, different detrending methods do not seem to greatly effect the MSPE values of the different estimation methods, with the exceptions of the 3rd level ATPS shown in Figures A.7d and A.8d, which had a problem fitting the trend surface with around 90% of missing data missing, and TS estimation method for all types of detrending. Looking at MAPE, however, the IDW estimation method showed improvement when FRS detrending was used compared to use of other detrending methods (Figure A.8e). With some exceptions (LSK at 50% missing data in Figure A.10e, for example) the statistical methods do not seem to be greatly affected by the choice of detrending surface used.

The ATPS trend fitting implementation was prone to errors that sometimes caused extreme points to be fitted, especially at the edges of the domain. When this occurred, the estimation method using that trend surface would see a huge increase in both MSPE and MAPE, allowing for fairly easy detection of the problem. The problem was likely caused by the choice of method for performing the inversion of the  $\mathbf{A}$  matrix discussed in section 3.2.4.3. The errors were easily detected and could usually be corrected by running the dataset again.

With regard to the MO data, there is a greater improvement between the different detrending methods. This can be seen by comparing Figure A.9b, where the hierarchical

methods increase to MSPE values around  $100 \text{ ppm}^2$  as the percentage of missing data crosses 50%, to Figure A.16d, where the hierarchical methods have MSPE values comparable to other methods for the entire range of missing data values. Also, Figure A.9d shows that 3rd level ATPS detrending gives the best TS estimate of all the detrending methods attempted. Choice of detrending surface has a greater effect on the MO dataset compared to the CT dataset; again, this is likely due to the increased spatial variation present in the MO dataset.

MM MSPE values for the different estimation and detrending methods are shown in Figures A.14 and A.16 for the CT and MO datasets, respectively. Compared to the randomly removed datasets, these missing middle datasets have much higher errors. This is understandable, not only because of the higher percentage of missing data due to the immediate removal of the center third, but also because it was a large continuous region. Without any information in the region, predictions are made based on the data on either side; if these data are not representative, predictions suffer. An added difficulty lies in fitting a trend surface with no information about the center of the domain.

For the CT datasets, the MRSM method is now outperformed by the IDW estimation for most of the detrending methods. The MURS predictions, however show more relative improvement than the MRSM in this missing data configuration, compared to the RR runs. Data points have been removed from Figures A.14d and A.8d because of very high errors reported for the TS estimation. This was not due to the computational problems discussed previously, it is due to a poor trend fit with the particular amount of missing data. Data points for all estimations have also been removed from Figures A.14e, A.15e, and A.18e because of very high errors; this time the errors are associated with problems fitting the FRS trend to data for which information is extremely limited.

With regard to the MO data, there is again a greater dependence on the detrending method selected, especially for the hierarchical methods. For most detrending surfaces used, the MRSM and MURS have MSPE values higher than the other statistical methods. However, use of the ATPS detrending surface allows these methods to attain smaller errors.

With regard to MSPE, IDW seems to be a good performer for this configuration of missing data, achieving errors close to that of the kriging methods for some detrending methods (Figure A.16b).

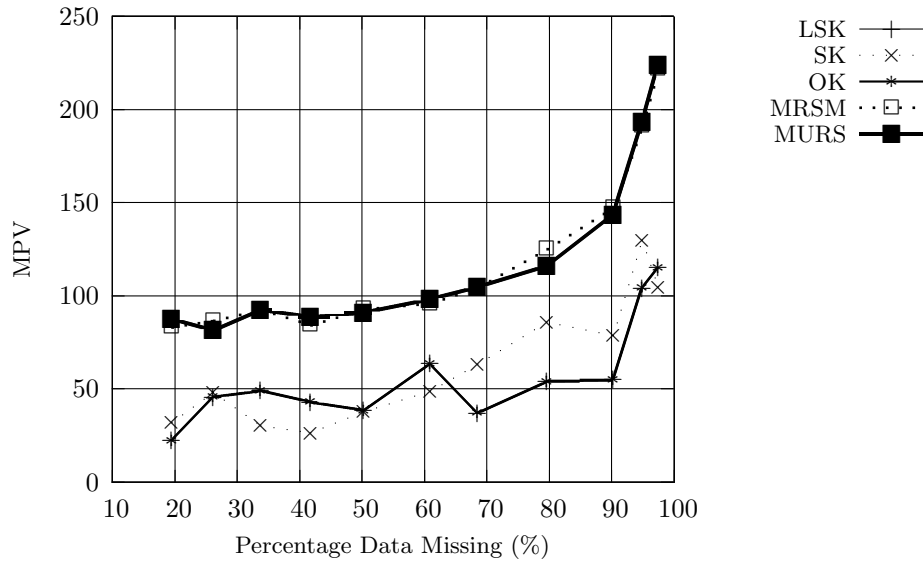


Figure 3.15: MO data, simple mean removal, MPV.

### 3.5.1.3 Variance Comparison

As expected, the MPV values for kriging based methods are generally lower than for the hierarchical methods. An example of this trend is shown in Figure 3.15. However, this is not the case for 3rd level ATPS detrended MO data (Figure 3.16). Interestingly, the MPV values for OK and LSK estimations are roughly equal for all detrending methods and amounts of missing data.

The sudden drop in MPV values for large percentages of missing data, as shown in Figure 3.17, is likely due to problems in variogram estimation, and stem from a dearth of data points, combined with the lower spatial variation present in the CT dataset. The MO dataset has MPV values that generally increase with an increasing amount of missing data. Although this case suffers from the same problem of too few points for proper variogram estimation, the larger spatial variation in the dataset increases the likelihood of a high sill and short range being selected for variogram parameters. This then translates into larger prediction variances for predictions made far away from informed points.

Similar to RR, in the MM case, kriging based methods generally have lower MPV values. Surprisingly, the MPV values move lower with decreasing amounts of data. This is likely because with so few data points, there is nothing to hint at the true variability of the data,

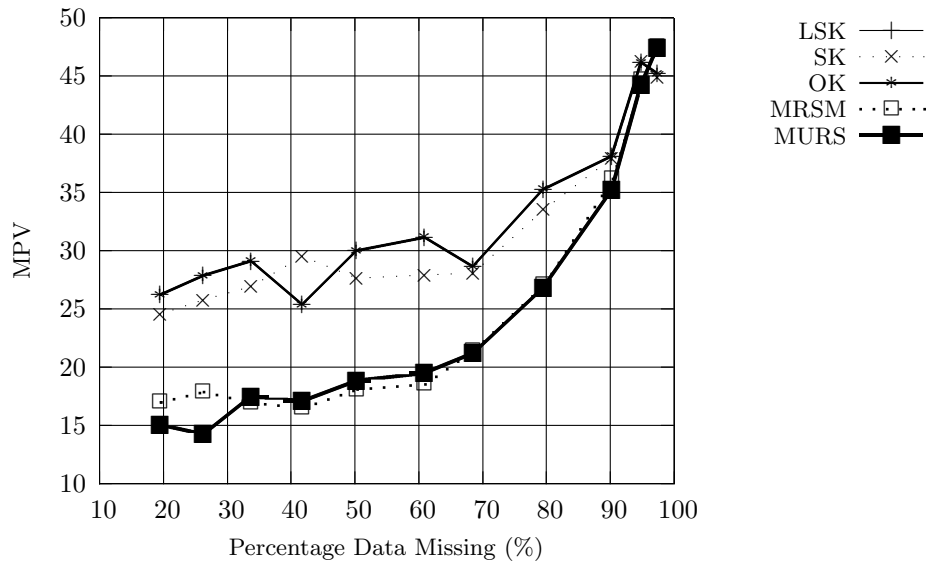


Figure 3.16: MO data, 3rd level ATPS detrending, MPV.

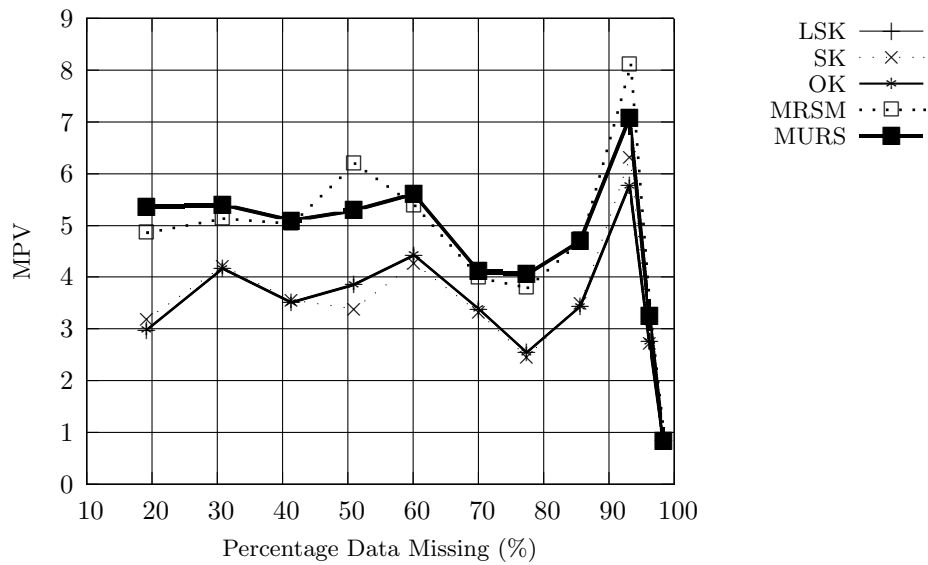


Figure 3.17: CT data, 3rd level ATPS detrending, MPV.

especially with a large region in the middle being removed.

Plots of the MPV values calculated for different detrending and estimations methods not shown here are located in Appendix A.1.2 (Figures A.11 (CT RR), A.12 (MO RR), A.18(CT MM), and A.19(MO MM)).

#### 3.5.1.4 Speed Comparison

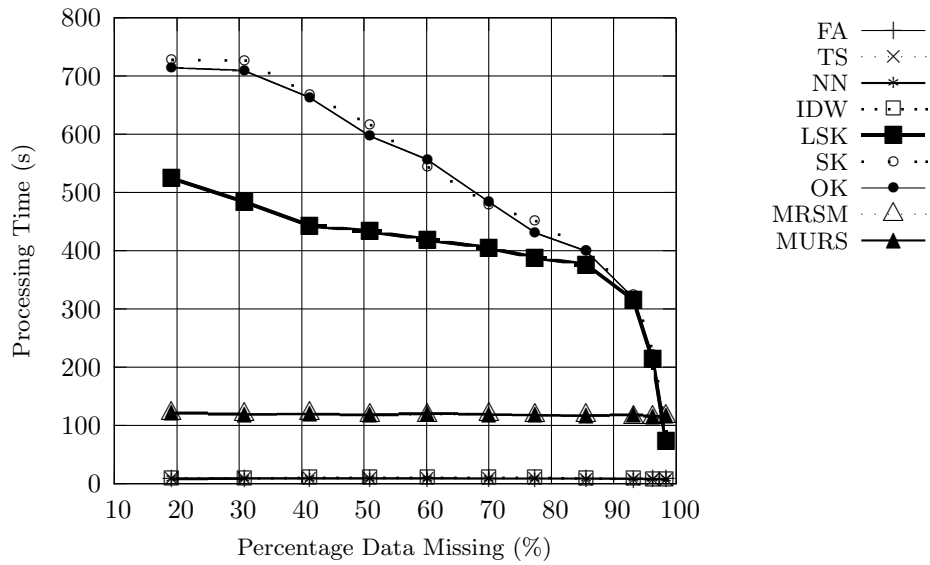
Processing times for the different estimation methods, detrending schemes and datasets are shown in Figure 3.18. Generally, and regardless of the detrending method employed, the non-statistical estimation methods are, as expected, much faster than any of the statistical methods. The next fastest methods are the hierarchical methods: the bulk of their processing comes from the two parameter fitting steps that must be performed. These methods also show little dependence on the amount of missing data. In contrast, SK and OK clearly gave the longest processing times for low amounts of missing data, and they exhibit the greatest dependence on the amount of data being processed.

Since all of the different data types were mapped to the same resolution ( $64 \times 64$  grid cells), the data variability in the different data types became an important factor in processing time. Long range spatial correlation resulted in denser matrix inversions for the kriging methods, as well as a larger kriging neighbourhood for local simple kriging. This spatial correlation also caused detrending methods that relied on the covariance matrix  $C$  to take longer.

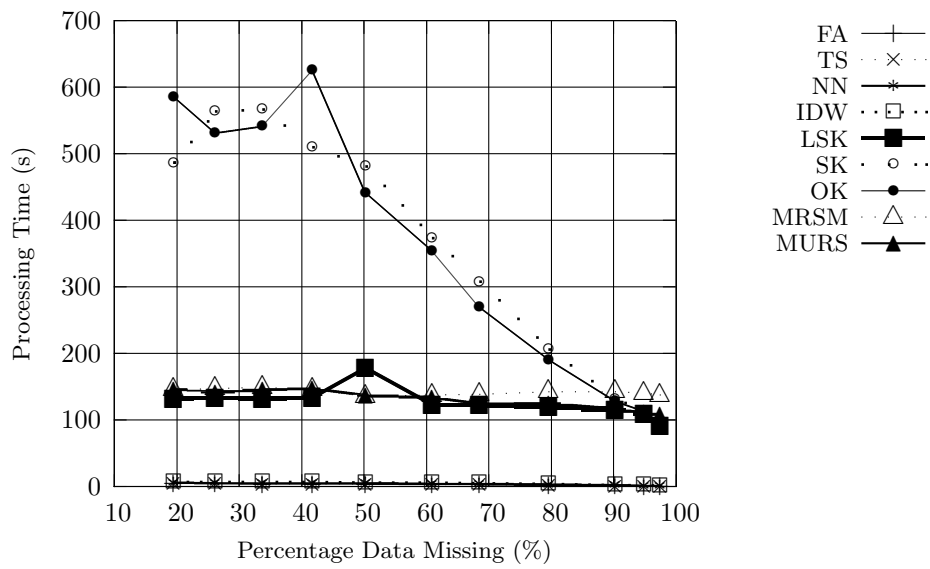
The effects of differing spatial correlation among the different data sets is illustrated in Figures 3.18a and 3.18b. These figures show the times for SM detrended CT and MO data, respectively. With the longer spatial correlations present in the CT dataset, the LSK neighbourhood is larger, leading to the increased processing time shown. The reverse occurs for the MO data, where a short correlation range results in computation times closer to those of the hierarchical methods. The long average times for FRS detrending, seen in Figures 3.18c and 3.18d are likely caused by a problem with the implementation of the algorithm.

Performing any detrending beyond SM increases the processing time for all estimation methods. More importantly, the more advanced methods add a processing step dependant on the number of data points present, which is an undesirable trait where spatially dense

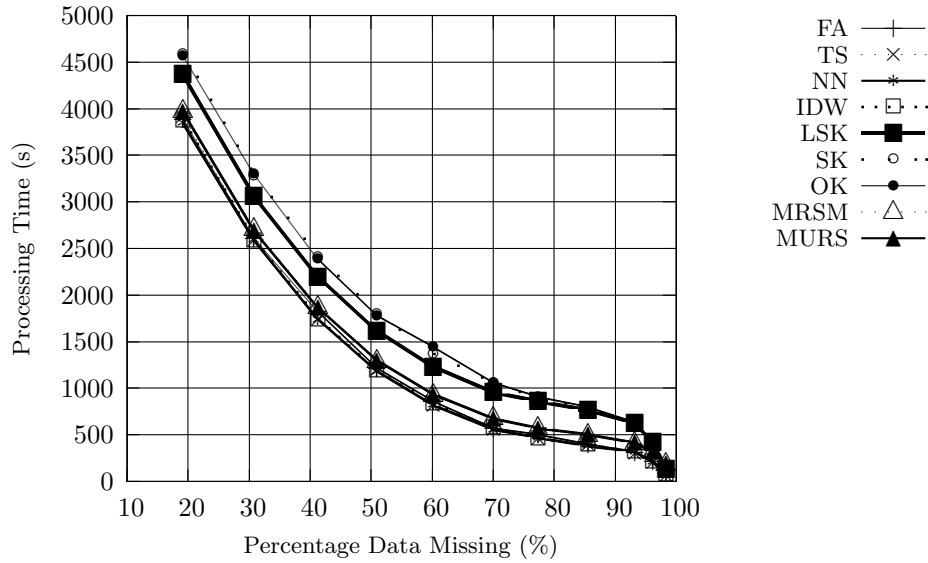
datasets are concerned. The methods each had a parameter that affected the processing time, e.g., the aggregation level for ATPS and the surface order for GLS, which allows for tradeoffs between time and surface fit. Unfortunately, implementation of the FRS detrending method, a method able to handle large amounts of data, had a numerical problem that resulted in it taking the longest time and having a high dependency on the amount of data used. This should be corrected to achieve the speeds reported in [17].



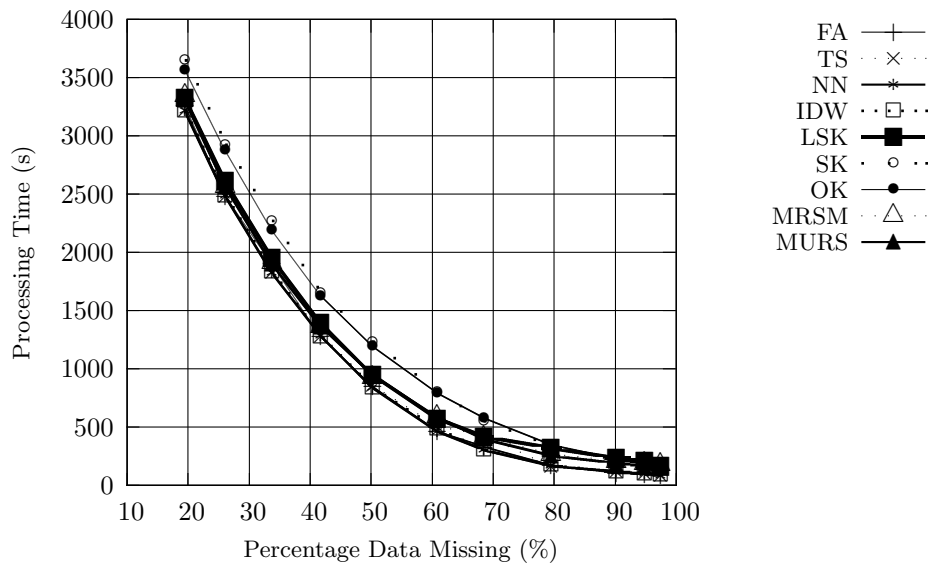
(a) CT data, simple mean removal, time.



(b) MO data, simple mean removal, time.



(c) CT data, 3rd level FRS detrending, time.



(d) MO data, 3rd level FRS detrending, time.

Figure 3.18: Processing time comparisons (RR data).

Table 3.9: MSPE values for non-hierarchical methods using randomly removed data.

Method	MSPE Values
	MO
FA	85.538
TS	85.538
NN	21.322
IDW	26.794
SK	28.819
LSK	43.731
OK	28.819

Table 3.10: MSPE values for static hierarchical methods using randomly removed data.

Subdomains	Method	MRSM	MURS
	MO Data	1	19.711
4		22.621	17.882
16		24.422	19.564

## 3.5.2 Dynamic Results

### 3.5.2.1 Random Data Removal

A dataset was created consisting of MO data where roughly 50% of the data points in each time step was removed. The MSPE values for the nonhierarchical estimation methods are shown in Table 3.9. Values for the static hierarchical methods, broken down by number of subdomains, are shown in Table 3.10. Because of the random distribution of missing data, the inclusion of dynamics to the hierarchical estimation methods was not expected to provide any improvement over the static cases. For the main domain, and subdomain splits being considered, it was likely that for any area considered, there would be enough data dispersed within to make good predictions without relying on historical information. As Table 3.10 shows, the splitting up of the domain into smaller subdomains, causes a decrease in prediction accuracy. This is due to the independent nature of the hierarchical trees: through splitting, each hierarchical tree has less spatial data to work with.

MSPE values for different DMM and DMURS predictions are shown in Table 3.11. The FNN method of dynamic inclusion failed to produce predictions for the  $2 \times 2$  subdomain split and have been excluded. In general, and as expected, the dynamic inclusions did not provide any appreciable improvement over the static case. Also of note is that the KBF method of

Table 3.11: Selected MSPE values for dynamic hierarchical methods using RR dataset, MO.

Sub-domains	Dynamic Model	Parameters	MSPE Values			
			DMM	DMURS	$\frac{DMM}{MRSM}$	$\frac{MURS}{DMURS}$
1	3ES	$\alpha=0.6, \beta=0.8, \gamma=0.9, L=24$	19.711	14.515	1.000	1.000
1	3ES	$\alpha=0.6, \beta=0.8, \gamma=0.9, L=4$	19.710	14.471	1.000	1.000
4	3ES	$\alpha=0.6, \beta=0.8, \gamma=0.9, L=24$	22.600	17.857	0.999	0.999
4	3ES	$\alpha=0.6, \beta=0.8, \gamma=0.9, L=4$	22.600	17.857	0.999	0.999
1	2ES	$\alpha=0.6, \beta=0.8$	22.580	17.835	0.998	0.997
4	2ES	$\alpha=0.6, \beta=0.8$	22.580	17.835	0.998	0.997
1	FNN	$LR=0.2, L=24$	19.832	14.877	1.006	1.011
1	FNN	$LR=0.2, L=24$	19.832	14.565	1.006	0.997
1	FNN	$LR=0.2, L=48$	19.832	14.574	1.006	1.006
1	FNN	$LR=0.2, L=48$	19.832	14.570	1.006	1.007
1	KBF	$\alpha=0.02, \beta=0.05, \Lambda=3, L=3$	19.711	14.535	1.000	1.000
4	KBF	$\alpha=4, \beta=4, \Lambda=2.6, L=3$	9565.228	17.845	536.028	0.998
4	KBF	$\alpha=4, \beta=4, \Lambda=2.6, L=2$	22.623	17.845	1.268	0.998
4	KBF	$\alpha=4, \beta=4, \Lambda=2.6, L=1$	22.617	17.845	1.2674	0.998
16	KBF	$\alpha=5, \beta=16, \Lambda=2.6, L=3$	23.965	18.410	1.302	0.942
16	KBF	$\alpha=5, \beta=16, \Lambda=2.6, L=2$	23.992	18.410	1.303	0.941
16	KBF	$\alpha=5, \beta=16, \Lambda=2.6, L=1$	23.987	18.403	1.303	0.940
4096	KBF	$\alpha=20, \beta=48, \Lambda=2.6, L=3$	50.821	-	0.594	-
4096	KBF	$\alpha=20, \beta=48, \Lambda=2.6, L=2$	50.254	-	0.317	-
4096	KBF	$\alpha=20, \beta=48, \Lambda=2.6, L=1$	46.527	-	0.279	-

dynamic inclusion demonstrated a greater dependence on the number of time steps used in the prediction. Whereas the 3ES could make use of many previous values without adverse effects, the KBF predictions could use only a much smaller number, otherwise a small error would be introduced during the prediction of the time series and would gradually become larger and larger. This error likely comes from the nonstationarity of the time series used, as well as the blanket application of the estimated temporal variogram to all spatial regions present. While SM was used solely to reduce the amount of processing time, other detrending methods may reduce the amount of spatial nonstationarity present and make the application of a single temporal variogram to the entire area more appropriate.

### 3.5.2.2 ‘3rd Step Good’ Dataset

In remotely sensed data from orbiting satellites, there may be a pattern to the way the missing data occurs. For example, the GOSAT satellite measures the same spot on the earth once every three days. If the domain of interest does not intersect two measurement ‘swaths,’ there will be three days between any measured points located in the domain. As this is potentially a place where dynamic models could be highly useful, an experimental dataset was created in which this property was present. MO data and CT data were both used. The dataset consisted of 48 time steps of relatively well informed frames while in

Table 3.12: MSPE values for non-hierarchical methods using 3SG datasets.

Method	MSPE Values		
	MO1	MO2	CT
FA	113.411	98.165	172.135
TS	113.411	98.165	172.135
NN	125.331	86.878	117.267
IDW	88.596	64.339	85.219
SK	110.979	73.395	171.839
LSK	111.270	76.101	171.999
OK	110.979	76.101	171.840

the rest of the frames only every third day was well informed, and the rest had very few data points. An additional dataset was created using MO data where a ‘good’ day had far fewer data points than the other MO data set. Here the set with the better informed days is labelled MO1, and the other is labelled MO2. The detrending used was a simple mean removal, and the data removal itself was random without any structure within the frames. MSPE was the performance metric used for comparison across all frames.

For the different dynamic models, parameters were varied, as were the number of subdomains that the main domain was split into. Hierarchical methods generally provided slightly worse results when the dynamic model was used on a single subdomain. By splitting up the domain into a number of smaller subdomains, the dynamic model was able to provide improvement over static predictions. However, generally, the amount of error increased with the number of subdomains created from the original domain. This highlights the relative importance of spatial vs. temporal dependence present in this data.

The MSPE values of nonhierarchical methods for both CT and MO data are shown in Table 3.12. The nonhierarchical methods always considered the entire domain. However, the MSPE values for the static hierarchical method had to be calculated for each configuration of subdomains used. These values are shown in Table 3.13. The lower values for the MO2 data compared to the MO1 data occur because of the large difference in the number of data points being predicted. Using the few data points present in the domain on an uninformed time step, the prediction methods are generally able to predict a reasonable value for the missing points. The lack of data points caused the total squared error to be larger. However, when divided among the much larger number of predicted points, the result is a lower MSPE.

Table 3.13: MSPE values for static hierarchical methods using 3SG datasets.

Subdomains	Method	MRS	MURS
		1	108.538
MO1 Data	4	110.044	109.695
	16	110.695	110.527
	1	70.882	66.434
MO2 Data	4	76.178	75.775
	16	77.515	78.060
	1	98.976	79.022
CT Data	4	181.342	146.807
	16	155.250	142.785

**Model Output Data** Tables of MSPE values for different dynamic model parameters applied to the MO1 and MO2 datasets are shown in Tables 3.14 and 3.15, respectively. For the MO1 dataset, which has the well informed days, the subdomain split produced MSPE errors that were not only below the static hierarchical values for the split case, but were also below the single domain values of the static case. The MO2 dataset did not produce the same result, likely because the lower amount of data every third time step puts increased weighting on the historical information. Also, because of the low amount of data for these time steps, the dynamic models are not able to track the temporal trends as well. When these poor trends are used, the models had a higher error than if only spatial information had been used. This is well illustrated by the MSPE values seen when using the FNN dynamics in MO2. Since the neural networks are trained when a threshold of informed points is passed, less data leads to less training, and ultimately poor predictions.

Table 3.14 describes a run using the hierarchical methods with the primary domain split into  $64 \times 64$  subdomains; that is, each original cell in the domain was considered as a single tree. For the static case this caused the estimates made to be equal to whatever trend surface had been used, i.e., SM in these cases. The MURS estimation as implemented was not useful with this scheme, since individual trees are independent.

While this is a promising result for this dataset, the implemented software took a very long time to process, as it was not designed with this use in mind. Another implementation could be created to allow for faster processing and more testing. However, allowing each data cell to hold its own set of dynamic parameters may increase hardware requirements

Table 3.14: Selected MSPE values for dynamic hierarchical methods using 3SG datasets, MO1.

Sub-domains	Dynamic Model	Parameters	MSPE Values			
			DMM	DMURS	$\frac{DMM}{MRSM}$	$\frac{MURS}{DMURS}$
1	3ES	$\alpha=0.6, \beta=0.8, \gamma=0.9, L=24$	108.536	107.556	1.000	1.000
1	3ES	$\alpha=0.6, \beta=0.8, \gamma=0.9, L=4$	108.536	107.551	1.000	1.000
4	3ES	$\alpha=0.6, \beta=0.8, \gamma=0.9, L=24$	102.374	102.099	0.930	0.931
4096	3ES	$\alpha=0.6, \beta=0.8, \gamma=0.9, L=34$	63.099	-	0.556	-
4	2ES	$\alpha=0.6, \beta=0.8$	102.667	102.384	0.933	0.933
4096	2ES	$\alpha=0.6, \beta=0.8$	56.622	-	0.499	-
1	FNN	$LR=0.2, L=24$	108.534	107.553	1.000	1.000
1	FNN	$LR=0.2, L=24$	108.534	107.551	1.000	1.000
1	FNN	$LR=0.2, L=48$	108.534	107.551	1.000	1.000
1	FNN	$LR=0.2, L=48$	108.534	107.555	1.000	1.000
4	FNN	$LR=0.2, L=24$	110.429	110.046	1.003	1.003
4	FNN	$LR=0.2, L=24$	110.429	110.046	1.003	1.003
4	FNN	$LR=0.2, L=24$	110.429	110.046	1.003	1.003
4	FNN	$LR=0.2, L=24$	110.429	110.046	1.003	1.003
1	KBF	$\alpha=0.02, \beta=0.05, \Lambda=3, L=3$	108.535	107.546	1.000	1.000
4	KBF	$\alpha=5, \beta=16, \Lambda=2.6, L=3$	102.099	110.042	0.928	1.003
4	KBF	$\alpha=5, \beta=16, \Lambda=2.6, L=2$	101.316	110.042	0.921	1.003
4	KBF	$\alpha=5, \beta=16, \Lambda=2.6, L=1$	100.230	110.042	0.911	1.003
16	KBF	$\alpha=4, \beta=4, \Lambda=2.6, L=3$	7.006E62	110.801	6.328E60	1.002
16	KBF	$\alpha=4, \beta=4, \Lambda=2.6, L=2$	2.836E58	110.801	2.562E56	1.002
16	KBF	$\alpha=4, \beta=4, \Lambda=2.6, L=1$	78.730	110.801	0.711	1.002
4096	KBF	$\alpha=20, \beta=48, \Lambda=2.6, L=3$	58.639	-	0.517	-
4096	KBF	$\alpha=20, \beta=48, \Lambda=2.6, L=2$	56.555	-	0.499	-
4096	KBF	$\alpha=20, \beta=48, \Lambda=2.6, L=1$	45.918	-	0.405	-

for spatiotemporal datasets of a scale larger than considered here, possibly negating any improvements made.

As with the RR data, the problem of too many time steps being included for KBF is demonstrated here and is even more dramatic. For the certain resolutions and dynamic time step inclusion values, the MSPE values for the entire time series prediction became huge, primarily due to the gradually increasing error previously mentioned.

**CarbonTracker Data** Results of the different estimation methods applied to the the CT 3SG data are shown in Table 3.16. As with the other cases, inclusion of dynamic information at the single root node did not provide any improvement over the static hierarchical cases. The splitting of the domain into subdomains allowed for the dynamic information to make an improvement; however, similar to the majority of other cases, improvement in error due to the dynamic inclusion is far outweighed by the negative effect of domain splitting.

Table 3.15: Selected MSPE values for dynamic hierarchical methods using 3SG datasets, MO2.

Sub-domains	Dynamic Model	Parameters	MSPE Values			
			DMM	DMURS	$\frac{DMM}{MRSM}$	$\frac{MURS}{DMURS}$
1	3ES	$\alpha=0.6, \beta=0.8, \gamma=0.9, L=24$	75.553	73.951	0.976	0.976
1	3ES	$\alpha=0.6, \beta=0.8, \gamma=0.9, L=4$	71.409	67.296	1.007	1.013
4	3ES	$\alpha=0.6, \beta=0.8, \gamma=0.9, L=24$	75.553	73.951	0.976	0.976
4	3ES	$\alpha=0.6, \beta=0.8, \gamma=0.9, L=4$	75.424	73.824	0.975	0.974
4	2ES	$\alpha=0.6, \beta=0.8$	76.346	74.735	0.987	0.986
1	FNN	$LR=0.2, L=24$	110.247	105.865	1.555	1.594
1	FNN	$LR=0.2, L=24$	110.247	105.865	1.555	1.594
1	FNN	$LR=0.2, L=48$	110.247	105.865	1.555	1.594
1	FNN	$LR=0.2, L=48$	110.247	105.865	1.555	1.594
4	FNN	$LR=0.2, L=24$	200.327	198.714	2.589	2.622
4	FNN	$LR=0.2, L=24$	200.327	198.707	2.589	2.622
4	FNN	$LR=0.2, L=24$	200.327	198.713	2.589	2.622
4	FNN	$LR=0.2, L=24$	200.327	198.709	2.589	2.622
1	KBF	$\alpha=0.02, \beta=0.05, \Lambda=3, L=3$	71.562	67.435	1.010	1.014
4	KBF	$\alpha=4, \beta=4, \Lambda=2.6, L=3$	3.302E93	76.179	4.335E91	1.005
4	KBF	$\alpha=4, \beta=4, \Lambda=2.6, L=2$	2.441E109	76.179	3.204E107	1.005
4	KBF	$\alpha=4, \beta=4, \Lambda=2.6, L=1$	73.570	76.179	0.966	1.005
16	KBF	$\alpha=5, \beta=16, \Lambda=2.6, L=3$	68.541	77.514	0.884	0.993
16	KBF	$\alpha=5, \beta=16, \Lambda=2.6, L=2$	67.655	77.515	0.873	0.993
16	KBF	$\alpha=5, \beta=16, \Lambda=2.6, L=1$	65.665	77.513	0.847	0.993
4096	KBF	$\alpha=20, \beta=48, \Lambda=2.6, L=3$	99.428	-	1.013	-
4096	KBF	$\alpha=20, \beta=48, \Lambda=2.6, L=2$	104.262	-	1.062	-
4096	KBF	$\alpha=20, \beta=48, \Lambda=2.6, L=1$	120.986	-	1.232	-

### 3.6 Summary

With regard to prediction accuracy, kriging based methods generally outperformed other implemented methods for all types of detrending. However, as expected, the processing time required was much greater for larger amounts of data. For datasets where kriging is no longer feasible, the hierarchical methods may be a good choice, although nonstatistical NN and IDW methods provided unexpectedly low errors for the tested datasets. With regard to dynamic hierarchical estimation methods, the simple dynamic models implemented were unable to provide a large reduction in MSPE for most of the created datasets. However, when the domain was split into multiple subdomains, the dynamic models provided a reduction of error when compared with static versions applied in a similar manner. Unfortunately, in most cases this reduction was insufficient to allow the dynamic models to outperform the single domain static version. One case exhibited the desired improvement, that is, the split domain dynamic MSPE values became lower than the unsplit domain static versions. While this was an extreme case involving swings between near incomplete and near complete information (3SG MO1 data), it illustrates the potential usefulness this method. Through the use of more advanced dynamic models and better treatment of temporal/spatial stationarity,

Table 3.16: Selected MSPE values for hierarchical methods using 3SG datasets, CT data.

Sub-domains	Dynamic Model	Parameters	MSPE Values			
			DMM	DMURS	$\frac{DMM}{MRSM}$	$\frac{MURS}{DMURS}$
1	3ES	$\alpha=0.6, \beta=0.8, \gamma=0.9, L=24$	98.976	78.994	1.000	0.999
1	3ES	$\alpha=0.6, \beta=0.8, \gamma=0.9, L=4$	98.976	79.037	1.000	1.000
4	3ES	$\alpha=0.6, \beta=0.8, \gamma=0.9, L=24$	175.691	138.222	0.969	0.942
4	3ES	$\alpha=0.6, \beta=0.8, \gamma=0.9, L=4$	175.731	138.144	0.969	0.941
4	2ES	$\alpha=0.6, \beta=0.8$	175.0617	137.075	0.965	0.934
1	FNN	$LR=0.2, L=24$	98.975	79.048	1.000	1.000
1	FNN	$LR=0.2, L=24$	98.975	79.040	1.000	1.000
1	FNN	$LR=0.2, L=48$	98.975	79.028	1.000	1.000
1	FNN	$LR=0.2, L=48$	98.975	79.035	1.000	1.000
4	FNN	$LR=0.2, L=24$	174.751	135.908	0.964	0.926
4	FNN	$LR=0.2, L=24$	174.751	135.908	0.964	0.926
4	FNN	$LR=0.2, L=24$	174.751	135.909	0.964	0.926
4	FNN	$LR=0.2, L=24$	174.751	135.908	0.964	0.926
1	KBF	$\alpha=0.1E-027, \beta=1.75E-026, \Lambda=0.78, L=3$	98.975	78.974	1.000	0.999
4	KBF	$\alpha=0.1E-027, \beta=3.8, \Lambda=1, L=3$	177.127	137.391	0.977	0.936
16	KBF	$\alpha=20, \beta=16.5, \Lambda=0.8, L=3$	123.628	111.299	0.796	0.779
4096	KBF	$\alpha=8, \beta=140, \Lambda=0.8, L=3$	1.697E83	-	9.86E83	-
4096	KBF	$\alpha=8, \beta=140, \Lambda=0.8, L=2$	158.269	-	0.919	-
4096	KBF	$\alpha=8, \beta=140, \Lambda=0.8, L=1$	160.923	-	0.935	-

this improvement may be seen in more general cases.

## Chapter 4

# Inventory Prediction

As explained in section 2.2, emission inventories are crucial for the success of modelling CO<sub>2</sub> concentrations and surface fluxes, but they are rarely available in a timely fashion.

Here, updated emissions values for three greenhouse gases (CO<sub>2</sub>, CH<sub>4</sub>, and N<sub>2</sub>O) are predicted without the need for any spatial allocation step. Information about the location in question is fed into a model and the updated emission estimate is produced. Data about the location includes previous emission value, population, average temperature data, monthly temperature anomaly data, and various socioeconomic variables. The time interval used between the base and updated inventory is five years.

Two different models were used to perform the predictions. The first is the random forest model (section 4.3.1) and the second is the extreme learning machine model (section 4.3.2).

### 4.1 Data Sources

The EDGAR emissions inventories were the primary data source. The motivation for this choice was to make use of data that had already been spatially distributed, and then use more recent data to update the emission values. Since the emissions of interest are anthropogenic, data sources were sought that would reflect human activity.

The EDGAR emissions database is available in a format broken down into gas and emissions sectors. For this work, emissions of CO<sub>2</sub>, N<sub>2</sub>O, CH<sub>4</sub>, and livestock emissions of N<sub>2</sub>O and CH<sub>4</sub> were predicted for the agriculture, energy, oil and gas production, residential,

and road transportation sectors.

Gridded world population data (GPWv3) [45] and national boundary data [46] are both provided at a resolution of 2.5 arc minutes ( $0.04167^\circ$ ). Monthly temperature averages came from [47]. These monthly averages were created from temperature readings taken during the period of 1961–1990. This dataset has a resolution of  $5^\circ \times 5^\circ$ . Temperature anomaly data comes on a  $2^\circ \times 2^\circ$  grid (GISTEMP [48]). The information about temperature anomalies could provide insight into increases and decreases in the amount of energy used for heating and cooling.

Socioeconomic data, provided at the country level, was taken from the World Development Indicator [49] (WDI). Due to missing data, the entire dataset could not be used. The variables used in the final completed dataset are listed in Appendix B. They have been broken down into two classes: regular variables (section B.1), provided only on a country-wide basis and per capita variables (section B.2), which are provided on a per person (or similar) basis. While some of the variables in the second class are not strictly per capita, they are all somehow related to the population (e.g. per 1000 people, percentage of the population etc.). The value assigned to a given cell is its population value multiplied by the value of the variables. This provides spatial distribution of data values.

## 4.2 Data Preprocessing

One of the challenges of using the different data sources is the differing resolutions. Fortunately, due to the nature of the data, this was relatively straightforward. EDGAR resolution cells were used since the other datasets lent themselves more to the aggregation. While this meant that there mapping in the EDGAR data needed no aggregation, in order to make the values more meaningful, the original units of  $\text{kg}/(\text{m}^2 \text{ second})$  were scaled to give units of  $\text{kg}/(\text{m}^2 \text{ year})$ .

Since the population was at a higher resolution than the EDGAR data, the population cells that fell inside each EDGAR data cell were determined and their populations summed. Similarly, the national boundary data was all assigned to the EDGAR cell that contained them, but instead of summing the numerical codes, the country assignment of the EDGAR data cell was selected as the last entry into this pool. Due to the order in which the mapping

was performed, the final dataset has a slight bias to the north.

The opposite took place for the temperature data. In this case the EDGAR cells were much smaller in comparison, and the EDGAR cells that fell in each temperature cell were determined, and their temperature values were assigned accordingly.

Socioeconomic data, reported at the country level, were assigned to the spatial grid. This was done using the previously assigned country code values. The mapping of country codes between those used in the gridded dataset and the ones used in the socioeconomic dataset was not one-to-one. A number of small islands that are formally part of other countries had been given their own country codes in the gridded dataset. These codes were replaced with the codes of their political parents. The country codes were ignored in cases where countries appeared between datasets due to country breakup. These country codes were not expected to have a large impact on worldwide emissions.

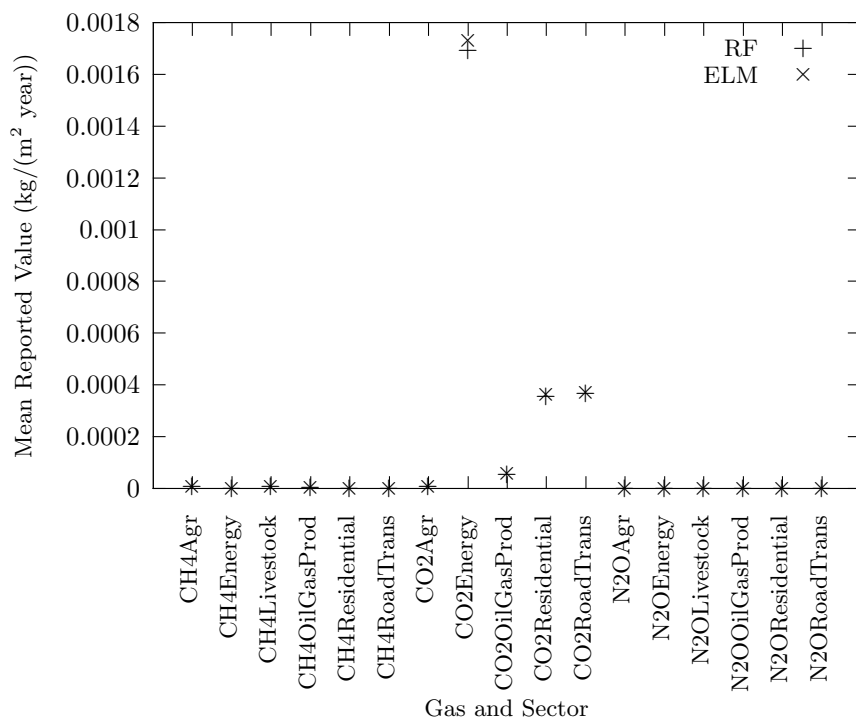
The datasets used to train and test the random forest prediction methods were slightly different from the datasets used with the extreme learning machine method. Because a different input format was required by each function, and a variable removed from one dataset may not have been removed from the other, the random forest dataset contains slightly more data points than the extreme learning machine dataset. The resulting datasets do not vary much in their summary statistics (provided in Appendix C); they were used despite this difference, mainly because of the processing time required to retrain the models. Averages for reported data are shown in Figure 4.1.

## 4.3 Model Building

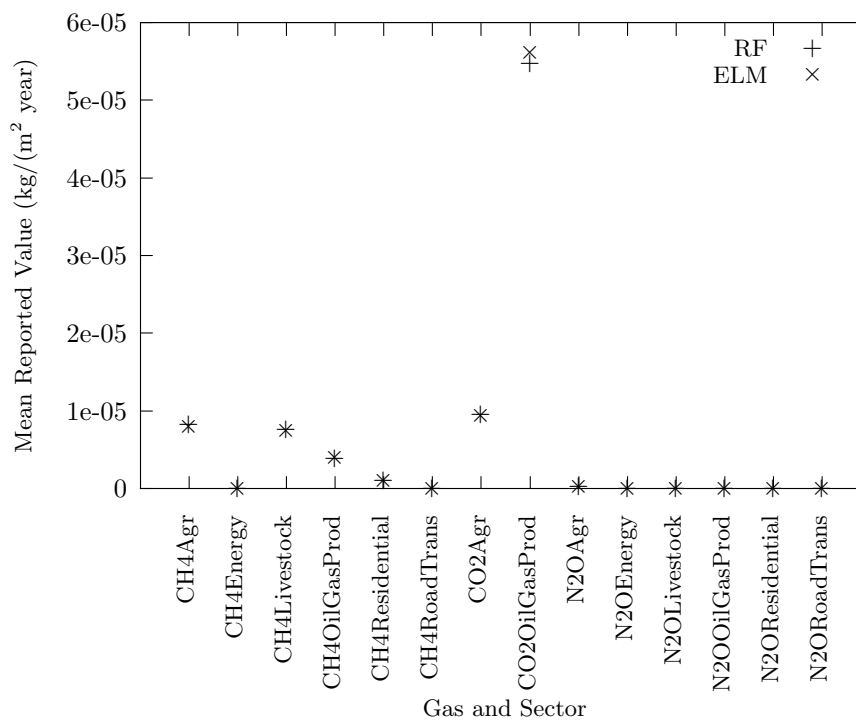
For both models, the goal was to predict values for different gases which had been broken down by sector based on previous pollutant values, current and previous temperature data, population data, and socioeconomic data.

### 4.3.1 Random Forests

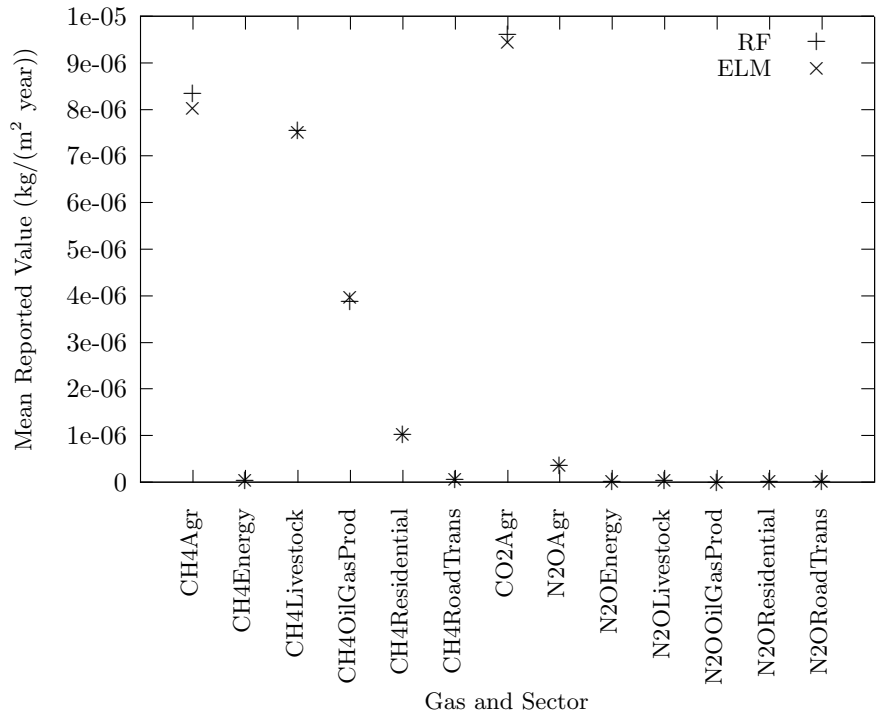
Random forests are a method of classification and regression in which many tree predictors are created and they either vote for the class for assignment (classification), or have their predicted numerical values averaged with the other predictors in the forest to arrive at a



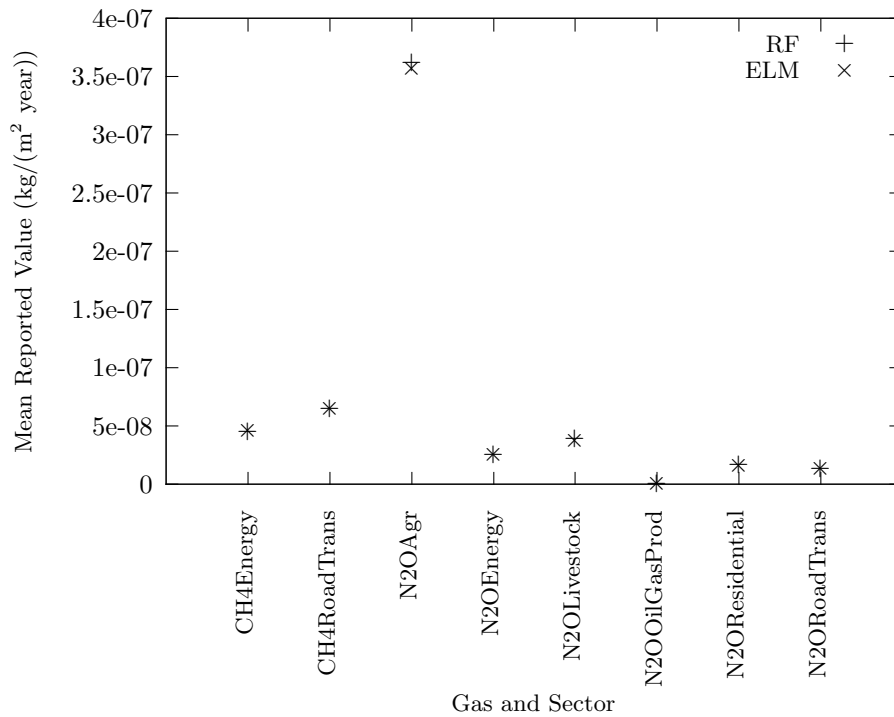
(a) Complete categories.



(b) Categories removed to show scale.



(c) Categories removed to show scale.



(d) Categories removed to show scale.

Figure 4.1: Mean reported value comparison.

final predicted value (regression) [50].

The creation of a single regression tree involves the splitting up of the complete dataset at nodes using the different predictor variables present [51]. This process continues until a terminal node is reached, and a value is assigned to the target variable for the points falling in this node. In the case of a regression tree, splitting of the dataset involves searching for the split that will result in the greatest reduction of MSPE for the entire tree. When left to fulfill this requirement, the produced trees are very large, complex, and will contain very few data points in each terminal node. The strategy for overcoming this problem is to first grow a large and complex tree, then to prune branches as to minimize an error-complexity measure [51, p.233]. The result of this pruning is a smaller tree that has a higher error rate with respect to the training data, but much lower error when generalised to previously unseen data.

In the case of random forests, multiple regression trees are grown and used for prediction. The predicted values from all trees are averaged to use as the final prediction. The creation of the trees for a random forest differs in a few ways from the creation of a single regression tree in that only samples of the training data are used for training the individual trees, not all predictor variables are considered when searching for the best possible split at each node, and the largest tree is always grown with out any pruning [52]. The use of random features provides comparable accuracy to other methods, increased robustness to noise and outliers, increased speed compared to similar methods, and simplicity [50].

The analysis was performed using the `randomForest` package [53] in the R statistical program [54]. Data subsets were created that contained all previous emission values, all other data variables, and the emission variable of interest. A sample was taken from this subset and used to grow the random forest. After training, the entire subset was applied to the forest, with the target value withheld. The withheld values were predicted and the percentage error between true and predicted values was calculated.

### **4.3.2 Extreme Machine Learning**

The extreme learning machine (ELM) [55] is a learning algorithm for a feed forward neural network. The method of training with this type of network is to set all of the input weights and hidden node weights randomly and train only the weights connecting the hidden layer

to the output layer. This training takes place through the compact representation of the network output as a matrix equation, which is used to solve for the unknown weights. The benefit of this method compared to the usual gradient based decent methods is primarily speed. The lack of iterative learning steps can make this training method much faster allowing for more training samples to be used in a similar time.

More formally, a set of  $N$  samples is defined, each sample having  $n$  input values and  $m$  output values,  $\mathbf{x}_i$  is defined as the vector containing the  $i^{th}$  set of input values and  $\mathbf{t}_i$  is defined as the vector containing the  $i^{th}$  set of output values. Moving on to define the neural network, we first define  $\tilde{N}$  as the number of hidden neurons in the network. The weight vector connecting the  $i^{th}$  hidden neuron to the input neurons is denoted by  $\mathbf{w}_i$  and the weight vector connecting the  $i^{th}$  hidden neuron to the output neurons is  $\beta_i$ . Each hidden neuron has a threshold value, denoted by  $b_i$ . Further defining the activation function of the hidden neurons as  $g(x)$ , the output of the network is calculated with

$$\sum_{i=1}^{\tilde{N}} \beta_i g(\mathbf{w}_i \cdot \mathbf{x}_j + b_i) = t_j, \quad j = 1, \dots, \tilde{N},$$

where  $\mathbf{w}_i \cdot \mathbf{x}_j$  denotes the inner product between vectors  $\mathbf{w}_i$  and  $\mathbf{x}_j$ .

$\beta$  is defined as the  $\tilde{N} \times m$  matrix of all  $\beta_i$  vectors,  $\mathbf{T}$  is the  $N \times m$  matrix of all  $\mathbf{t}_i$  vectors, and a matrix  $\mathbf{H}$  is defined as follows,

$$\mathbf{H} = \begin{bmatrix} g(\mathbf{w}_1 \cdot \mathbf{x}_1 + b_1) & \dots & g(\mathbf{w}_{\tilde{N}} \cdot \mathbf{x}_1 + b_{\tilde{N}}) \\ \vdots & & \vdots \\ g(\mathbf{w}_1 \cdot \mathbf{x}_N + b_1) & \dots & g(\mathbf{w}_{\tilde{N}} \cdot \mathbf{x}_N + b_{\tilde{N}}) \end{bmatrix}.$$

The output out the network can be more compactly represented by

$$\mathbf{H}\beta = \mathbf{T}.$$

Finally, as discussed in [55], since all weights, except the weights between the hidden and output neurons, and biases have been randomly assigned, the training of the network is accomplished through the setting of the weights connecting the hidden and output layers. This is done by solving the equation

$$\hat{\beta} = \mathbf{H}^\dagger \mathbf{T},$$

where  $\mathbf{H}^\dagger$  is the Moore-Penrose generalised inverse of  $\mathbf{H}$ . After solving for  $\hat{\beta}$ , estimates of new samples can be made by creating a new matrix  $\mathbf{H}$  using the previous randomly assigned values for  $\mathbf{w}_i$  and  $\mathbf{b}_i$ , and the new input values, then solving the equation

$$\mathbf{H}\hat{\beta} = \mathbf{T},$$

where  $\mathbf{H}$  and  $\mathbf{T}$  now reflect values from the new samples.

The procedure for use of the extreme learning machine was implemented in the R scripting language based on the description from [55].

As with the random forest predictions, a sample of the data was taken and used to train the model. Again, similar to the random forest protocol, the entire dataset was then passed to the trained model with the target values withheld, and predictions were made. Percentage errors between true and predicted data values were calculated. Since this can result in infinite values in locations where there are no reported emissions, these infinite values were removed prior to the calculation of the summary statistics of the percentage error distribution.

## 4.4 Results and Discussion

Figure 4.2 shows the MAPE for the different prediction methods, gases, and sectors. In order to relate these errors to the reported values, a ratio of MAPE to mean reported value was taken (shown in Figure 4.3). Values below 1 indicate a mean absolute error that is less than the mean reported value, while values above 1 indicate mean absolute errors above the reported mean. Plots of percentage error for the different gas/sector combinations are shown in Figure 4.4.

Taking a more global approach to the inventory updating, the predictions were summed and the result was compared to the sum of the reported values for the different gases and sectors using percentage difference. The results of these comparisons are shown in Figure 4.5.

Tables of the five number statistical summaries (median, min, max, 1st and 3rd quartiles)

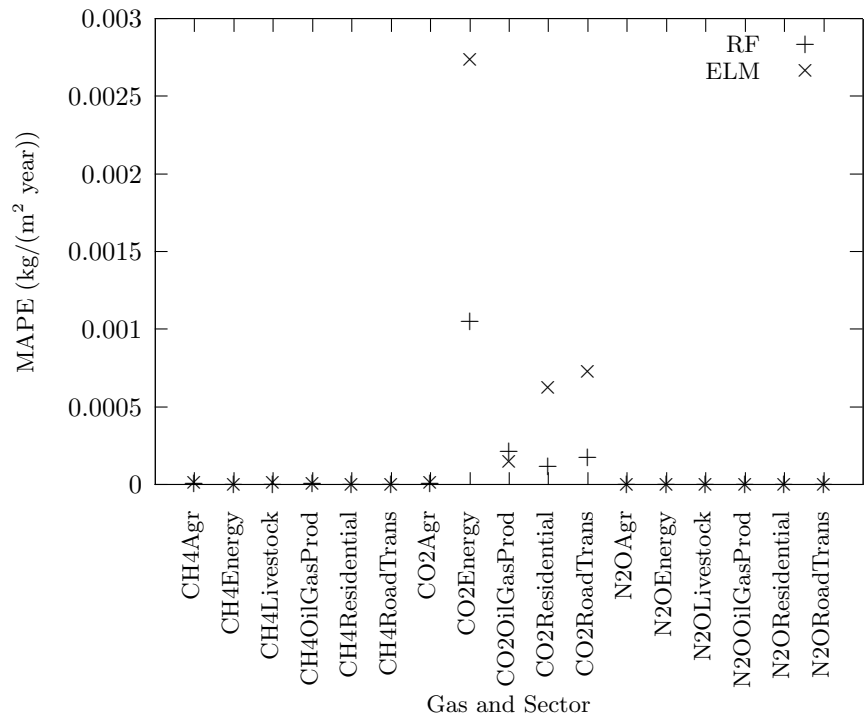
for data used by the RF and ELM prediction methods, the predictions, the absolute error and the percentage error (with infinite values removed) are located in Appendix C. Summary statistics for the distributions of the percentage error for random forest and extreme learning machine predictions are located in Tables C.7, and C.8, respectively.

Considering what is shown in Figure 4.2, it seems that some gas/sector combinations are more difficult to predict than others. More generally, CO<sub>2</sub> seems to be the most difficult gas to predict using these methods, followed by CH<sub>4</sub>, and finally N<sub>2</sub>O. Providing context to the errors of these updating schemes, Figure 4.3 shows that the mean absolute error is most often higher than the mean reported value, especially for the case of ELM predictions. RF predictions perform somewhat better in most cases but the predictions are generally poor. This is also shown by the high values in the plots of mean percentage error in Figure 4.4.

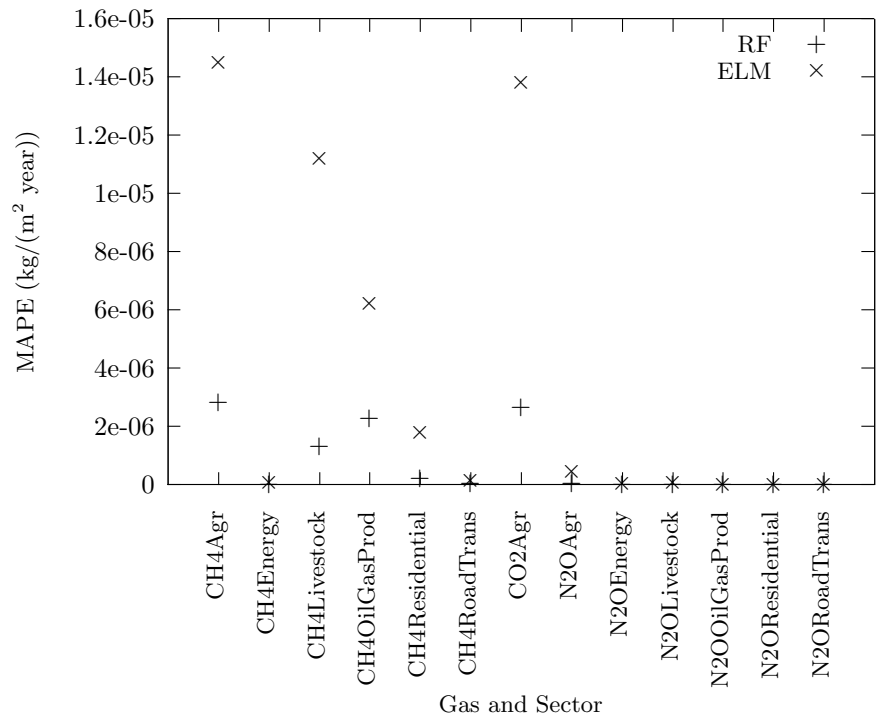
Ideally, if all of the predictions were summed, the total would be equal to the sum of all of the reported values. This is checked using Figure 4.5. In this regard, the prediction schemes do much better. Here we also see more sectors where ELM predictions outperform those made using RF. This difference is due to the fact that the RF method was able to make predictions that were exactly equal to zero, which was the case for much of the spatial area processed, generally leading to smaller MAE and MPE values. On the other hand, ELM sometimes predicts small negative values for large areas. Anthropogenic emissions, as presented in the EDGAR dataset, are never negative so this leads to higher values of MAE and MPE. However, these negative values appear to be offsetting over-predicted values, in some cases leading to total emissions closer to reported values.

The apparent difficulty in predicting some gas/sector combinations likely stems from the fact that some emission categories, for example, CO<sub>2</sub>Energy and CO<sub>2</sub>OilAndGasProd, have large emissions concentrated in relatively small areas. This can introduce two problems. The first is that since random samples are taken for training, the most important areas for the emissions may be left out. The second problem is related to the fact that the prediction algorithms try to minimize the average error; because of the relative frequency of high emission cells compared to low emission cells, estimating on the low side gives a better mean error.

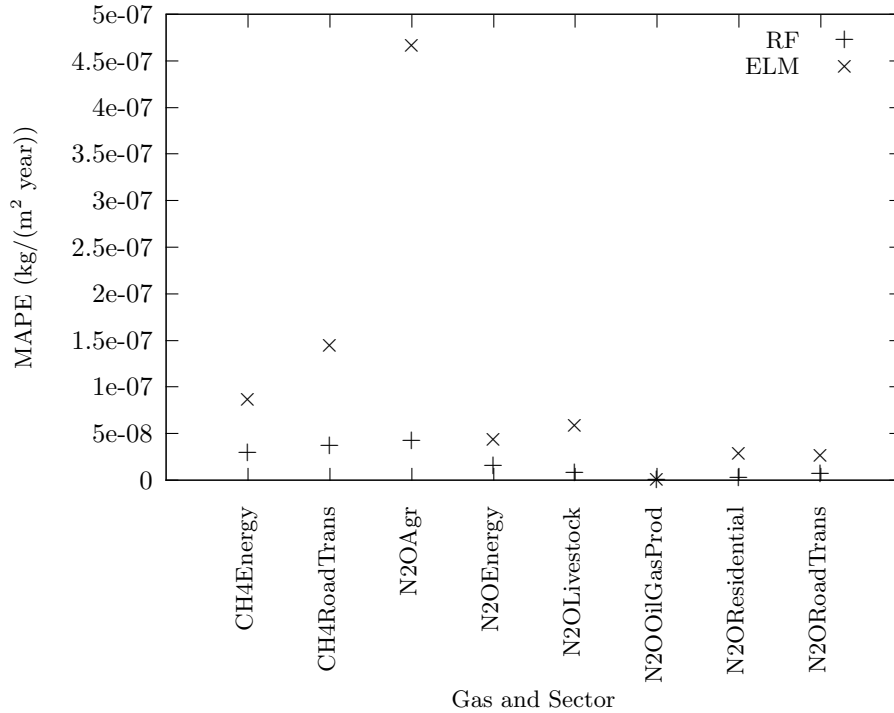
For some gas/sector combinations, there may be little correlation with the chosen explanatory variables. For example, power plants are not usually built in areas of high pop-



(a) Complete categories.



(b) Reduced categories to show scale.



(c) Further reduced categories to show scale.

Figure 4.2: MAPE Comparison

ulation, but a low population does not mean that a power plant is present. Similarly, for temperature anomalies, a higher than average temperature may mean more energy use in areas of high population, but these models are currently not able to determine where the increase in CO<sub>2</sub> due to energy production should occur. This would be very hard to implement properly, since knowledge of the locations of many different facilities would be needed. Taking into account that the consumed energy does not always come from the closest power plant, the model could quickly become very complex.

A bottom up approach, the method of emissions inventory updating used here, does not compare favourably with the more commonly used top down approach, in which total regional emissions are forecasted with the aid of energy-use statistics, and then spatially allocated using some other surrogate value. This top down approach has a distinct advantage that regional energy-use forecasts are readily included, and changing regional energy policy may be easily incorporated in these forecasts. Simple and fast methods have been used to

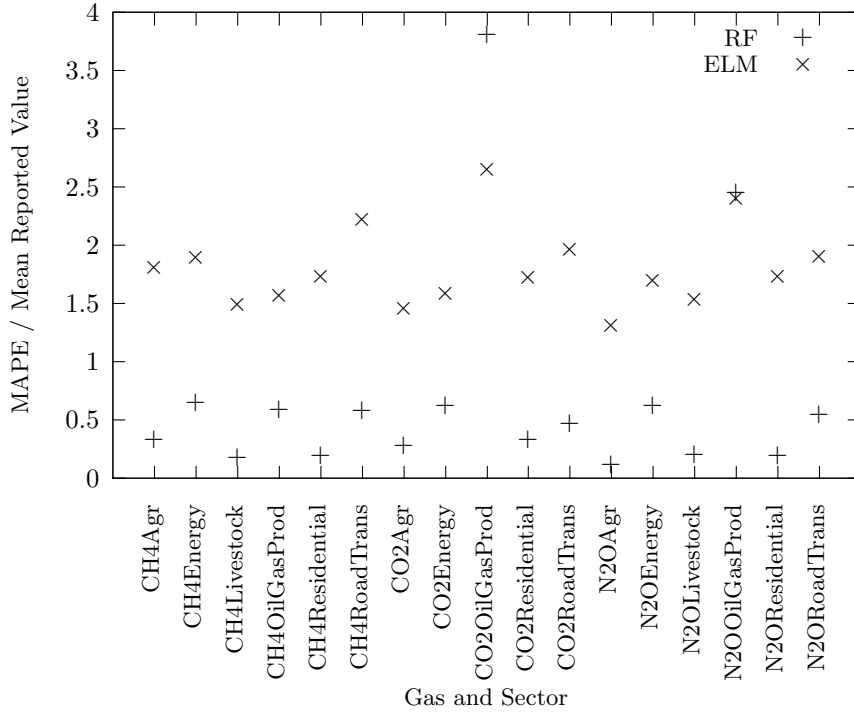
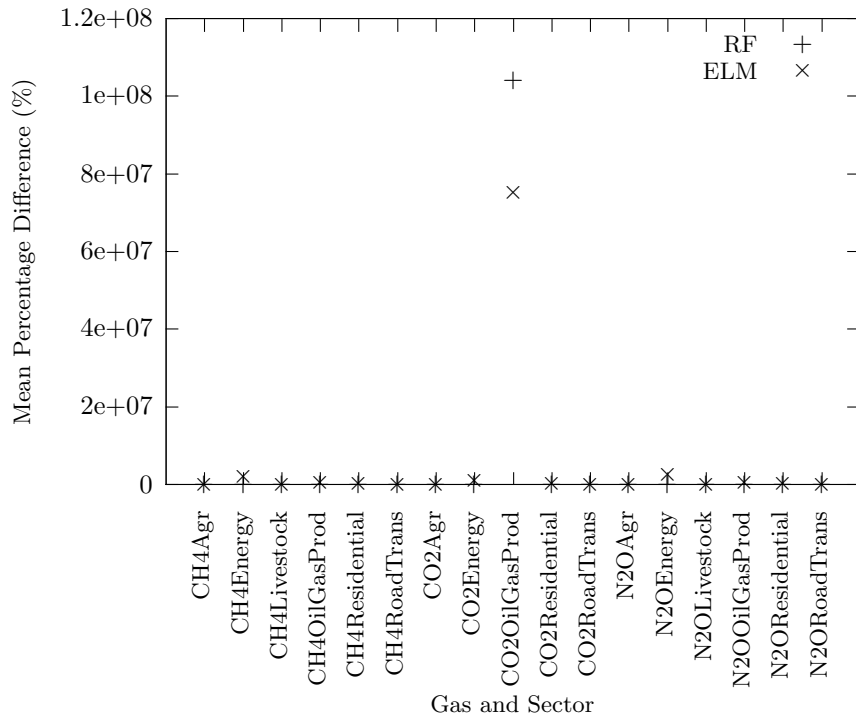


Figure 4.3: MAPE over mean reported value comparison.

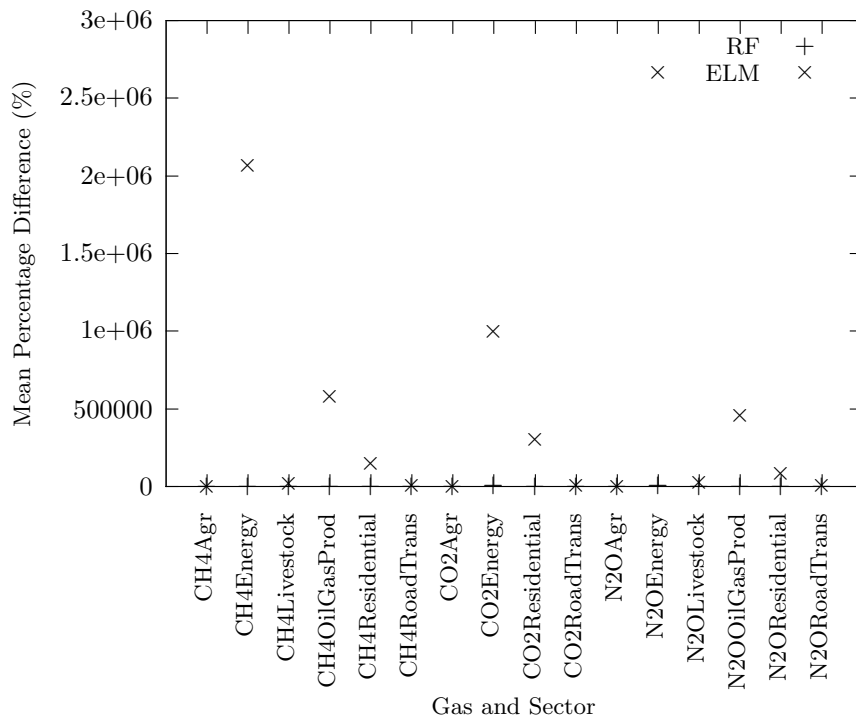
produce large scale regional emissions updating systems with good accuracy [23]. Continuing improvements in spatial allocation handling, i.e., using images of night-time lights as surrogate data [56], make the top down approach more accurate and reliable.

## 4.5 Summary

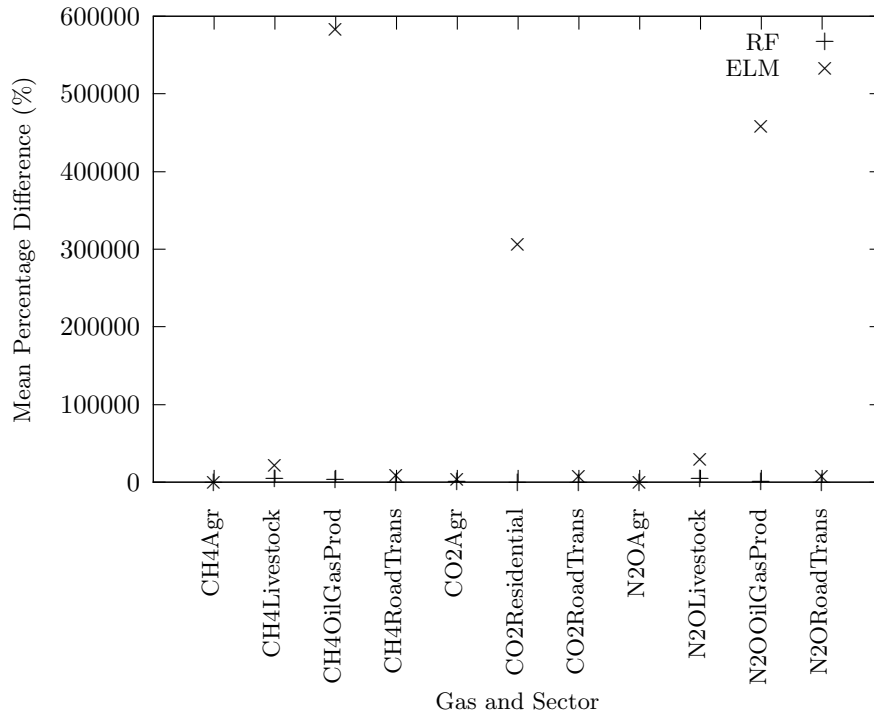
Two methods of updating a spatially distributed anthropogenic emissions inventory of three greenhouse gases were explored, namely random forest regression and a feed-forward neural network scheme called an extreme learning machine. Input datasets were created that included population, climatic temperature, temperature anomalies, various socioeconomic values, and the emissions values themselves. The dataset was sampled and used to train the models. The complete datasets were then processed and the results were compared. The random forest regression generally outperformed the extreme learning machine when the results were compared in a spatially distributed manner. Performance of the extreme learning machine improved when the totals of all predictions made were considered. Unfortunately,



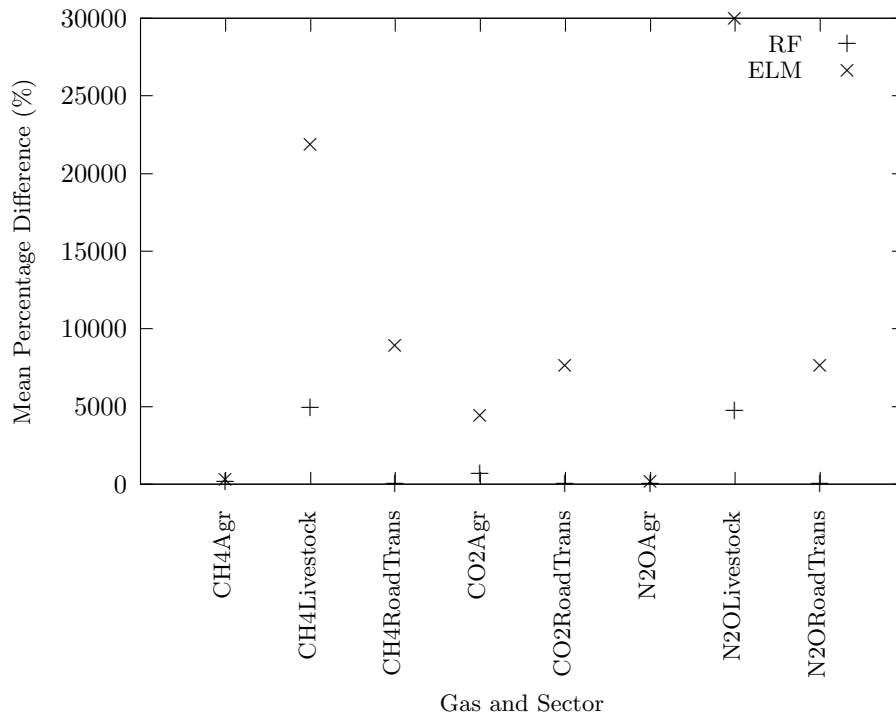
(a) Complete categories.



(b) Reduced categories to show scale.

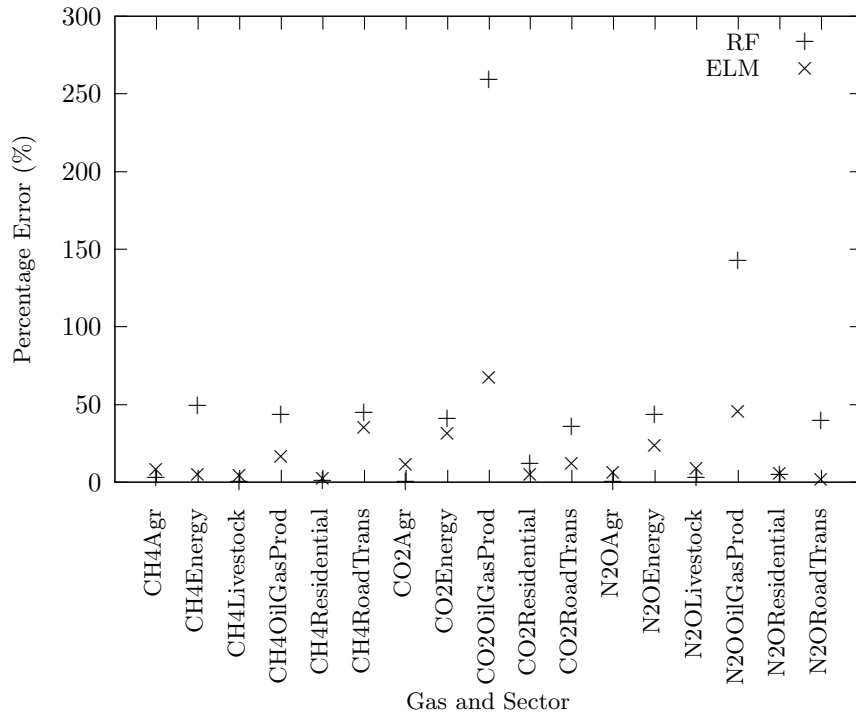


(c) Complete categories.

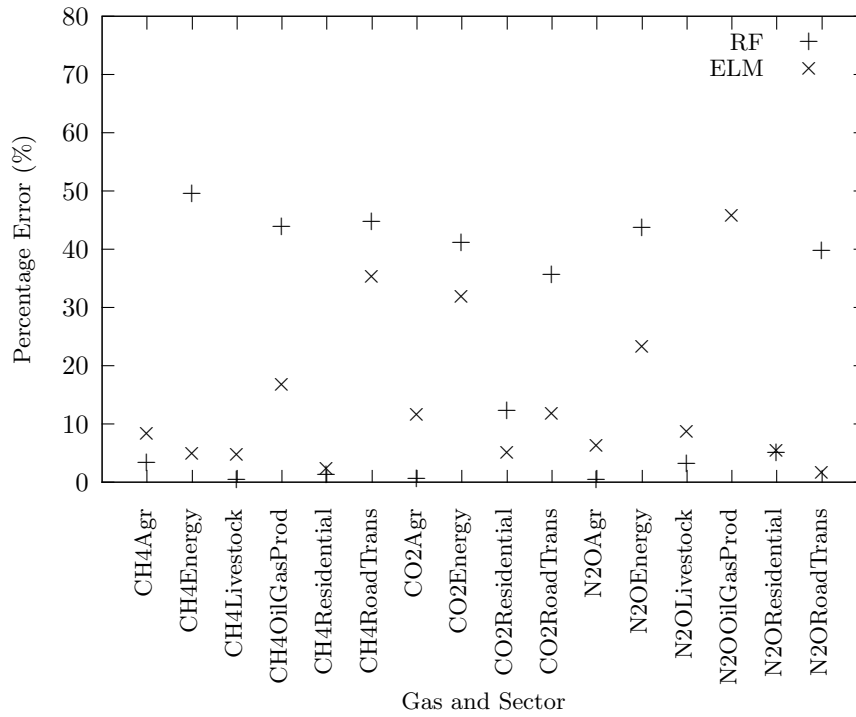


(d) Reduced categories to show scale.

Figure 4.4: MPE comparison



(a) Complete categories.



(b) Categories removed for scale.

Figure 4.5: Total percentage difference comparison.

the errors for both methods were such that these schemes are not suitable for practical use.

## Chapter 5

# Conclusions, Contributions, and Future Work

### 5.1 Conclusions

The choice of detrending and estimation method, depends on the end goal. If values at different resolutions will be required, then the hierarchical models are a clear choice. If prediction variances are not required, and speed is a priority, then nearest neighbour and inverse distance weighted interpolation can both be acceptable choices. Prediction variances require that a choice can be made between speed and prediction accuracy. Kriging based methods provide higher confidence predictions that are more accurate, but at the cost of a much longer processing time.

Of the spatial prediction methods implemented, the traditional kriging approaches were the most reliable with the datasets tested. The LSK estimation method provided a good trade-off between prediction accuracy and processing time, but was affected by the spatial variation of the data. Hierarchical method predictions were only slightly less accurate than kriging method predictions and required much less processing time. MURS consistently outperformed the MRSM estimation method.

The MO dataset benefited the most from detrending, particularly with the hierarchical methods. The 3rd level ATPS detrending surface showed the best improvement, but numer-

ical problems arose in a few cases. The FRS detrending surface should be reimplemented to correct the long processing time.

The simple dynamic models used to incorporate historical information were not useful in the majority of datasets tested, but did provide an improvement in one extreme case. More thorough treatments of temporal and spatial stationarity may allow for the gains seen in the extreme case to be present in more general cases.

Neither of the two inventory prediction methods explored provided forecasts accurate enough for real world use. Method improvement is possible but may not provide a useful performance increase. Updating inventory estimations, such as including the incorporating of governmental policy changes and energy-use statistics, is more easily with a top down approach, rather than the bottom up approach. Improvements in data and in methods to carry out temporal and spatial disaggregation from a national/global inventory are continually improving. The poor output from the bottom up approach does not warrant the long process of building the dataset and training the models.

## **5.2 Thesis Contributions**

The objectives described in section 1.2 were used as a guide for the contributions to the area of computer modelling of greenhouse gas emissions described here.

### **5.2.1 Missing Data**

A number of spatial prediction algorithms were implemented to test their performance with regard to error and speed in the context of atmospheric CO<sub>2</sub> concentrations. The methods implemented included nearest neighbour, inverse distance weighting, simple kriging, local simple kriging, ordinary kriging, multiresolution spatial models, and multiresolution spatial predictors. The incorporation of historical information was introduced to the hierarchical methods through double and triple exponential smoothing, a feed forward neural network, and a kriging based forecast. Different methods of trend removal were also implemented and applied as part of the spatial prediction system, including simple mean removal, general least squares, thin plate splines and fixed rank smoothing. Experimental datasets with missing values were created using available model data and the implemented methods were applied.

## 5.2.2 Inventory Prediction

Two methods of updating spatially distributed, anthropogenic greenhouse gas emissions were tested, including random forest regression (available in an R package) and extreme machine learning neural networks (implemented in R). Input data from a variety of sources, including previous emissions data, climatological sources, and socioeconomic data, were processed to create the dataset used for prediction. The models were trained using subsets of the larger dataset, then applied to the entire set in order to test prediction accuracy.

## 5.3 Future Work

### 5.3.1 Missing Data

#### 5.3.1.1 Consideration for Use with Remotely Sensed Data

The GOSAT satellite [57] is one of the newest earth observing satellites capable of taking the necessary measurements to estimate atmospheric concentrations of greenhouse gases. The sparsity of data measurements resulting from cloud cover, atmospheric dust, and other measurement issues make it far more difficult to use GOSAT data to predict global CO<sub>2</sub> concentrations than to use the data discussed in this work. GOSAT problems are further compounded by the satellite's sun synchronous orbit.

Data sparsity introduces a number of problems. For example, getting enough pairs to estimate parameters for a variogram model may be difficult. A possible solution may be to carry information about the variogram forward in a dynamic fashion. The fit variogram from previous steps could be passed forward in time and updated with the current variogram information. This may also reduce the computation required for variogram parameter estimation as it would no longer need to be performed from scratch each time.

Data sparsity also causes problems with any dynamic modelling that is undertaken. For example, the triple exponential smoothing method of including dynamic information requires one whole 'season,' which may be difficult to find when using real remotely sensed data. This could potentially be handled by using data modelled for a typical season at the desired spatial scale to fit the dynamic parameters and, using these parameters, estimate missing values based on the measured data.

### **5.3.1.2 Exclusion of Anisotropy**

Anisotropy was ignored for all work presented in this thesis in order to reduce the processing time and simplify calculations. This could result in the loss of useful information present in the data, especially in the case of kriging predictions. Inclusion of anisotropy could improve both prediction error and provide better estimates of variance. However, because spatial patterns present in the data, the simple anisotropy models usually seen may not provide meaningful improvement.

In a geological context, the creation of an locally varying anisotropy (LVA) field is accomplished through the combination of expert knowledge, an understanding of the deposit in question, and data [58]. In an atmospheric prediction context, the generation of an LVA field may require the use of tracer models and numerical weather prediction, in order to gain an understanding of atmospheric gas concentrations, and how they change. Additionally, it may be difficult to implement a version of ‘expert intelligence’ in software to allow automatic processing of the large amount of data that is expected. Regardless, the addition of numerical weather prediction and tracer models for use of LVA fields would likely render their use infeasible from a computation time standpoint.

Despite these difficulties, potential performance improvements may make it desirable to implement simplified methods of handling LVA. While the gains may not be worth the extra processing required in all cases, there may be some cases where large improvements are evident. High resolution data may be one such case.

## **5.3.2 Inventory Prediction**

### **5.3.2.1 Data Availability**

Data selection was frustrated by the unavailability of potentially relevant socioeconomic data points. The period of time examined in regard to EDGAR emissions did not have many of the variables collected. This situation seems to be improving, as more recent years generally contain more data. The World Development Indicators report depends on statistics collected from individual countries, and as more countries begin to collect statistic, the overall dataset is expected improve.

### 5.3.2.2 Long Updating Interval

The period between the base year and the year being updated was perhaps far too long. A five year period (1990 to 1995) was chosen because GPWv3 data were available every five years from 1990 to 2015 (with the last few datasets being projections). In [22], forecasts of 1-3 years are called a medium range, which perhaps makes this emissions updating scheme too long range considering the accuracy that was desired.

Despite the availability of more recent population data, in which there was a potential for more available socioeconomic data to be found, the emissions updating of 1990 to 1995 was attempted in order to reserve more recent EDGAR data. Models that were trained using the 1990 and 1995 datasets, had they shown more reasonable accuracy, would have then been presented with the 1995 data in order to attempt the update to year 2000 values, in order to test them on data with which they had not been trained.

### 5.3.2.3 The Importance of Point-Source Emissions

The presented updating scheme is ill suited to make estimates of point-source emissions. This can be inferred from the fact that sector/gas combinations where emissions come mainly from point-sources are generally predicted with less accuracy than those where emissions have been spatially allocated over a larger area. Two possible explanations are that random samples used to train the models had a much higher representation of area-sources and the explanatory variables used are not likely well correlated to point-source emissions.

Larger facilities are often required to keep track of and report emissions to a governing body. The EDGAR dataset makes use of this information by geolocating it on the grid. The data for some of these facilities comes from the CARMA [59] dataset, and due to the fuzzy matching used to estimate the facility location, will occasionally have the reported location differing greatly from the real location [60].

### 5.3.2.4 Clustering

A dataset that represents the whole world contains a huge amount of diversity in regards to population, wealth and industrialisation. If data clustering methods were applied to separate the dataset into intuitive groups such as areas of high and low population and train-

ing/prediction was applied to the different groups, prediction error might be improved. For example, areas of low population and industrialisation would be expected to have low emissions compared to areas of high population and industrialisation. Thus, emission predictions could begin on a logical basis.

# References

- [1] S. Arrhenius, “On the influence of carbonic acid in the air upon the temperature of the ground,” *Philosophical Magazine and Journal of Science*, vol. 41, pp. 237+, apr 1896.
- [2] S.C. Doney, V.J. Fabry, R.A. Feely, and J.A. Kleypas, “Ocean acidification: The other CO<sub>2</sub> problem,” *Annual Review of Marine Science*, vol. 1, no. 1, pp. 169–192, 2009.
- [3] F.I. Woodward, G.B. Thompson, and I.F. McKee, “The effects of elevated concentrations of carbon dioxide on individual plants, populations, communities and ecosystems,” *Annals of Botany*, vol. 67, no. Suppl. 1, pp. 23–38, JUN 1991.
- [4] O.L. Phillips, S.L. Lewis, T.R. Baker, K.J. Chao, and N. Higuchi, “The changing amazon forest,” *Philosophical Transactions of the Royal Society B: Biological Sciences*, vol. 363, no. 1498, pp. 1819–1827, May 2008, PMID: 18267900 PMCID: 2374914.
- [5] S. Solomon, D. Qin, M. Manning, Z. Chen, M. Marquis, K. B. Averyt, M. Tignor, and H. L. Miller, Eds., *Climate Change 2007 - The Physical Science Basis: Working Group I Contribution to the Fourth Assessment Report of the IPCC*, Cambridge University Press, Cambridge, UK and New York, NY, USA, Sept. 2007.
- [6] A. Pasini and F. Sofri, *From observations to simulations*, World Scientific, 2005.
- [7] E. Dufour and F.M. Breon, “Spaceborne estimate of atmospheric CO<sub>2</sub> column by use of the differential absorption method: Error analysis,” *Applied Optics*, vol. 42, no. 18, pp. 3595–3609, June 2003.
- [8] D.P. Wylie and W.P. Menzel, “Eight years of high cloud statistics using HIRS,” Internet: [http://journals.ametsoc.org/doi/abs/10.1175/1520-0442\(1999\)012%3C0170%3AEYOHCS%3E2.0.CO%3B2](http://journals.ametsoc.org/doi/abs/10.1175/1520-0442(1999)012%3C0170%3AEYOHCS%3E2.0.CO%3B2) [Accessed April 08, 2001], Feb. 2010.
- [9] N. Cressie, “The origins of kriging,” *Mathematical Geology*, vol. 22, no. 3, pp. 239–252, 1990.
- [10] R.P. Barry and R.K. Pace, “Kriging with large data sets using sparse matrix techniques,” *Communications in Statistics - Simulation and Computation*, vol. 26, no. 2, pp. 619, 1997.
- [11] N. Cressie, *Statistics for Spatial Data*, Wiley, New York, rev. ed edition, 1993, Series: Wiley series in probability and mathematical statistics. Applied probability and statistics Bibliography note: Includes bibliographical references (p. 803-872) and index Series: (Wiley series in probability and mathematical statistics. Applied probability and statistics).

- [12] A.G. Journel and M.E. Rossi, “When do we need a trend model in kriging?,” *Mathematical Geology*, vol. 21, no. 7, pp. 715–739, 1989.
- [13] D. Shepard, “A two-dimensional interpolation function for irregularly-spaced data,” in *Proceedings of the 1968 23rd ACM national conference*. 1968, pp. 517–524, ACM.
- [14] H.C. Huang, N. Cressie, and J. Gabrosek, “Fast, resolution-consistent spatial prediction of global processes from satellite data,” *Journal of Computational and Graphical Statistics*, vol. 11, no. 1, pp. 63–88, 2002.
- [15] S.L. Tzeng, H.C. Huang, and N. Cressie, “A fast, optimal spatial-prediction method for massive datasets,” *Journal of the American Statistical Association*, vol. 100, no. 472, pp. 1343–1357, 2005.
- [16] N. Cressie, T. Shi, and E.L. Kang, “Fixed rank filtering for Spatio-Temporal data,” *Journal of Computational and Graphical Statistics*, vol. 19, no. 3, pp. 724–745, Sept. 2010.
- [17] N. Cressie and G. Johannesson, “Fixed rank kriging for very large spatial data sets,” *Journal of the Royal Statistical Society Series B-Statistical*, vol. 70, pp. 209–226, 2008.
- [18] G. Johannesson, H.C. Huang, and N. Cressie, “Dynamic multi-resolution spatial models,” *Environmental and Ecological Statistics*, vol. 14, no. 1, pp. 5–25, January 2007.
- [19] T. Bailey and T. Gatrell, *Interactive Spatial Data Analysis*, Prentice Hall, 1 edition, June 1995.
- [20] G. Johannesson and N. Cressie, “Finding large-scale spatial trends in massive, global, environmental datasets,” *Environmetrics*, vol. 15, pp. 1–44, 2004.
- [21] Joint Research Centre (JRC)/Netherlands Environmental Assessment Agency (PBL) European Commission, “Emission database for global atmospheric research (EDGAR), release version 4.0,” <http://edgar.jrc.ec.europa.eu>, 2009, Accessed February 10, 2010.
- [22] I. Samoilov and A. Nakhutin, “Estimation and medium-term forecasting of anthropogenic carbon dioxide and methane emission in russia with statistical methods,” *Russian Meteorology and Hydrology*, vol. 34, no. 6, pp. 348–353, June 2009.
- [23] G. Myhre, K. Alterskjaer, and D. Lowe, “A fast method for updating global fossil fuel carbon dioxide emissions,” *Environmental Research Letters*, vol. 4, no. 3, Sept. 2009.
- [24] N. Vardar and Z. Yumurtaci, “Emissions estimation for lignite-fired power plants in turkey,” *Energy Policy*, vol. 38, no. 1, pp. 243–252, Jan. 2010.
- [25] M.G. Cortina-Januchs, J.M. Barron-Adame, A. Vega-Corona, and D. Andina, “Prevision of industrial SO<sub>2</sub> pollutant concentration applying ANNs,” *2009 7TH IEEE Internatinal Conference on Industrial Informatics, VOLS*, pp. 510–515, 2009.
- [26] W. Peters, A.R. Jacobson, C. Sweeney, A.E. Andrews, T.J. Conway, K. Masarie, J.B. Miller, L.M.P. Bruhwiler, G. Ptron, A.I. Hirsch, D.E.J. Worthy, G.R. van der Werf, J.T. Randerson, P.O. Wennberg, Maarten C. Krol, and P.P. Tans, “An atmospheric perspective on north american carbon dioxide exchange: CarbonTracker,” *Proceedings of the National Academy of Sciences*, vol. 104, no. 48, pp. 18925–18930, Nov. 2007.
- [27] ESRL Web Team and NOAA US Department of Commerce, “ESRL global monitoring division - CarbonTracker,” <http://carbontracker.noaa.gov>, 2008.

- [28] P. Musilek and P. Jurus, “Regional-scale modeling of greenhouse gas fluxes,” in *In Proc. of Symposium Reclamation And Restoration Of Boreal Peatland And Forest Ecosystems: Toward A Sustainable Future*, Edmonton, AB, Canada, March 2010, p. 22.
- [29] C.A. Gotway and L.J. Young, “Combining incompatible spatial data,” *Journal of the American Statistical Association*, vol. 97, no. 458, pp. 632–648, 2002.
- [30] S. Weinzierl, “Introduction to Monte Carlo methods,” Internet: <http://arxiv.org/abs/hep-ph/0006269>, June 2000, [Accessed April 04, 2011].
- [31] N. Cressie, “Fitting variogram models by weighted least squares,” *Mathematical Geology*, vol. 17, no. 5, pp. 563–586, July 1985.
- [32] D.L. Zimmerman and M.B. Zimmerman, “A comparison of spatial semivariogram estimators and corresponding ordinary kriging predictors,” *Technometrics*, vol. 33, no. 1, pp. 77–91, 1991.
- [33] P. Diamond and M. Armstrong, “Robustness of variograms and conditioning of kriging matrices,” *Journal of the International Association for Mathematical Geology*, vol. 16, no. 8, pp. 809–822, 1984.
- [34] A.G. Journel and Ch.J. Huijbregts, *Mining Geostatistics*, Academic Press, Feb. 1978.
- [35] X. Jiang, R.A. Olea, and Y.S. Yu, “Semivariogram modeling by weighted least squares,” *Computers & Geosciences*, vol. 22, no. 4, pp. 387–397, May 1996.
- [36] A. Singh and A.K. Singh, “Trend removal in spatially correlated datasets,” *Mathematical Geology*, vol. 28, no. 1, pp. 111–132, 1996.
- [37] M.R. Holdaway, “Spatial modeling and interpolation of monthly temperature using kriging,” *Climate Research*, vol. 6, no. 3, pp. 215–225, June 1996.
- [38] F.L. Bookstein, “Principal warps: thin-plate splines and the decomposition of deformations,” *Pattern Analysis and Machine Intelligence, IEEE Transactions on*, vol. 11, no. 6, pp. 567–585, 1989.
- [39] G. Wahba, *Spline models for observational data*, SIAM, Sept. 1990.
- [40] T.H. Li, “Multiscale representation and analysis of spherical data by spherical wavelets,” *SIAM Journal on Scientific Computing*, vol. 21, no. 3, pp. 924–953, Dec. 1999.
- [41] “Eigen 2: C++ template library for linear algebra,” [http://http://eigen.tuxfamily.org/](http://eigen.tuxfamily.org/).
- [42] T.A. Davis, “Algorithm 832: UMFPACK v4.3—an unsymmetric-pattern multifrontal method,” *ACM Trans. Math. Softw.*, vol. 30, no. 2, pp. 196–199, 2004.
- [43] S. Magnussen, E. Nsset, and M.A. Wulder, “Efficient multiresolution spatial predictions for large data arrays,” *Remote Sensing of Environment*, vol. 109, no. 4, pp. 451–463, Aug. 2007.
- [44] NIST/SEMATECH, “Nist/sematech e-handbook of statistical methods,” <http://www.itl.nist.gov/div898/handbook/>, June 2003, Accessed August 10, 2010.

- [45] Socioeconomic Data and Applications Center (SEDAC), “Gridded population of the world version 3 (GPWv3): Population grids,” Tech. Rep., Center for International Earth Science Information Network (CIESIN), Columbia University; and Centro Internacional de Agricultura Tropical (CIAT), 2005, <http://sedac.ciesin.columbia.edu/gpw>, Accessed March 15, 2010.
- [46] Socioeconomic Data and Applications Center (SEDAC), “Gridded population of the world version 3 (GPWv3): National identifier grid,” Tech. Rep., Center for International Earth Science Information Network (CIESIN), Columbia University; and Centro Internacional de Agricultura Tropical (CIAT), 2005, <http://sedac.ciesin.columbia.edu/gpw>, Accessed March 15, 2010.
- [47] Climatic Research Unit, School of Environmental Sciences, University of East Anglia, “Absolute temperatures for the base period 1961-90,” <http://www.cru.uea.ac.uk/cru/data/temperature/>, December 2009, Accessed October 7, 2010.
- [48] Earth Science Division, Goddard Institute for Space Studies, National Aeronautic and Space Administration, “GISS surface temperature analysis temperature anomaly data,” <http://data.giss.nasa.gov/gistemp/>, 2010, Accessed February 10, 2010.
- [49] S.S. Lee, “World development indicators,” Tech. Rep., The World Bank, 2010, <http://data.worldbank.org/data-catalog/world-development-indicators>, Accessed October 20, 2010.
- [50] L. Breiman, “Random forests,” *Machine Learning*, vol. 45, no. 1, pp. 5–32, Oct. 2001.
- [51] L. Breiman, J. Friedman, C.J. Stone, and R.A. Olshen, *Classification and Regression Trees*, Wadsworth International Group, 1 edition, Jan. 1984.
- [52] L. Breiman, M. Last, and J. Rice, “Random forests: Finding quasars,” *Statistical Challenges in Astronomy*, pp. 243–254, 2003.
- [53] Andy Liaw and Matthew Wiener, “Classification and regression by randomforest,” *R News*, vol. 2, no. 3, pp. 18–22, 2002.
- [54] R Development Core Team, *R: A Language and Environment for Statistical Computing*, R Foundation for Statistical Computing, Vienna, Austria, 2008, ISBN 3-900051-07-0.
- [55] G.B. Huang, Q.Y. Zhu, and C.K. Siew, “Extreme learning machine: a new learning scheme of feedforward neural networks,” in *Neural Networks, 2004. Proceedings. 2004 IEEE International Joint Conference on*, 2004, vol. 2, pp. 985–990 vol.2.
- [56] T. Oda and S. Maksyutov, “A very high-resolution (1 km  $\times$  1 km) global fossil fuel CO<sub>2</sub> emission inventory derived using a point source database and satellite observations of nighttime lights,” *Atmos. Chem. Phys.*, vol. 11, no. 2, pp. 543–556, Jan. 2011.
- [57] T. Yokota, Y. Yoshida, N. Eguchi, Y. Ota, T. Tanaka, H. Watanabe, and S. Maksyutov, “Global concentrations of CO<sub>2</sub> and CH<sub>4</sub> retrieved from gosat: First preliminary results,” *SOLA*, vol. 5, pp. 160–163, 2009.
- [58] J.B. Boisvert, J.G. Manchuk, and C.V. Deutsch, “Kriging in the presence of locally varying anisotropy using Non-Euclidean distances,” *Mathematical Geosciences*, vol. 41, no. 5, pp. 585–601, 2009.

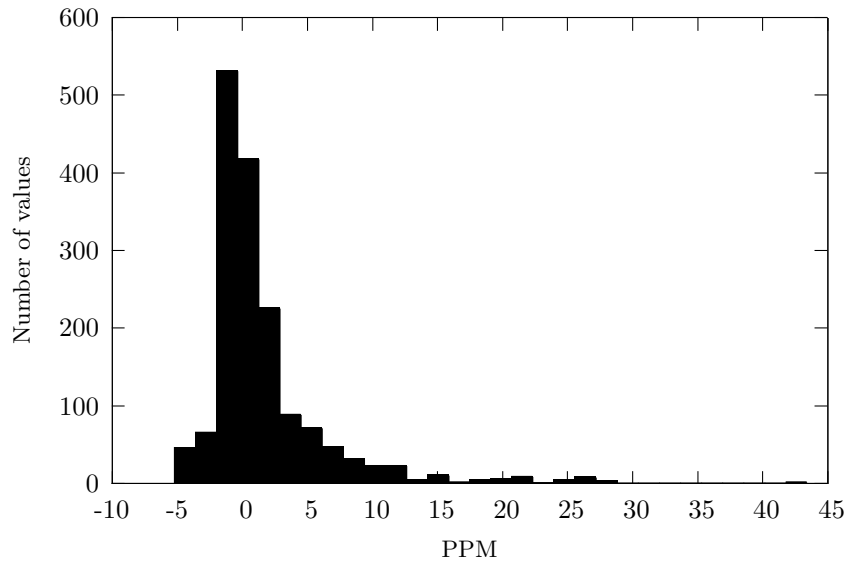
- [59] Center for Global Development, “Carbon monitoring for action (CARMA),” <http://www.carma.org>, 2010, Accessed May 25, 2010.
- [60] D. Wheeler and K. Ummel, “Calculating CARMA: global estimation of CO<sub>2</sub> emissions from the power sector,” Tech. Rep., Center for Global Development, May 2008.

## Appendix A

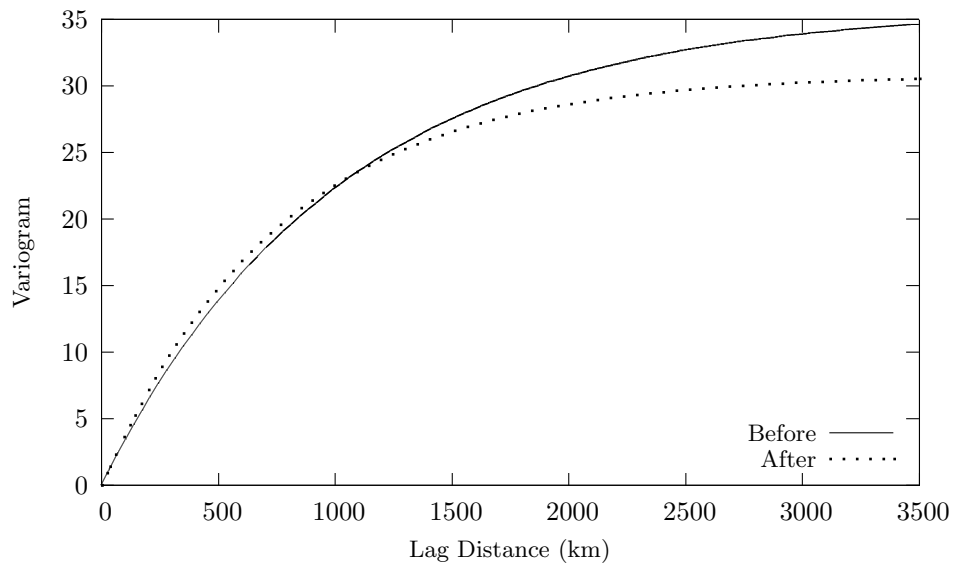
# Missing Data Prediction Supplementary Material

### A.1 Complete Graphs

#### A.1.1 Detrending

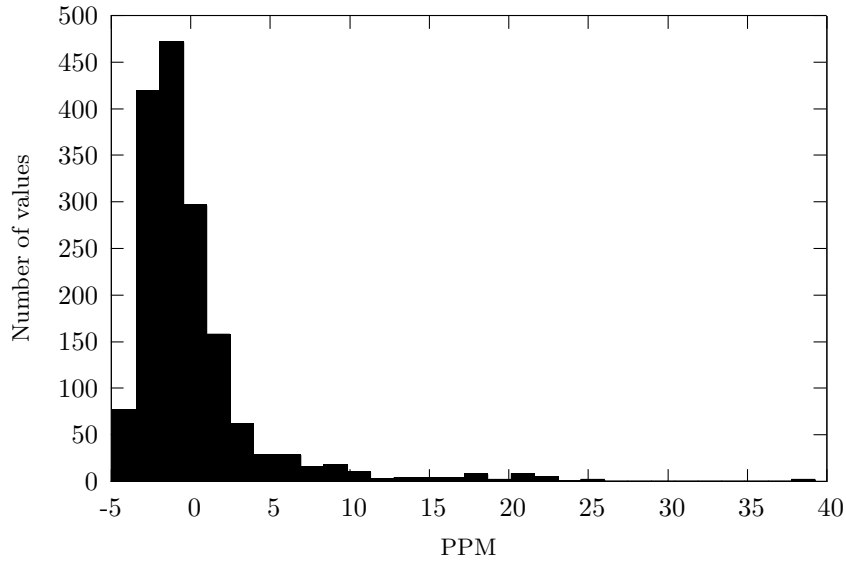


(a) Histogram of residual values after detrending.

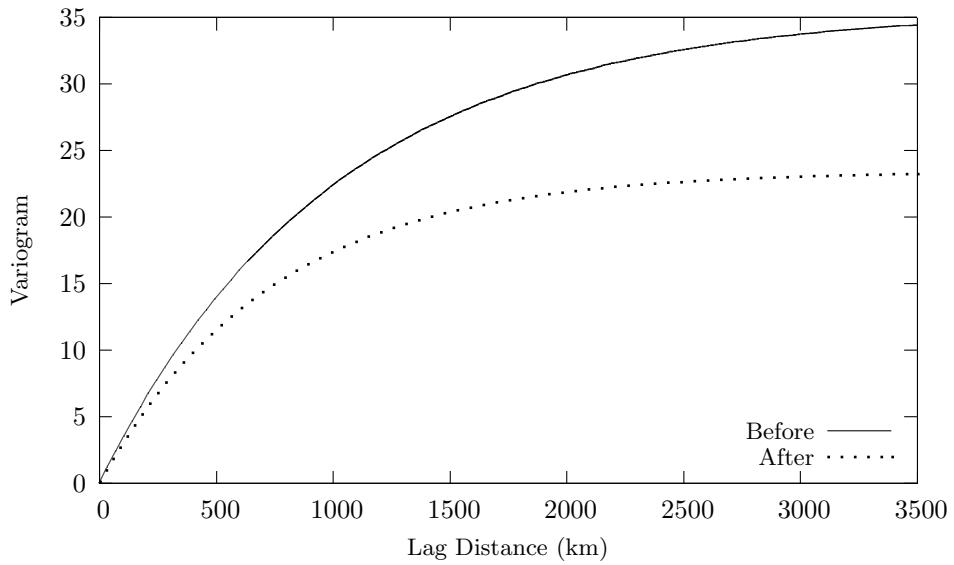


(b) Fit variograms before and after detrending.

Figure A.1: Effect of 1st order GLS detrending on CT data

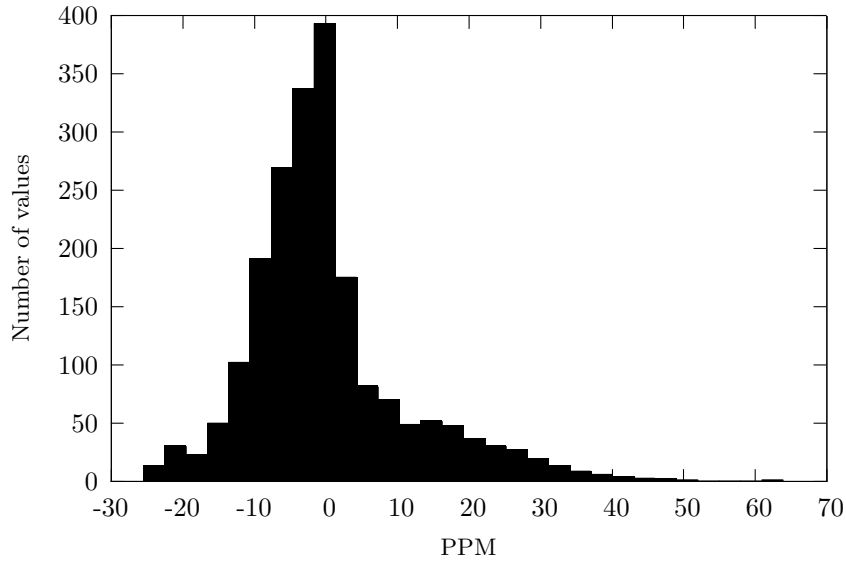


(a) Histogram of residual values after detrending.

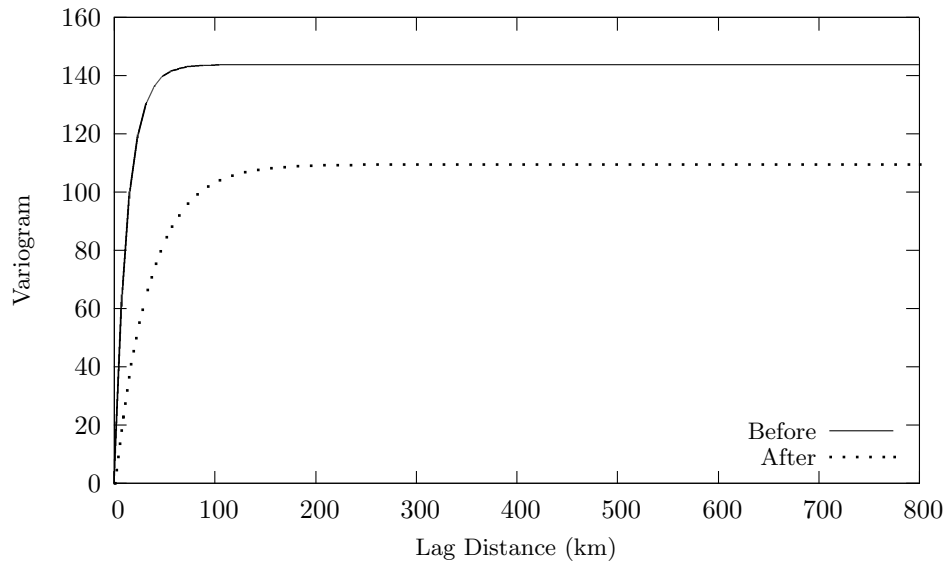


(b) Fit variograms before and after 3rd order GLS Detrending.

Figure A.2: Effect of 3rd order GLS detrending on CT data.

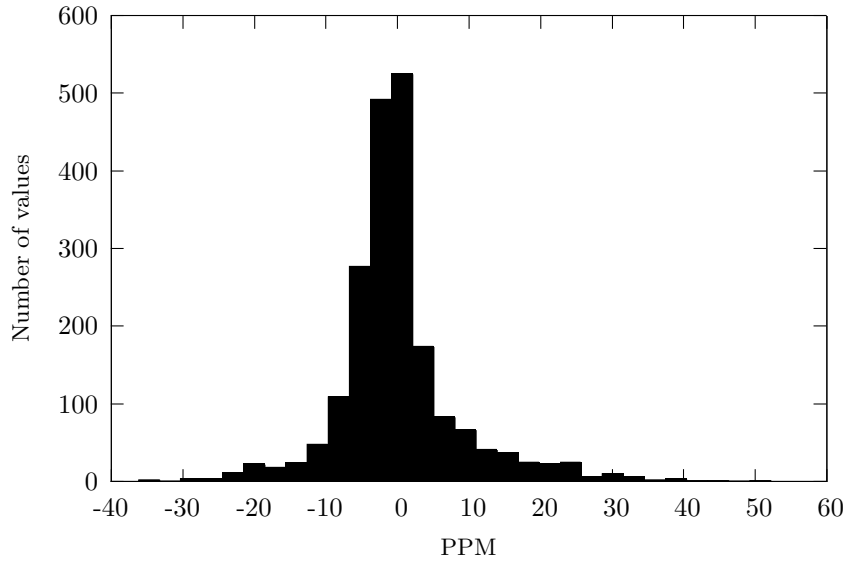


(a) Histogram of residual values after detrending.

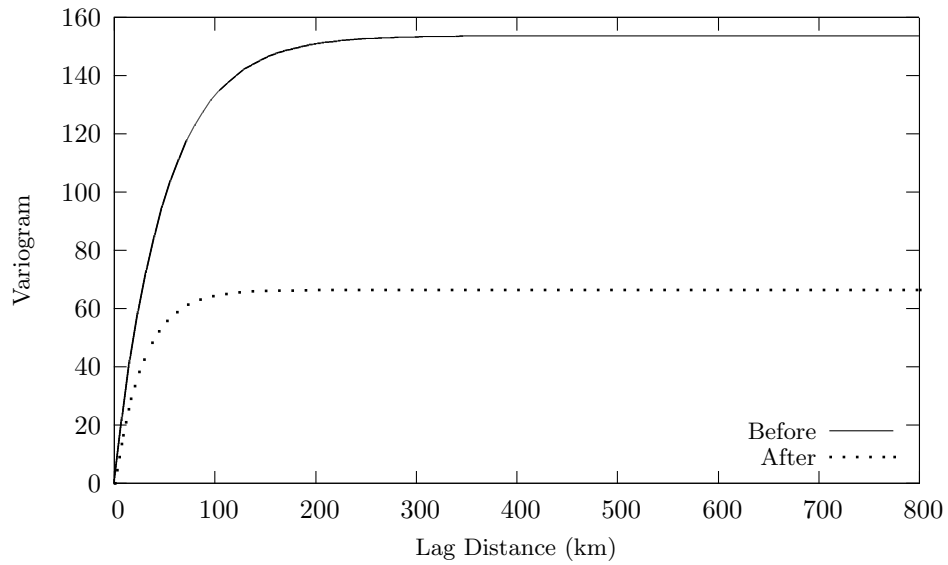


(b) Fit variograms before and after detrending.

Figure A.3: Effect of 1st order GLS detrending on MO data

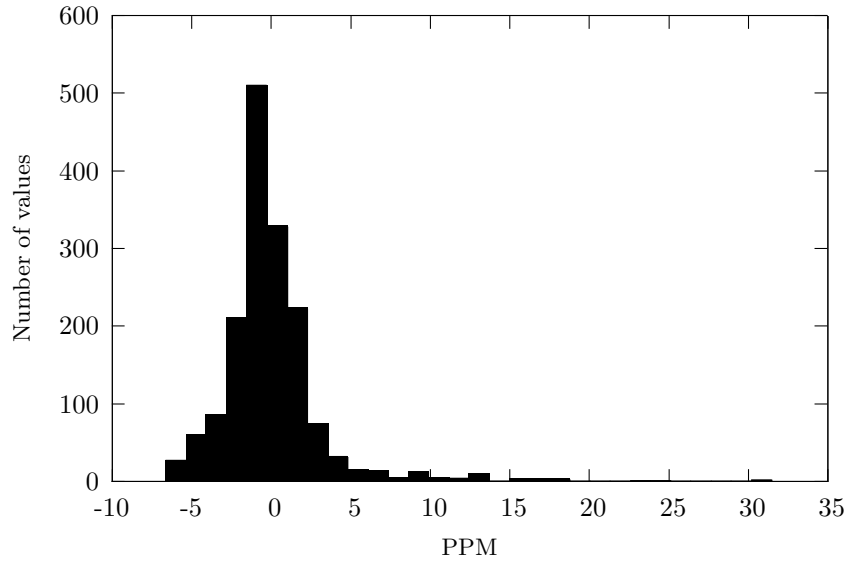


(a) Histogram of residual values after detrending.

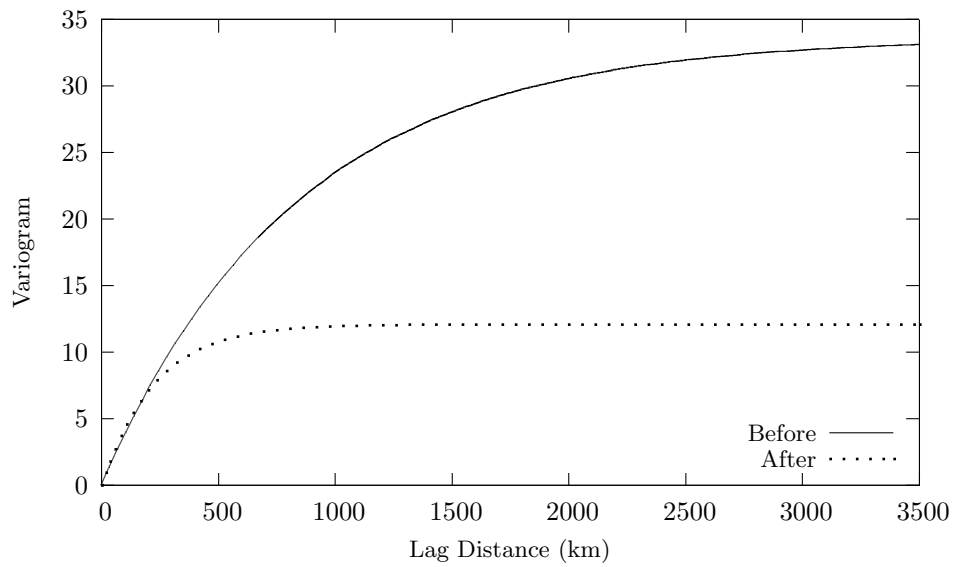


(b) Fit variograms before and after detrending.

Figure A.4: Effect of 3rd order GLS detrending on MO data.

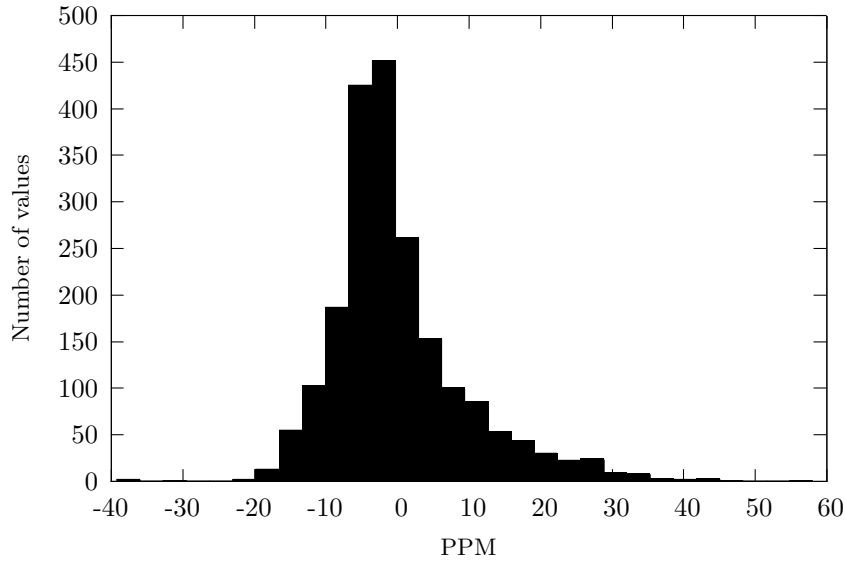


(a) Histogram of residual values after detrending.

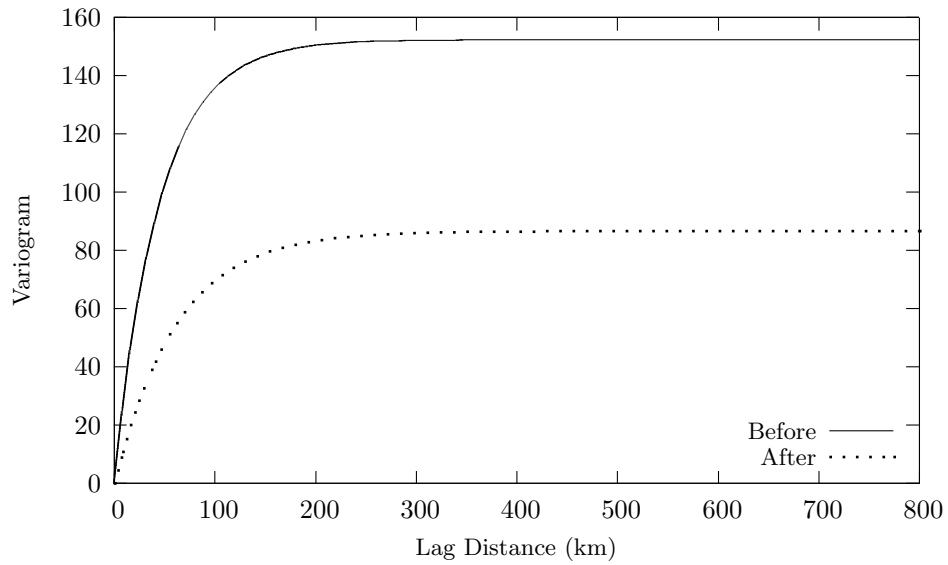


(b) Fit variograms before and after detrending.

Figure A.5: Effect of 3rd level FRS detrending on CT data.



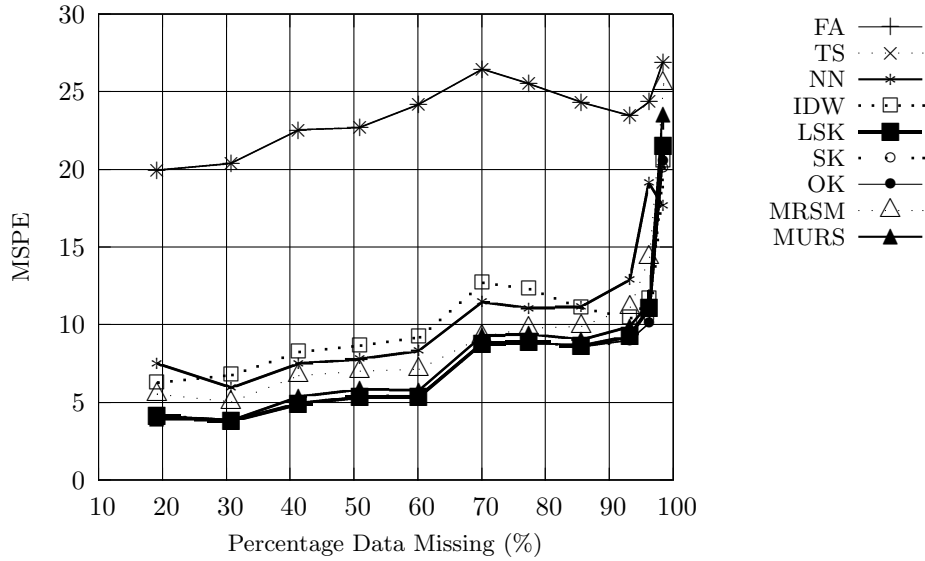
(a) Histogram of residual values after detrending.



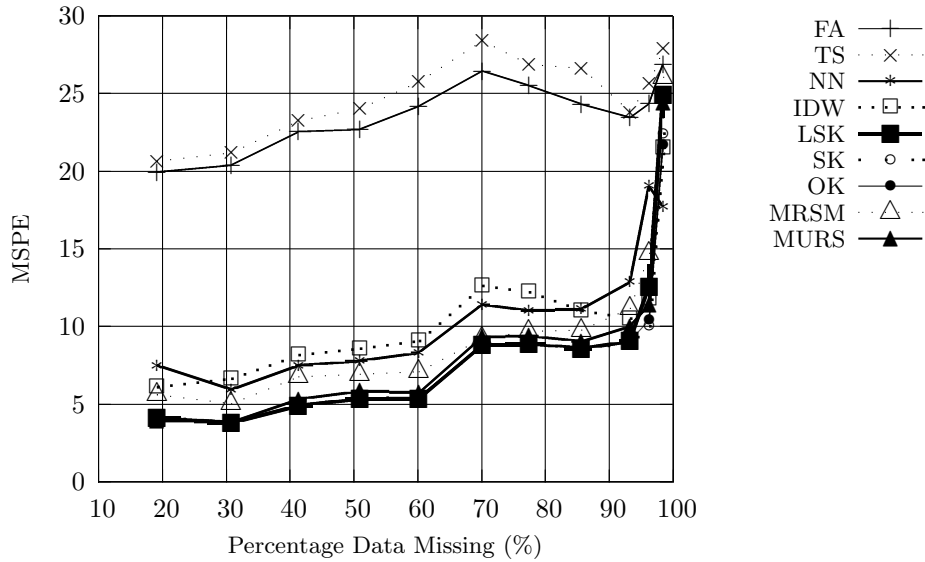
(b) Fit variograms before and after detrending.

Figure A.6: Effect of 3rd level FRS detrending on MO data.

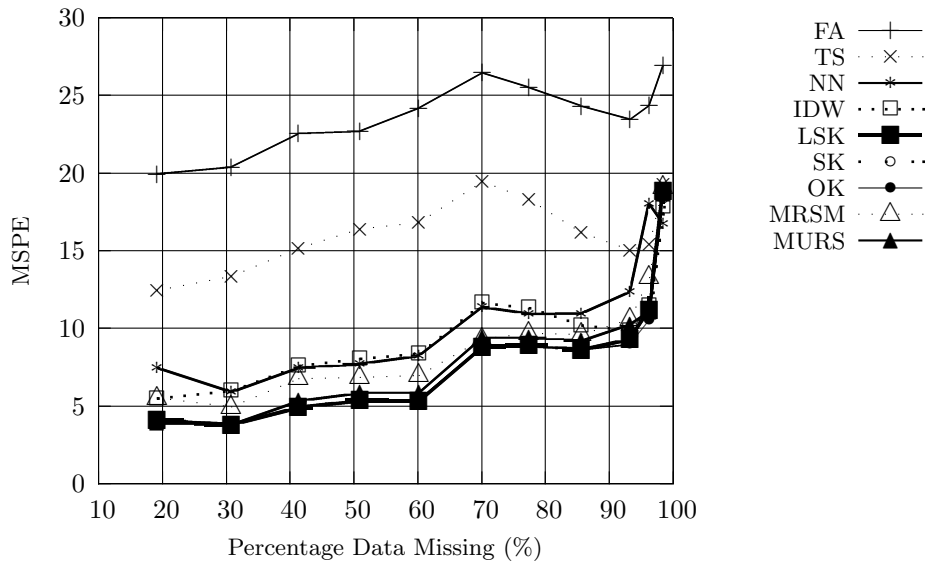
### A.1.2 Error Graphs



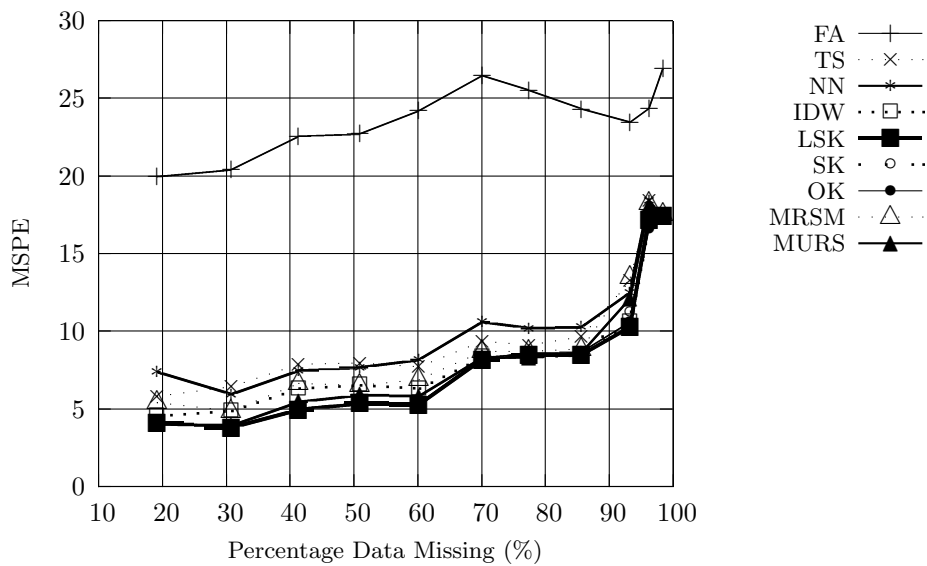
(a) Simple mean removal, MSPE.



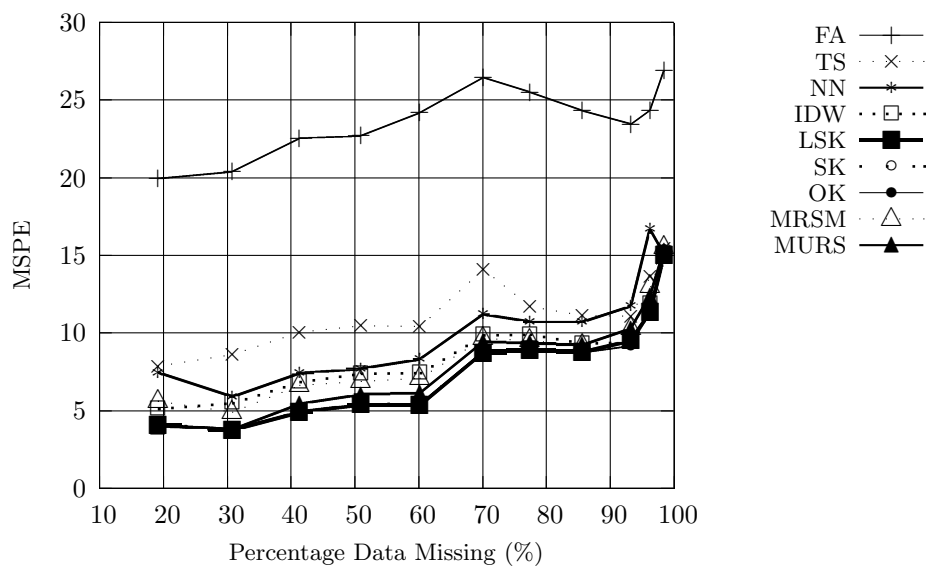
(b) 1st order GLS detrending, MSPE.



(c) 3rd order GLS detrending, MSPE.

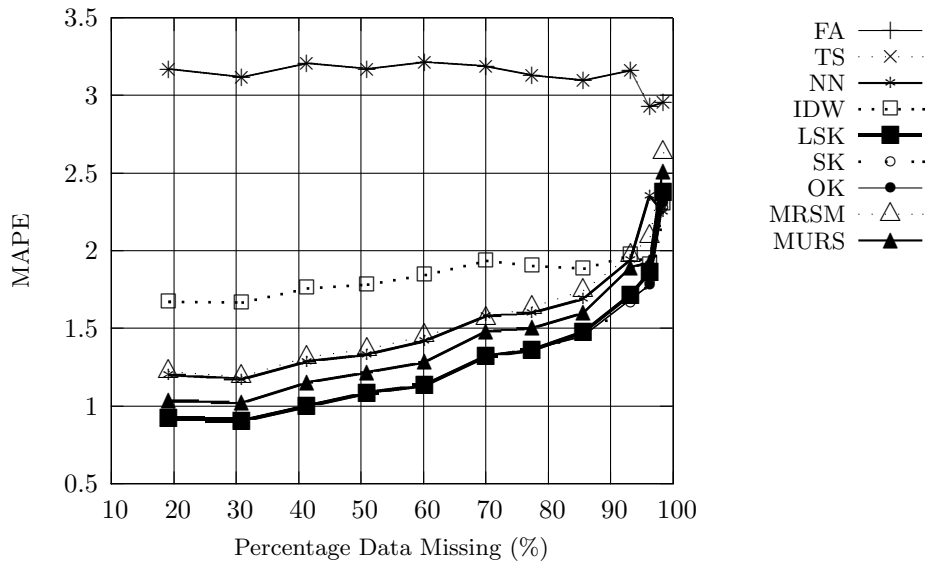


(d) 3rd level ATPS detrending, MSPE.

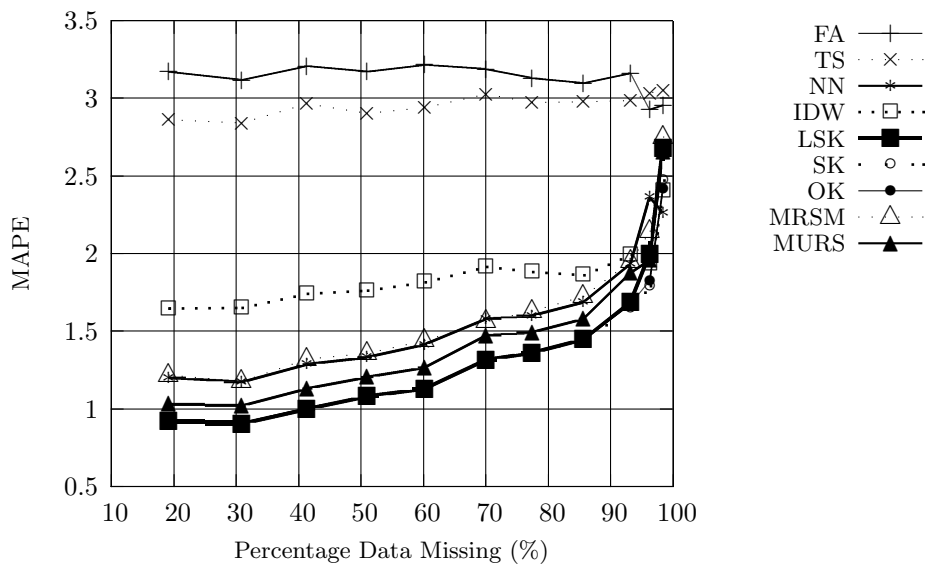


(e) 3rd level FRS detrending, MSPE.

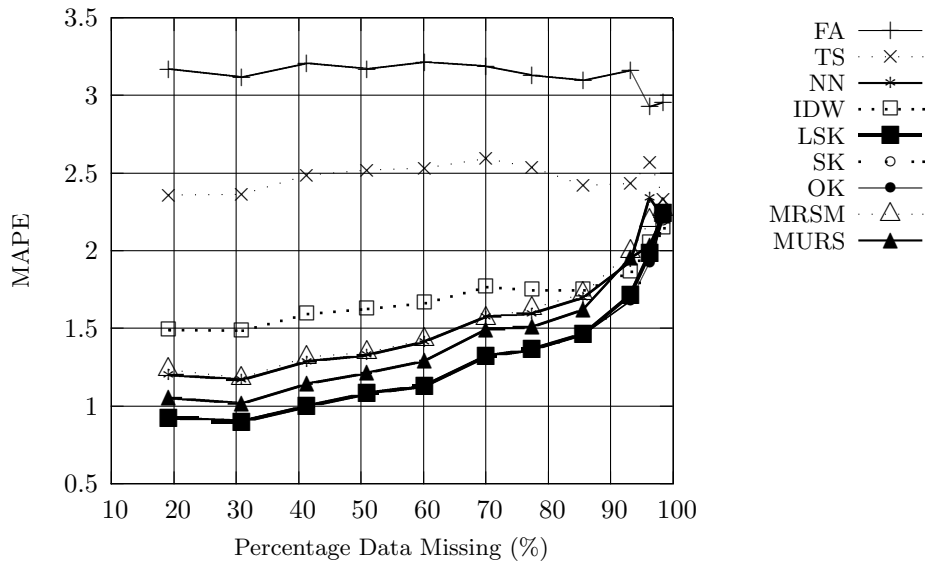
Figure A.7: MSPE comparisons for different detrending methods applied to CT data.



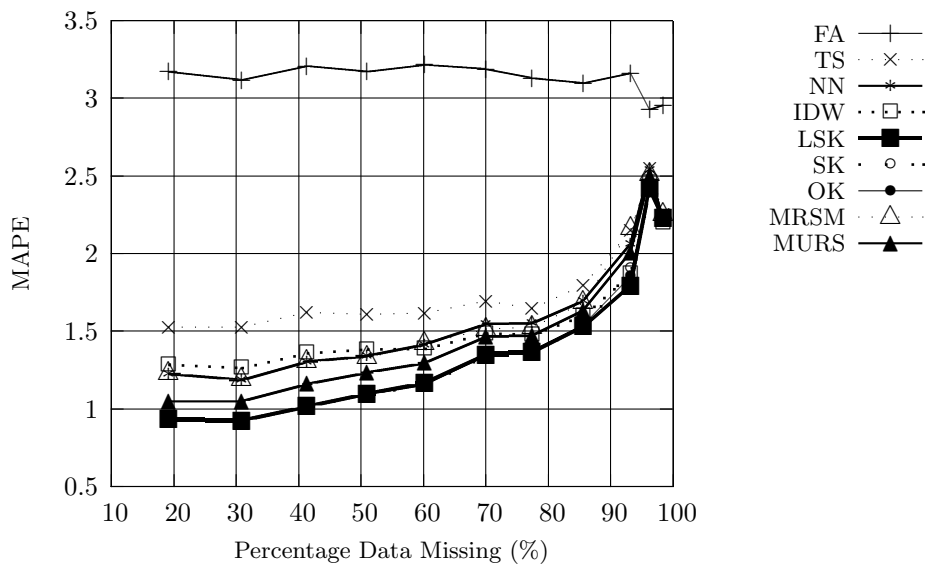
(a) Simple mean removal, MAPE.



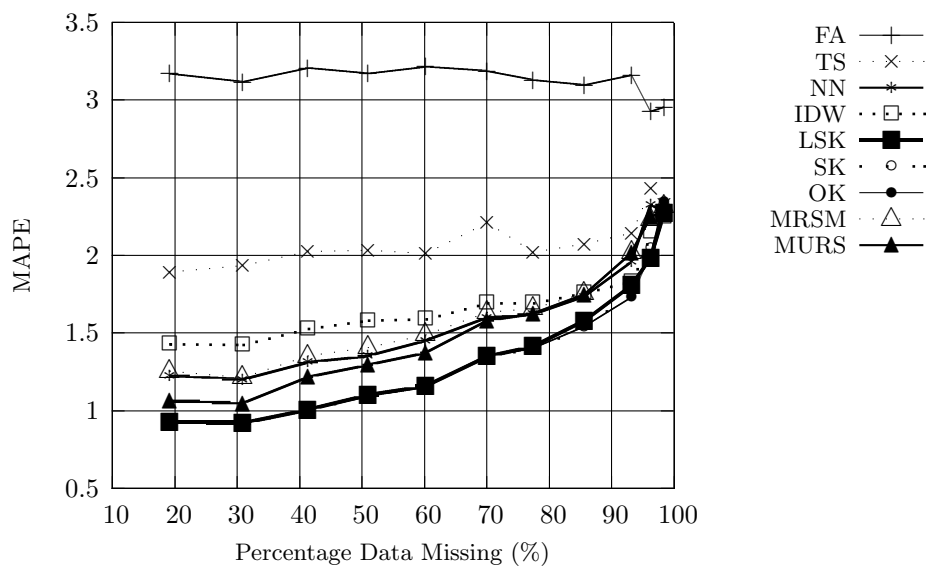
(b) 1st order GLS detrending, MAPE.



(c) 3rd order GLS detrending, MAPE.

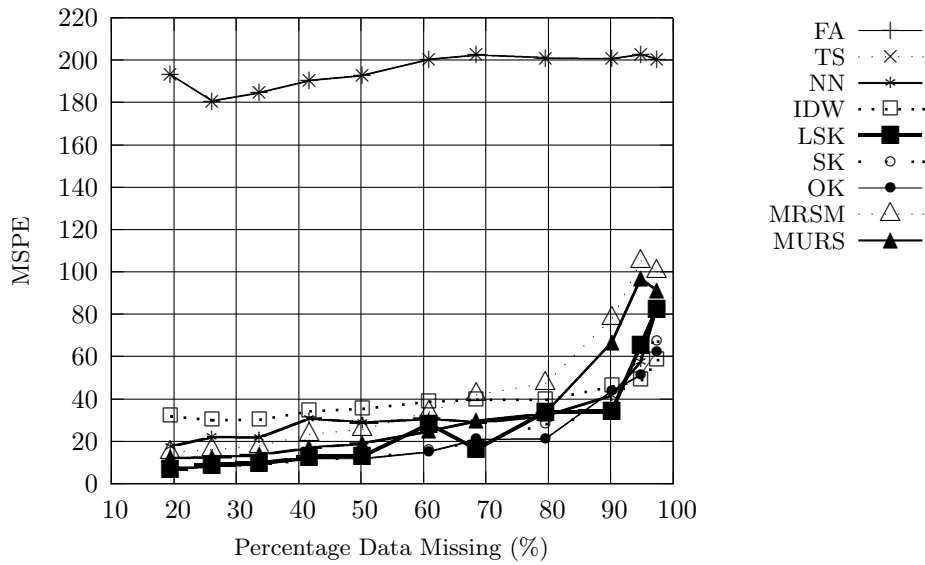


(d) 3rd level ATPS detrending, MAPE.

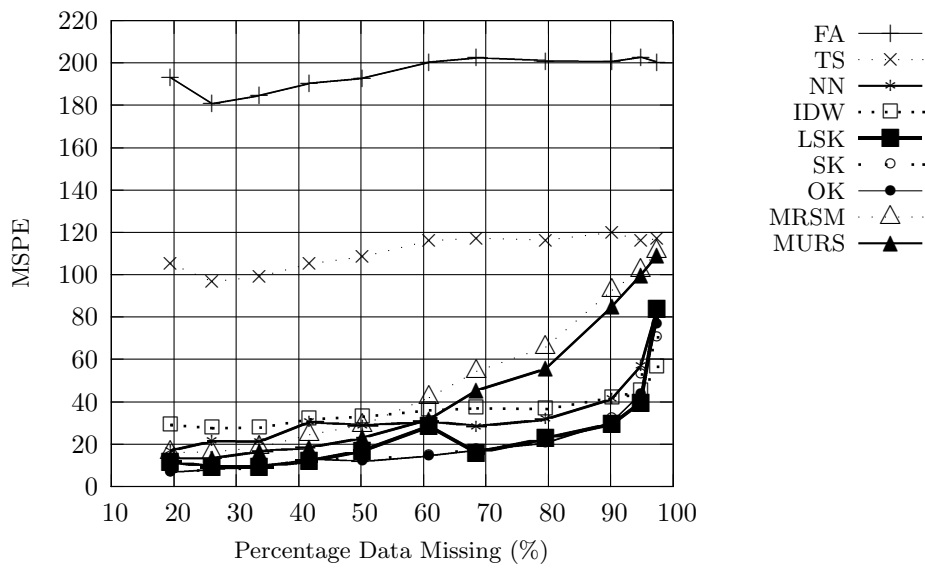


(e) 3rd level FRS detrending, MAPE.

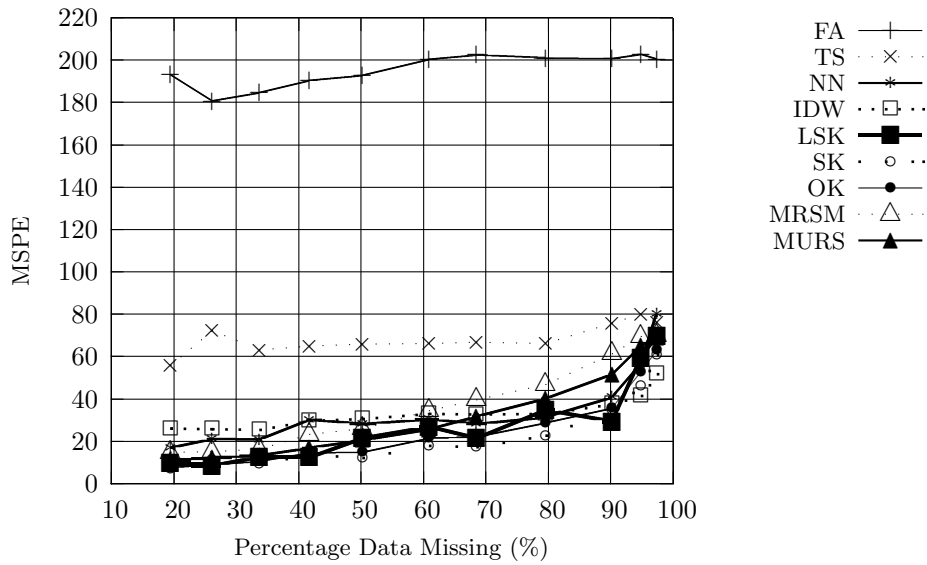
Figure A.8: MAPE comparisons for different detrending methods applied to RR CT data.



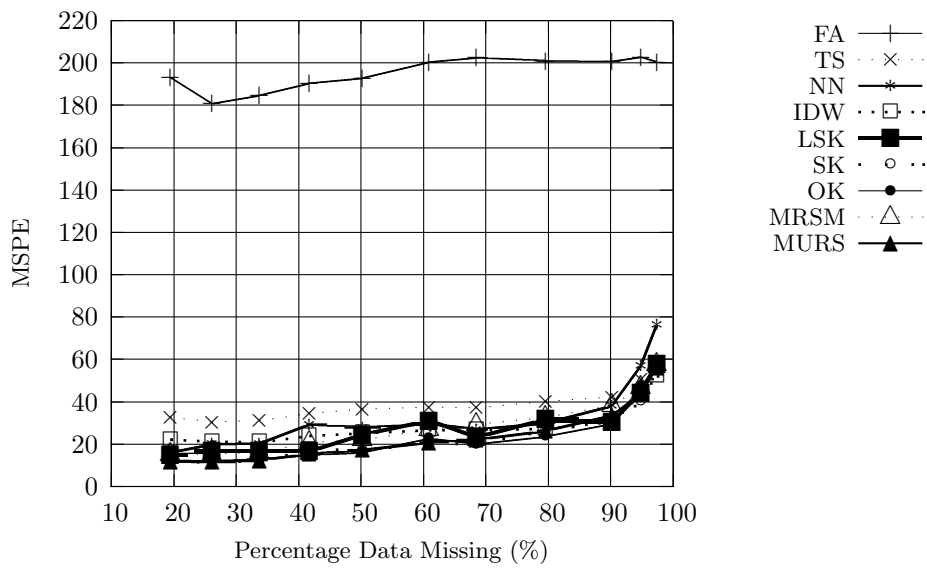
(a) Simple mean removal, MSPE.



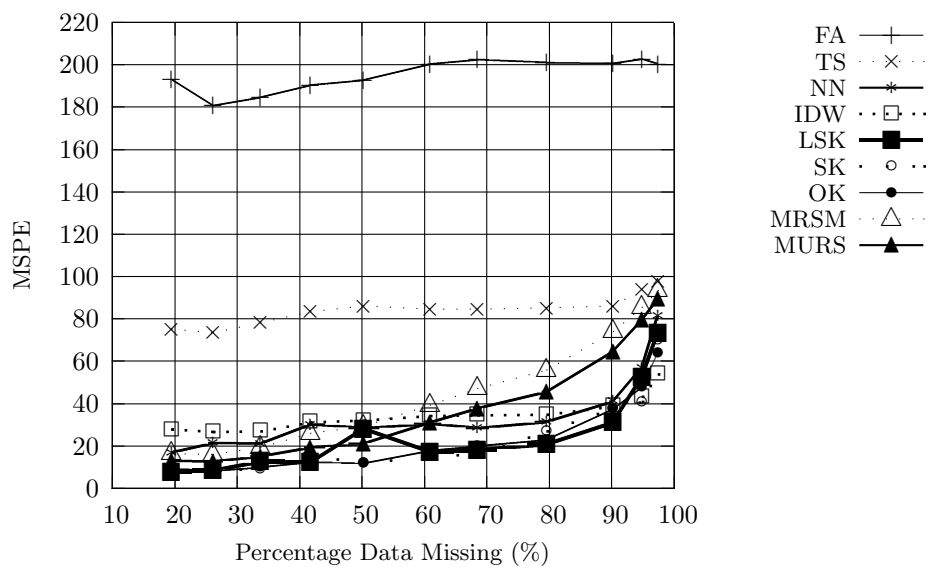
(b) 1st order GLS detrending, MSPE.



(c) 3rd order GLS detrending, MSPE.

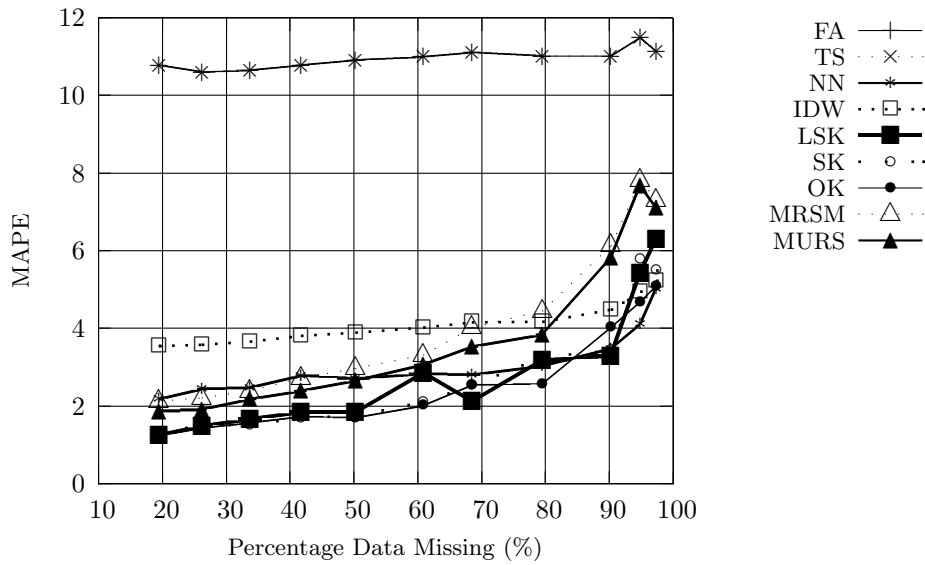


(d) 3rd level ATPS detrending, MSPE.

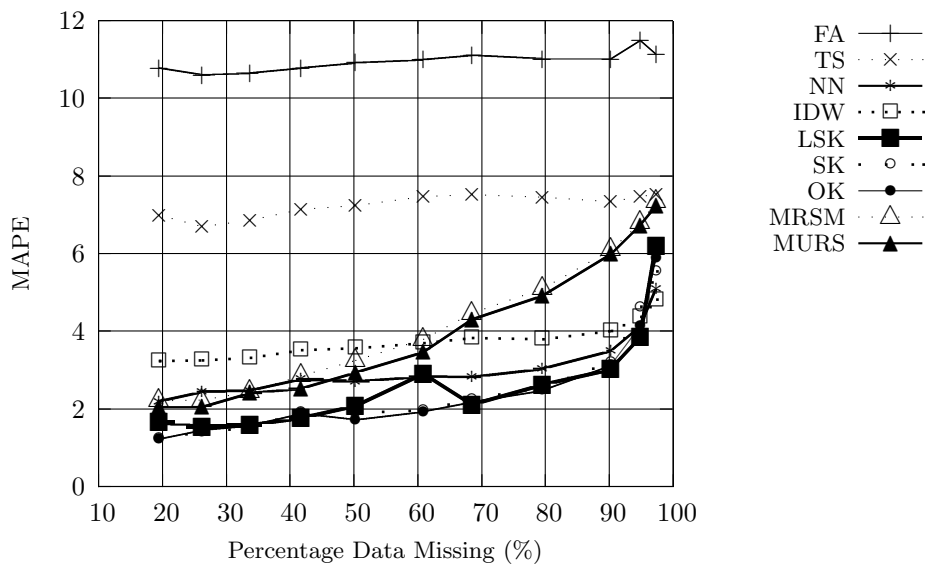


(e) 3rd level FRS detrending, MSPE.

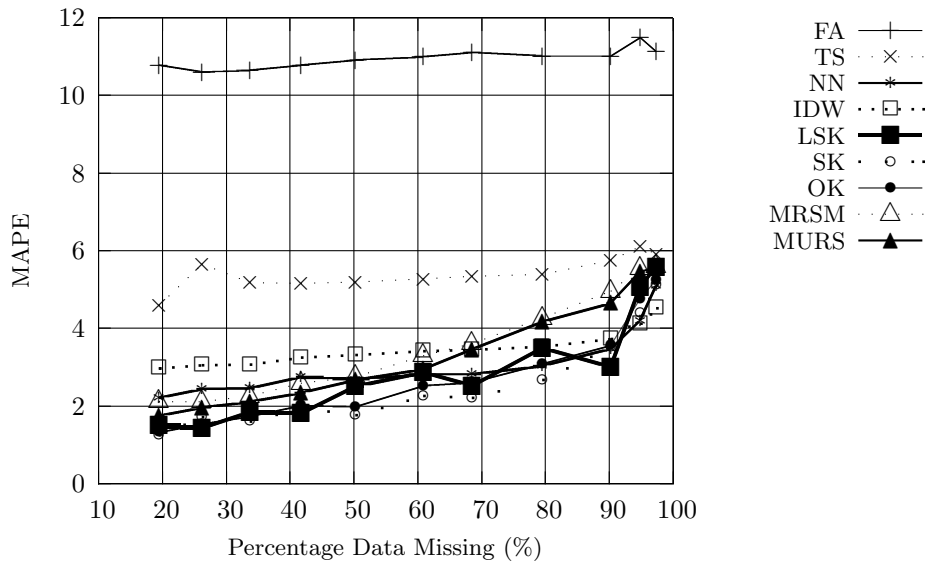
Figure A.9: MSPE comparison for different detrending methods applied to RR MO data.



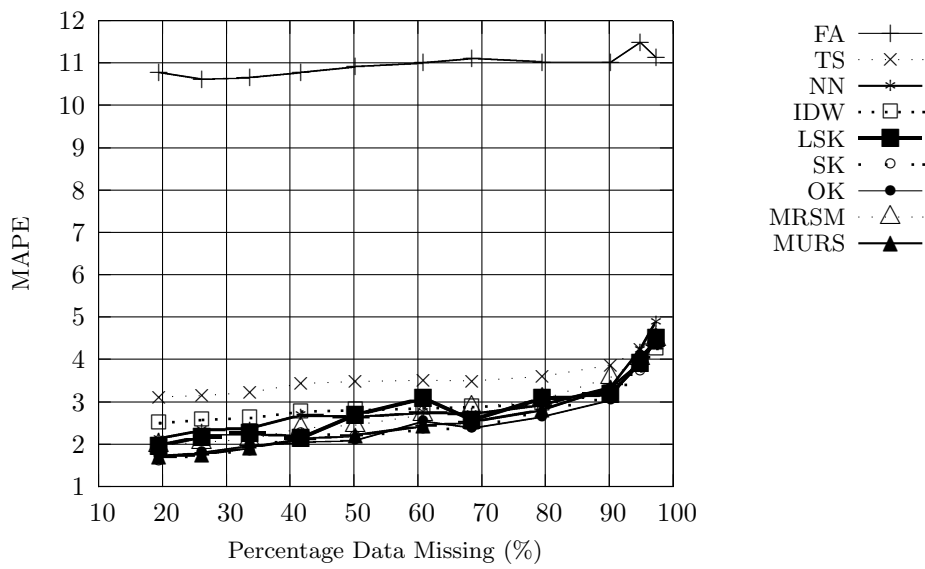
(a) Simple mean removal, MAPE.



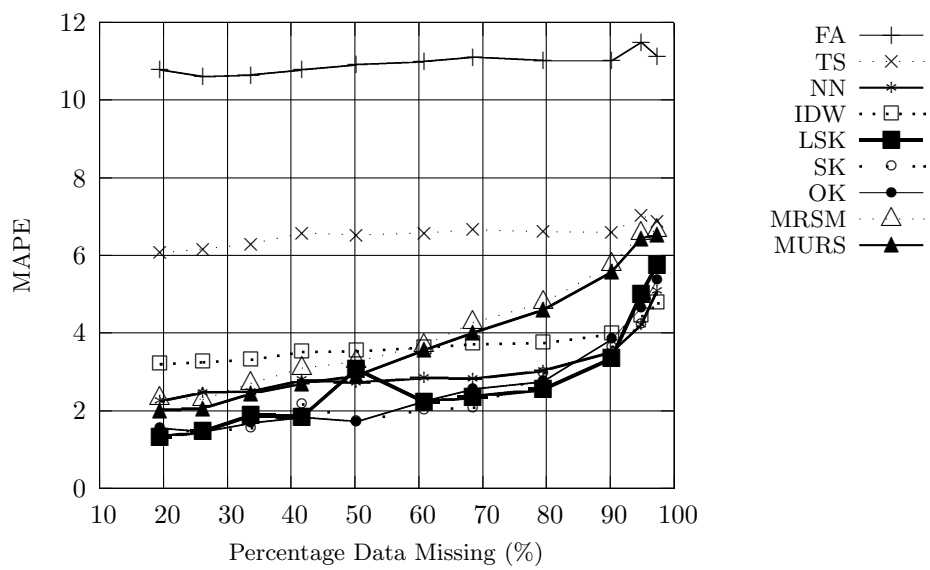
(b) 1st order GLS detrending, MAPE.



(c) 3rd order GLS detrending, MAPE.

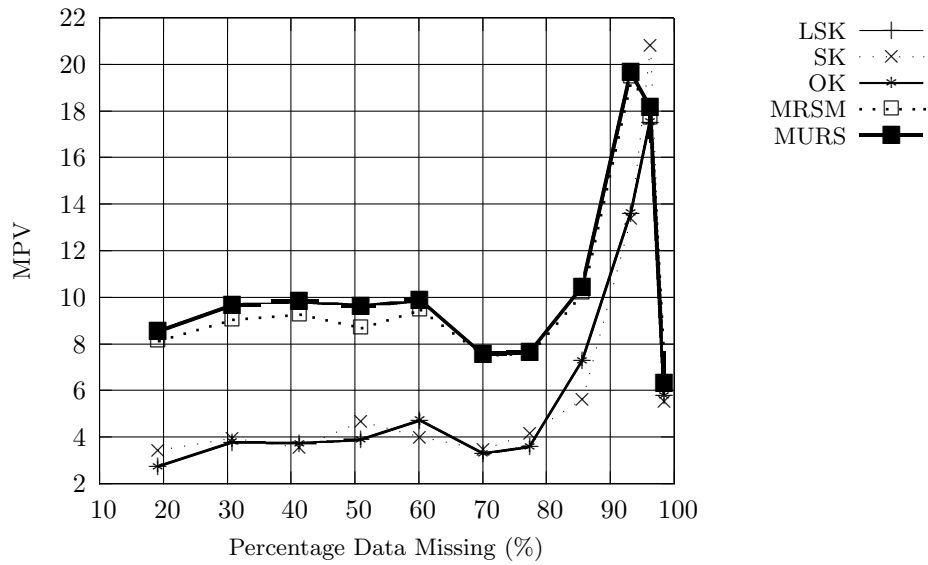


(d) 3rd level ATPS detrending, MAPE.

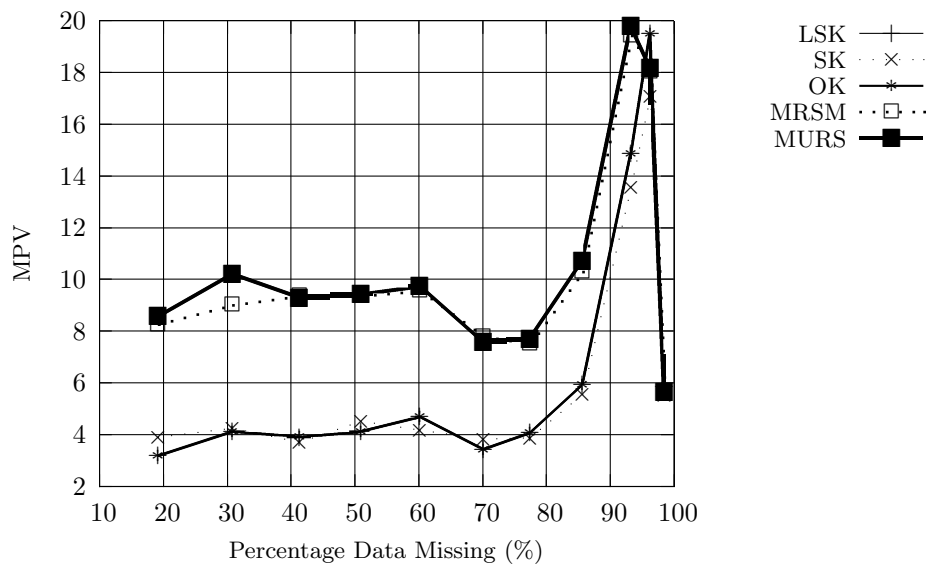


(e) 3rd level FRS detrending, MAPE.

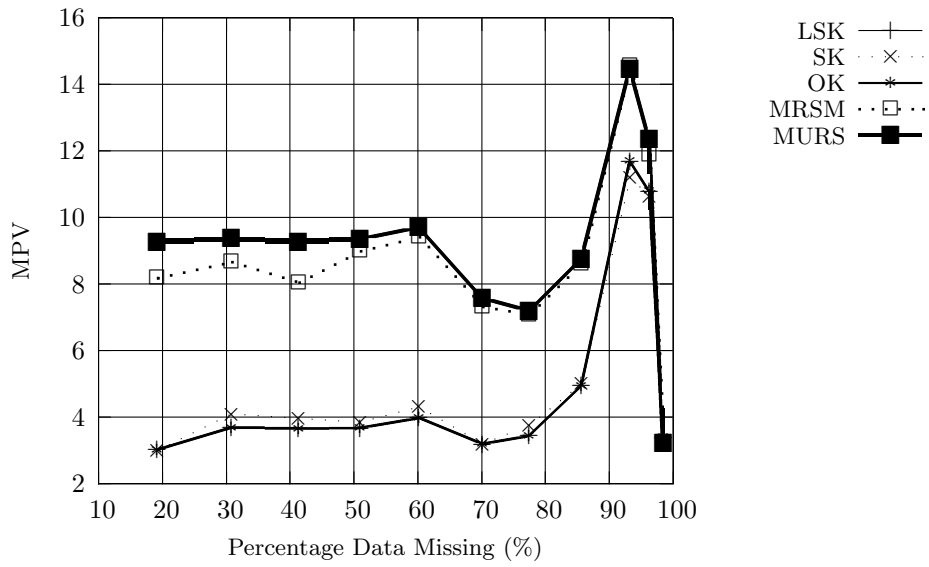
Figure A.10: MAPE comparison for different detrending methods applied to RR MO data.



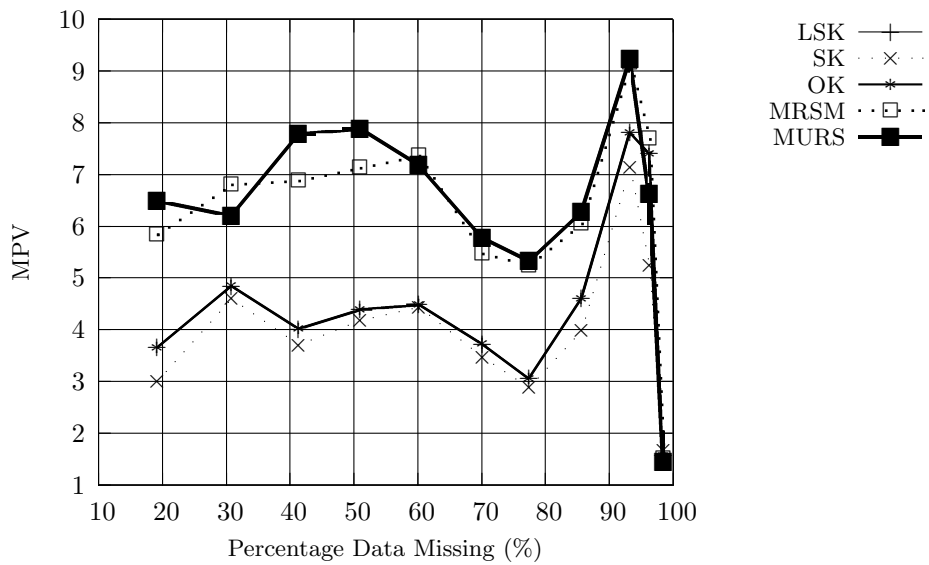
(a) Simple mean removal, MPV.



(b) 1st order GLS detrending, MPV.

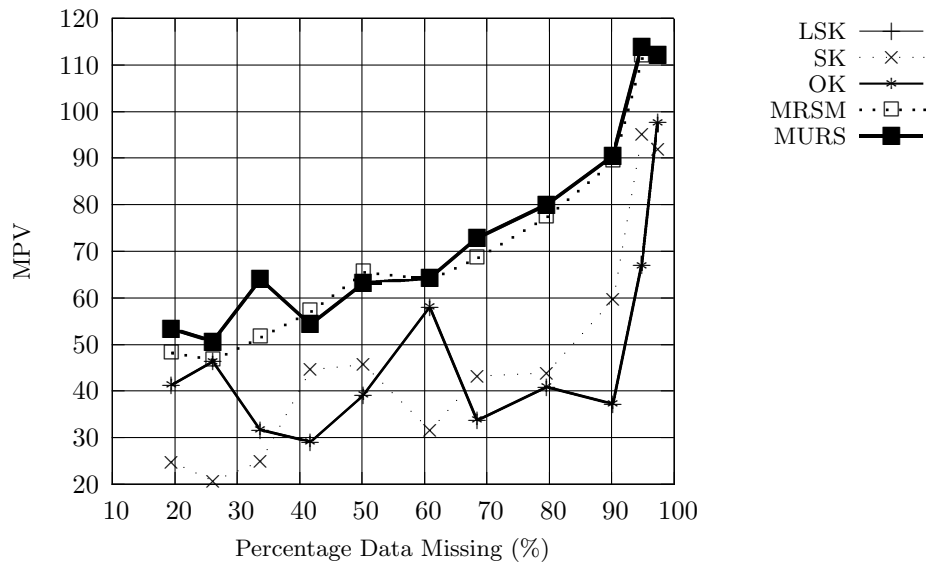


(c) 3rd order GLS detrending, MPV.

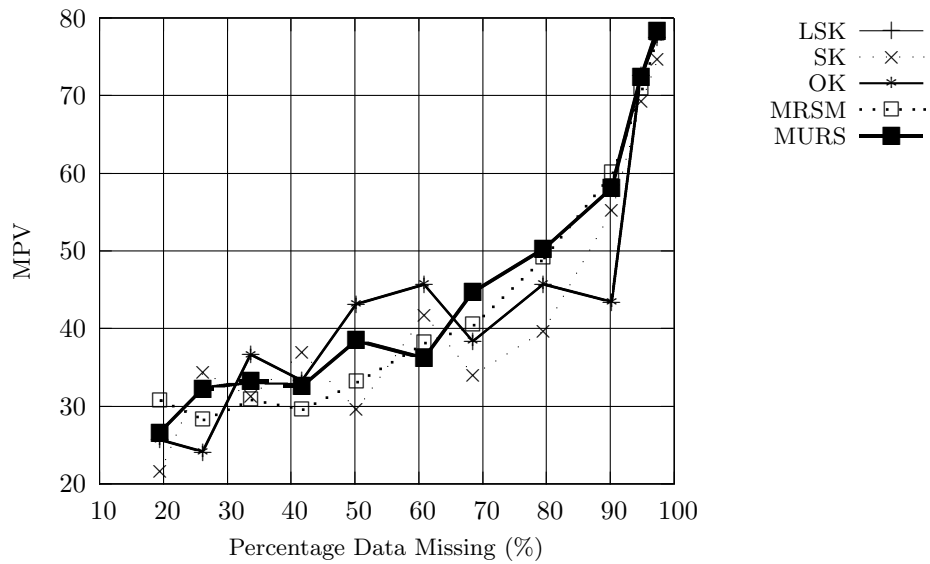


(d) 3rd level FRS detrending, MPV.

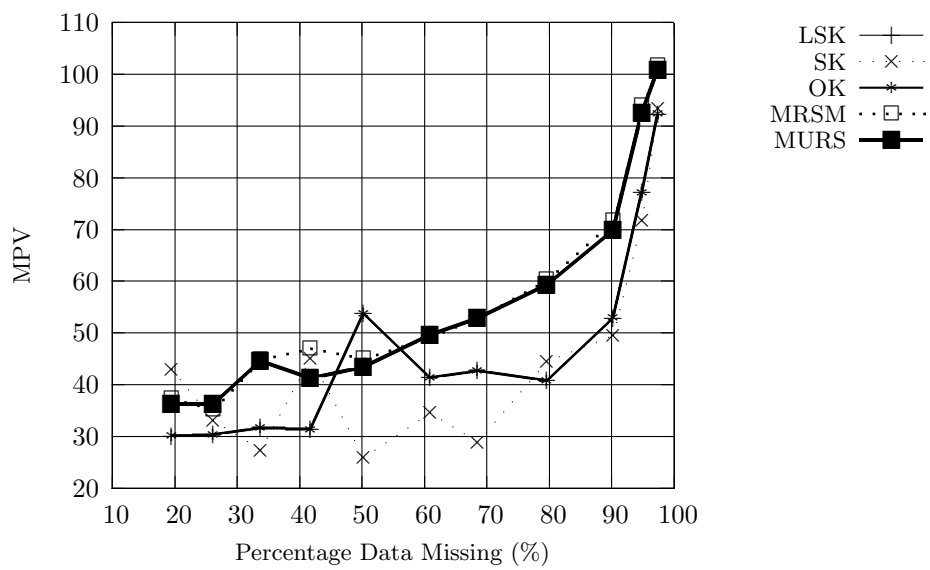
Figure A.11: MPV comparisons for different detrending methods applied to RR CT data.



(a) 1st order GLS detrending, MPV.

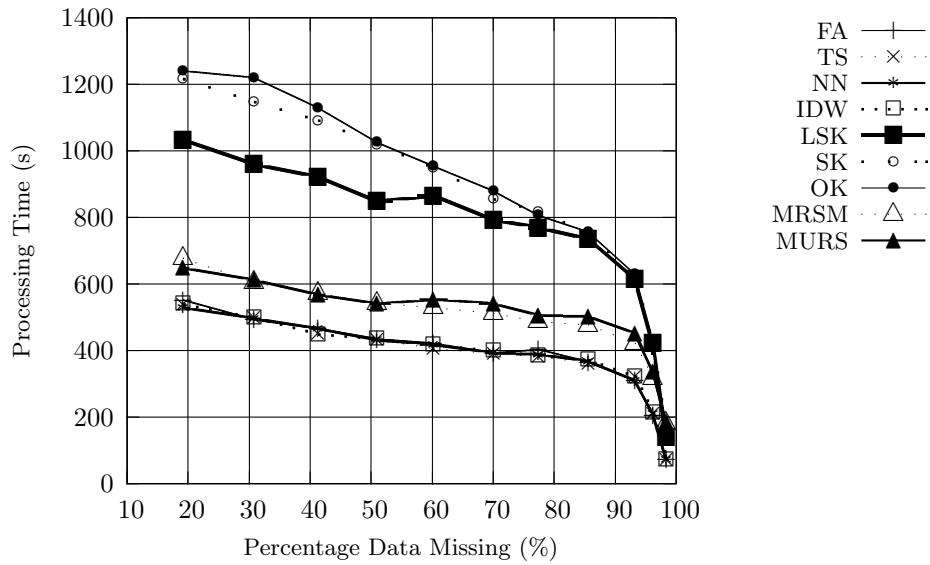


(b) 3rd order GLS detrending, MPV.

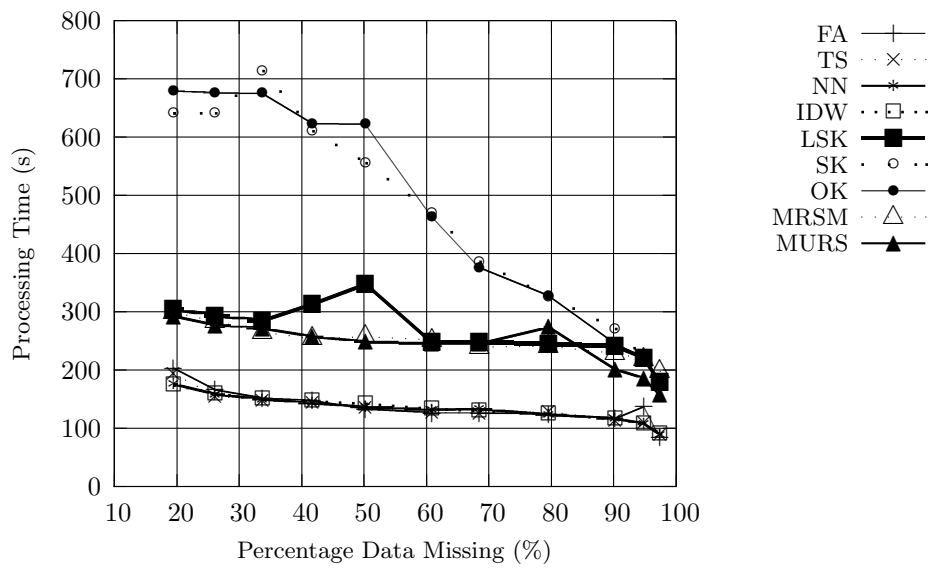


(c) 3rd level FRS detrending, MPV.

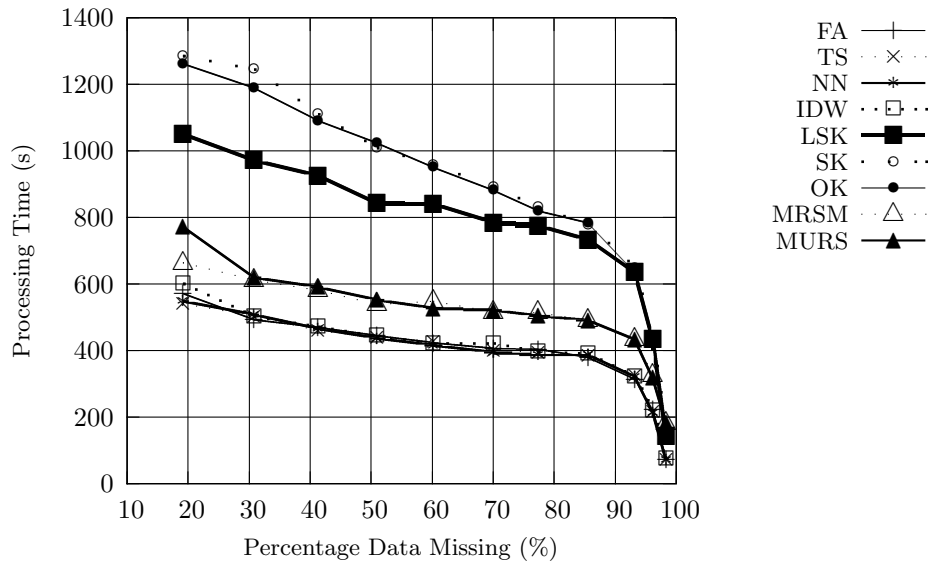
Figure A.12: MPV comparison for different detrending methods applied to RR MO data.



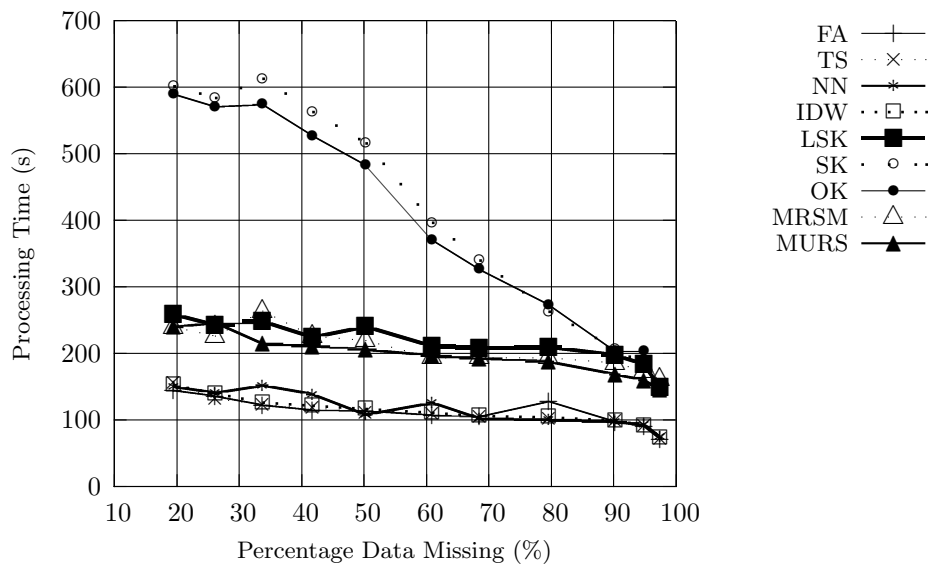
(a) CT data, 1st order GLS detrending, time.



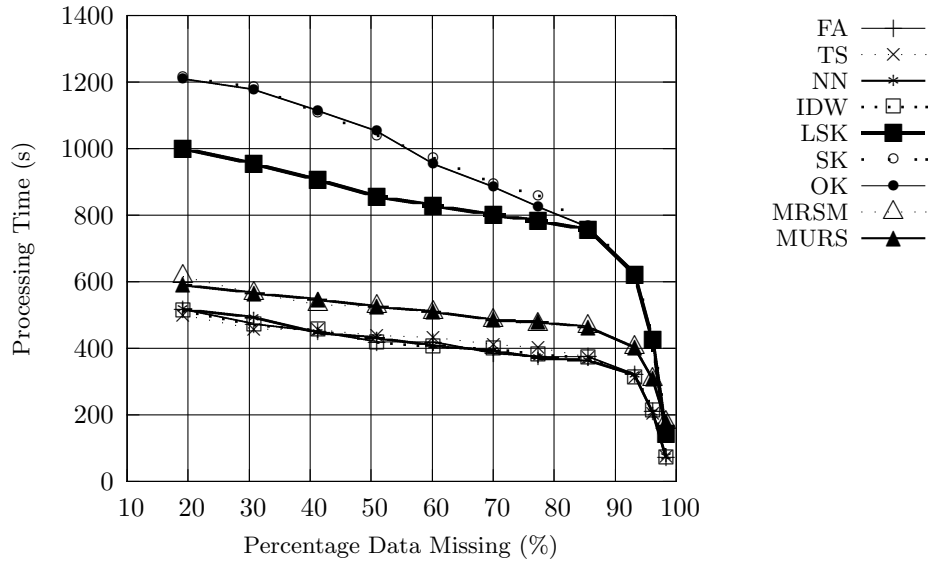
(b) MO data, 1st order GLS detrending, time.



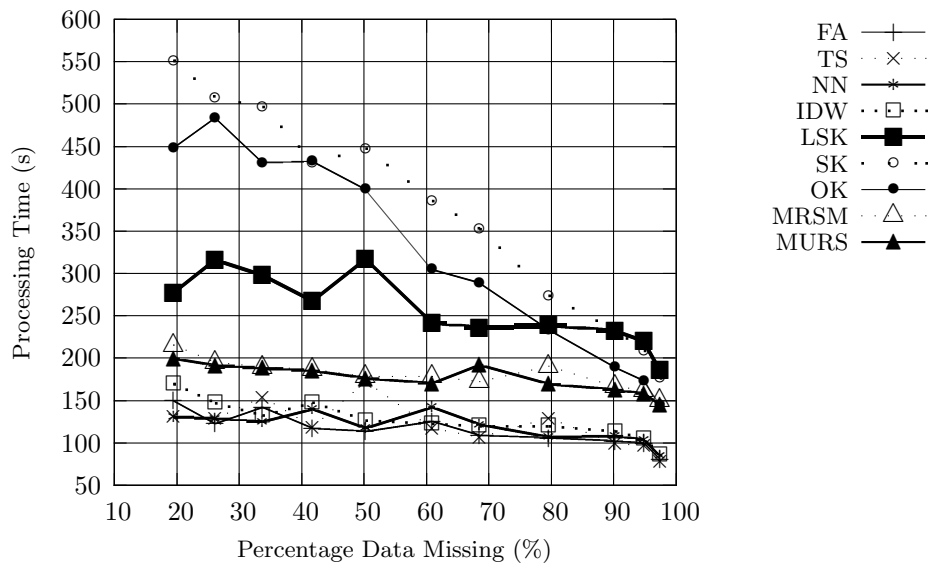
(c) CT data, 3rd order GLS detrending, time.



(d) MO data, 3rd order GLS detrending, time.

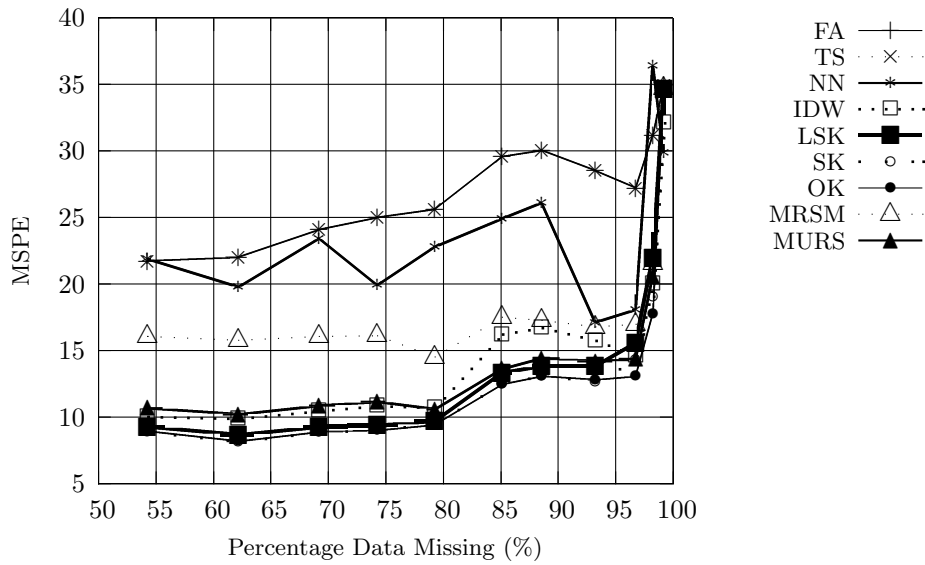


(e) CT data, 3rd level ATPS detrending, time.

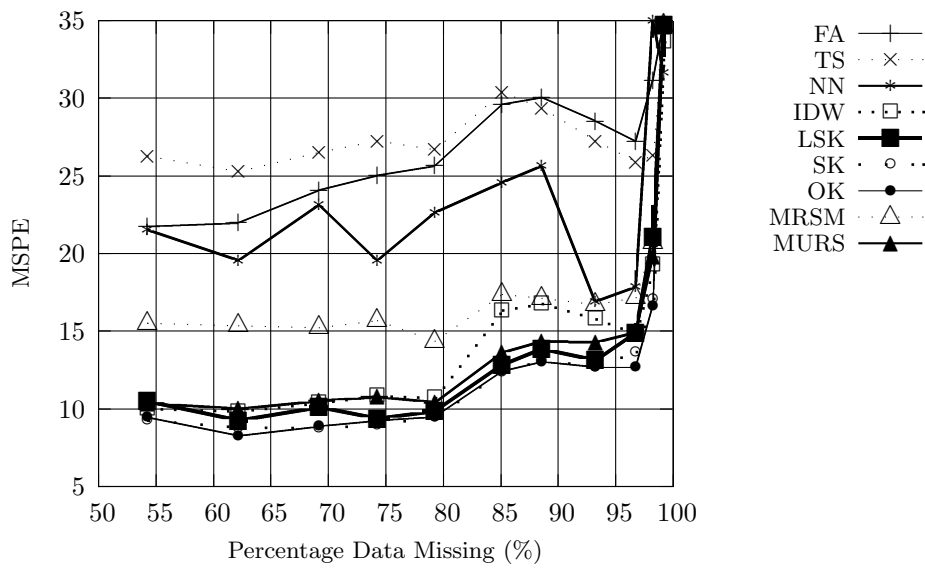


(f) MO data, 3rd level ATPS detrending, time.

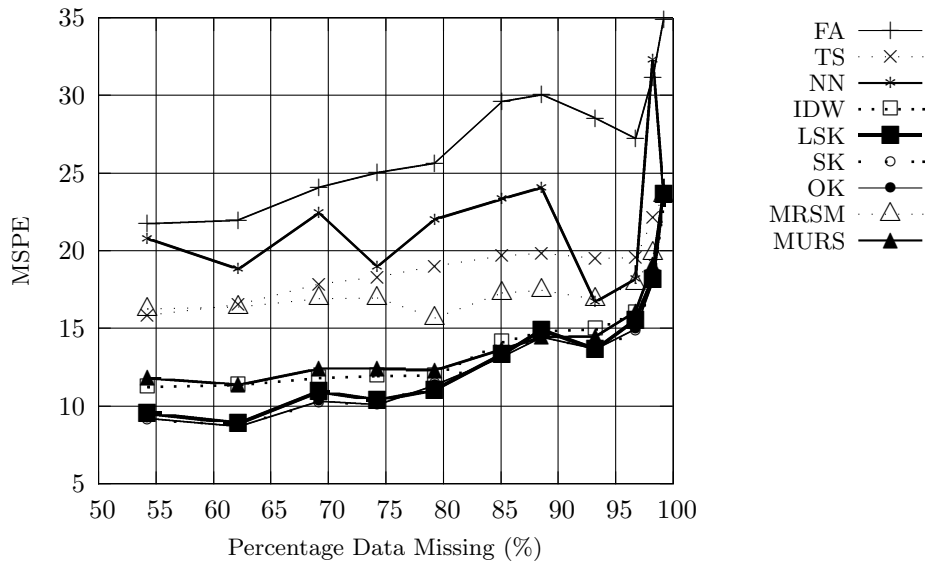
Figure A.13: Processing time comparisons (RR data).



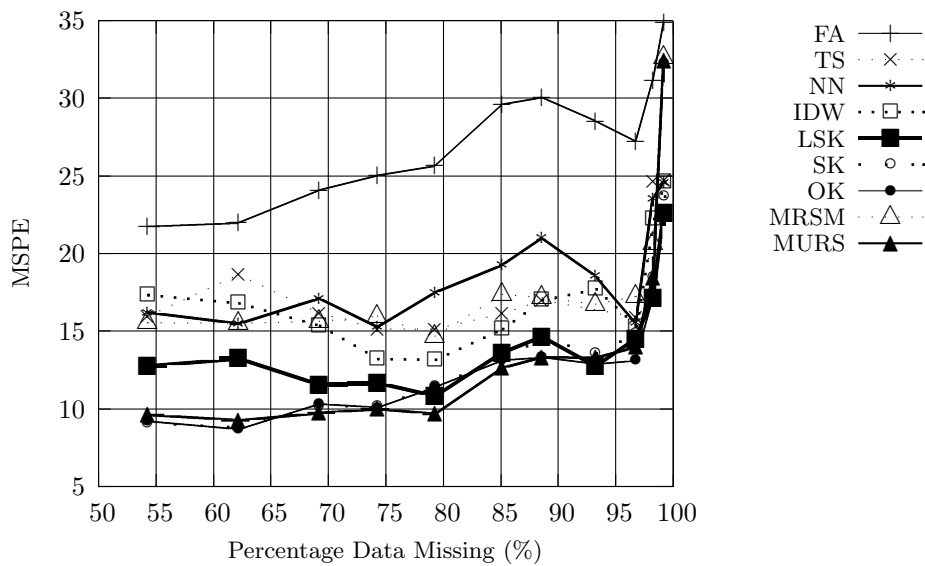
(a) Simple mean removal, MSPE.



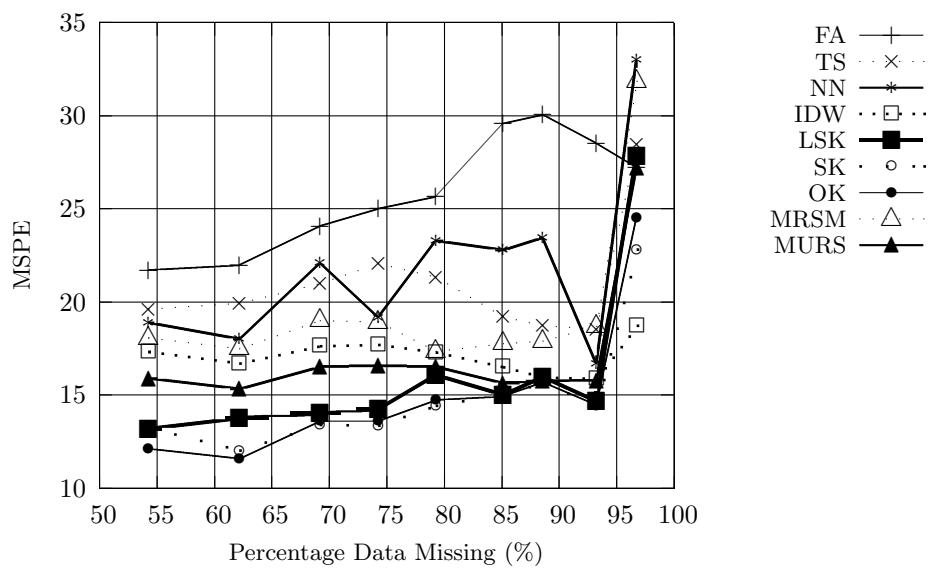
(b) 1st order GLS detrending, MSPE.



(c) 3rd order GLS detrending, MSPE.

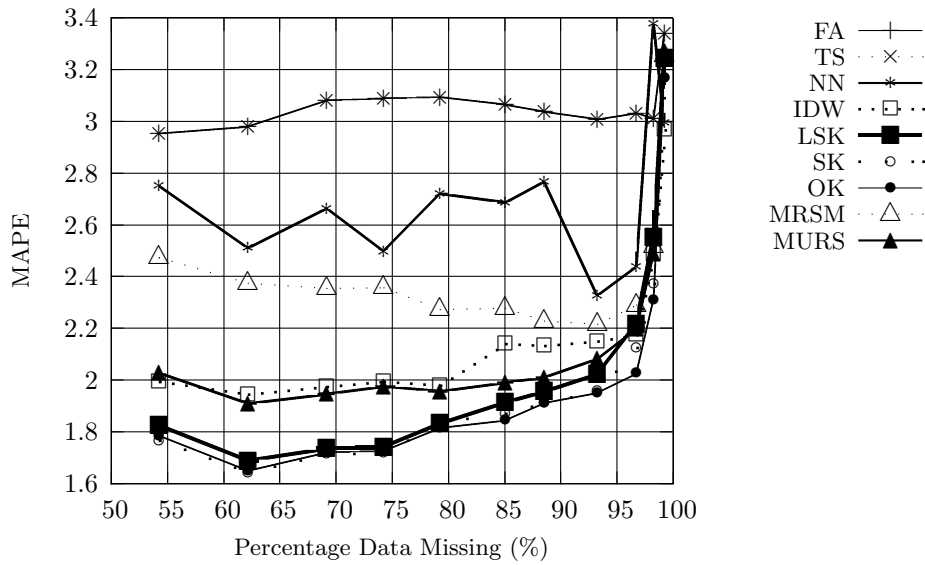


(d) 3rd level ATPS detrending, MSPE.

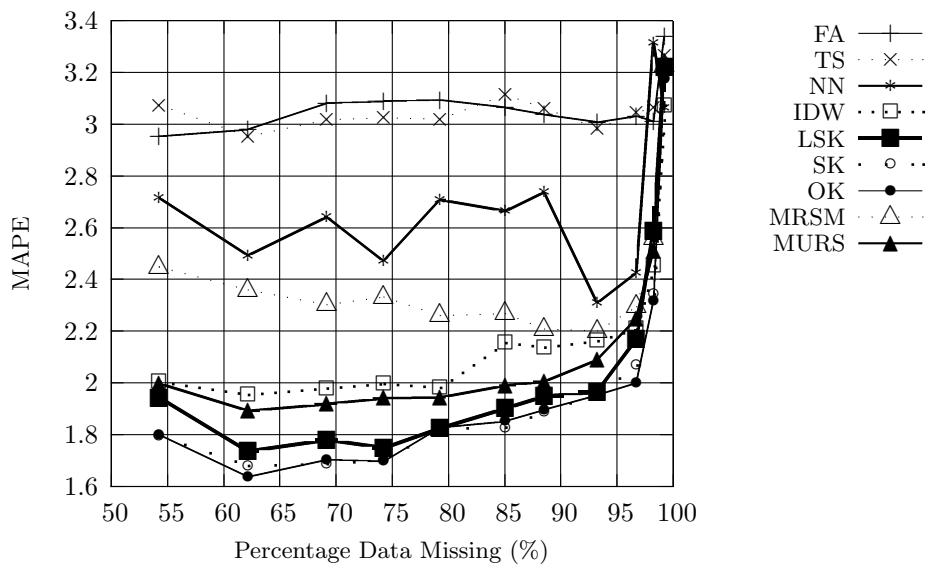


(e) 3rd level FRS detrending, MSPE.

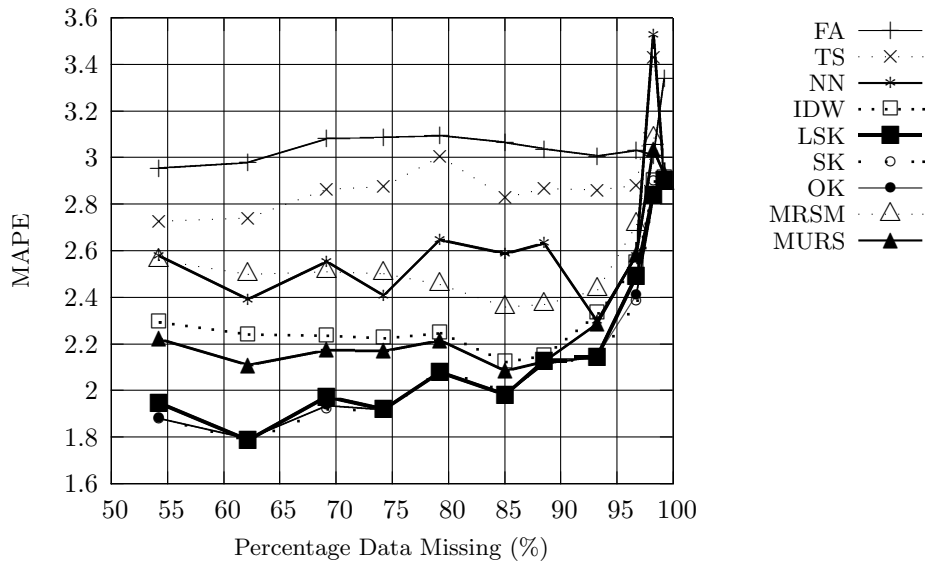
Figure A.14: MSPE comparisons for different detrending methods applied to MM CT data.



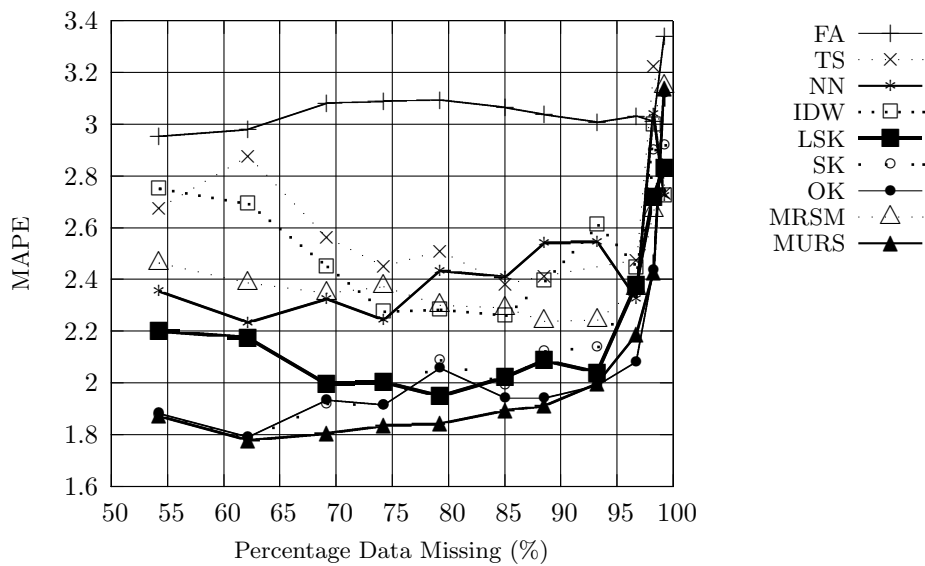
(a) Simple mean removal, MAPE.



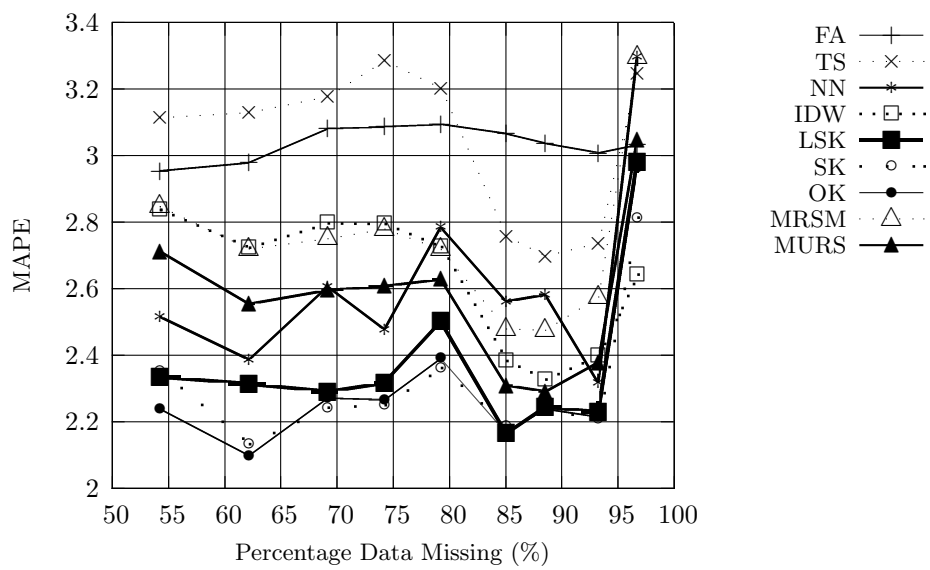
(b) 1st order GLS detrending, MAPE.



(c) 3rd order GLS detrending, MAPE.

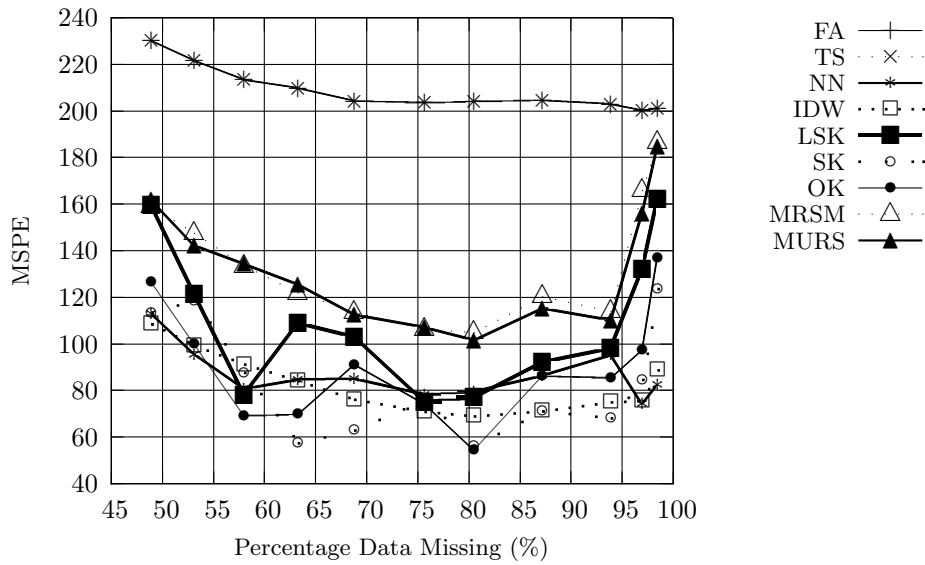


(d) 3rd level ATPS detrending, MAPE.

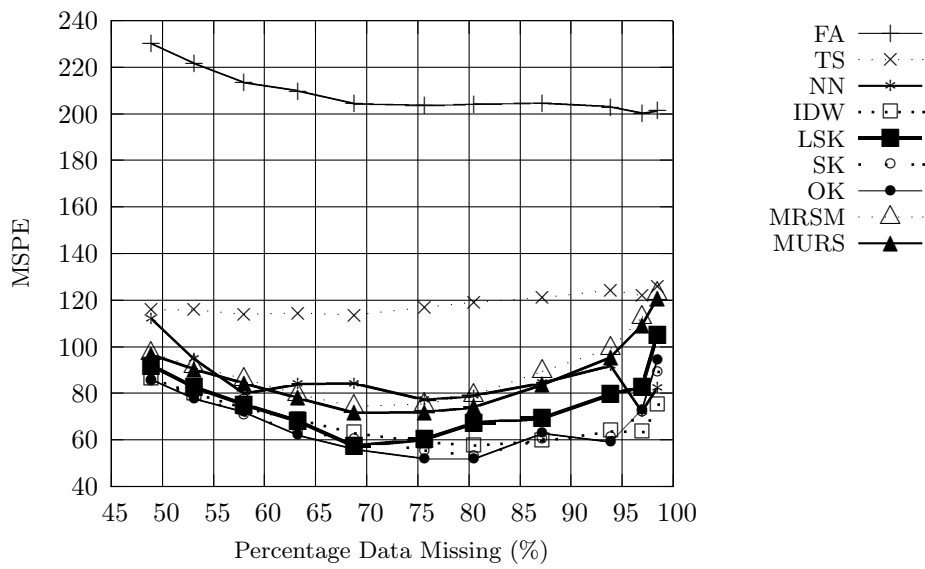


(e) 3rd level FRS detrending, MAPE.

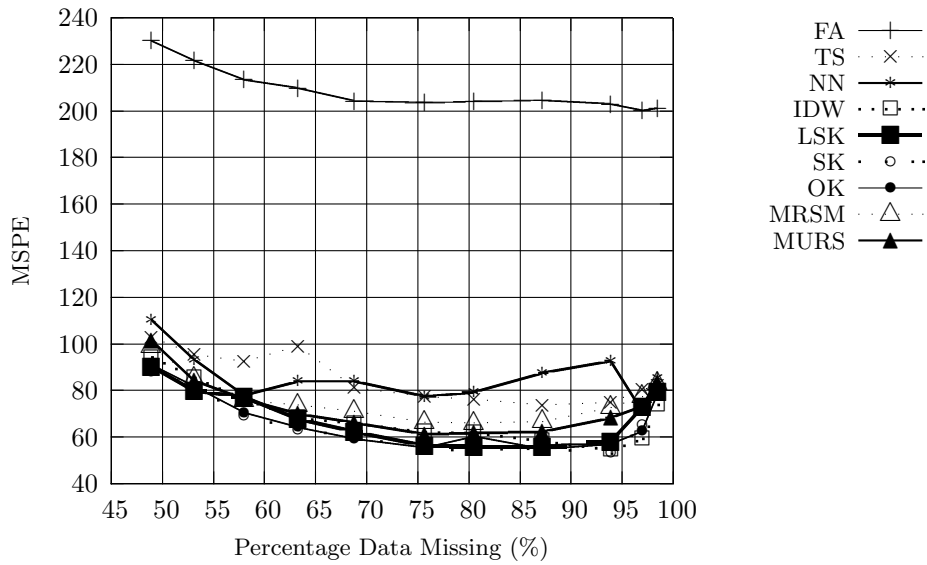
Figure A.15: MAPE comparisons for different detrending methods applied to MM CT data.



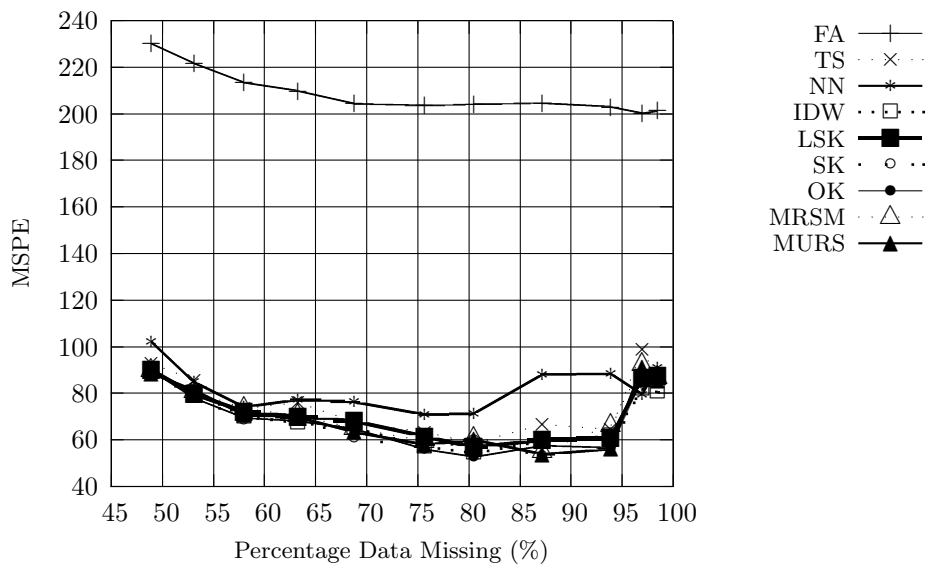
(a) Simple mean removal, MSPE.



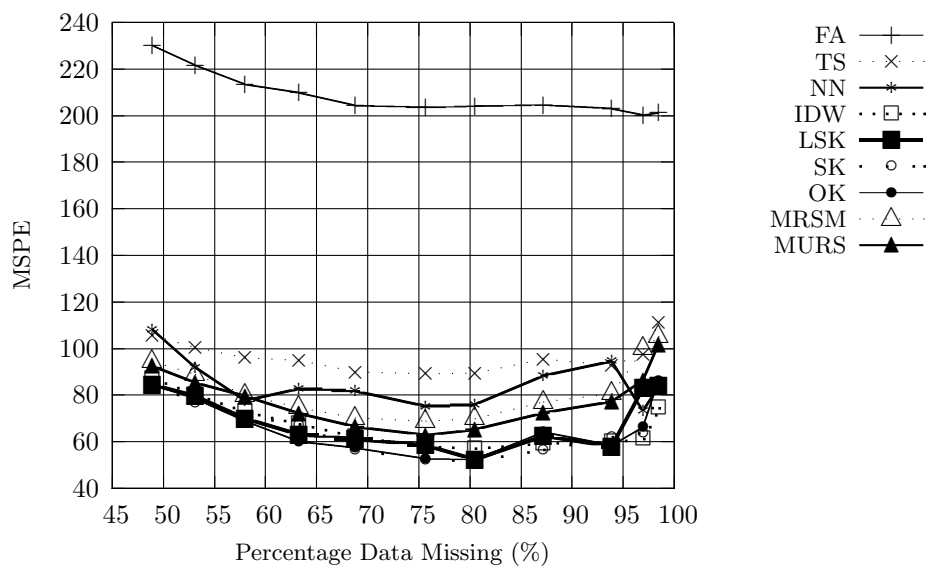
(b) 1st order GLS detrending, MSPE.



(c) 3rd order GLS detrending, MSPE.

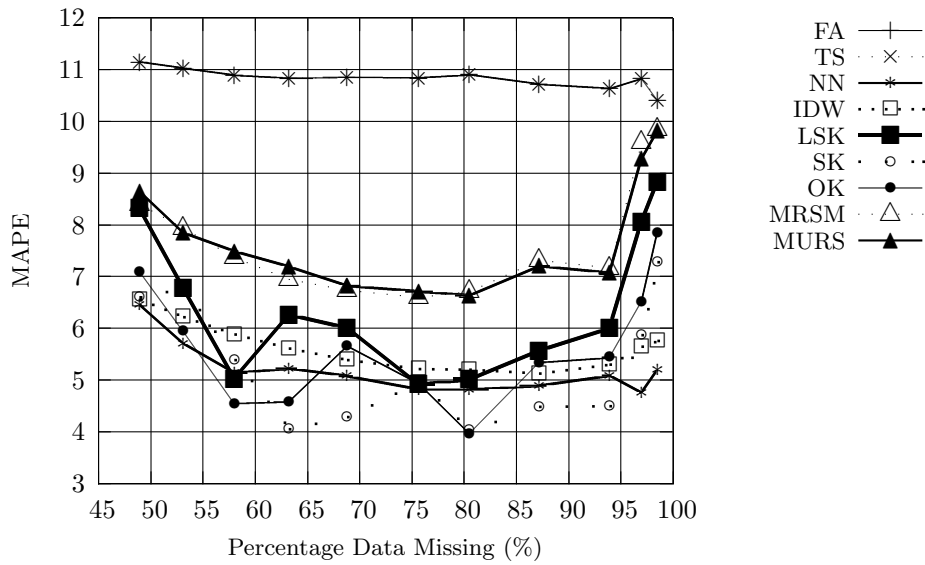


(d) 3rd level ATPS detrending, MSPE.

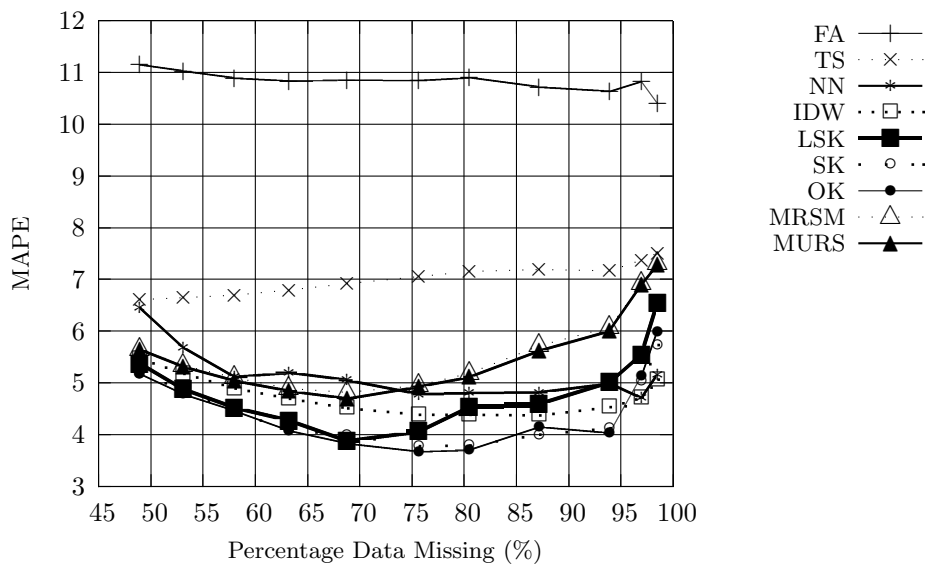


(e) 3rd level FRS detrending, MSPE.

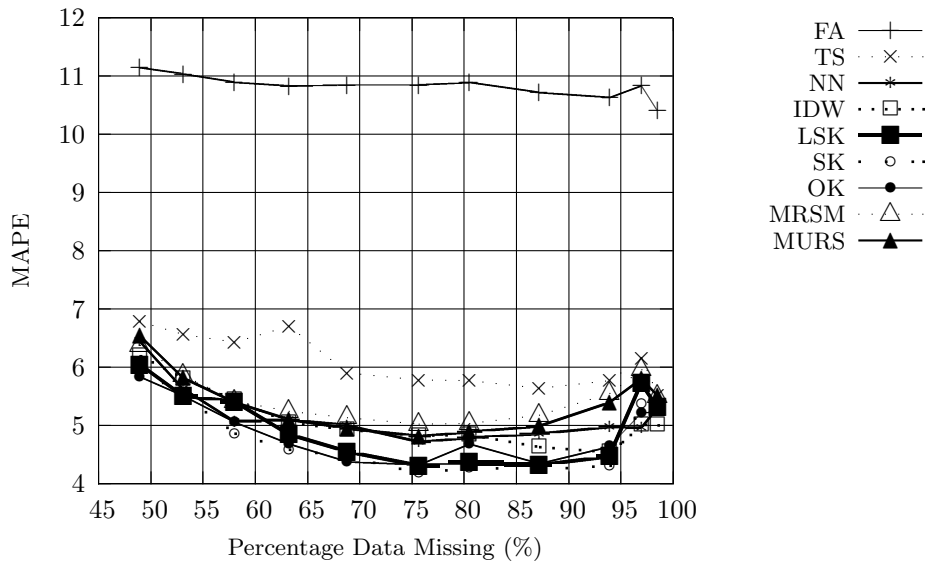
Figure A.16: MSPE comparison for different detrending methods applied to MM MO data.



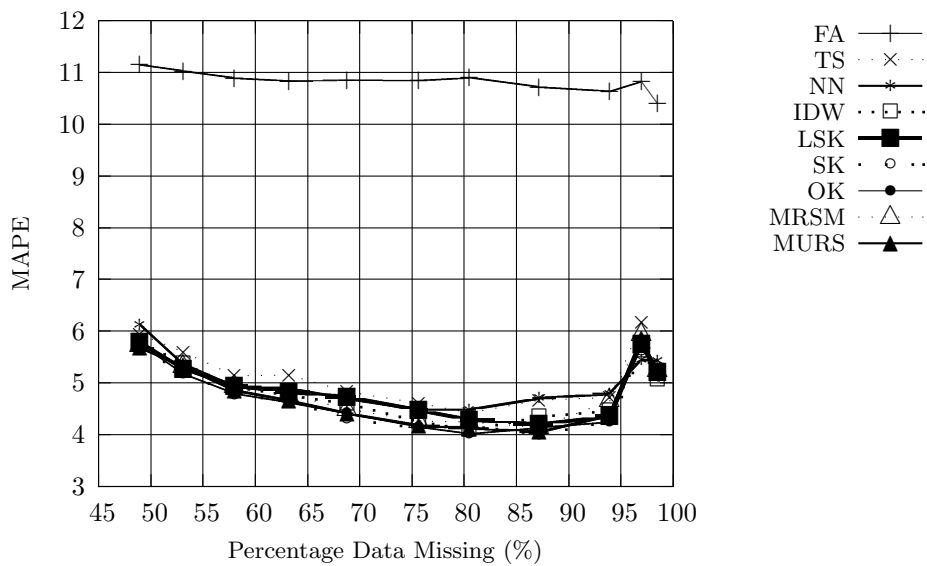
(a) Simple mean removal, MAPE.



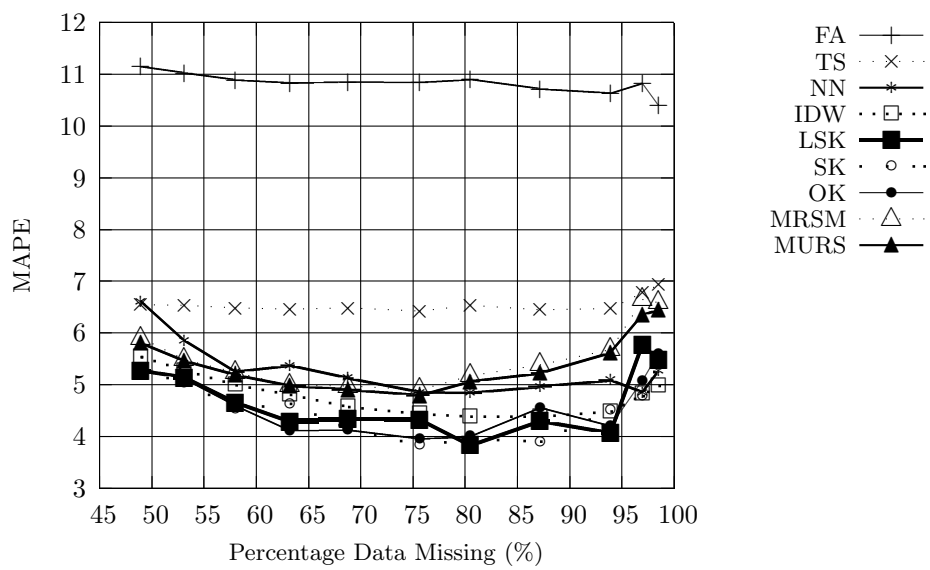
(b) 1st order GLS detrending, MAPE.



(c) 3rd order GLS detrending, MAPE.

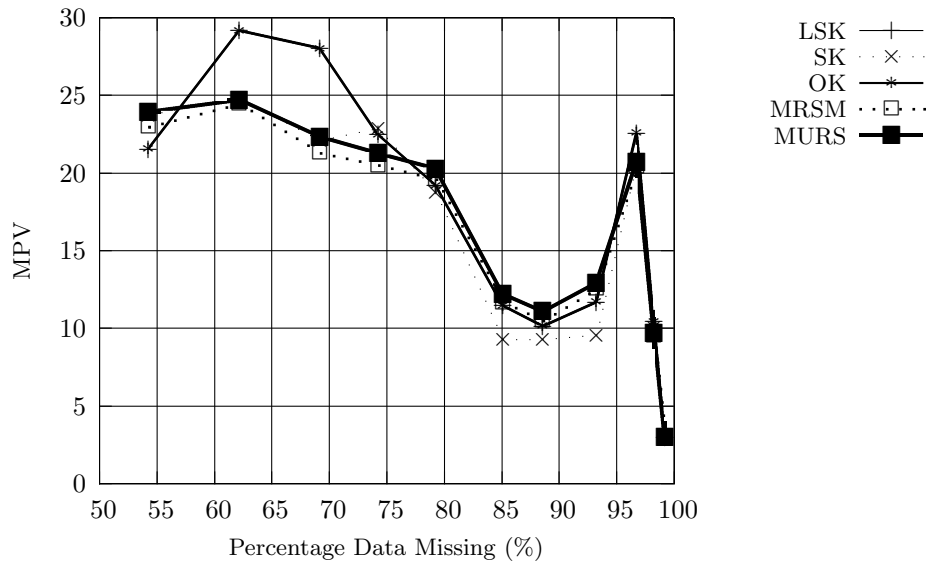


(d) 3rd level ATPS detrending, MAPE.

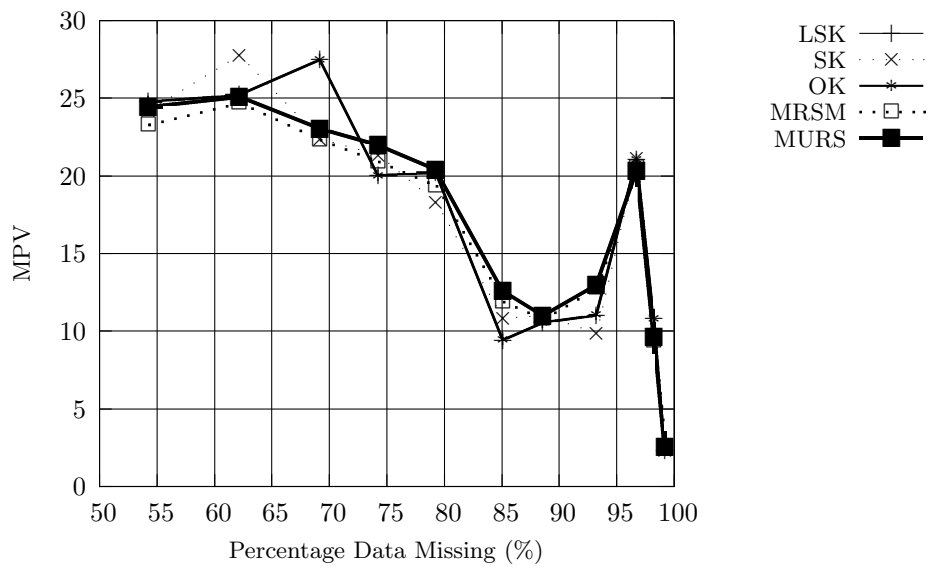


(e) 3rd level FRS detrending, MAPE.

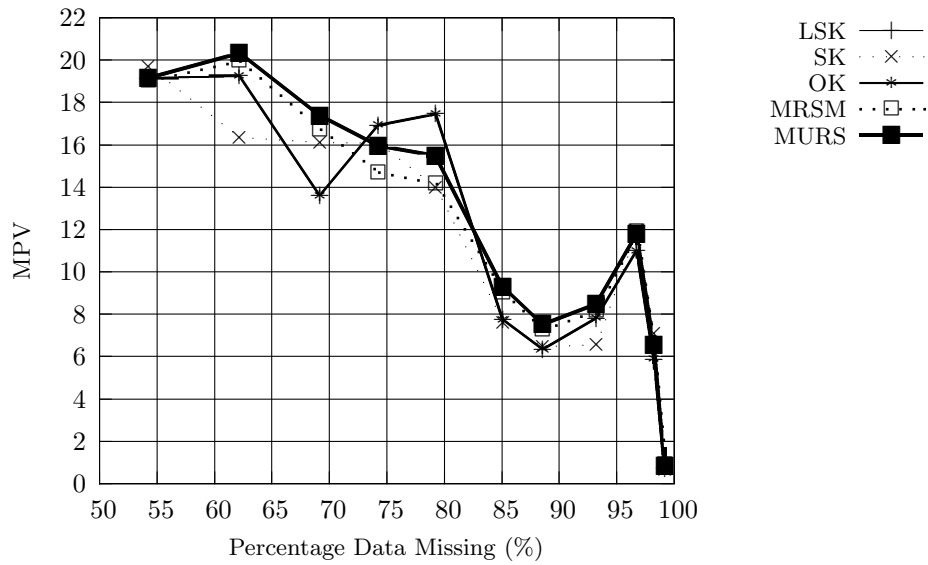
Figure A.17: MAPE comparison for different detrending methods applied to MM MO data.



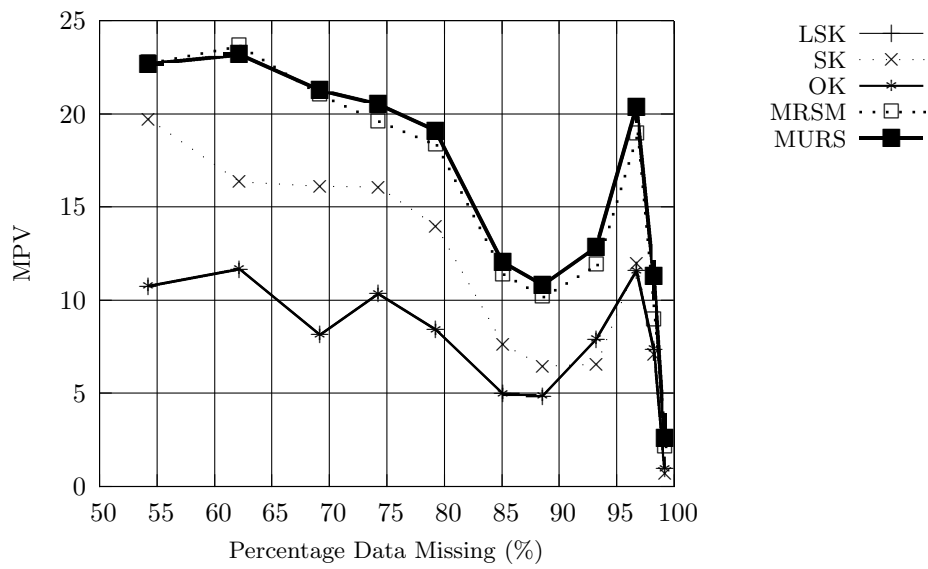
(a) Simple mean removal, MPV.



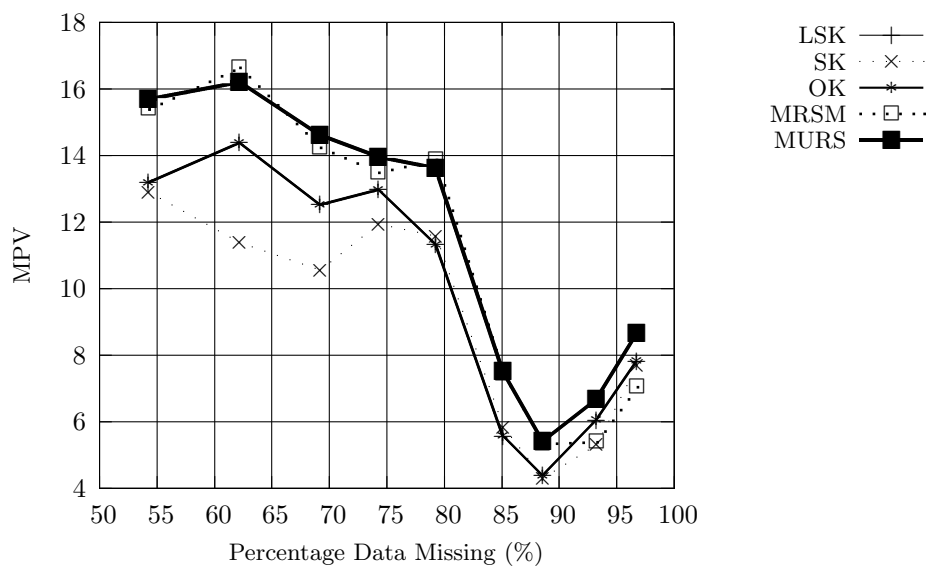
(b) 1st order GLS detrending, MPV.



(c) 3rd order GLS detrending, MPV.

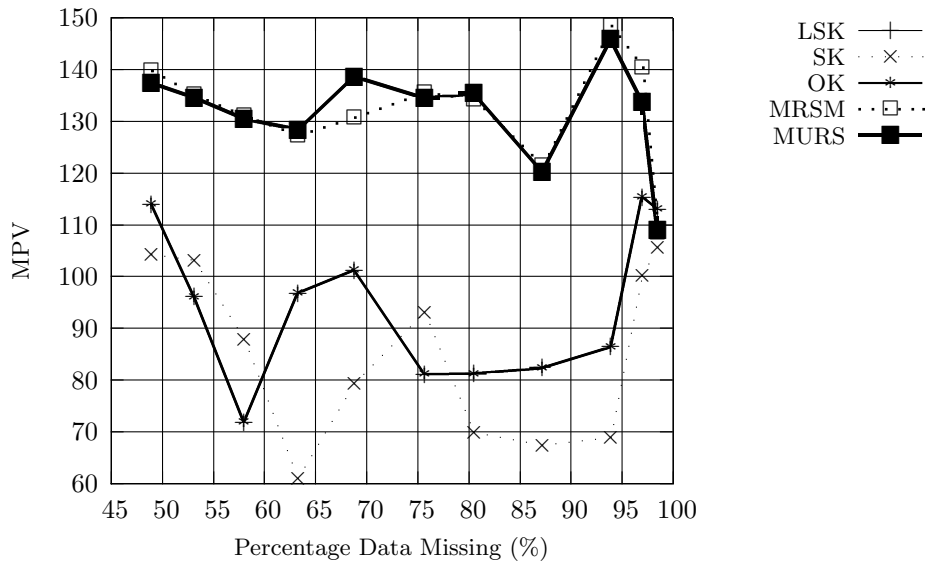


(d) 3rd level ATPS detrending, MPV.

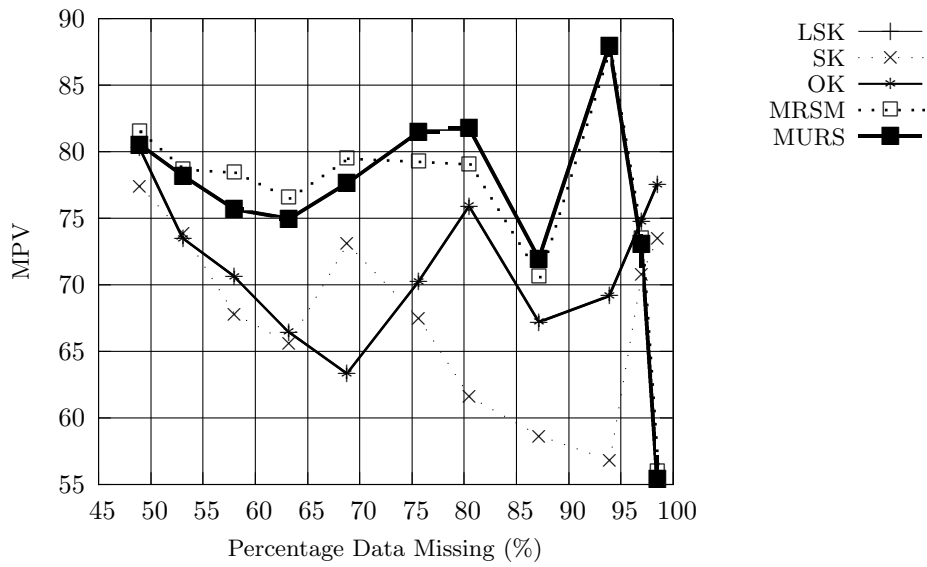


(e) 3rd level FRS detrending, MPV.

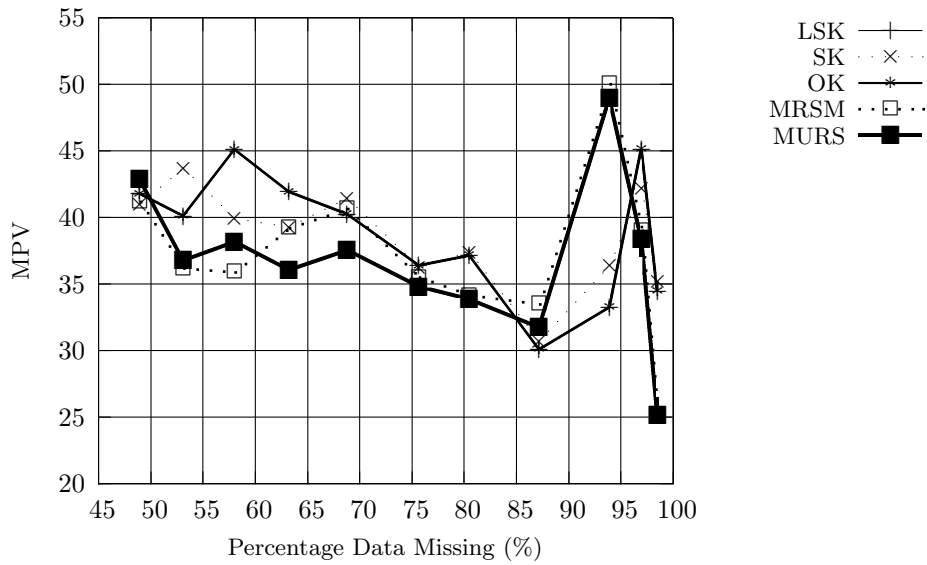
Figure A.18: MPV comparisons for different detrending methods applied to MM CT data.



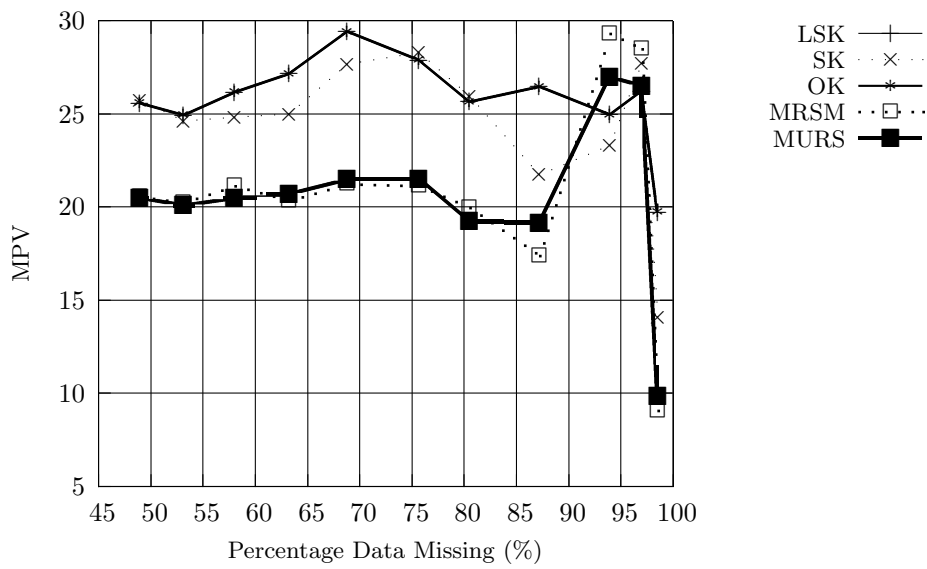
(a) Simple mean removal, MPV.



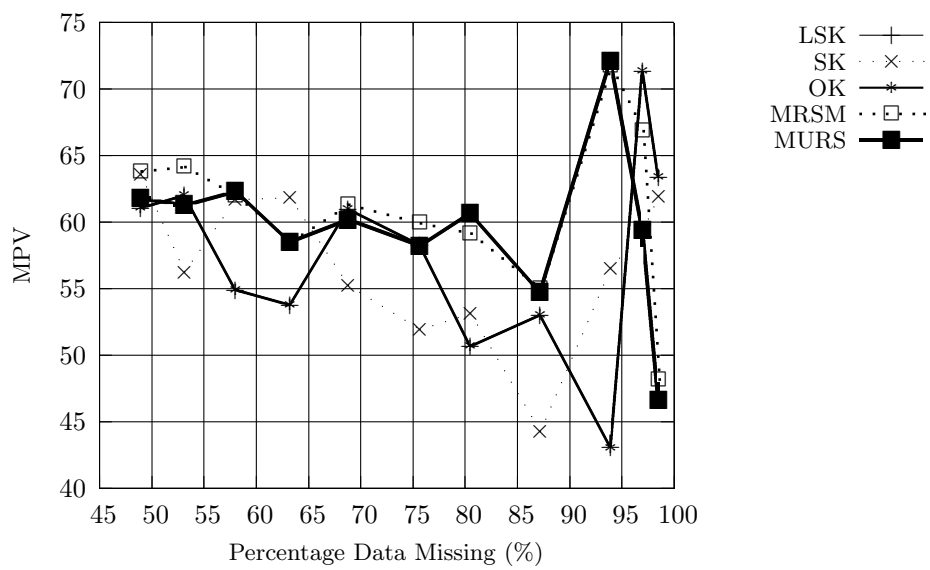
(b) 1st order GLS detrending, MPV.



(c) 3rd order GLS detrending, MPV.



(d) 3rd level ATPS detrending, MPV.



(e) 3rd level FRS detrending, MPV.

Figure A.19: MPV comparison for different detrending methods applied to MM MO data.

## A.2 Method Rankings

Table A.1: CT RR, methods ranked by MSPE, pt1.

Percentage Data Removed									
19.26		30.88		41.33		50.98		60.21	
MURS	3GLS	LSK	3FRS	LSK	3FRS	LSK	3GLS	LSK	3ATPS
MURS	1GLS	SK	3FRS	LSK	3GLS	LSK	3ATPS	LSK	3GLS
MURS	SM	MURS	3FRS	LSK	1GLS	LSK	1GLS	SK	3ATPS
MURS	3FRS	OK	3FRS	LSK	SM	LSK	SM	LSK	1GLS
MURS	3ATPS	LSK	3GLS	LSK	3ATPS	SK	3ATPS	OK	3ATPS
LSK	3FRS	LSK	1GLS	SK	3FRS	LSK	3FRS	LSK	SM
LSK	3ATPS	LSK	SM	OK	3FRS	OK	3ATPS	LSK	3FRS
LSK	3GLS	MURS	3GLS	SK	3GLS	SK	3GLS	SK	3GLS
LSK	1GLS	LSK	3ATPS	OK	3GLS	OK	3GLS	OK	3GLS
LSK	SM	SK	3ATPS	OK	1GLS	OK	1GLS	SK	1GLS
SK	3ATPS	OK	3GLS	SK	1GLS	SK	1GLS	OK	1GLS
OK	3FRS	SK	3GLS	SK	SM	OK	SM	OK	3FRS
OK	3ATPS	OK	3ATPS	SK	3ATPS	SK	SM	SK	SM
SK	3FRS	SK	1GLS	OK	SM	SK	3FRS	OK	SM
OK	3GLS	OK	1GLS	OK	3ATPS	OK	3FRS	SK	3FRS
SK	1GLS	SK	SM	MURS	1GLS	MURS	1GLS	MURS	1GLS
SK	3GLS	OK	SM	MURS	3GLS	MURS	3GLS	MURS	SM
OK	1GLS	MURS	SM	MURS	SM	MURS	SM	MURS	3ATPS
OK	SM	MURS	1GLS	MURS	3FRS	MURS	3ATPS	MURS	3GLS
SK	SM	MURS	3ATPS	MURS	3ATPS	MURS	3FRS	MURS	3FRS
IDW	3ATPS	MRSM	3ATPS	IDW	3ATPS	IDW	3ATPS	IDW	3ATPS
IDW	3FRS	IDW	3ATPS	MRSM	3FRS	MRSM	3ATPS	MRSM	3ATPS
MRSM	3ATPS	MRSM	3FRS	MRSM	3ATPS	MRSM	3GLS	MRSM	3GLS
IDW	3GLS	MRSM	3GLS	MRSM	SM	MRSM	3FRS	MRSM	1GLS
MRSM	3GLS	MRSM	1GLS	MRSM	1GLS	MRSM	1GLS	MRSM	3FRS
MRSM	SM	MRSM	SM	MRSM	3GLS	MRSM	SM	MRSM	SM
MRSM	1GLS	IDW	3FRS	IDW	3FRS	IDW	3FRS	IDW	3FRS
MRSM	3FRS	NN	3FRS	NN	3FRS	NN	3ATPS	TS	3ATPS
TS	3ATPS	NN	3GLS	NN	3ATPS	NN	3FRS	NN	3ATPS
IDW	1GLS	NN	3ATPS	NN	3GLS	NN	3GLS	NN	3GLS
IDW	SM	NN	1GLS	NN	1GLS	NN	1GLS	NN	3FRS
NN	3ATPS	NN	SM	NN	SM	NN	SM	NN	1GLS
NN	3FRS	IDW	3GLS	IDW	3GLS	TS	3ATPS	NN	SM
NN	3GLS	TS	3ATPS	TS	3ATPS	IDW	3GLS	IDW	3GLS
NN	SM	IDW	1GLS	IDW	1GLS	IDW	1GLS	IDW	1GLS
NN	1GLS	IDW	SM	IDW	SM	IDW	SM	IDW	SM
TS	3FRS	TS	3FRS	TS	3FRS	TS	3FRS	TS	3FRS
TS	3GLS	TS	3GLS	TS	3GLS	TS	3GLS	TS	3GLS
FA	1GLS	FA	1GLS	FA	1GLS	FA	1GLS	FA	1GLS
FA	3ATPS	FA	3ATPS	FA	3ATPS	FA	3ATPS	FA	3ATPS
FA	3FRS	FA	3FRS	FA	3FRS	FA	3FRS	FA	3FRS
FA	3GLS	FA	3GLS	FA	3GLS	FA	3GLS	FA	3GLS
FA	SM	FA	SM	FA	SM	FA	SM	FA	SM
TS	SM	TS	SM	TS	SM	TS	SM	TS	SM
TS	1GLS	TS	1GLS	TS	1GLS	TS	1GLS	TS	1GLS

Table A.2: CT RR, methods ranked by MSPE, pt.2.

Percentage Data Removed											
70.12		77.44		85.67		93.24		96.26		98.46	
LSK	3ATPS	MURS	3ATPS	IDW	3ATPS	SK	1GLS	SK	1GLS	LSK	3FRS
MURS	3ATPS	IDW	3ATPS	LSK	3ATPS	SK	SM	OK	SM	NN	3FRS
OK	3ATPS	LSK	3ATPS	SK	3ATPS	OK	3GLS	SK	SM	IDW	3FRS
SK	3ATPS	SK	3ATPS	SK	1GLS	OK	SM	OK	1GLS	SK	3FRS
IDW	3ATPS	OK	3ATPS	OK	1GLS	SK	3GLS	OK	3GLS	MURS	3FRS
MRSRM	3ATPS	MRSRM	3ATPS	OK	SM	OK	1GLS	SK	3GLS	OK	3FRS
LSK	3FRS	OK	3GLS	LSK	1GLS	LSK	1GLS	LSK	SM	TS	3FRS
LSK	3GLS	LSK	SM	SK	SM	OK	3FRS	MURS	3GLS	MRSRM	3FRS
LSK	1GLS	SK	3GLS	MURS	3ATPS	LSK	SM	LSK	3GLS	NN	3GLS
SK	3FRS	SK	3FRS	SK	3GLS	SK	3FRS	OK	3FRS	IDW	3ATPS
LSK	SM	LSK	3GLS	OK	3GLS	LSK	3GLS	MURS	SM	NN	3ATPS
OK	3GLS	OK	3FRS	LSK	SM	IDW	3FRS	LSK	3FRS	OK	3ATPS
OK	3FRS	OK	SM	LSK	3GLS	LSK	3FRS	MURS	1GLS	SK	3ATPS
SK	SM	SK	1GLS	OK	3ATPS	IDW	3GLS	IDW	3GLS	MURS	3ATPS
OK	SM	LSK	1GLS	SK	3FRS	MURS	SM	SK	3FRS	LSK	3ATPS
SK	3GLS	LSK	3FRS	OK	3FRS	MURS	1GLS	IDW	SM	MRSRM	3ATPS
OK	1GLS	SK	SM	LSK	3FRS	LSK	3ATPS	IDW	1GLS	TS	3ATPS
SK	1GLS	OK	1GLS	MRSRM	3ATPS	MURS	3GLS	IDW	3FRS	NN	SM
MRSRM	SM	TS	3ATPS	MURS	1GLS	MURS	3FRS	MURS	3FRS	NN	1GLS
MRSRM	1GLS	MURS	3FRS	MURS	SM	MRSRM	3FRS	LSK	1GLS	IDW	3GLS
MURS	SM	MURS	SM	MRSRM	3FRS	IDW	SM	MRSRM	3FRS	SK	3GLS
MRSRM	3GLS	MURS	1GLS	MURS	3GLS	IDW	1GLS	MRSRM	3GLS	OK	3GLS
MURS	1GLS	MURS	3GLS	MURS	3FRS	IDW	3ATPS	TS	3FRS	MURS	3GLS
TS	3ATPS	MRSRM	3FRS	IDW	3FRS	MRSRM	3GLS	MRSRM	SM	LSK	3GLS
MURS	3GLS	MRSRM	3GLS	MRSRM	3GLS	OK	3ATPS	MRSRM	1GLS	MRSRM	3GLS
MURS	3FRS	MRSRM	1GLS	TS	3ATPS	TS	3FRS	TS	3GLS	TS	3GLS
MRSRM	3FRS	MRSRM	SM	MRSRM	1GLS	MRSRM	SM	OK	3ATPS	SK	SM
IDW	3FRS	IDW	3FRS	MRSRM	SM	MRSRM	1GLS	SK	3ATPS	OK	SM
NN	3ATPS	NN	3ATPS	IDW	3GLS	SK	3ATPS	NN	3FRS	IDW	SM
NN	3FRS	NN	3FRS	NN	3ATPS	NN	3FRS	LSK	3ATPS	LSK	SM
NN	3GLS	NN	3GLS	NN	3FRS	MURS	3ATPS	IDW	3ATPS	IDW	1GLS
NN	1GLS	NN	1GLS	NN	3GLS	NN	3GLS	NN	3GLS	OK	1GLS
NN	SM	NN	SM	IDW	1GLS	NN	3ATPS	MURS	3ATPS	SK	1GLS
IDW	3GLS	IDW	3GLS	IDW	SM	NN	1GLS	MRSRM	3ATPS	MURS	SM
IDW	1GLS	TS	3FRS	TS	3FRS	NN	SM	NN	3ATPS	MURS	1GLS
IDW	SM	IDW	1GLS	NN	1GLS	TS	3ATPS	TS	3ATPS	LSK	1GLS
TS	3FRS	IDW	SM	NN	SM	MRSRM	3ATPS	NN	1GLS	MRSRM	SM
TS	3GLS	TS	3GLS	TS	3GLS	TS	3GLS	NN	SM	MRSRM	1GLS
FA	1GLS	FA	1GLS	FA	1GLS	FA	1GLS	FA	1GLS	FA	1GLS
FA	3ATPS	FA	3ATPS	FA	3ATPS	FA	3ATPS	FA	3ATPS	FA	3ATPS
FA	3FRS	FA	3FRS	FA	3FRS	FA	3FRS	FA	3FRS	FA	3FRS
FA	3GLS	FA	3GLS	FA	3GLS	FA	3GLS	FA	3GLS	FA	3GLS
FA	SM	FA	SM	FA	SM	FA	SM	FA	SM	FA	SM
TS	SM	TS	SM	TS	SM	TS	SM	TS	SM	TS	SM
TS	1GLS	TS	1GLS	TS	1GLS	TS	1GLS	TS	1GLS	TS	1GLS

Table A.3: CT RR, methods ranked by MAPE, pt1.

Percentage Data Removed									
19.26		30.88		41.33		50.98		60.21	
LSK	3GLS	LSK	3GLS	LSK	3GLS	SK	3GLS	LSK	1GLS
LSK	1GLS	LSK	1GLS	LSK	1GLS	OK	3GLS	LSK	3GLS
LSK	SM	LSK	SM	LSK	SM	OK	1GLS	SK	1GLS
LSK	3FRS	SK	3GLS	OK	3GLS	SK	1GLS	OK	1GLS
OK	1GLS	OK	3GLS	SK	3GLS	LSK	3GLS	SK	3GLS
SK	1GLS	SK	1GLS	SK	1GLS	LSK	1GLS	OK	3GLS
SK	3GLS	OK	1GLS	OK	1GLS	OK	SM	LSK	SM
SK	SM	OK	SM	LSK	3FRS	SK	SM	SK	SM
OK	3GLS	SK	SM	SK	SM	LSK	SM	OK	SM
OK	SM	OK	3FRS	OK	SM	SK	3ATPS	OK	3ATPS
OK	3FRS	SK	3FRS	OK	3FRS	SK	3FRS	OK	3FRS
SK	3FRS	LSK	3FRS	SK	3FRS	OK	3ATPS	SK	3ATPS
LSK	3ATPS	OK	3ATPS	LSK	3ATPS	OK	3FRS	LSK	3FRS
OK	3ATPS	SK	3ATPS	SK	3ATPS	LSK	3ATPS	SK	3FRS
SK	3ATPS	LSK	3ATPS	OK	3ATPS	LSK	3FRS	LSK	3ATPS
MURS	1GLS	MURS	3GLS	MURS	1GLS	MURS	1GLS	MURS	1GLS
MURS	SM	MURS	SM	MURS	3GLS	MURS	3GLS	MURS	SM
MURS	3ATPS	MURS	1GLS	MURS	SM	MURS	SM	MURS	3GLS
MURS	3GLS	MURS	3FRS	MURS	3ATPS	MURS	3ATPS	MURS	3ATPS
MURS	3FRS	MURS	3ATPS	MURS	3FRS	MURS	3FRS	MURS	3FRS
NN	1GLS	NN	3GLS	NN	1GLS	MRSM	3ATPS	IDW	3ATPS
NN	SM	NN	1GLS	NN	SM	NN	3GLS	NN	3ATPS
NN	3GLS	NN	SM	NN	3GLS	NN	1GLS	NN	1GLS
MRSM	1GLS	MRSM	1GLS	NN	3ATPS	NN	SM	NN	3GLS
MRSM	SM	MRSM	3GLS	MRSM	3ATPS	NN	3ATPS	NN	SM
NN	3ATPS	NN	3ATPS	NN	3FRS	MRSM	3GLS	MRSM	3ATPS
MRSM	3ATPS	MRSM	SM	MRSM	3GLS	NN	3FRS	MRSM	3GLS
NN	3FRS	MRSM	3ATPS	MRSM	SM	MRSM	1GLS	MRSM	1GLS
MRSM	3GLS	NN	3FRS	MRSM	1GLS	MRSM	SM	MRSM	SM
MRSM	3FRS	MRSM	3FRS	MRSM	3FRS	IDW	3ATPS	NN	3FRS
IDW	3ATPS	IDW	3ATPS	IDW	3ATPS	MRSM	3FRS	MRSM	3FRS
IDW	3FRS	IDW	3FRS	IDW	3FRS	IDW	3FRS	IDW	3FRS
IDW	3GLS	IDW	3GLS	IDW	3GLS	TS	3ATPS	TS	3ATPS
TS	3ATPS	TS	3ATPS	TS	3ATPS	IDW	3GLS	IDW	3GLS
IDW	1GLS	IDW	1GLS	IDW	1GLS	IDW	1GLS	IDW	1GLS
IDW	SM	IDW	SM	IDW	SM	IDW	SM	IDW	SM
TS	3FRS	TS	3FRS	TS	3FRS	TS	3FRS	TS	3FRS
TS	3GLS	TS	3GLS	TS	3GLS	TS	3GLS	TS	3GLS
TS	1GLS	TS	1GLS	TS	1GLS	TS	1GLS	TS	1GLS
FA	1GLS	FA	1GLS	FA	1GLS	FA	1GLS	FA	1GLS
FA	3ATPS	FA	3ATPS	FA	3ATPS	FA	3ATPS	FA	3ATPS
FA	3FRS	FA	3FRS	FA	3FRS	FA	3FRS	FA	3FRS
FA	3GLS	FA	3GLS	FA	3GLS	FA	3GLS	FA	3GLS
FA	SM	FA	SM	FA	SM	FA	SM	FA	SM
TS	SM	TS	SM	TS	SM	TS	SM	TS	SM

Table A.4: CT RR, methods ranked by MAPE, pt2.

Percentage Data Removed											
70.12		77.44		85.67		93.24		96.26		98.46	
LSK	1GLS	OK	3GLS	SK	1GLS	SK	1GLS	OK	SM	IDW	3GLS
LSK	3GLS	SK	1GLS	OK	1GLS	SK	SM	SK	1GLS	SK	3GLS
OK	1GLS	SK	3GLS	LSK	1GLS	OK	1GLS	SK	SM	IDW	3ATPS
LSK	SM	LSK	SM	SK	SM	OK	3GLS	OK	1GLS	OK	3GLS
SK	1GLS	LSK	1GLS	OK	SM	LSK	1GLS	LSK	SM	NN	3ATPS
OK	3GLS	LSK	3GLS	OK	3GLS	OK	SM	IDW	SM	OK	3ATPS
SK	3GLS	OK	1GLS	SK	3GLS	SK	3GLS	OK	3GLS	NN	3GLS
SK	SM	OK	SM	LSK	3GLS	LSK	3GLS	MURS	SM	SK	3ATPS
OK	SM	LSK	3ATPS	LSK	SM	LSK	SM	IDW	1GLS	MURS	3GLS
SK	3ATPS	SK	SM	SK	3ATPS	OK	3FRS	SK	3GLS	MURS	3ATPS
OK	3ATPS	SK	3ATPS	LSK	3ATPS	SK	3FRS	MURS	1GLS	LSK	3ATPS
LSK	3FRS	OK	3ATPS	OK	3ATPS	LSK	3ATPS	LSK	3FRS	LSK	3GLS
LSK	3ATPS	SK	3FRS	SK	3FRS	LSK	3FRS	LSK	3GLS	NN	SM
SK	3FRS	OK	3FRS	OK	3FRS	IDW	3FRS	LSK	1GLS	IDW	3FRS
OK	3FRS	LSK	3FRS	MURS	1GLS	OK	3ATPS	OK	3FRS	MRSM	3ATPS
MURS	3ATPS	MURS	3ATPS	LSK	3FRS	IDW	3GLS	MURS	3GLS	TS	3ATPS
MURS	1GLS	IDW	3ATPS	MURS	SM	IDW	3ATPS	SK	3FRS	NN	1GLS
MURS	SM	MURS	1GLS	IDW	3ATPS	MURS	1GLS	IDW	3GLS	MRSM	3GLS
IDW	3ATPS	MURS	SM	MURS	3GLS	MURS	SM	MRSM	SM	SK	SM
MURS	3GLS	MURS	3GLS	MURS	3ATPS	SK	3ATPS	MRSM	1GLS	LSK	3FRS
MRSM	3ATPS	MRSM	3ATPS	MRSM	3ATPS	NN	3GLS	IDW	3FRS	SK	3FRS
NN	3ATPS	NN	3ATPS	NN	1GLS	NN	1GLS	MRSM	3GLS	NN	3FRS
MRSM	3GLS	NN	3GLS	NN	SM	NN	SM	MRSM	3FRS	MURS	3FRS
MRSM	1GLS	NN	1GLS	NN	3ATPS	MRSM	1GLS	MURS	3FRS	IDW	SM
MRSM	SM	NN	SM	NN	3GLS	MURS	3GLS	NN	3FRS	OK	SM
NN	3GLS	NN	3FRS	MRSM	3GLS	NN	3FRS	NN	3GLS	MRSM	3FRS
MURS	3FRS	MURS	3FRS	MRSM	1GLS	MRSM	SM	NN	SM	TS	3FRS
NN	1GLS	MRSM	1GLS	NN	3FRS	IDW	SM	NN	1GLS	TS	3GLS
NN	SM	MRSM	3GLS	IDW	3GLS	IDW	1GLS	OK	3ATPS	OK	3FRS
NN	3FRS	MRSM	SM	MRSM	SM	MRSM	3GLS	SK	3ATPS	LSK	SM
MRSM	3FRS	TS	3ATPS	MURS	3FRS	MURS	3ATPS	LSK	3ATPS	IDW	1GLS
IDW	3FRS	MRSM	3FRS	IDW	3FRS	MURS	3FRS	TS	3FRS	OK	1GLS
TS	3ATPS	IDW	3FRS	MRSM	3FRS	MRSM	3FRS	IDW	3ATPS	SK	1GLS
IDW	3GLS	IDW	3GLS	TS	3ATPS	NN	3ATPS	MURS	3ATPS	MURS	SM
IDW	1GLS	IDW	1GLS	IDW	1GLS	TS	3FRS	MRSM	3ATPS	MRSM	SM
IDW	SM	IDW	SM	IDW	SM	TS	3ATPS	NN	3ATPS	MURS	1GLS
TS	3FRS	TS	3FRS	TS	3FRS	MRSM	3ATPS	TS	3ATPS	LSK	1GLS
TS	3GLS	TS	3GLS	TS	3GLS	TS	3GLS	TS	3GLS	MRSM	1GLS
TS	1GLS	TS	1GLS	TS	1GLS	TS	1GLS	FA	1GLS	FA	1GLS
FA	1GLS	FA	1GLS	FA	1GLS	FA	1GLS	FA	3ATPS	FA	3ATPS
FA	3ATPS	FA	3ATPS	FA	3ATPS	FA	3ATPS	FA	3FRS	FA	3FRS
FA	3FRS	FA	3FRS	FA	3FRS	FA	3FRS	FA	3GLS	FA	3GLS
FA	3GLS	FA	3GLS	FA	3GLS	FA	3GLS	FA	SM	FA	SM
FA	SM	FA	SM	FA	SM	FA	SM	TS	SM	TS	SM
TS	SM	TS	SM	TS	SM	TS	SM	TS	1GLS	TS	1GLS

Table A.5: MO RR, methods ranked by MSPE, pt1.

Percentage Data Removed											
19.53		26.20		33.79		41.77		50.24		60.91	
MURS	3ATPS	MURS	3ATPS	MURS	3ATPS	MURS	3ATPS	MURS	3ATPS	MURS	3ATPS
MRSM	3ATPS	MRSM	3ATPS	MRSM	3ATPS	MRSM	3ATPS	MRSM	3ATPS	MRSM	3ATPS
OK	1GLS	SK	1GLS	SK	SM	SK	SM	OK	SM	OK	1GLS
OK	SM	OK	SM	SK	1GLS	OK	SM	OK	1GLS	SK	1GLS
SK	1GLS	OK	1GLS	SK	3FRS	LSK	1GLS	OK	3FRS	OK	SM
LSK	SM	OK	3FRS	OK	SM	OK	3FRS	SK	3FRS	SK	3FRS
SK	3GLS	LSK	3GLS	OK	1GLS	LSK	3GLS	SK	SM	SK	SM
SK	SM	SK	3FRS	LSK	1GLS	LSK	3FRS	SK	3GLS	LSK	3FRS
OK	3GLS	LSK	3FRS	SK	3GLS	LSK	SM	LSK	SM	SK	3GLS
LSK	3FRS	SK	SM	LSK	SM	OK	1GLS	SK	1GLS	OK	3FRS
SK	3FRS	LSK	SM	OK	3FRS	SK	1GLS	OK	3GLS	SK	3ATPS
OK	3FRS	OK	3GLS	OK	3GLS	SK	3GLS	OK	3ATPS	OK	3GLS
LSK	3GLS	LSK	1GLS	SK	3ATPS	OK	3GLS	LSK	1GLS	OK	3ATPS
SK	3ATPS	SK	3GLS	LSK	3FRS	OK	3ATPS	SK	3ATPS	MURS	SM
MURS	3GLS	SK	3ATPS	LSK	3GLS	SK	3FRS	MURS	SM	MURS	3GLS
LSK	1GLS	OK	3ATPS	OK	3ATPS	LSK	3ATPS	MURS	3GLS	IDW	3ATPS
MURS	SM	MURS	3GLS	MURS	3GLS	MURS	SM	MURS	3FRS	LSK	3GLS
OK	3ATPS	MURS	SM	MURS	SM	MURS	3GLS	LSK	3GLS	LSK	SM
MURS	3FRS	MURS	3FRS	MURS	3FRS	SK	3ATPS	MURS	1GLS	LSK	1GLS
MURS	1GLS	MURS	1GLS	MRSM	3GLS	MURS	1GLS	LSK	3ATPS	NN	3ATPS
MRSM	3GLS	MRSM	3GLS	MURS	1GLS	MURS	3FRS	IDW	3ATPS	NN	3GLS
MRSM	SM	MRSM	SM	LSK	3ATPS	MRSM	3GLS	MRSM	SM	NN	3FRS
LSK	3ATPS	MRSM	3FRS	MRSM	SM	MRSM	SM	MRSM	3GLS	NN	1GLS
MRSM	1GLS	MRSM	1GLS	MRSM	1GLS	IDW	3ATPS	NN	3ATPS	NN	SM
NN	3ATPS	LSK	3ATPS	MRSM	3FRS	MRSM	1GLS	NN	3GLS	LSK	3ATPS
MRSM	3FRS	NN	3ATPS	NN	3ATPS	MRSM	3FRS	LSK	3FRS	MURS	3FRS
NN	1GLS	IDW	3ATPS	NN	3GLS	NN	3ATPS	NN	3FRS	MURS	1GLS
NN	3FRS	NN	3GLS	IDW	3ATPS	IDW	3GLS	NN	1GLS	IDW	3GLS
NN	3GLS	NN	3FRS	NN	3FRS	NN	3GLS	NN	SM	MRSM	SM
NN	SM	NN	1GLS	NN	1GLS	NN	3FRS	MRSM	1GLS	IDW	3FRS
IDW	3ATPS	NN	SM	NN	SM	NN	1GLS	MRSM	3FRS	MRSM	3GLS
IDW	3GLS	IDW	3GLS	IDW	3GLS	NN	SM	IDW	3GLS	IDW	1GLS
IDW	3FRS	IDW	3FRS	IDW	3FRS	IDW	3FRS	IDW	3FRS	TS	3ATPS
IDW	1GLS	IDW	1GLS	IDW	1GLS	IDW	1GLS	IDW	1GLS	IDW	SM
IDW	SM	IDW	SM	IDW	SM	IDW	SM	IDW	SM	MRSM	3FRS
TS	3ATPS	TS	3ATPS	TS	3ATPS	TS	3ATPS	TS	3ATPS	MRSM	1GLS
TS	3GLS	TS	3GLS	TS	3GLS	TS	3GLS	TS	3GLS	TS	3GLS
TS	3FRS	TS	3FRS	TS	3FRS	TS	3FRS	TS	3FRS	TS	3FRS
TS	1GLS	TS	1GLS	TS	1GLS	TS	1GLS	TS	1GLS	TS	1GLS
FA	1GLS	FA	1GLS	FA	1GLS	FA	1GLS	FA	1GLS	FA	1GLS
FA	3ATPS	FA	3ATPS	FA	3ATPS	FA	3ATPS	FA	3ATPS	FA	3ATPS
FA	3FRS	FA	3FRS	FA	3FRS	FA	3FRS	FA	3FRS	FA	3FRS
FA	3GLS	FA	3GLS	FA	3GLS	FA	3GLS	FA	3GLS	FA	3GLS
FA	SM	FA	SM	FA	SM	FA	SM	FA	SM	FA	SM
TS	SM	TS	SM	TS	SM	TS	SM	TS	SM	TS	SM

Table A.6: MO RR, methods ranked by MSPE, pt2.

Percentage Data Removed									
68.48		79.59		90.26		94.90		97.44	
MURS	3ATPS	MURS	3ATPS	MURS	3ATPS	MURS	3ATPS	MURS	3ATPS
MRSM	3ATPS	MRSM	3ATPS	MRSM	3ATPS	MRSM	3ATPS	MRSM	3ATPS
SK	3FRS	OK	1GLS	LSK	3GLS	LSK	1GLS	IDW	3GLS
LSK	1GLS	LSK	3FRS	OK	3ATPS	SK	3ATPS	IDW	3ATPS
LSK	SM	OK	SM	LSK	1GLS	SK	3FRS	IDW	3FRS
OK	1GLS	SK	1GLS	LSK	3ATPS	IDW	3GLS	SK	3ATPS
SK	3GLS	LSK	1GLS	OK	1GLS	IDW	3FRS	IDW	1GLS
SK	1GLS	SK	3GLS	IDW	3ATPS	OK	1GLS	OK	3ATPS
LSK	3FRS	OK	3FRS	SK	3ATPS	IDW	3ATPS	LSK	3ATPS
SK	SM	OK	3ATPS	LSK	3FRS	LSK	3ATPS	IDW	SM
OK	3FRS	SK	3ATPS	SK	1GLS	IDW	1GLS	TS	3ATPS
OK	3ATPS	SK	3FRS	SK	SM	SK	3GLS	SK	3GLS
SK	3ATPS	IDW	3ATPS	LSK	SM	OK	3ATPS	OK	SM
OK	SM	SK	SM	SK	3GLS	OK	3FRS	OK	3GLS
LSK	3GLS	OK	3GLS	OK	3GLS	IDW	SM	OK	3FRS
OK	3GLS	NN	3ATPS	OK	3FRS	TS	3ATPS	SK	SM
LSK	3ATPS	NN	3GLS	IDW	3GLS	OK	SM	MURS	3GLS
IDW	3ATPS	NN	3FRS	SK	3FRS	OK	3GLS	LSK	3GLS
NN	3ATPS	LSK	3ATPS	NN	3ATPS	LSK	3FRS	MRSM	3GLS
NN	3GLS	NN	1GLS	IDW	3FRS	SK	1GLS	SK	3FRS
NN	3FRS	NN	SM	NN	3GLS	NN	3GLS	SK	1GLS
NN	1GLS	IDW	3GLS	NN	3FRS	NN	1GLS	LSK	3FRS
NN	SM	MURS	SM	NN	1GLS	NN	3ATPS	TS	3GLS
MURS	SM	LSK	SM	NN	SM	NN	3FRS	NN	3ATPS
MURS	3GLS	IDW	3FRS	IDW	1GLS	NN	SM	OK	1GLS
IDW	3GLS	LSK	3GLS	TS	3ATPS	LSK	3GLS	NN	3GLS
IDW	3FRS	IDW	1GLS	OK	SM	MURS	3GLS	NN	3FRS
IDW	1GLS	IDW	SM	IDW	SM	LSK	SM	LSK	SM
TS	3ATPS	MURS	3GLS	MURS	3GLS	SK	SM	NN	SM
MURS	3FRS	TS	3ATPS	MRSM	3GLS	MRSM	3GLS	NN	1GLS
IDW	SM	MURS	3FRS	MURS	3FRS	MURS	3FRS	LSK	1GLS
MRSM	3GLS	MRSM	3GLS	MURS	SM	TS	3GLS	MURS	3FRS
MRSM	SM	MRSM	SM	MRSM	3FRS	MRSM	3FRS	MURS	SM
MURS	1GLS	MURS	1GLS	TS	3GLS	TS	3FRS	MRSM	3FRS
MRSM	3FRS	MRSM	3FRS	MRSM	SM	MURS	SM	TS	3FRS
MRSM	1GLS	MRSM	1GLS	MURS	1GLS	MURS	1GLS	MRSM	SM
TS	3GLS	TS	3GLS	TS	3FRS	MRSM	1GLS	MURS	1GLS
TS	3FRS	TS	3FRS	MRSM	1GLS	MRSM	SM	MRSM	1GLS
TS	1GLS	TS	1GLS	TS	1GLS	TS	1GLS	TS	1GLS
FA	1GLS	FA	1GLS	FA	1GLS	FA	1GLS	FA	1GLS
FA	3ATPS	FA	3ATPS	FA	3ATPS	FA	3ATPS	FA	3ATPS
FA	3FRS	FA	3FRS	FA	3FRS	FA	3FRS	FA	3FRS
FA	3GLS	FA	3GLS	FA	3GLS	FA	3GLS	FA	3GLS
FA	SM	FA	SM	FA	SM	FA	SM	FA	SM
TS	SM	TS	SM	TS	SM	TS	SM	TS	SM

Table A.7: MO RR, methods ranked by MAPE, pt1.

Percentage Data Removed											
19.53		26.20		33.79		41.77		50.24		60.91	
OK	1GLS	SK	1GLS	SK	1GLS	SK	SM	OK	SM	OK	1GLS
OK	SM	LSK	3GLS	SK	SM	OK	SM	OK	1GLS	SK	1GLS
SK	1GLS	OK	SM	SK	3FRS	LSK	1GLS	OK	3FRS	OK	SM
SK	3GLS	OK	1GLS	OK	SM	LSK	3GLS	SK	3FRS	SK	3FRS
LSK	SM	OK	3FRS	OK	1GLS	OK	3FRS	SK	SM	SK	SM
OK	3GLS	LSK	3FRS	LSK	1GLS	LSK	3FRS	SK	3GLS	LSK	3FRS
LSK	3FRS	SK	3FRS	SK	3GLS	LSK	SM	LSK	SM	OK	3FRS
SK	SM	LSK	SM	LSK	SM	OK	1GLS	SK	1GLS	SK	3GLS
SK	3FRS	SK	SM	OK	3FRS	SK	1GLS	OK	3GLS	SK	3ATPS
LSK	3GLS	LSK	1GLS	OK	3GLS	SK	3GLS	LSK	1GLS	MURS	3ATPS
OK	3FRS	OK	3GLS	SK	3ATPS	OK	3GLS	OK	3ATPS	OK	3GLS
SK	3ATPS	SK	3GLS	LSK	3GLS	OK	3ATPS	SK	3ATPS	OK	3ATPS
LSK	1GLS	MURS	3ATPS	LSK	3FRS	MURS	3ATPS	MURS	3ATPS	MRSM	3ATPS
MURS	3ATPS	SK	3ATPS	MURS	3ATPS	LSK	3ATPS	MRSM	3ATPS	NN	3ATPS
OK	3ATPS	OK	3ATPS	OK	3ATPS	SK	3FRS	LSK	3GLS	NN	3GLS
MURS	3GLS	MURS	SM	MURS	3GLS	SK	3ATPS	NN	3ATPS	NN	SM
MURS	SM	MURS	3GLS	MRSM	3ATPS	MURS	3GLS	MURS	SM	IDW	3ATPS
LSK	3ATPS	MURS	1GLS	MURS	SM	MRSM	3ATPS	MURS	3GLS	NN	1GLS
MRSM	3ATPS	MRSM	3ATPS	MRSM	3GLS	MURS	SM	NN	3GLS	LSK	SM
MURS	3FRS	MURS	3FRS	LSK	3ATPS	MURS	1GLS	LSK	3ATPS	NN	3FRS
MURS	1GLS	MRSM	3GLS	NN	3ATPS	MRSM	3GLS	NN	SM	LSK	3GLS
MRSM	3GLS	LSK	3ATPS	MRSM	SM	NN	3ATPS	NN	1GLS	LSK	1GLS
MRSM	SM	MRSM	SM	MURS	1GLS	MURS	3FRS	NN	3FRS	MURS	3GLS
NN	3ATPS	MRSM	1GLS	MURS	3FRS	MRSM	SM	MRSM	3GLS	MURS	SM
NN	SM	MRSM	3FRS	MRSM	1GLS	NN	3GLS	IDW	3ATPS	LSK	3ATPS
NN	1GLS	NN	3ATPS	NN	3GLS	IDW	3ATPS	MURS	3FRS	MRSM	3GLS
MRSM	1GLS	NN	3GLS	NN	1GLS	NN	1GLS	MURS	1GLS	MRSM	SM
NN	3GLS	NN	1GLS	NN	SM	NN	SM	MRSM	SM	IDW	3GLS
NN	3FRS	NN	SM	NN	3FRS	NN	3FRS	LSK	3FRS	MURS	1GLS
MRSM	3FRS	NN	3FRS	IDW	3ATPS	MRSM	1GLS	MRSM	1GLS	TS	3ATPS
IDW	3ATPS	IDW	3ATPS	MRSM	3FRS	MRSM	3FRS	MRSM	3FRS	MURS	3FRS
IDW	3GLS	IDW	3GLS	IDW	3GLS	IDW	3GLS	IDW	3GLS	IDW	3FRS
TS	3ATPS	TS	3ATPS	TS	3ATPS	TS	3ATPS	TS	3ATPS	MRSM	3FRS
IDW	3FRS	IDW	1GLS	IDW	1GLS	IDW	1GLS	IDW	3FRS	IDW	1GLS
IDW	1GLS	IDW	3FRS	IDW	3FRS	IDW	3FRS	IDW	1GLS	MRSM	1GLS
IDW	SM	IDW	SM	IDW	SM	IDW	SM	IDW	SM	IDW	SM
TS	3GLS	TS	3GLS	TS	3GLS	TS	3GLS	TS	3GLS	TS	3GLS
TS	3FRS	TS	3FRS	TS	3FRS	TS	3FRS	TS	3FRS	TS	3FRS
TS	1GLS	TS	1GLS	TS	1GLS	TS	1GLS	TS	1GLS	TS	1GLS
FA	1GLS	FA	1GLS	FA	1GLS	FA	1GLS	FA	1GLS	FA	1GLS
FA	3ATPS	FA	3ATPS	FA	3ATPS	FA	3ATPS	FA	3ATPS	FA	3ATPS
FA	3FRS	FA	3FRS	FA	3FRS	FA	3FRS	FA	3FRS	FA	3FRS
FA	3GLS	FA	3GLS	FA	3GLS	FA	3GLS	FA	3GLS	FA	3GLS
FA	SM	FA	SM	FA	SM	FA	SM	FA	SM	FA	SM
TS	SM	TS	SM	TS	SM	TS	SM	TS	SM	TS	SM

Table A.8: MO RR, methods ranked by MAPE, pt2.

Percentage Data Removed									
68.48		79.59		90.26		94.90		97.44	
SK	3FRS	OK	1GLS	LSK	3GLS	SK	3ATPS	IDW	3ATPS
LSK	1GLS	LSK	3FRS	LSK	1GLS	LSK	1GLS	SK	3ATPS
LSK	SM	SK	1GLS	OK	3ATPS	IDW	3ATPS	MURS	3ATPS
OK	1GLS	OK	SM	OK	1GLS	LSK	3ATPS	OK	3ATPS
SK	3GLS	LSK	1GLS	SK	3ATPS	MURS	3ATPS	MRSM	3ATPS
SK	1GLS	OK	3ATPS	LSK	3ATPS	MRSM	3ATPS	LSK	3ATPS
LSK	3FRS	SK	3GLS	IDW	3ATPS	OK	3ATPS	IDW	3GLS
OK	3ATPS	OK	3FRS	SK	1GLS	NN	SM	TS	3ATPS
SK	3ATPS	SK	3ATPS	LSK	SM	OK	1GLS	IDW	3FRS
MURS	3ATPS	MURS	3ATPS	NN	3ATPS	IDW	3GLS	IDW	1GLS
LSK	3GLS	NN	3ATPS	MURS	3ATPS	NN	1GLS	NN	3ATPS
SK	SM	IDW	3ATPS	LSK	3FRS	NN	3FRS	NN	SM
OK	SM	SK	3FRS	SK	SM	NN	3GLS	NN	3FRS
OK	3FRS	NN	3FRS	NN	SM	SK	3FRS	NN	3GLS
LSK	3ATPS	NN	1GLS	NN	3GLS	NN	3ATPS	OK	SM
OK	3GLS	NN	SM	NN	1GLS	TS	3ATPS	NN	1GLS
NN	3ATPS	NN	3GLS	NN	3FRS	IDW	1GLS	SK	3GLS
NN	SM	MRSM	3ATPS	SK	3GLS	SK	3GLS	IDW	SM
NN	3GLS	OK	3GLS	OK	3GLS	IDW	3FRS	OK	3GLS
NN	1GLS	LSK	3ATPS	MRSM	3ATPS	OK	3FRS	OK	3FRS
NN	3FRS	LSK	SM	SK	3FRS	SK	1GLS	SK	SM
MRSM	3ATPS	SK	SM	IDW	3GLS	OK	SM	SK	1GLS
IDW	3ATPS	LSK	3GLS	OK	3FRS	OK	3GLS	MURS	3GLS
IDW	3GLS	IDW	3GLS	TS	3ATPS	IDW	SM	LSK	3GLS
MURS	3GLS	TS	3ATPS	IDW	3FRS	LSK	3FRS	MRSM	3GLS
TS	3ATPS	IDW	3FRS	IDW	1GLS	LSK	3GLS	SK	3FRS
MURS	SM	IDW	1GLS	OK	SM	LSK	SM	LSK	3FRS
MRSM	3GLS	MURS	SM	IDW	SM	MURS	3GLS	OK	1GLS
IDW	3FRS	IDW	SM	MURS	3GLS	MRSM	3GLS	TS	3GLS
IDW	1GLS	MURS	3GLS	MRSM	3GLS	SK	SM	LSK	1GLS
MURS	3FRS	MRSM	3GLS	MURS	3FRS	TS	3GLS	LSK	SM
MRSM	SM	MRSM	SM	TS	3GLS	MURS	3FRS	MURS	3FRS
IDW	SM	MURS	3FRS	MRSM	3FRS	MRSM	3FRS	MRSM	3FRS
MRSM	3FRS	MRSM	3FRS	MURS	SM	MURS	1GLS	TS	3FRS
MURS	1GLS	MURS	1GLS	MURS	1GLS	MRSM	1GLS	MURS	SM
MRSM	1GLS	MRSM	1GLS	MRSM	1GLS	TS	3FRS	MURS	1GLS
TS	3GLS	TS	3GLS	MRSM	SM	TS	1GLS	MRSM	SM
TS	3FRS	TS	3FRS	TS	3FRS	MURS	SM	MRSM	1GLS
TS	1GLS	TS	1GLS	TS	1GLS	MRSM	SM	TS	1GLS
FA	1GLS	FA	1GLS	FA	1GLS	FA	1GLS	FA	1GLS
FA	3ATPS	FA	3ATPS	FA	3ATPS	FA	3ATPS	FA	3ATPS
FA	3FRS	FA	3FRS	FA	3FRS	FA	3FRS	FA	3FRS
FA	3GLS	FA	3GLS	FA	3GLS	FA	3GLS	FA	3GLS
FA	SM	FA	SM	FA	SM	FA	SM	FA	SM
TS	SM	TS	SM	TS	SM	TS	SM	TS	SM

Table A.9: CT MM, methods ranked by MSPE, pt1.

Percentage Data Removed									
54.30		62.21		69.21		74.27		79.27	
SK	SM	SK	SM	SK	1GLS	SK	1GLS	OK	SM
OK	SM	OK	SM	SK	SM	OK	SM	SK	1GLS
SK	3ATPS	OK	1GLS	OK	1GLS	SK	SM	OK	1GLS
SK	3GLS	LSK	SM	OK	SM	OK	1GLS	SK	SM
OK	3ATPS	OK	3ATPS	LSK	SM	LSK	SM	MURS	3ATPS
OK	3GLS	OK	3GLS	MURS	3ATPS	LSK	1GLS	LSK	SM
SK	1GLS	SK	3ATPS	LSK	1GLS	MURS	3ATPS	LSK	1GLS
LSK	SM	SK	3GLS	SK	3ATPS	OK	3ATPS	MURS	1GLS
OK	1GLS	SK	1GLS	SK	3GLS	OK	3GLS	MURS	SM
LSK	3GLS	LSK	3GLS	OK	3ATPS	SK	3ATPS	IDW	1GLS
MURS	3ATPS	MURS	3ATPS	OK	3GLS	SK	3GLS	IDW	SM
IDW	1GLS	LSK	1GLS	IDW	1GLS	LSK	3GLS	LSK	3ATPS
IDW	SM	IDW	1GLS	IDW	SM	MURS	1GLS	LSK	3GLS
MURS	1GLS	IDW	SM	MURS	1GLS	IDW	1GLS	OK	3GLS
LSK	1GLS	MURS	1GLS	MURS	SM	IDW	SM	OK	3ATPS
MURS	SM	MURS	SM	LSK	3GLS	MURS	SM	SK	3ATPS
IDW	3GLS	IDW	3GLS	LSK	3ATPS	LSK	3ATPS	SK	3GLS
MURS	3GLS	MURS	3GLS	IDW	3GLS	IDW	3GLS	IDW	3GLS
OK	3FRS	OK	3FRS	MURS	3GLS	MURS	3GLS	MURS	3GLS
LSK	3ATPS	SK	3FRS	SK	3FRS	IDW	3ATPS	IDW	3ATPS
LSK	3FRS	LSK	3ATPS	OK	3FRS	SK	3FRS	MRSRM	1GLS
SK	3FRS	LSK	3FRS	LSK	3FRS	OK	3FRS	SK	3FRS
MRSRM	1GLS	MURS	3FRS	MRSRM	1GLS	LSK	3FRS	MRSRM	SM
MRSRM	3ATPS	MRSRM	1GLS	IDW	3ATPS	TS	3ATPS	MRSRM	3ATPS
TS	3GLS	NN	3ATPS	MRSRM	3ATPS	NN	3ATPS	OK	3FRS
MURS	3FRS	MRSRM	3ATPS	MRSRM	SM	MRSRM	1GLS	TS	3ATPS
TS	3ATPS	MRSRM	SM	TS	3ATPS	MRSRM	3ATPS	MRSRM	3GLS
MRSRM	SM	MRSRM	3GLS	MURS	3FRS	MRSRM	SM	LSK	3FRS
NN	3ATPS	TS	3GLS	MRSRM	3GLS	MURS	3FRS	MURS	3FRS
MRSRM	3GLS	IDW	3FRS	NN	3ATPS	MRSRM	3GLS	IDW	3FRS
IDW	3ATPS	IDW	3ATPS	IDW	3FRS	IDW	3FRS	MRSRM	3FRS
IDW	3FRS	MRSRM	3FRS	TS	3GLS	TS	3GLS	NN	3ATPS
MRSRM	3FRS	NN	3FRS	MRSRM	3FRS	MRSRM	3FRS	TS	3GLS
NN	3FRS	TS	3ATPS	TS	3FRS	NN	3GLS	TS	3FRS
TS	3FRS	NN	3GLS	NN	3FRS	NN	3FRS	NN	3GLS
NN	3GLS	NN	1GLS	NN	3GLS	NN	1GLS	NN	1GLS
NN	1GLS	NN	SM	NN	1GLS	NN	SM	NN	SM
FA	1GLS	TS	3FRS	NN	SM	TS	3FRS	NN	3FRS
FA	3ATPS	FA	1GLS	FA	1GLS	FA	1GLS	FA	1GLS
FA	3FRS	FA	3ATPS	FA	3ATPS	FA	3ATPS	FA	3ATPS
FA	3GLS	FA	3FRS	FA	3FRS	FA	3FRS	FA	3FRS
FA	SM	FA	3GLS	FA	3GLS	FA	3GLS	FA	3GLS
TS	SM	FA	SM	FA	SM	FA	SM	FA	SM
NN	SM	TS	SM	TS	SM	TS	SM	TS	SM
TS	1GLS	TS	1GLS	TS	1GLS	TS	1GLS	TS	1GLS

Table A.10: CT MM, methods ranked by MSPE, pt2.

Percentage Data Removed											
85.11		88.57		93.26		96.75		98.27		99.24	
SK	1GLS	OK	1GLS	SK	SM	OK	1GLS	OK	1GLS	LSK	3ATPS
OK	1GLS	OK	SM	OK	1GLS	OK	SM	SK	1GLS	MRSM	3GLS
OK	SM	SK	SM	SK	1GLS	OK	3ATPS	OK	3ATPS	OK	3GLS
SK	SM	SK	1GLS	LSK	3ATPS	SK	1GLS	LSK	3ATPS	LSK	3GLS
MURS	3ATPS	MURS	3ATPS	OK	SM	MURS	3ATPS	OK	SM	TS	3GLS
LSK	1GLS	OK	3ATPS	OK	3ATPS	SK	SM	OK	3GLS	SK	3ATPS
OK	3ATPS	LSK	SM	LSK	1GLS	MURS	SM	LSK	3GLS	SK	3GLS
OK	3GLS	LSK	1GLS	MURS	3ATPS	LSK	3ATPS	IDW	3GLS	IDW	3GLS
SK	3ATPS	MURS	1GLS	SK	3ATPS	IDW	SM	MURS	3ATPS	MURS	3GLS
SK	3GLS	MURS	SM	SK	3GLS	IDW	1GLS	SK	3ATPS	NN	3GLS
LSK	SM	MURS	3GLS	OK	3GLS	SK	3ATPS	SK	3GLS	NN	3ATPS
LSK	3GLS	OK	3GLS	LSK	3GLS	SK	3GLS	SK	SM	IDW	3ATPS
MURS	1GLS	SK	3ATPS	LSK	SM	LSK	1GLS	MURS	3GLS	TS	3ATPS
LSK	3ATPS	SK	3GLS	MURS	SM	MURS	1GLS	IDW	1GLS	NN	SM
MURS	SM	LSK	3ATPS	MURS	1GLS	OK	3GLS	MURS	1GLS	NN	1GLS
MURS	3GLS	IDW	3GLS	SK	3FRS	IDW	3ATPS	MRSM	3GLS	IDW	SM
IDW	3GLS	LSK	3GLS	OK	3FRS	NN	3ATPS	IDW	SM	OK	3ATPS
OK	3FRS	SK	3FRS	MURS	3GLS	LSK	3GLS	MURS	SM	MURS	3ATPS
LSK	3FRS	OK	3FRS	LSK	3FRS	LSK	SM	MRSM	3ATPS	MRSM	3ATPS
SK	3FRS	MURS	3FRS	IDW	3GLS	TS	3ATPS	MRSM	1GLS	IDW	1GLS
IDW	3ATPS	IDW	3FRS	IDW	SM	IDW	3GLS	LSK	1GLS	SK	SM
MURS	3FRS	LSK	3FRS	IDW	1GLS	MURS	3GLS	MRSM	SM	OK	SM
TS	3ATPS	IDW	SM	MURS	3FRS	MRSM	SM	LSK	SM	OK	1GLS
IDW	SM	IDW	1GLS	IDW	3FRS	MRSM	1GLS	TS	3GLS	SK	1GLS
IDW	1GLS	TS	3ATPS	NN	3FRS	MRSM	3ATPS	IDW	3ATPS	LSK	SM
IDW	3FRS	IDW	3ATPS	NN	3GLS	NN	1GLS	NN	3ATPS	MRSM	SM
MRSM	3GLS	MRSM	1GLS	MRSM	1GLS	MRSM	3GLS	TS	3ATPS	MURS	SM
MRSM	3ATPS	MRSM	3ATPS	MRSM	3ATPS	NN	SM	TS	1GLS	LSK	1GLS
MRSM	1GLS	MRSM	SM	MRSM	SM	NN	3GLS	FA	1GLS	MRSM	1GLS
MRSM	SM	MRSM	3GLS	MRSM	3GLS	IDW	3FRS	FA	3ATPS	MURS	1GLS
MRSM	3FRS	MRSM	3FRS	NN	1GLS	TS	3GLS	FA	3FRS	TS	1GLS
TS	3FRS	TS	3FRS	NN	SM	SK	3FRS	FA	3GLS	FA	1GLS
NN	3ATPS	TS	3GLS	IDW	3ATPS	OK	3FRS	FA	SM	FA	3ATPS
TS	3GLS	NN	3ATPS	NN	3ATPS	TS	1GLS	TS	SM	FA	3FRS
NN	3FRS	NN	3FRS	TS	3FRS	MURS	3FRS	NN	3GLS	FA	3GLS
NN	3GLS	NN	3GLS	MRSM	3FRS	FA	1GLS	NN	1GLS	FA	SM
NN	1GLS	NN	1GLS	TS	3GLS	FA	3ATPS	NN	SM	TS	SM
NN	SM	NN	SM	TS	1GLS	FA	3FRS	SK	3FRS	LSK	3FRS
FA	1GLS	TS	1GLS	FA	1GLS	FA	3GLS	OK	3FRS	IDW	3FRS
FA	3ATPS	FA	1GLS	FA	3ATPS	FA	SM	MURS	3FRS	NN	3FRS
FA	3FRS	FA	3ATPS	FA	3FRS	TS	SM	IDW	3FRS	TS	3FRS
FA	3GLS	FA	3FRS	FA	3GLS	LSK	3FRS	NN	3FRS	MURS	3FRS
FA	SM	FA	3GLS	FA	SM	TS	3FRS	LSK	3FRS	SK	3FRS
TS	SM	FA	SM	TS	SM	MRSM	3FRS	MRSM	3FRS	OK	3FRS
TS	1GLS	TS	SM	TS	3ATPS	NN	3FRS	TS	3FRS	MRSM	3FRS

Table A.11: CT MM, methods ranked by MAPE, pt1.

Percentage Data Removed									
54.30		62.21		69.21		74.27		79.27	
SK	SM	OK	1GLS	SK	1GLS	OK	1GLS	OK	SM
OK	SM	SK	SM	OK	1GLS	SK	1GLS	SK	1GLS
SK	1GLS	OK	SM	SK	SM	SK	SM	LSK	1GLS
OK	1GLS	SK	1GLS	OK	SM	OK	SM	OK	1GLS
LSK	SM	LSK	SM	LSK	SM	LSK	SM	LSK	SM
MURS	3ATPS	LSK	1GLS	LSK	1GLS	LSK	1GLS	SK	SM
SK	3ATPS	MURS	3ATPS	MURS	3ATPS	MURS	3ATPS	MURS	3ATPS
OK	3ATPS	SK	3ATPS	SK	3ATPS	SK	3ATPS	MURS	1GLS
LSK	1GLS	OK	3ATPS	MURS	1GLS	OK	3ATPS	LSK	3ATPS
IDW	SM	MURS	1GLS	OK	3ATPS	MURS	1GLS	MURS	SM
MURS	1GLS	MURS	SM	MURS	SM	MURS	SM	IDW	SM
IDW	1GLS	IDW	SM	IDW	SM	IDW	SM	IDW	1GLS
MURS	SM	IDW	1GLS	IDW	1GLS	IDW	1GLS	OK	3ATPS
LSK	3ATPS	OK	3FRS	LSK	3ATPS	LSK	3ATPS	SK	3ATPS
OK	3FRS	SK	3FRS	IDW	3GLS	IDW	3GLS	IDW	3GLS
IDW	3GLS	LSK	3ATPS	SK	3FRS	NN	3ATPS	MRSRM	1GLS
LSK	3FRS	NN	3ATPS	OK	3FRS	SK	3FRS	MRSRM	SM
SK	3FRS	IDW	3GLS	LSK	3FRS	OK	3FRS	IDW	3ATPS
NN	3ATPS	LSK	3FRS	MRSRM	1GLS	IDW	3ATPS	MRSRM	3ATPS
MRSRM	1GLS	MRSRM	1GLS	NN	3ATPS	LSK	3FRS	SK	3FRS
MRSRM	3ATPS	MRSRM	SM	MRSRM	3ATPS	MRSRM	1GLS	OK	3FRS
MRSRM	SM	MRSRM	3ATPS	MRSRM	SM	MRSRM	SM	NN	3ATPS
NN	3FRS	NN	3FRS	IDW	3ATPS	MRSRM	3ATPS	LSK	3FRS
NN	3GLS	NN	3GLS	NN	3GLS	NN	3GLS	TS	3ATPS
TS	3ATPS	NN	1GLS	TS	3ATPS	TS	3ATPS	MURS	3FRS
MURS	3FRS	NN	SM	MURS	3FRS	NN	1GLS	NN	3GLS
NN	1GLS	MURS	3FRS	NN	3FRS	NN	3FRS	NN	1GLS
TS	3GLS	IDW	3ATPS	NN	1GLS	NN	SM	MRSRM	3FRS
NN	SM	MRSRM	3FRS	NN	SM	MURS	3FRS	NN	SM
IDW	3ATPS	IDW	3FRS	MRSRM	3FRS	MRSRM	3FRS	IDW	3FRS
IDW	3FRS	TS	3GLS	IDW	3FRS	IDW	3FRS	NN	3FRS
MRSRM	3FRS	TS	3ATPS	TS	3GLS	TS	3GLS	TS	3GLS
FA	1GLS	TS	1GLS	TS	1GLS	TS	1GLS	TS	1GLS
FA	3ATPS	FA	1GLS	FA	1GLS	FA	1GLS	FA	1GLS
FA	3FRS	FA	3ATPS	FA	3ATPS	FA	3ATPS	FA	3ATPS
FA	3GLS	FA	3FRS	FA	3FRS	FA	3FRS	FA	3FRS
FA	SM	FA	3GLS	FA	3GLS	FA	3GLS	FA	3GLS
TS	SM	FA	SM	FA	SM	FA	SM	FA	SM
TS	1GLS	TS	SM	TS	SM	TS	SM	TS	SM
TS	3FRS	TS	3FRS	TS	3FRS	TS	3FRS	TS	3FRS
SK	3GLS	OK	3GLS	SK	3GLS	OK	3GLS	LSK	3GLS
OK	3GLS	SK	3GLS	OK	3GLS	SK	3GLS	OK	3GLS
LSK	3GLS	LSK	3GLS	LSK	3GLS	LSK	3GLS	SK	3GLS
MURS	3GLS	MURS	3GLS	MURS	3GLS	MURS	3GLS	MURS	3GLS
MRSRM	3GLS	MRSRM	3GLS	MRSRM	3GLS	MRSRM	3GLS	MRSRM	3GLS

Table A.12: CT MM, methods ranked by MAPE, pt2.

Percentage Data Removed											
85.11		88.57		93.26		96.75		98.27		99.24	
SK	1GLS	SK	1GLS	OK	SM	OK	1GLS	OK	SM	IDW	3ATPS
OK	SM	OK	1GLS	OK	1GLS	OK	SM	OK	1GLS	NN	3ATPS
OK	1GLS	SK	SM	SK	1GLS	SK	1GLS	SK	1GLS	TS	3ATPS
SK	SM	OK	SM	SK	SM	OK	3ATPS	SK	SM	LSK	3ATPS
MURS	3ATPS	MURS	3ATPS	LSK	1GLS	SK	SM	MURS	3ATPS	IDW	3GLS
LSK	1GLS	OK	3ATPS	OK	3ATPS	LSK	1GLS	OK	3ATPS	TS	3GLS
LSK	SM	LSK	1GLS	MURS	3ATPS	IDW	SM	IDW	1GLS	SK	3ATPS
OK	3ATPS	LSK	SM	LSK	SM	MURS	3ATPS	IDW	SM	NN	3GLS
MURS	1GLS	MURS	1GLS	LSK	3ATPS	MURS	SM	MURS	SM	IDW	SM
MURS	SM	MURS	SM	MURS	SM	IDW	1GLS	MURS	1GLS	NN	SM
SK	3ATPS	LSK	3ATPS	MURS	1GLS	LSK	SM	MRSRM	SM	NN	1GLS
LSK	3ATPS	SK	3ATPS	SK	3ATPS	MURS	1GLS	LSK	SM	IDW	1GLS
IDW	3GLS	IDW	SM	IDW	SM	MRSRM	SM	MRSRM	1GLS	OK	3ATPS
IDW	SM	IDW	1GLS	IDW	1GLS	MRSRM	1GLS	LSK	1GLS	MURS	3ATPS
IDW	1GLS	IDW	3GLS	MRSRM	1GLS	NN	3ATPS	MRSRM	3ATPS	MRSRM	3ATPS
LSK	3FRS	MRSRM	1GLS	SK	3FRS	MRSRM	3ATPS	LSK	3ATPS	SK	SM
OK	3FRS	MRSRM	SM	OK	3FRS	LSK	3ATPS	SK	3ATPS	OK	SM
SK	3FRS	SK	3FRS	MRSRM	SM	SK	3ATPS	IDW	3GLS	OK	1GLS
IDW	3ATPS	MRSRM	3ATPS	LSK	3FRS	NN	1GLS	IDW	3ATPS	SK	1GLS
MRSRM	1GLS	OK	3FRS	MRSRM	3ATPS	NN	SM	FA	1GLS	LSK	1GLS
MRSRM	SM	LSK	3FRS	NN	3GLS	IDW	3ATPS	FA	3ATPS	MRSRM	1GLS
MRSRM	3ATPS	MURS	3FRS	NN	1GLS	TS	3ATPS	FA	3FRS	MURS	1GLS
MURS	3FRS	IDW	3FRS	NN	3FRS	IDW	3GLS	FA	3GLS	LSK	SM
TS	3ATPS	IDW	3ATPS	NN	SM	NN	3GLS	FA	SM	MRSRM	SM
IDW	3FRS	TS	3ATPS	IDW	3GLS	IDW	3FRS	TS	SM	TS	1GLS
NN	3ATPS	MRSRM	3FRS	MURS	3FRS	SK	3FRS	NN	3ATPS	MURS	SM
MRSRM	3FRS	NN	3ATPS	IDW	3FRS	TS	3GLS	TS	1GLS	FA	1GLS
NN	3FRS	NN	3FRS	NN	3ATPS	OK	3FRS	TS	3ATPS	FA	3ATPS
NN	3GLS	NN	3GLS	MRSRM	3FRS	LSK	3FRS	NN	1GLS	FA	3FRS
NN	1GLS	TS	3FRS	IDW	3ATPS	FA	1GLS	NN	SM	FA	3GLS
NN	SM	NN	1GLS	TS	3FRS	FA	3ATPS	TS	3GLS	FA	SM
TS	3FRS	NN	SM	TS	3GLS	FA	3FRS	NN	3GLS	TS	SM
TS	3GLS	TS	3GLS	TS	1GLS	FA	3GLS	SK	3FRS	IDW	3FRS
FA	1GLS	FA	1GLS	FA	1GLS	FA	SM	MURS	3FRS	LSK	3FRS
FA	3ATPS	FA	3ATPS	FA	3ATPS	TS	SM	OK	3FRS	NN	3FRS
FA	3FRS	FA	3FRS	FA	3FRS	TS	1GLS	NN	3FRS	TS	3FRS
FA	3GLS	FA	3GLS	FA	3GLS	MURS	3FRS	MRSRM	3FRS	MURS	3FRS
FA	SM	FA	SM	FA	SM	TS	3FRS	IDW	3FRS	SK	3FRS
TS	SM	TS	SM	TS	SM	MRSRM	3FRS	LSK	3FRS	OK	3FRS
TS	1GLS	TS	1GLS	TS	3ATPS	NN	3FRS	TS	3FRS	MRSRM	3FRS
OK	3GLS	MURS	3GLS	SK	3GLS	SK	3GLS	OK	3GLS	MRSRM	3GLS
SK	3GLS	OK	3GLS	OK	3GLS	OK	3GLS	LSK	3GLS	OK	3GLS
LSK	3GLS	SK	3GLS	LSK	3GLS	LSK	3GLS	SK	3GLS	LSK	3GLS
MURS	3GLS	LSK	3GLS	MURS	3GLS	MURS	3GLS	MURS	3GLS	SK	3GLS
MRSRM	3GLS	MRSRM	3GLS	MRSRM	3GLS	MRSRM	3GLS	MRSRM	3GLS	MURS	3GLS

Table A.13: MO MM, methods ranked by MSPE, pt1.

Percentage Data Removed											
48.97		53.13		58.06		63.28		68.80		75.6	
SK	3FRS	SK	3FRS	SK	3ATPS	SK	SM	OK	1GLS	OK	1GLS
LSK	3FRS	OK	1GLS	OK	3FRS	OK	3FRS	SK	3FRS	SK	3FRS
OK	3FRS	OK	3ATPS	SK	3GLS	OK	1GLS	OK	3FRS	OK	3FRS
SK	1GLS	SK	3ATPS	OK	SM	SK	3GLS	LSK	1GLS	SK	3GLS
OK	1GLS	OK	3FRS	OK	3ATPS	LSK	3FRS	OK	3GLS	SK	1GLS
IDW	1GLS	SK	1GLS	IDW	3ATPS	SK	1GLS	SK	1GLS	OK	3GLS
IDW	3FRS	LSK	3ATPS	LSK	3FRS	OK	3GLS	SK	3GLS	OK	3ATPS
SK	3GLS	LSK	3FRS	SK	1GLS	IDW	3ATPS	SK	3ATPS	LSK	3GLS
SK	3ATPS	LSK	3GLS	OK	3GLS	SK	3FRS	LSK	3FRS	SK	3ATPS
MURS	3ATPS	IDW	1GLS	MURS	3ATPS	IDW	3FRS	IDW	3FRS	IDW	3ATPS
IDW	3ATPS	IDW	3FRS	SK	3FRS	LSK	3GLS	LSK	3GLS	MURS	3ATPS
OK	3ATPS	IDW	3ATPS	OK	1GLS	LSK	1GLS	IDW	1GLS	IDW	3FRS
MRSRM	3ATPS	MRSRM	3ATPS	LSK	3ATPS	IDW	3GLS	SK	SM	LSK	3FRS
LSK	3ATPS	MURS	3ATPS	IDW	3FRS	OK	3ATPS	MURS	3ATPS	IDW	1GLS
LSK	3GLS	SK	3GLS	TS	3ATPS	IDW	1GLS	OK	3ATPS	MRSRM	3ATPS
OK	3GLS	OK	3GLS	IDW	1GLS	SK	3ATPS	IDW	3ATPS	LSK	1GLS
LSK	1GLS	LSK	1GLS	MRSRM	3ATPS	OK	SM	MRSRM	3ATPS	MURS	3GLS
MURS	3FRS	MURS	3GLS	NN	3ATPS	MURS	3ATPS	IDW	3GLS	LSK	3ATPS
TS	3ATPS	NN	3ATPS	LSK	1GLS	LSK	3ATPS	MURS	3GLS	IDW	3GLS
IDW	3GLS	MRSRM	3GLS	MRSRM	3GLS	MURS	3GLS	MURS	3FRS	MURS	3FRS
MRSRM	3FRS	MURS	3FRS	IDW	3GLS	MRSRM	3ATPS	TS	3ATPS	TS	3ATPS
MURS	1GLS	IDW	3GLS	MURS	3GLS	MURS	3FRS	LSK	3ATPS	MRSRM	3GLS
MRSRM	1GLS	TS	3ATPS	LSK	3GLS	MRSRM	3GLS	MRSRM	3FRS	MRSRM	3FRS
MRSRM	3GLS	MRSRM	3FRS	NN	3FRS	MRSRM	3FRS	MRSRM	3GLS	IDW	SM
MURS	3GLS	MURS	1GLS	NN	3GLS	TS	3ATPS	MURS	1GLS	NN	3ATPS
NN	3ATPS	MRSRM	1GLS	LSK	SM	NN	3ATPS	MRSRM	1GLS	MURS	1GLS
TS	3GLS	NN	3FRS	MURS	3FRS	MURS	1GLS	IDW	SM	OK	SM
TS	3FRS	NN	3GLS	NN	1GLS	MRSRM	1GLS	NN	3ATPS	LSK	SM
NN	3FRS	NN	1GLS	MRSRM	3FRS	NN	3FRS	TS	3GLS	NN	3FRS
IDW	SM	NN	SM	NN	SM	NN	3GLS	NN	3FRS	MRSRM	1GLS
NN	3GLS	TS	3GLS	MURS	1GLS	NN	1GLS	NN	3GLS	SK	SM
NN	1GLS	IDW	SM	MRSRM	1GLS	IDW	SM	NN	1GLS	NN	1GLS
NN	SM	OK	SM	SK	SM	NN	SM	NN	SM	TS	3GLS
SK	SM	TS	3FRS	IDW	SM	TS	3FRS	TS	3FRS	NN	3GLS
TS	1GLS	TS	1GLS	TS	3GLS	TS	3GLS	OK	SM	NN	SM
OK	SM	SK	SM	TS	3FRS	LSK	SM	LSK	SM	TS	3FRS
MRSRM	SM	LSK	SM	TS	1GLS	TS	1GLS	MURS	SM	MRSRM	SM
LSK	SM	MURS	SM	MRSRM	SM	MRSRM	SM	MRSRM	SM	MURS	SM
MURS	SM	MRSRM	SM	MURS	SM	MURS	SM	TS	1GLS	TS	1GLS
FA	1GLS	FA	1GLS	FA	1GLS	FA	1GLS	FA	1GLS	FA	1GLS
FA	3ATPS	FA	3ATPS	FA	3ATPS	FA	3ATPS	FA	3ATPS	FA	3ATPS
FA	3FRS	FA	3FRS	FA	3FRS	FA	3FRS	FA	3FRS	FA	3FRS
FA	3GLS	FA	3GLS	FA	3GLS	FA	3GLS	FA	3GLS	FA	3GLS
FA	SM	FA	SM	FA	SM	FA	SM	FA	SM	FA	SM
TS	SM	TS	SM	TS	SM	TS	SM	TS	SM	TS	SM

Table A.14: MO MM, methods ranked by MSPE, pt2.

Percentage Data Removed									
80.54		87.21		93.95		96.97		98.51	
OK	1GLS	SK	3ATPS	SK	3GLS	IDW	3GLS	IDW	3GLS
SK	3FRS	MURS	3ATPS	IDW	3GLS	IDW	3FRS	IDW	3FRS
LSK	3FRS	OK	3GLS	MURS	3ATPS	OK	3GLS	IDW	1GLS
OK	3FRS	SK	3GLS	OK	3ATPS	IDW	1GLS	OK	3GLS
OK	3ATPS	MRSM	3ATPS	OK	3GLS	SK	3FRS	LSK	3GLS
SK	1GLS	LSK	3GLS	SK	3ATPS	SK	3GLS	IDW	3ATPS
IDW	3ATPS	SK	3FRS	LSK	3GLS	OK	3FRS	SK	3GLS
OK	SM	OK	3ATPS	LSK	3FRS	NN	3GLS	TS	3GLS
SK	3GLS	IDW	3GLS	OK	3FRS	SK	1GLS	NN	1GLS
LSK	3GLS	IDW	3FRS	OK	1GLS	NN	1GLS	NN	SM
SK	SM	IDW	1GLS	IDW	3FRS	LSK	3GLS	MRSM	3GLS
LSK	3ATPS	IDW	3ATPS	LSK	3ATPS	OK	1GLS	MURS	3GLS
IDW	3FRS	LSK	3ATPS	SK	1GLS	NN	3FRS	SK	3FRS
IDW	1GLS	SK	1GLS	IDW	3ATPS	MURS	3GLS	NN	3FRS
TS	3ATPS	MURS	3GLS	SK	3FRS	NN	SM	LSK	3FRS
SK	3ATPS	LSK	3FRS	IDW	1GLS	IDW	SM	TS	3ATPS
MURS	3ATPS	OK	1GLS	TS	3ATPS	MRSM	3GLS	NN	3GLS
OK	3GLS	OK	3FRS	MRSM	3ATPS	NN	3ATPS	MURS	3ATPS
MRSM	3ATPS	TS	3ATPS	SK	SM	TS	3GLS	SK	3ATPS
MURS	3GLS	MRSM	3GLS	MURS	3GLS	IDW	3ATPS	OK	3FRS
IDW	3GLS	LSK	1GLS	MRSM	3GLS	LSK	1GLS	MRSM	3ATPS
MURS	3FRS	SK	SM	IDW	SM	LSK	3FRS	OK	3ATPS
MRSM	3GLS	IDW	SM	TS	3GLS	SK	3ATPS	LSK	3ATPS
LSK	1GLS	MURS	3FRS	MURS	3FRS	SK	SM	IDW	SM
IDW	SM	TS	3GLS	LSK	1GLS	OK	3ATPS	SK	1GLS
MRSM	3FRS	MRSM	3FRS	MRSM	3FRS	MURS	3FRS	NN	3ATPS
NN	3ATPS	MURS	1GLS	OK	SM	LSK	3ATPS	OK	1GLS
MURS	1GLS	NN	1GLS	NN	3ATPS	MURS	3ATPS	MURS	3FRS
NN	3FRS	OK	SM	NN	1GLS	MRSM	3ATPS	LSK	1GLS
TS	3GLS	NN	SM	TS	3FRS	OK	SM	MRSM	3FRS
LSK	SM	NN	3GLS	NN	3GLS	TS	3FRS	TS	3FRS
NN	1GLS	NN	3ATPS	NN	3FRS	TS	3ATPS	MURS	1GLS
MRSM	1GLS	NN	3FRS	NN	SM	MRSM	3FRS	MRSM	1GLS
NN	3GLS	MRSM	1GLS	MURS	1GLS	MURS	1GLS	SK	SM
NN	SM	LSK	SM	LSK	SM	MRSM	1GLS	TS	1GLS
TS	3FRS	TS	3FRS	MRSM	1GLS	TS	1GLS	OK	SM
MURS	SM	MURS	SM	MURS	SM	LSK	SM	LSK	SM
MRSM	SM	MRSM	SM	MRSM	SM	MURS	SM	MURS	SM
TS	1GLS	TS	1GLS	TS	1GLS	MRSM	SM	MRSM	SM
FA	1GLS	FA	1GLS	FA	1GLS	FA	1GLS	FA	1GLS
FA	3ATPS	FA	3ATPS	FA	3ATPS	FA	3ATPS	FA	3ATPS
FA	3FRS	FA	3FRS	FA	3FRS	FA	3FRS	FA	3FRS
FA	3GLS	FA	3GLS	FA	3GLS	FA	3GLS	FA	3GLS
FA	SM	FA	SM	FA	SM	FA	SM	FA	SM
TS	SM	TS	SM	TS	SM	TS	SM	TS	SM

Table A.15: MO MM, methods ranked by MAPE, pt1.

Percentage Data Removed											
48.97		53.13		58.06		63.28		68.80		75.6	
SK	1GLS	OK	1GLS	SK	1GLS	SK	SM	OK	1GLS	OK	1GLS
OK	1GLS	SK	1GLS	OK	1GLS	OK	1GLS	LSK	1GLS	SK	1GLS
SK	3FRS	LSK	1GLS	LSK	1GLS	SK	1GLS	SK	1GLS	SK	3FRS
LSK	3FRS	SK	3FRS	SK	3FRS	OK	3FRS	OK	3FRS	OK	3FRS
OK	3FRS	OK	3FRS	OK	SM	LSK	1GLS	SK	3FRS	LSK	1GLS
LSK	1GLS	LSK	3FRS	OK	3FRS	LSK	3FRS	SK	SM	SK	3ATPS
IDW	1GLS	IDW	1GLS	LSK	3FRS	OK	SM	SK	3ATPS	OK	3ATPS
IDW	3FRS	OK	3ATPS	SK	3ATPS	SK	3GLS	LSK	3FRS	SK	3GLS
MURS	1GLS	SK	3ATPS	OK	3ATPS	OK	3ATPS	OK	3GLS	MURS	3ATPS
SK	3ATPS	LSK	3ATPS	MURS	3ATPS	SK	3FRS	MURS	3ATPS	IDW	3ATPS
MRS	1GLS	IDW	3FRS	SK	3GLS	SK	3ATPS	OK	3ATPS	MRS	3ATPS
MRS	3ATPS	MURS	3ATPS	IDW	1GLS	MURS	3ATPS	SK	3GLS	LSK	3GLS
MRS	3ATPS	MURS	1GLS	IDW	3ATPS	OK	3GLS	MRS	3ATPS	OK	3GLS
OK	3ATPS	MRS	3ATPS	NN	3ATPS	IDW	1GLS	IDW	1GLS	LSK	3FRS
IDW	3ATPS	MRS	1GLS	MRS	3ATPS	IDW	3ATPS	LSK	3GLS	IDW	1GLS
LSK	3ATPS	NN	3ATPS	LSK	3ATPS	MRS	3ATPS	IDW	3FRS	IDW	3FRS
MURS	3FRS	IDW	3ATPS	IDW	3FRS	IDW	3FRS	IDW	3ATPS	LSK	3ATPS
OK	3GLS	MURS	3FRS	LSK	SM	LSK	3ATPS	MURS	1GLS	NN	3ATPS
MRS	3FRS	MRS	3FRS	MURS	1GLS	MURS	1GLS	NN	3ATPS	TS	3ATPS
TS	3ATPS	SK	3GLS	OK	3GLS	LSK	3GLS	LSK	3ATPS	NN	3GLS
SK	3GLS	OK	3GLS	NN	3GLS	NN	3ATPS	MRS	1GLS	NN	1GLS
LSK	3GLS	LSK	3GLS	MRS	1GLS	MRS	1GLS	TS	3ATPS	MURS	3FRS
NN	3ATPS	TS	3ATPS	NN	1GLS	MURS	3FRS	MURS	3FRS	MURS	3GLS
IDW	3GLS	NN	3GLS	TS	3ATPS	MRS	3FRS	IDW	3GLS	NN	SM
MRS	3GLS	NN	1GLS	NN	SM	IDW	3GLS	MURS	3GLS	IDW	3GLS
NN	1GLS	NN	SM	MURS	3FRS	MURS	3GLS	MRS	3FRS	NN	3FRS
NN	SM	IDW	3GLS	MRS	3FRS	NN	3GLS	NN	3GLS	MRS	3FRS
NN	3GLS	MURS	3GLS	NN	3FRS	TS	3ATPS	NN	1GLS	LSK	SM
MURS	3GLS	MRS	3GLS	SK	SM	NN	1GLS	NN	SM	MURS	1GLS
TS	3FRS	NN	3FRS	MURS	3GLS	NN	SM	NN	3FRS	OK	SM
IDW	SM	OK	SM	LSK	3GLS	MRS	3GLS	MRS	3GLS	MRS	1GLS
SK	SM	IDW	SM	MRS	3GLS	NN	3FRS	IDW	SM	SK	SM
NN	3FRS	TS	3FRS	IDW	3GLS	IDW	SM	OK	SM	MRS	3GLS
TS	1GLS	TS	3GLS	IDW	SM	LSK	SM	TS	3GLS	IDW	SM
TS	3GLS	TS	1GLS	TS	3GLS	TS	3FRS	LSK	SM	TS	3GLS
OK	SM	SK	SM	TS	3FRS	TS	3GLS	TS	3FRS	TS	3FRS
LSK	SM	LSK	SM	TS	1GLS	TS	1GLS	MRS	SM	MRS	SM
MRS	SM	MURS	SM	MRS	SM	MRS	SM	MURS	SM	MURS	SM
MURS	SM	MRS	SM	MURS	SM	MURS	SM	TS	1GLS	TS	1GLS
FA	1GLS	FA	1GLS	FA	1GLS	FA	1GLS	FA	1GLS	FA	1GLS
FA	3ATPS	FA	3ATPS	FA	3ATPS	FA	3ATPS	FA	3ATPS	FA	3ATPS
FA	3FRS	FA	3FRS	FA	3FRS	FA	3FRS	FA	3FRS	FA	3FRS
FA	3GLS	FA	3GLS	FA	3GLS	FA	3GLS	FA	3GLS	FA	3GLS
FA	SM	FA	SM	FA	SM	FA	SM	FA	SM	FA	SM
TS	SM	TS	SM	TS	SM	TS	SM	TS	SM	TS	SM

Table A.16: MO MM, methods ranked by MAPE, pt2.

Percentage Data Removed									
80.54		87.21		93.95		96.97		98.51	
OK	1GLS	SK	3FRS	OK	1GLS	NN	1GLS	IDW	3FRS
SK	1GLS	SK	3ATPS	LSK	3FRS	IDW	1GLS	IDW	3GLS
LSK	3FRS	SK	1GLS	SK	1GLS	NN	SM	IDW	3ATPS
SK	3FRS	MURS	3ATPS	OK	3FRS	SK	3FRS	IDW	1GLS
OK	SM	OK	3ATPS	OK	3ATPS	IDW	3FRS	NN	1GLS
OK	3FRS	MRSM	3ATPS	SK	3ATPS	NN	3FRS	OK	3ATPS
OK	3ATPS	OK	1GLS	SK	3GLS	NN	3GLS	NN	SM
SK	SM	LSK	3ATPS	LSK	3ATPS	IDW	3GLS	TS	3ATPS
IDW	3ATPS	SK	3GLS	MURS	3ATPS	SK	1GLS	LSK	3ATPS
MURS	3ATPS	LSK	3FRS	IDW	3ATPS	OK	3FRS	SK	3ATPS
SK	3ATPS	LSK	3GLS	LSK	3GLS	OK	1GLS	MURS	3ATPS
MRSM	3ATPS	OK	3GLS	IDW	3FRS	OK	3GLS	OK	3GLS
SK	3GLS	IDW	3ATPS	SK	SM	SK	3GLS	MRSM	3ATPS
LSK	3ATPS	IDW	1GLS	SK	3FRS	NN	3ATPS	NN	3FRS
LSK	3GLS	IDW	3FRS	IDW	1GLS	LSK	1GLS	NN	3GLS
IDW	3FRS	SK	SM	IDW	3GLS	SK	3ATPS	LSK	3GLS
IDW	1GLS	OK	3FRS	OK	3GLS	IDW	3ATPS	SK	3GLS
TS	3ATPS	LSK	1GLS	MRSM	3ATPS	IDW	SM	NN	3ATPS
NN	3ATPS	IDW	3GLS	TS	3ATPS	LSK	3GLS	LSK	3FRS
LSK	1GLS	TS	3ATPS	NN	3ATPS	OK	3ATPS	SK	3FRS
OK	3GLS	NN	3ATPS	NN	3GLS	LSK	3ATPS	MRSM	3GLS
NN	3GLS	NN	1GLS	NN	1GLS	LSK	3FRS	TS	3GLS
NN	1GLS	NN	3GLS	LSK	1GLS	MURS	3GLS	MURS	3GLS
NN	SM	NN	SM	NN	SM	MURS	3ATPS	OK	3FRS
IDW	3GLS	NN	3FRS	NN	3FRS	SK	SM	SK	1GLS
NN	3FRS	MURS	3GLS	IDW	SM	MRSM	3ATPS	IDW	SM
MURS	3GLS	IDW	SM	MURS	3GLS	MRSM	3GLS	OK	1GLS
LSK	SM	MRSM	3GLS	OK	SM	TS	3GLS	MURS	3FRS
MRSM	3GLS	MURS	3FRS	MRSM	3GLS	TS	3ATPS	LSK	1GLS
MURS	3FRS	OK	SM	MURS	3FRS	MURS	3FRS	MRSM	3FRS
MURS	1GLS	MRSM	3FRS	MRSM	3FRS	OK	SM	TS	3FRS
MRSM	3FRS	LSK	SM	TS	3GLS	MRSM	3FRS	MURS	1GLS
MRSM	1GLS	MURS	1GLS	LSK	SM	TS	3FRS	SK	SM
IDW	SM	TS	3GLS	MURS	1GLS	MURS	1GLS	MRSM	1GLS
TS	3GLS	MRSM	1GLS	MRSM	1GLS	MRSM	1GLS	TS	1GLS
TS	3FRS	TS	3FRS	TS	3FRS	TS	1GLS	OK	SM
MURS	SM	TS	1GLS	MURS	SM	LSK	SM	LSK	SM
MRSM	SM	MURS	SM	MRSM	SM	MURS	SM	MURS	SM
TS	1GLS	MRSM	SM	TS	1GLS	MRSM	SM	MRSM	SM
FA	1GLS	FA	1GLS	FA	1GLS	FA	1GLS	FA	1GLS
FA	3ATPS	FA	3ATPS	FA	3ATPS	FA	3ATPS	FA	3ATPS
FA	3FRS	FA	3FRS	FA	3FRS	FA	3FRS	FA	3FRS
FA	3GLS	FA	3GLS	FA	3GLS	FA	3GLS	FA	3GLS
FA	SM	FA	SM	FA	SM	FA	SM	FA	SM
TS	SM	TS	SM	TS	SM	TS	SM	TS	SM

## A.3 MSPE and MAPE Values

### A.3.1 Grouped by Estimation Method

Table A.17: CT RR, MSPE grouped by estimation method.

		Percentage Data Removed										
		19.26	30.88	41.33	50.98	60.21	70.12	77.44	85.67	93.24	96.26	98.46
FA	SM	19.94	20.39	22.55	22.71	24.17	26.45	25.52	24.32	23.47	24.37	26.91
	1GLS	19.94	20.39	22.55	22.71	24.17	26.45	25.52	24.32	23.47	24.37	26.91
	3GLS	19.94	20.39	22.55	22.71	24.17	26.45	25.52	24.32	23.47	24.37	26.91
	3ATPS	19.94	20.39	22.55	22.71	24.17	26.45	25.52	24.32	23.47	24.37	26.91
	3FRS	19.94	20.39	22.55	22.71	24.17	26.45	25.52	24.32	23.47	24.37	26.91
TS	SM	19.94	20.39	22.55	22.71	24.17	26.45	25.52	24.32	23.47	24.37	26.91
	1GLS	20.65	21.19	23.26	24.04	25.77	28.41	26.88	26.64	23.81	25.67	27.91
	3GLS	12.45	13.35	15.15	16.42	16.82	19.46	18.30	16.16	15.03	15.42	19.24
	3ATPS	5.83	6.43	7.86	7.95	7.73	9.34	9.12	9.64	13.27	18.42	17.53
	3FRS	7.87	8.60	10.07	10.45	10.42	14.11	11.72	11.14	11.08	13.68	15.47
NN	SM	7.48	5.95	7.50	7.80	8.33	11.45	11.03	11.15	12.88	19.13	17.62
	1GLS	7.49	5.94	7.49	7.79	8.32	11.44	11.02	11.15	12.85	19.05	17.74
	3GLS	7.45	5.90	7.46	7.72	8.26	11.36	10.90	10.96	12.38	18.05	16.73
	3ATPS	7.38	5.92	7.45	7.66	8.14	10.58	10.18	10.25	12.48	18.36	17.34
	3FRS	7.44	5.88	7.42	7.71	8.31	11.21	10.73	10.72	11.76	16.70	15.07
IDW	SM	6.25	6.74	8.24	8.66	9.19	12.68	12.28	11.05	10.43	11.67	20.57
	1GLS	6.11	6.63	8.16	8.57	9.06	12.61	12.20	10.99	10.49	11.75	21.52
	3GLS	5.49	5.97	7.58	8.05	8.35	11.62	11.28	10.16	9.83	11.43	17.80
	3ATPS	4.54	4.88	6.29	6.50	6.31	8.33	8.34	8.46	10.60	17.21	17.31
	3FRS	5.12	5.46	6.85	7.39	7.40	9.86	9.91	9.32	9.39	11.87	15.14
LSK	SM	4.10	3.79	4.91	5.37	5.35	8.80	8.87	8.62	9.25	11.04	21.51
	1GLS	4.10	3.79	4.91	5.37	5.34	8.79	8.89	8.56	9.08	12.56	24.89
	3GLS	4.10	3.79	4.90	5.36	5.33	8.79	8.88	8.63	9.32	11.21	18.87
	3ATPS	4.08	3.80	4.92	5.36	5.29	8.17	8.43	8.48	10.28	17.17	17.44
	3FRS	4.07	3.76	4.89	5.39	5.37	8.74	8.89	8.77	9.50	11.34	15.02
SK	SM	4.16	3.82	4.96	5.41	5.44	8.82	8.90	8.56	8.93	10.35	20.06
	1GLS	4.15	3.82	4.96	5.41	5.43	8.84	8.89	8.55	8.89	10.01	22.40
	3GLS	4.16	3.81	4.96	5.40	5.41	8.82	8.88	8.61	9.05	10.59	18.35
	3ATPS	4.11	3.80	4.96	5.39	5.33	8.30	8.55	8.55	11.24	16.68	17.37
	3FRS	4.13	3.77	4.93	5.42	5.46	8.79	8.88	8.71	9.28	11.62	15.31
OK	SM	4.16	3.82	4.96	5.41	5.44	8.82	8.89	8.56	9.02	10.11	20.55
	1GLS	4.16	3.82	4.96	5.40	5.43	8.83	8.91	8.56	9.06	10.40	21.68
	3GLS	4.14	3.81	4.96	5.40	5.41	8.82	8.87	8.61	9.00	10.49	18.45
	3ATPS	4.12	3.81	4.97	5.39	5.34	8.28	8.58	8.64	10.60	16.58	17.37
	3FRS	4.11	3.78	4.93	5.42	5.43	8.82	8.88	8.74	9.19	11.25	15.32
MRSM	SM	5.52	5.05	6.74	6.99	7.11	9.22	9.77	9.90	11.13	14.36	25.52
	1GLS	5.59	5.01	6.76	6.92	7.09	9.24	9.70	9.77	11.15	14.71	26.04
	3GLS	5.52	4.95	6.77	6.85	6.96	9.30	9.67	9.61	10.60	13.28	19.07
	3ATPS	5.40	4.85	6.65	6.52	6.89	8.69	8.69	8.86	13.48	18.22	17.52
	3FRS	5.62	4.92	6.62	6.89	7.09	9.65	9.52	9.18	10.29	12.97	15.50
MURS	SM	3.95	3.83	5.35	5.85	5.78	9.28	9.38	9.04	9.88	11.32	23.47
	1GLS	3.94	3.84	5.30	5.84	5.75	9.31	9.39	9.02	10.01	11.36	24.38
	3GLS	3.92	3.80	5.32	5.85	5.86	9.41	9.41	9.19	10.28	11.08	18.68
	3ATPS	4.02	3.91	5.43	5.87	5.80	8.26	8.33	8.58	12.08	18.06	17.43
	3FRS	3.98	3.78	5.43	6.06	6.12	9.44	9.36	9.25	10.28	12.39	15.32

Table A.18: CT RR, MAPE grouped by estimation method.

		Percentage Data Removed										
		19.26	30.88	41.33	50.98	60.21	70.12	77.44	85.67	93.24	96.26	98.46
FA	SM	3.17	3.12	3.21	3.17	3.22	3.18	3.13	3.10	3.16	2.93	2.96
	1GLS	3.17	3.12	3.21	3.17	3.22	3.18	3.13	3.10	3.16	2.93	2.96
	3GLS	3.17	3.12	3.21	3.17	3.22	3.18	3.13	3.10	3.16	2.93	2.96
	3ATPS	3.17	3.12	3.21	3.17	3.22	3.18	3.13	3.10	3.16	2.93	2.96
	3FRS	3.17	3.12	3.21	3.17	3.22	3.18	3.13	3.10	3.16	2.93	2.96
TS	SM	3.17	3.12	3.21	3.17	3.22	3.18	3.13	3.10	3.16	2.93	2.96
	1GLS	2.86	2.84	2.96	2.90	2.94	3.02	2.97	2.98	2.98	3.03	3.05
	3GLS	2.36	2.36	2.49	2.52	2.53	2.59	2.54	2.42	2.43	2.57	2.33
	3ATPS	1.52	1.53	1.62	1.61	1.62	1.70	1.65	1.80	2.15	2.55	2.25
	3FRS	1.89	1.93	2.02	2.03	2.01	2.21	2.02	2.07	2.14	2.43	2.33
NN	SM	1.20	1.17	1.29	1.33	1.42	1.58	1.60	1.69	1.94	2.35	2.25
	1GLS	1.20	1.17	1.29	1.33	1.42	1.58	1.60	1.69	1.94	2.36	2.26
	3GLS	1.20	1.17	1.29	1.33	1.42	1.58	1.60	1.70	1.93	2.34	2.22
	3ATPS	1.22	1.18	1.30	1.34	1.41	1.55	1.55	1.70	2.06	2.54	2.21
	3FRS	1.23	1.20	1.31	1.35	1.45	1.60	1.62	1.73	1.96	2.33	2.28
IDW	SM	1.67	1.66	1.76	1.78	1.85	1.94	1.90	1.89	1.97	1.91	2.30
	1GLS	1.65	1.65	1.74	1.76	1.82	1.91	1.88	1.86	1.99	1.93	2.40
	3GLS	1.49	1.48	1.59	1.62	1.66	1.76	1.74	1.74	1.86	2.05	2.15
	3ATPS	1.28	1.26	1.36	1.38	1.39	1.48	1.47	1.60	1.87	2.45	2.19
	3FRS	1.43	1.42	1.53	1.58	1.59	1.69	1.69	1.76	1.83	2.15	2.25
LSK	SM	0.92	0.90	1.00	1.08	1.13	1.32	1.36	1.48	1.72	1.86	2.37
	1GLS	0.92	0.90	1.00	1.08	1.13	1.32	1.36	1.45	1.68	1.99	2.68
	3GLS	0.92	0.90	1.00	1.08	1.13	1.32	1.36	1.47	1.71	1.98	2.25
	3ATPS	0.93	0.92	1.01	1.10	1.17	1.35	1.36	1.53	1.79	2.42	2.23
	3FRS	0.93	0.92	1.01	1.10	1.16	1.35	1.41	1.58	1.81	1.98	2.27
SK	SM	0.93	0.91	1.01	1.08	1.14	1.33	1.37	1.45	1.66	1.80	2.27
	1GLS	0.93	0.91	1.00	1.08	1.13	1.32	1.36	1.44	1.64	1.79	2.47
	3GLS	0.93	0.91	1.00	1.08	1.13	1.32	1.36	1.46	1.69	1.94	2.19
	3ATPS	0.94	0.92	1.02	1.09	1.16	1.34	1.37	1.53	1.91	2.40	2.22
	3FRS	0.93	0.92	1.01	1.09	1.17	1.35	1.40	1.54	1.76	2.05	2.28
OK	SM	0.93	0.91	1.01	1.08	1.14	1.33	1.36	1.45	1.69	1.78	2.31
	1GLS	0.93	0.91	1.01	1.08	1.13	1.32	1.36	1.45	1.67	1.82	2.41
	3GLS	0.93	0.91	1.00	1.08	1.13	1.32	1.36	1.46	1.68	1.92	2.20
	3ATPS	0.93	0.92	1.02	1.09	1.15	1.34	1.37	1.54	1.85	2.39	2.21
	3FRS	0.93	0.92	1.01	1.10	1.15	1.35	1.40	1.54	1.73	2.00	2.34
MRSM	SM	1.22	1.19	1.31	1.36	1.45	1.57	1.64	1.75	1.97	2.09	2.63
	1GLS	1.22	1.18	1.32	1.36	1.44	1.56	1.63	1.72	1.95	2.14	2.75
	3GLS	1.23	1.18	1.31	1.34	1.43	1.56	1.63	1.72	2.00	2.19	2.27
	3ATPS	1.23	1.19	1.31	1.33	1.42	1.52	1.53	1.68	2.16	2.51	2.25
	3FRS	1.25	1.21	1.35	1.41	1.49	1.63	1.66	1.76	2.02	2.23	2.31
MURS	SM	1.04	1.02	1.15	1.22	1.28	1.48	1.50	1.60	1.89	1.93	2.51
	1GLS	1.03	1.02	1.13	1.20	1.27	1.47	1.49	1.58	1.88	1.96	2.65
	3GLS	1.05	1.01	1.14	1.21	1.29	1.49	1.51	1.62	1.96	2.03	2.22
	3ATPS	1.05	1.05	1.16	1.23	1.30	1.46	1.47	1.63	2.01	2.50	2.23
	3FRS	1.06	1.05	1.22	1.30	1.37	1.58	1.62	1.75	2.02	2.25	2.29

Table A.19: CT RR, time grouped by estimation method.

		Percentage Data Removed										
		19.26	30.88	41.33	50.98	60.21	70.12	77.44	85.67	93.24	96.26	98.46
FA	SM	9.90	9.80	10.40	10.30	9.60	8.50	8.70	8.60	8.10	8.40	8.50
	1GLS	551.80	491.50	464.90	433.90	420.20	392.30	404.00	365.90	310.20	205.90	72.50
	3GLS	570.20	492.40	468.50	445.00	423.30	405.10	403.00	379.80	313.40	223.90	72.60
	3ATPS	517.80	472.70	449.10	418.40	418.60	384.00	375.50	374.80	321.80	211.20	70.50
	3FRS	3887.00	2606.50	1822.00	1213.30	858.80	570.20	498.90	399.00	314.60	221.00	80.60
TS	SM	8.40	8.60	8.40	8.60	8.50	8.80	8.30	8.00	7.50	6.90	7.20
	1GLS	538.40	500.10	451.90	433.00	405.00	390.60	381.90	360.70	321.00	211.70	73.50
	3GLS	539.60	504.20	459.00	437.50	428.70	402.70	394.70	385.70	326.80	216.80	72.80
	3ATPS	500.40	458.50	456.30	438.30	433.40	412.00	402.10	373.40	313.10	205.20	74.20
	3FRS	3916.10	2587.70	1742.00	1198.50	818.30	566.00	462.90	398.20	303.20	204.30	69.10
NN	SM	7.90	8.50	8.80	9.20	9.20	9.00	9.30	8.30	8.30	7.90	7.40
	1GLS	529.00	496.40	465.50	430.00	418.00	392.90	388.70	367.40	308.90	210.30	74.00
	3GLS	548.20	507.10	466.20	437.40	416.20	394.40	387.20	386.00	320.90	213.70	71.40
	3ATPS	517.10	492.20	445.60	430.50	407.80	391.80	371.30	363.30	318.70	207.90	73.20
	3FRS	3848.70	2586.30	1738.20	1183.20	819.80	559.40	464.20	379.60	315.10	206.40	71.40
IDW	SM	9.20	9.30	10.10	10.10	9.50	9.60	9.50	9.20	7.40	5.80	5.90
	1GLS	538.20	497.70	447.70	434.40	417.20	397.80	384.50	370.20	320.30	211.30	71.00
	3GLS	599.50	502.40	471.10	442.20	421.50	420.30	396.90	390.10	321.70	217.60	74.70
	3ATPS	511.00	468.30	454.10	417.80	404.20	398.20	379.90	371.30	311.00	212.00	71.40
	3FRS	3868.30	2582.50	1735.80	1179.30	827.80	568.70	454.30	388.20	312.60	203.30	70.70
LSK	SM	523.80	483.40	442.50	432.80	418.90	404.40	388.30	375.80	315.30	212.80	73.40
	1GLS	1033.20	959.80	920.50	847.60	864.80	791.50	769.80	733.90	615.00	421.00	141.10
	3GLS	1049.40	972.10	925.30	842.70	839.90	784.10	774.70	732.90	633.70	434.60	143.50
	3ATPS	999.50	954.60	905.90	855.90	829.30	800.70	782.70	756.50	621.10	424.60	142.30
	3FRS	4368.60	3063.30	2189.90	1614.70	1226.60	953.40	859.40	764.10	627.40	415.80	138.60
SK	SM	727.60	726.20	666.90	615.50	542.50	477.80	450.30	399.10	323.40	220.90	72.20
	1GLS	1215.10	1145.60	1090.90	1016.90	948.60	854.00	816.40	751.10	615.80	411.90	140.10
	3GLS	1284.40	1244.40	1109.50	1008.60	958.10	890.60	829.90	777.00	648.20	432.90	141.90
	3ATPS	1214.20	1184.50	1106.30	1038.40	970.70	893.60	857.00	767.20	623.90	418.70	139.60
	3FRS	4589.20	3273.70	2405.40	1793.80	1365.90	1051.00	895.40	786.40	621.80	423.30	142.20
OK	SM	714.70	708.70	662.80	596.80	556.00	483.80	430.60	398.60	318.70	214.80	70.90
	1GLS	1241.30	1220.00	1128.90	1025.20	954.40	878.50	805.70	755.30	629.20	412.80	139.80
	3GLS	1261.80	1188.10	1090.80	1022.30	950.30	881.30	818.60	781.80	633.80	428.90	140.20
	3ATPS	1208.80	1176.60	1112.70	1051.60	954.70	884.90	824.90	763.90	628.10	419.80	141.10
	3FRS	4564.50	3295.80	2380.80	1778.90	1442.80	1054.50	903.50	794.60	630.30	416.60	138.80
MRSM	SM	120.40	119.50	121.00	116.50	117.60	118.70	117.40	117.30	114.10	113.90	115.90
	1GLS	677.40	603.90	571.90	541.70	529.20	511.90	485.70	476.70	421.80	317.20	182.80
	3GLS	663.60	611.60	580.20	538.60	549.00	515.80	513.90	490.50	432.50	325.50	183.00
	3ATPS	615.50	564.80	531.30	525.50	507.20	485.40	472.10	467.90	404.00	307.50	179.00
	3FRS	3970.90	2707.10	1866.30	1288.10	926.30	682.90	572.00	497.50	414.10	316.80	179.40
MURS	SM	122.40	118.90	119.30	118.00	120.90	118.90	117.60	116.10	118.50	115.10	116.40
	1GLS	647.40	611.30	567.70	541.10	553.70	540.80	506.50	502.10	452.50	336.70	186.30
	3GLS	771.40	618.90	589.80	551.00	527.40	522.10	503.80	490.30	432.10	318.00	182.60
	3ATPS	589.70	564.80	546.70	525.00	510.40	484.20	477.90	463.30	401.90	307.60	179.50
	3FRS	3968.20	2690.70	1859.40	1301.40	935.80	670.20	571.10	499.30	410.20	321.50	182.80

Table A.20: MO RR, MSPE grouped by estimation method.

		Percentage Data Removed										
		19.53	26.20	33.79	41.77	50.24	60.91	68.48	79.59	90.26	94.90	97.44
FA	SM	192.96	180.62	184.53	190.36	192.95	200.39	202.35	201.05	200.74	202.65	200.29
	1GLS	192.96	180.62	184.53	190.36	192.95	200.39	202.35	201.05	200.74	202.65	200.29
	3GLS	192.96	180.62	184.53	190.36	192.95	200.39	202.35	201.05	200.74	202.65	200.29
	3ATPS	192.96	180.62	184.53	190.36	192.95	200.39	202.35	201.05	200.74	202.65	200.29
	3FRS	192.96	180.62	184.53	190.36	192.95	200.39	202.35	201.05	200.74	202.65	200.29
TS	SM	192.96	180.62	184.53	190.36	192.95	200.39	202.35	201.05	200.74	202.65	200.29
	1GLS	105.28	96.83	99.27	105.23	108.43	116.13	117.34	116.40	120.05	116.16	116.96
	3GLS	55.84	72.26	63.13	65.11	65.90	66.18	66.73	66.29	75.73	79.98	76.11
	3ATPS	32.67	30.67	31.11	34.60	36.57	37.54	37.25	40.30	42.16	50.43	58.48
	3FRS	75.25	73.34	78.39	83.52	86.07	84.53	84.63	85.10	85.98	93.94	97.81
NN	SM	17.42	21.91	21.74	30.75	28.85	30.89	28.66	31.91	41.60	57.46	82.51
	1GLS	17.02	21.56	21.30	30.49	28.59	30.70	28.45	31.78	41.29	56.81	82.67
	3GLS	17.06	21.26	20.91	30.23	28.11	30.49	28.11	31.37	40.70	56.44	80.41
	3ATPS	15.95	19.86	20.15	29.33	27.77	29.49	26.79	29.88	38.00	56.91	76.26
	3FRS	17.05	21.42	21.11	30.35	28.34	30.61	28.27	31.44	41.22	57.14	81.65
IDW	SM	31.60	29.89	30.14	34.15	35.36	38.70	39.46	39.59	46.06	49.08	58.23
	1GLS	29.07	27.59	27.73	31.75	32.84	36.06	36.88	36.60	42.00	45.41	56.56
	3GLS	26.10	25.68	25.48	29.47	30.64	33.04	32.63	32.95	37.53	41.48	51.78
	3ATPS	21.97	21.11	20.95	23.88	25.20	26.70	26.62	27.22	30.60	44.06	52.10
	3FRS	27.91	26.62	26.86	31.00	31.89	34.14	34.57	34.67	38.73	43.22	53.65
LSK	SM	6.94	8.66	9.77	12.68	13.12	28.13	16.28	33.92	34.03	65.41	82.51
	1GLS	11.66	9.06	9.24	11.99	16.81	28.39	16.12	22.57	29.69	39.67	83.78
	3GLS	10.10	8.33	12.63	12.47	21.54	26.99	21.38	34.86	29.31	59.14	69.71
	3ATPS	14.88	16.65	16.87	16.52	24.59	31.05	23.22	31.64	30.53	44.24	58.02
	3FRS	7.59	8.51	12.60	12.54	28.12	17.38	18.26	20.87	31.13	52.64	73.36
SK	SM	7.47	8.57	8.80	11.40	12.06	15.82	19.88	27.99	33.33	65.55	67.09
	1GLS	6.85	7.87	8.80	13.28	13.14	14.68	17.69	21.41	32.24	52.75	70.29
	3GLS	7.00	11.31	9.32	13.72	12.23	17.86	17.28	22.58	34.79	46.37	60.70
	3ATPS	10.73	11.84	11.84	17.49	17.35	19.95	20.26	26.35	30.77	40.32	56.29
	3FRS	8.78	8.37	8.97	15.27	11.91	15.17	15.90	26.94	37.69	40.71	70.24
OK	SM	6.71	8.14	9.02	11.65	11.74	15.14	20.98	21.12	43.68	51.24	62.31
	1GLS	6.69	8.19	9.11	12.90	11.75	14.51	17.09	20.68	30.57	43.85	76.72
	3GLS	7.55	9.02	10.46	14.65	14.71	21.34	22.12	28.76	35.64	52.45	62.73
	3ATPS	12.28	11.98	13.03	14.92	16.14	22.53	20.06	23.69	29.49	47.54	56.57
	3FRS	9.39	8.24	9.84	12.33	11.86	17.89	19.96	23.03	37.35	47.81	63.65
MRSM	SM	14.72	15.90	17.71	23.40	25.57	33.79	42.02	47.56	78.20	105.29	99.88
	1GLS	15.94	16.34	18.42	24.41	29.14	41.86	54.39	65.92	92.62	102.09	111.11
	3GLS	14.71	15.14	16.18	23.34	25.85	34.37	39.64	46.89	61.46	69.40	70.22
	3ATPS	1.99	2.05	2.12	2.37	2.45	2.70	2.86	3.05	3.58	4.02	4.48
	3FRS	16.40	16.10	19.20	26.01	29.28	39.22	47.20	55.91	74.10	85.64	93.43
MURS	SM	12.17	12.29	13.70	16.89	19.02	24.86	29.73	33.35	66.85	96.84	91.1
	1GLS	13.23	13.26	16.53	18.42	22.84	31.78	45.23	55.68	84.88	99.67	108.70
	3GLS	11.24	12.20	13.16	16.90	20.62	25.72	31.59	40.08	51.59	65.08	68.82
	3ATPS	1.70	1.75	1.91	2.12	2.21	2.43	2.52	2.82	3.35	3.92	4.43
	3FRS	12.92	12.58	15.06	19.36	21.25	31.13	37.81	45.55	64.70	79.43	89.51

Table A.21: MO RR, MAPE grouped by estimation method.

		Percentage Data Removed										
		19.53	26.20	33.79	41.77	50.24	60.91	68.48	79.59	90.26	94.90	97.44
FA	SM	10.78	10.60	10.65	10.77	10.91	11.00	11.11	11.02	11.01	11.49	11.12
	1GLS	10.78	10.60	10.65	10.77	10.91	11.00	11.11	11.02	11.01	11.49	11.12
	3GLS	10.78	10.60	10.65	10.77	10.91	11.00	11.11	11.02	11.01	11.49	11.12
	3ATPS	10.78	10.60	10.65	10.77	10.91	11.00	11.11	11.02	11.01	11.49	11.12
TS	SM	10.78	10.60	10.65	10.77	10.91	11.00	11.11	11.02	11.01	11.49	11.12
	1GLS	6.99	6.70	6.86	7.13	7.24	7.47	7.52	7.45	7.33	7.46	7.53
	3GLS	4.60	5.66	5.17	5.15	5.19	5.28	5.34	5.39	5.76	6.11	5.90
	3ATPS	3.11	3.14	3.23	3.43	3.47	3.50	3.50	3.60	3.87	4.26	4.53
NN	SM	2.18	2.44	2.48	2.78	2.70	2.83	2.81	3.03	3.48	4.10	5.03
	1GLS	2.19	2.44	2.47	2.78	2.70	2.84	2.82	3.03	3.50	4.13	5.10
	3GLS	2.21	2.44	2.45	2.75	2.68	2.83	2.81	3.03	3.48	4.20	5.09
	3ATPS	2.13	2.33	2.38	2.70	2.63	2.75	2.71	2.93	3.34	4.23	4.90
IDW	SM	3.55	3.58	3.66	3.81	3.89	4.03	4.15	4.17	4.48	4.95	5.23
	1GLS	3.23	3.25	3.32	3.50	3.55	3.70	3.83	3.80	4.01	4.37	4.82
	3GLS	2.96	3.04	3.07	3.25	3.31	3.41	3.44	3.52	3.73	4.13	4.51
	3ATPS	2.50	2.57	2.61	2.77	2.79	2.84	2.87	2.94	3.20	3.87	4.25
LSK	SM	1.25	1.49	1.66	1.85	1.85	2.84	2.12	3.18	3.30	5.42	6.31
	1GLS	1.65	1.53	1.58	1.76	2.08	2.91	2.11	2.62	3.01	3.84	6.20
	3GLS	1.50	1.43	1.84	1.81	2.50	2.87	2.52	3.49	3.01	5.05	5.58
	3ATPS	1.97	2.18	2.27	2.14	2.69	3.08	2.57	3.09	3.18	3.91	4.50
SK	SM	1.34	1.50	1.52	1.69	1.75	2.10	2.53	3.26	3.43	5.79	5.48
	1GLS	1.25	1.40	1.52	1.92	1.89	1.96	2.26	2.56	3.21	4.63	5.54
	3GLS	1.25	1.71	1.60	1.94	1.76	2.27	2.20	2.68	3.52	4.40	5.11
	3ATPS	1.59	1.77	1.83	2.26	2.19	2.35	2.38	2.79	3.12	3.72	4.43
OK	SM	1.49	1.47	1.55	2.15	1.73	2.02	2.08	2.97	3.65	4.22	5.70
	SM	1.23	1.43	1.56	1.73	1.70	2.01	2.54	2.57	4.03	4.68	5.09
	1GLS	1.22	1.44	1.57	1.88	1.71	1.93	2.18	2.47	3.12	4.12	5.89
	3GLS	1.32	1.54	1.73	2.00	1.99	2.53	2.61	3.08	3.56	4.74	5.24
MRSM	SM	1.72	1.80	1.96	2.04	2.09	2.54	2.37	2.65	3.04	4.08	4.44
	3ATPS	1.55	1.45	1.69	1.82	1.72	2.25	2.55	2.76	3.84	4.63	5.35
	SM	2.13	2.20	2.40	2.72	2.96	3.31	4.03	4.44	6.14	7.82	7.29
	1GLS	2.20	2.23	2.44	2.85	3.24	3.79	4.47	5.10	6.10	6.80	7.35
MURS	3GLS	2.10	2.11	2.27	2.59	2.76	3.30	3.62	4.26	4.97	5.56	5.59
	3ATPS	1.99	2.05	2.12	2.37	2.45	2.70	2.86	3.05	3.58	4.02	4.48
	3FRS	2.32	2.29	2.71	3.09	3.26	3.69	4.27	4.78	5.77	6.56	6.64
	SM	1.86	1.92	2.17	2.39	2.65	3.07	3.53	3.84	5.82	7.68	7.10
MURS	1GLS	2.04	2.05	2.41	2.53	2.93	3.46	4.30	4.91	5.98	6.72	7.23
	3GLS	1.74	1.96	2.11	2.34	2.67	2.96	3.47	4.18	4.64	5.46	5.56
	3ATPS	1.70	1.75	1.91	2.12	2.21	2.43	2.52	2.82	3.35	3.92	4.43
	3FRS	2.00	2.05	2.43	2.70	2.90	3.56	4.01	4.59	5.57	6.43	6.55

Table A.22: MO RR, time grouped by estimation method.

		Percentage Data Removed										
		19.53	26.20	33.79	41.77	50.24	60.91	68.48	79.59	90.26	94.90	97.44
FA	SM	4.70	4.40	4.00	3.60	3.60	3.00	2.50	2.00	1.60	0.60	0.80
	1GLS	202.90	165.50	151.90	147.20	132.90	126.30	126.50	123.80	116.70	137.40	84.40
	3GLS	144.60	135.90	122.40	114.60	113.00	106.70	104.40	128.20	96.90	90.80	71.30
	3ATPS	149.80	122.50	141.80	117.10	113.70	125.60	108.80	105.70	101.90	99.60	81.30
	3FRS	3260.60	2481.20	1901.10	1275.20	848.20	464.10	331.50	168.00	106.10	92.90	83.00
TS	SM	4.60	4.50	4.10	3.70	3.40	3.00	2.70	2.00	1.30	0.80	0.50
	1GLS	193.90	154.40	148.80	144.40	135.30	127.70	125.70	128.80	114.50	110.70	90.00
	3GLS	156.00	131.70	122.80	118.10	111.80	110.40	105.90	102.10	99.10	91.40	73.50
	3ATPS	131.40	128.90	154.00	118.50	172.70	117.10	106.30	129.20	98.90	97.00	79.00
	3FRS	3219.60	2484.50	1827.00	1275.50	858.00	508.20	425.90	160.60	117.50	98.20	84.50
NN	SM	5.30	5.10	4.90	5.00	4.50	4.10	3.80	3.00	1.70	1.30	1.20
	1GLS	175.40	158.10	149.80	142.40	136.60	132.00	133.20	123.20	116.60	107.90	88.60
	3GLS	150.20	140.20	151.80	138.10	107.50	126.30	102.40	100.00	97.10	93.10	74.80
	3ATPS	130.50	128.90	125.00	139.60	116.90	142.00	121.90	106.90	107.90	103.40	84.80
	3FRS	3213.40	2485.70	1826.00	1286.40	833.40	460.30	300.90	165.60	113.70	99.20	81.80
IDW	SM	6.40	6.60	6.50	6.40	6.10	5.80	4.60	3.70	2.30	1.60	1.20
	1GLS	173.90	158.80	149.60	146.70	141.40	133.00	129.40	123.70	115.50	108.10	89.60
	3GLS	151.50	139.00	125.50	121.60	116.40	110.10	105.70	104.10	99.40	91.30	72.80
	3ATPS	169.00	146.50	132.20	147.10	126.20	122.40	119.80	119.30	113.30	104.30	85.50
	3FRS	3216.90	2483.90	1827.10	1275.60	834.00	483.20	299.90	168.40	115.10	100.00	86.10
LSK	SM	131.80	132.50	131.60	133.70	177.60	122.60	122.00	119.70	115.50	109.10	91.40
	1GLS	304.10	293.10	284.80	313.50	347.80	247.10	248.30	244.90	240.40	221.30	179.00
	3GLS	258.30	242.10	248.10	224.40	240.50	210.80	207.40	210.00	197.30	184.00	149.80
	3ATPS	277.60	315.80	298.00	267.40	316.40	242.20	235.60	238.70	231.90	220.20	186.00
	3FRS	3326.60	2611.00	1949.00	1389.10	943.10	569.10	417.10	316.20	229.40	209.70	165.20
SK	SM	486.40	563.70	566.70	510.00	480.90	373.50	307.60	206.10	131.60	112.70	90.70
	1GLS	641.20	640.90	713.40	610.00	555.10	469.20	385.80	325.40	270.80	218.20	180.50
	3GLS	600.80	583.40	612.70	562.20	515.80	396.20	339.90	262.10	206.10	183.10	151.50
	3ATPS	550.80	506.70	496.60	430.60	447.30	385.50	352.30	273.50	231.90	208.70	175.80
	3FRS	3649.40	2924.70	2269.80	1649.80	1232.00	804.90	551.60	337.70	214.90	194.40	161.20
OK	SM	585.60	530.40	541.10	624.70	441.80	353.50	269.40	190.80	128.10	112.80	93.00
	1GLS	679.50	675.40	674.80	622.70	621.50	462.50	376.10	327.30	245.00	221.20	180.80
	3GLS	589.20	569.80	574.00	526.60	482.60	370.60	325.60	273.20	202.80	202.90	151.10
	3ATPS	448.00	483.30	430.80	432.60	398.80	304.50	288.40	233.90	189.20	173.30	145.30
	3FRS	3568.40	2872.10	2186.20	1624.10	1193.90	790.00	577.30	347.70	225.70	197.90	161.80
MRSM	SM	145.40	147.20	148.90	145.40	135.30	137.30	138.00	142.20	141.90	140.30	137.20
	1GLS	298.70	283.40	265.20	253.40	257.00	251.50	240.00	240.60	228.20	218.60	197.60
	3GLS	239.30	226.20	263.30	225.50	218.80	193.30	193.10	193.00	185.80	172.70	160.60
	3ATPS	215.70	195.00	190.00	186.50	178.20	178.30	172.70	190.50	166.30	162.80	150.80
	3FRS	3346.90	2566.20	1911.10	1368.70	930.30	595.70	411.60	270.80	207.60	193.40	175.10
MURS	SM	145.80	141.50	145.20	147.50	136.50	133.60	123.90	125.40	116.40	110.70	108.00
	1GLS	291.80	276.40	271.00	256.70	248.50	245.40	245.50	273.40	200.80	185.90	157.50
	3GLS	239.60	246.60	214.20	210.90	205.60	196.20	192.40	187.70	168.40	160.00	146.60
	3ATPS	199.50	191.10	188.40	185.10	176.40	170.10	192.20	169.30	162.70	158.40	145.10
	3FRS	3309.70	2564.20	1902.20	1360.50	947.70	583.80	398.10	253.50	185.20	171.60	157.50

Table A.23: CT MM, MSPE grouped by estimation method.

		Percentage Data Removed										
		54.30	62.21	69.21	74.27	79.27	85.11	88.57	93.26	96.75	98.27	99.24
FA	1GLS	21.72	22.00	24.07	25.01	25.64	29.58	30.04	28.52	27.22	31.17	34.89
	3ATPS	21.72	22.00	24.07	25.01	25.64	29.58	30.04	28.52	27.22	31.17	34.89
	3FRS	21.72	22.00	24.07	25.01	25.64	29.58	30.04	28.52	27.22	31.17	34.89
	3GLS	21.72	22.00	24.07	25.01	25.64	29.58	30.04	28.52	27.22	31.17	34.89
	SM	21.72	22.00	24.07	25.01	25.64	29.58	30.04	28.52	27.22	31.17	34.89
IDW	1GLS	9.99	9.83	10.37	10.80	10.67	16.34	16.73	15.77	14.83	19.28	33.61
	3ATPS	17.30	16.79	15.35	13.19	13.15	15.16	16.99	17.70	15.30	22.21	24.60
	3FRS	17.32	16.70	17.62	17.69	17.29	16.49	15.95	15.87	18.73	71.00	156.97
	3GLS	11.20	11.33	11.80	11.92	11.94	14.11	14.82	14.93	16.00	18.28	23.69
	SM	10.02	9.86	10.43	10.82	10.69	16.19	16.70	15.71	14.57	20.02	32.06
LSK	1GLS	10.49	9.25	10.09	9.38	9.85	12.82	13.85	13.14	14.91	21.08	34.70
	3ATPS	12.76	13.24	11.55	11.68	10.82	13.62	14.63	12.73	14.50	17.11	22.60
	3FRS	13.19	13.77	14.03	14.26	16.08	15.02	15.98	14.68	27.86	73.65	138.47
	3GLS	9.52	8.87	10.92	10.35	11.05	13.34	14.89	13.67	15.56	18.20	23.61
	SM	9.26	8.67	9.26	9.37	9.69	13.33	13.85	13.82	15.56	21.97	34.60
MRSM	1GLS	15.52	15.36	15.22	15.65	14.36	17.38	17.10	16.70	17.15	20.75	34.70
	3ATPS	15.53	15.49	15.64	15.97	14.70	17.38	17.16	16.72	17.23	20.65	32.59
	3FRS	18.08	17.48	18.99	18.94	17.36	17.77	17.90	18.67	31.85	74.15	250.22
	3GLS	16.23	16.36	16.91	16.93	15.68	17.27	17.46	16.87	17.91	19.83	23.56
	SM	16.05	15.75	16.04	16.11	14.52	17.50	17.25	16.76	16.98	21.56	34.66
MURS	1GLS	10.38	9.98	10.52	10.77	10.41	13.60	14.35	14.29	14.91	19.81	34.72
	3ATPS	9.60	9.23	9.73	9.97	9.65	12.63	13.32	13.30	13.99	18.42	32.40
	3FRS	15.92	15.32	16.53	16.58	16.53	15.65	15.77	15.79	27.19	68.87	181.84
	3GLS	11.81	11.33	12.42	12.42	12.30	13.64	14.42	14.47	16.09	19.11	23.73
	SM	10.67	10.20	10.86	11.17	10.56	13.63	14.40	14.20	14.37	20.56	34.67
NN	1GLS	21.52	19.54	23.15	19.56	22.65	24.57	25.65	16.93	17.87	34.95	31.68
	3ATPS	16.20	15.47	17.13	15.25	17.50	19.25	21.01	18.54	15.53	23.53	24.56
	3FRS	18.88	18.02	22.08	19.16	23.29	22.77	23.46	16.70	33.02	71.84	166.98
	3GLS	20.79	18.82	22.45	18.98	22.03	23.33	24.09	16.70	18.17	32.28	23.79
	SM	21.90	19.76	23.43	19.89	22.81	24.91	26.11	17.13	18.09	36.41	29.84
OK	1GLS	9.44	8.26	8.88	9.23	9.50	12.40	13.04	12.67	12.65	16.62	34.44
	3ATPS	9.20	8.67	10.32	10.07	11.38	13.11	13.32	12.86	13.12	17.10	32.27
	3FRS	12.14	11.56	13.62	13.60	14.75	14.93	15.69	14.45	24.51	64.17	245.83
	3GLS	9.20	8.67	10.32	10.07	11.34	13.15	14.43	13.64	14.96	17.92	23.57
	SM	8.96	8.16	8.89	8.99	9.44	12.47	13.06	12.78	13.07	17.73	34.23
SK	1GLS	9.25	8.81	8.76	8.97	9.48	12.37	13.13	12.71	13.67	17.09	34.49
	3ATPS	9.08	8.78	10.20	10.15	11.45	13.28	14.51	13.58	14.86	18.46	23.67
	3FRS	13.21	12.02	13.39	13.37	14.43	15.04	15.65	14.41	22.82	55.78	233.74
	3GLS	9.08	8.78	10.20	10.15	11.45	13.28	14.51	13.58	14.86	18.46	23.67
	SM	8.84	8.12	8.85	8.99	9.53	12.50	13.08	12.64	14.27	19.06	34.21
TS	1GLS	26.24	25.26	26.50	27.24	26.69	30.39	29.34	27.25	25.88	26.31	34.86
	3ATPS	15.98	18.66	16.16	15.13	15.15	16.14	16.98	447.69	15.93	24.64	24.74
	3FRS	19.62	19.92	20.98	22.04	21.32	19.21	18.73	18.57	28.48	75.76	168.74
	3GLS	15.84	16.53	17.84	18.32	19.00	19.65	19.84	19.50	19.56	22.13	23.67
	SM	21.72	22.00	24.07	25.01	25.64	29.58	30.04	28.52	27.22	31.17	34.89

Table A.24: CT MM, MAPE grouped by estimation method.

		Percentage Data Removed										
		54.30	62.21	69.21	74.27	79.27	85.11	88.57	93.26	96.75	98.27	99.24
FA	1GLS	2.95	2.98	3.08	3.09	3.09	3.06	3.04	3.01	3.03	3.01	3.34
	3ATPS	2.95	2.98	3.08	3.09	3.09	3.06	3.04	3.01	3.03	3.01	3.34
	3FRS	2.95	2.98	3.08	3.09	3.09	3.06	3.04	3.01	3.03	3.01	3.34
	3GLS SM	2.95	2.98	3.08	3.09	3.09	3.06	3.04	3.01	3.03	3.01	3.34
IDW	1GLS	2.00	1.95	1.98	2.00	1.98	2.15	2.14	2.16	2.21	2.45	3.07
	3ATPS	2.75	2.69	2.45	2.27	2.28	2.26	2.39	2.61	2.45	3.00	2.72
	3FRS	2.84	2.72	2.80	2.79	2.72	2.38	2.33	2.40	2.64	4.82	6.46
	3GLS SM	2.29	2.24	2.24	2.22	2.25	2.12	2.15	2.33	2.55	2.90	2.91
LSK	1GLS	1.94	1.74	1.78	1.75	1.83	1.90	1.95	1.97	2.17	2.59	3.22
	3ATPS	2.20	2.17	1.99	2.00	1.95	2.02	2.09	2.04	2.38	2.72	2.83
	3FRS	2.34	2.31	2.29	2.32	2.50	2.16	2.24	2.23	2.98	4.92	6.62
	3GLS SM	9.52	8.87	10.92	10.35	11.05	13.34	14.89	13.67	15.56	18.20	23.61
MRSM	1GLS	1.83	1.69	1.74	1.74	1.83	1.91	1.96	2.02	2.22	2.55	3.24
	3ATPS	2.45	2.36	2.30	2.33	2.26	2.27	2.21	2.20	2.29	2.56	3.23
	3FRS	2.46	2.39	2.35	2.37	2.30	2.29	2.24	2.24	2.36	2.67	3.15
	3GLS SM	2.85	2.72	2.75	2.78	2.72	2.48	2.48	2.57	3.29	4.77	8.91
MURS	1GLS	16.23	16.36	16.91	16.93	15.68	17.27	17.46	16.87	17.91	19.83	23.56
	3ATPS	2.47	2.37	2.35	2.36	2.27	2.28	2.23	2.22	2.29	2.52	3.25
	3FRS	2.00	1.89	1.92	1.94	1.94	1.99	2.00	2.09	2.25	2.51	3.23
	3GLS SM	1.87	1.78	1.81	1.84	1.84	1.89	1.91	2.00	2.19	2.43	3.14
NN	1GLS	2.71	2.55	2.60	2.61	2.63	2.31	2.29	2.38	3.05	4.72	7.30
	3ATPS	2.71	2.49	2.64	2.47	2.71	2.66	2.74	2.31	2.42	3.32	3.06
	3FRS	2.36	2.23	2.33	2.24	2.43	2.41	2.54	2.55	2.33	3.04	2.72
	3GLS SM	2.52	2.39	2.61	2.48	2.78	2.56	2.58	2.32	3.30	4.74	6.81
OK	1GLS	2.58	2.39	2.55	2.41	2.65	2.59	2.63	2.30	2.58	3.53	2.92
	3ATPS	2.75	2.51	2.66	2.50	2.72	2.69	2.77	2.33	2.44	3.38	3.00
	3FRS	1.80	1.64	1.71	1.70	1.83	1.85	1.90	1.95	2.00	2.31	3.17
	3GLS SM	1.88	1.79	1.93	1.91	2.06	1.94	1.94	1.99	2.08	2.44	3.12
SK	1GLS	2.24	2.10	2.27	2.27	2.39	2.17	2.24	2.21	2.96	4.73	8.69
	3ATPS	9.20	8.67	10.32	10.07	11.34	13.15	14.43	13.64	14.96	17.92	23.57
	3FRS	1.79	1.65	1.72	1.72	1.81	1.85	1.91	1.95	2.03	2.31	3.17
	3GLS SM	1.79	1.68	1.69	1.70	1.82	1.83	1.89	1.96	2.07	2.34	3.18
TS	1GLS	1.88	1.78	1.92	1.91	2.09	1.99	2.12	2.14	2.39	2.90	2.92
	3ATPS	2.35	2.13	2.24	2.25	2.36	2.19	2.24	2.21	2.81	4.42	8.62
	3FRS	9.08	8.78	10.20	10.15	11.45	13.28	14.51	13.58	14.86	18.46	23.67
	3GLS SM	1.76	1.64	1.71	1.72	1.84	1.87	1.91	1.96	2.12	2.37	3.16
TS	1GLS	3.07	2.95	3.02	3.02	3.02	3.11	3.06	2.98	3.04	3.07	3.27
	3ATPS	2.68	2.88	2.56	2.45	2.51	2.38	2.41	9.52	2.48	3.23	2.73
	3FRS	3.11	3.13	3.18	3.29	3.20	2.76	2.70	2.74	3.25	4.97	7.03
	3GLS SM	2.73	2.74	2.86	2.87	3.00	2.83	2.87	2.86	2.88	3.43	2.91

Table A.25: MO MM, MSPE grouped by estimation method.

		Percentage Data Removed										
		48.97	53.13	58.06	63.28	68.80	75.68	80.54	87.21	93.95	96.97	98.51
FA	SM	229.99	221.72	213.38	209.75	204.41	203.58	203.99	204.56	202.96	200.09	201.37
	1GLS	229.99	221.72	213.38	209.75	204.41	203.58	203.99	204.56	202.96	200.09	201.37
	3GLS	229.99	221.72	213.38	209.75	204.41	203.58	203.99	204.56	202.96	200.09	201.37
	3ATPS	229.99	221.72	213.38	209.75	204.41	203.58	203.99	204.56	202.96	200.09	201.37
	3FRS	229.99	221.72	213.38	209.75	204.41	203.58	203.99	204.56	202.96	200.09	201.37
TS	SM	229.99	221.72	213.38	209.75	204.41	203.58	203.99	204.56	202.96	200.09	201.37
	1GLS	115.77	115.96	114.01	114.52	113.59	116.95	119.09	121.08	124.37	121.89	126.10
	3GLS	102.93	95.59	92.47	99.14	81.12	77.33	76.39	73.89	74.85	80.35	81.90
	3ATPS	92.76	85.67	73.44	76.09	67.82	63.34	58.73	66.65	64.45	98.95	85.14
	3FRS	105.76	100.49	96.05	94.90	89.94	89.16	89.52	95.46	92.70	97.73	111.12
NN	SM	112.70	95.42	80.67	84.78	85.14	78.08	79.43	86.53	95.23	73.96	82.47
	1GLS	111.88	94.53	79.78	83.87	84.37	77.08	79.00	84.47	92.03	72.14	82.29
	3GLS	110.41	93.30	77.83	83.83	84.01	77.41	79.41	87.56	92.74	71.37	85.63
	3ATPS	102.04	84.88	74.18	77.35	76.25	70.86	71.38	88.02	88.33	79.68	90.73
	3FRS	108.12	91.89	77.71	82.94	81.88	75.24	75.95	88.22	94.60	73.14	83.49
IDW	SM	108.54	99.12	90.97	83.97	76.06	70.75	68.89	71.12	74.77	75.41	88.66
	1GLS	86.23	79.83	73.54	68.68	62.73	58.94	57.59	59.39	63.50	63.30	75.26
	3GLS	94.23	85.30	76.01	68.10	65.79	61.96	61.79	58.00	54.42	59.27	73.79
	3ATPS	89.11	80.25	69.89	67.14	64.92	57.12	54.39	59.57	61.77	81.72	80.47
	3FRS	87.02	80.00	72.69	67.49	61.99	57.99	56.94	59.11	59.71	61.29	74.40
LSK	SM	159.49	121.53	78.25	108.86	102.91	75.11	76.95	92.27	98.34	132.04	161.96
	1GLS	91.79	82.45	75.18	67.96	57.39	60.40	67.14	69.49	79.58	82.80	104.86
	3GLS	90.39	79.82	76.97	67.71	62.33	56.19	56.06	55.99	57.73	72.59	79.15
	3ATPS	89.98	79.43	72.04	69.83	67.97	61.29	56.87	60.00	60.64	86.47	87.52
	3FRS	84.47	79.52	69.94	63.13	61.13	58.47	52.35	62.53	57.98	82.85	83.88
SK	SM	113.43	118.70	87.66	57.37	62.79	75.90	56.13	70.97	68.15	84.59	123.43
	1GLS	85.17	79.21	70.42	63.64	60.24	55.28	53.19	60.20	61.17	72.08	89.18
	3GLS	88.17	81.58	69.12	62.95	60.43	54.23	54.65	55.16	52.88	64.96	80.79
	3ATPS	88.62	78.14	68.67	68.91	60.99	56.30	59.90	52.86	57.20	83.84	85.91
	3FRS	84.38	76.85	71.11	67.22	56.50	51.97	51.95	56.49	62.06	63.92	83.38
OK	SM	126.64	99.92	69.15	69.55	91.24	73.93	54.41	86.13	85.41	97.45	136.92
	1GLS	85.85	77.72	71.81	62.06	55.90	51.86	51.85	62.68	58.96	73.02	94.19
	3GLS	91.03	81.65	70.56	64.28	59.36	55.51	60.45	54.74	57.12	62.44	78.13
	3ATPS	89.77	77.92	69.49	68.13	64.59	56.01	52.72	57.65	56.60	85.91	86.58
	3FRS	84.52	78.47	68.81	60.06	57.30	52.77	52.37	64.29	58.42	66.50	86.00
MRSM	SM	158.99	147.40	133.28	121.94	113.58	106.10	104.87	120.22	113.90	165.71	186.47
	1GLS	97.16	91.70	86.24	79.61	74.36	75.37	79.22	89.49	99.28	112.77	122.84
	3GLS	99.03	84.93	75.84	73.76	71.15	66.30	66.13	66.72	72.68	77.37	83.12
	3ATPS	89.89	80.63	73.65	70.60	65.12	59.42	60.76	55.23	66.39	92.52	86.58
	3FRS	94.39	88.83	80.00	74.67	70.23	68.84	70.07	76.95	80.58	99.97	105.03
MURS	SM	161.75	142.11	134.28	125.41	112.61	106.99	101.51	115.33	110.16	156.06	184.78
	1GLS	96.64	90.37	84.14	78.02	71.52	71.94	73.95	83.81	95.51	109.21	120.68
	3GLS	101.45	84.21	76.18	70.03	65.99	61.29	61.68	62.34	68.21	73.27	83.35
	3ATPS	88.71	81.20	70.67	69.68	63.27	57.88	60.14	53.80	56.14	90.94	85.65
	3FRS	92.46	85.27	79.46	72.20	66.29	62.78	65.37	72.49	77.37	86.35	101.44

Table A.26: MO MM, MAPE grouped by estimation method.

		Percentage Data Removed										
		48.97	53.13	58.06	63.28	68.80	75.68	80.54	87.21	93.95	96.97	98.51
FA	SM	11.15	11.03	10.89	10.83	10.85	10.84	10.89	10.72	10.63	10.83	10.41
	1GLS	11.15	11.03	10.89	10.83	10.85	10.84	10.89	10.72	10.63	10.83	10.41
	3GLS	11.15	11.03	10.89	10.83	10.85	10.84	10.89	10.72	10.63	10.83	10.41
	3ATPS	11.15	11.03	10.89	10.83	10.85	10.84	10.89	10.72	10.63	10.83	10.41
	3FRS	11.15	11.03	10.89	10.83	10.85	10.84	10.89	10.72	10.63	10.83	10.41
TS	SM	11.15	11.03	10.89	10.83	10.85	10.84	10.89	10.72	10.63	10.83	10.41
	1GLS	6.61	6.65	6.69	6.80	6.91	7.06	7.16	7.19	7.17	7.38	7.52
	3GLS	6.78	6.57	6.43	6.70	5.90	5.78	5.77	5.63	5.77	6.16	5.51
	3ATPS	5.95	5.60	5.14	5.15	4.83	4.61	4.42	4.67	4.72	6.16	5.20
	3FRS	6.54	6.53	6.49	6.46	6.48	6.43	6.53	6.44	6.48	6.79	6.93
NN	SM	6.45	5.71	5.14	5.23	5.07	4.82	4.82	4.89	5.09	4.76	5.20
	1GLS	6.45	5.68	5.11	5.20	5.05	4.78	4.80	4.82	4.99	4.71	5.16
	3GLS	6.45	5.63	5.07	5.10	5.00	4.72	4.79	4.86	4.98	4.96	5.30
	3ATPS	6.13	5.36	4.93	4.89	4.69	4.49	4.49	4.70	4.80	5.44	5.42
	3FRS	6.61	5.85	5.24	5.37	5.13	4.85	4.85	4.97	5.10	4.85	5.26
IDW	SM	6.55	6.21	5.88	5.61	5.39	5.22	5.20	5.13	5.30	5.65	5.76
	1GLS	5.45	5.18	4.89	4.70	4.50	4.39	4.39	4.37	4.53	4.72	5.07
	3GLS	6.19	5.80	5.43	5.05	4.93	4.83	4.84	4.62	4.53	5.02	5.00
	3ATPS	5.79	5.36	4.92	4.75	4.60	4.25	4.09	4.35	4.46	5.62	5.05
	3FRS	5.53	5.28	4.99	4.81	4.57	4.44	4.38	4.38	4.48	4.81	4.98
LSK	SM	8.31	6.78	5.03	6.26	6.00	4.91	5.02	5.57	6.00	8.06	8.84
	1GLS	5.37	4.87	4.52	4.27	3.87	4.07	4.53	4.60	5.01	5.55	6.53
	3GLS	6.05	5.51	5.41	4.85	4.55	4.31	4.38	4.32	4.47	5.73	5.31
	3ATPS	5.79	5.27	4.95	4.82	4.73	4.47	4.28	4.19	4.36	5.74	5.21
	3FRS	5.27	5.13	4.65	4.29	4.34	4.32	3.83	4.30	4.07	5.77	5.49
SK	SM	6.60	6.76	5.39	4.05	4.29	4.97	4.03	4.48	4.50	5.87	7.28
	1GLS	5.18	4.85	4.43	4.08	3.99	3.78	3.79	4.01	4.13	5.03	5.73
	3GLS	5.97	5.49	4.86	4.59	4.46	4.17	4.27	4.25	4.30	5.37	5.41
	3ATPS	5.66	5.19	4.76	4.64	4.29	4.12	4.18	4.00	4.26	5.60	5.23
	3FRS	5.27	5.04	4.53	4.64	4.14	3.83	3.96	3.90	4.53	4.78	5.49
OK	SM	7.09	5.94	4.55	4.58	5.66	4.93	3.96	5.34	5.44	6.52	7.85
	1GLS	5.18	4.78	4.46	4.07	3.82	3.67	3.71	4.15	4.03	5.13	5.99
	3GLS	5.84	5.51	5.06	4.68	4.37	4.31	4.68	4.34	4.63	5.21	5.24
	3ATPS	5.76	5.18	4.79	4.62	4.41	4.16	4.01	4.13	4.25	5.73	5.16
	3FRS	5.32	5.11	4.59	4.11	4.12	3.95	4.01	4.56	4.20	5.08	5.59
MRSM	SM	8.39	7.93	7.37	6.94	6.73	6.60	6.71	7.32	7.16	9.60	9.83
	1GLS	5.66	5.33	5.10	4.90	4.81	4.95	5.19	5.72	6.07	6.93	7.32
	3GLS	6.38	5.85	5.41	5.24	5.13	5.02	5.04	5.18	5.55	5.96	5.51
	3ATPS	5.74	5.33	4.93	4.77	4.50	4.26	4.25	4.14	4.65	5.92	5.24
	3FRS	5.91	5.49	5.24	5.00	4.97	4.91	5.17	5.38	5.68	6.64	6.59
MURS	SM	8.64	7.85	7.48	7.19	6.82	6.71	6.63	7.21	7.06	9.27	9.81
	1GLS	5.64	5.31	5.04	4.84	4.69	4.93	5.11	5.63	6.01	6.90	7.28
	3GLS	6.54	5.81	5.40	5.10	4.94	4.81	4.88	4.99	5.39	5.81	5.52
	3ATPS	5.68	5.31	4.86	4.66	4.41	4.18	4.12	4.06	4.37	5.86	5.24
	3FRS	5.81	5.46	5.19	4.98	4.90	4.79	5.07	5.23	5.62	6.36	6.45

### A.3.2 Grouped by Detrending Method

Table A.27: CT RR, MSPE grouped by detrending method.

		Percentage Data Removed										
		19.26	30.88	41.33	50.98	60.21	70.12	77.44	85.67	93.24	96.26	98.46
1GLS	FA	19.94	20.39	22.55	22.71	24.17	26.45	25.52	24.32	23.47	24.37	26.91
	TS	20.65	21.19	23.26	24.04	25.77	28.41	26.88	26.64	23.81	25.67	27.91
	NN	7.49	5.94	7.49	7.79	8.32	11.44	11.02	11.15	12.85	19.05	17.74
	IDW	6.11	6.63	8.16	8.57	9.06	12.61	12.20	10.99	10.49	11.75	21.52
	LSK	4.10	3.79	4.91	5.37	5.34	8.79	8.89	8.56	9.08	12.56	24.89
	SK	4.15	3.82	4.96	5.41	5.43	8.84	8.89	8.55	8.89	10.01	22.40
	OK	4.16	3.82	4.96	5.40	5.43	8.83	8.91	8.56	9.06	10.40	21.68
	MRSM	5.59	5.01	6.76	6.92	7.09	9.24	9.70	9.77	11.15	14.71	26.04
	MURS	3.94	3.84	5.30	5.84	5.75	9.31	9.39	9.02	10.01	11.36	24.38
3ATPS	FA	19.94	20.39	22.55	22.71	24.17	26.45	25.52	24.32	23.47	24.37	26.91
	TS	5.83	6.43	7.86	7.95	7.73	9.34	9.12	9.64	13.27	18.42	17.53
	NN	7.38	5.92	7.45	7.66	8.14	10.58	10.18	10.25	12.48	18.36	17.34
	IDW	4.54	4.88	6.29	6.50	6.31	8.33	8.34	8.46	10.60	17.21	17.31
	LSK	4.08	3.80	4.92	5.36	5.29	8.17	8.43	8.48	10.28	17.17	17.44
	SK	4.11	3.80	4.96	5.39	5.33	8.30	8.55	8.55	11.24	16.68	17.37
	OK	4.12	3.81	4.97	5.39	5.34	8.28	8.58	8.64	10.60	16.58	17.37
	MRSM	5.40	4.85	6.65	6.52	6.89	8.69	8.69	8.86	13.48	18.22	17.52
	MURS	4.02	3.91	5.43	5.87	5.80	8.26	8.33	8.58	12.08	18.06	17.43
3FRS	FA	19.94	20.39	22.55	22.71	24.17	26.45	25.52	24.32	23.47	24.37	26.91
	TS	7.87	8.60	10.07	10.45	10.42	14.11	11.72	11.14	11.08	13.68	15.47
	NN	7.44	5.88	7.42	7.71	8.31	11.21	10.73	10.72	11.76	16.70	15.07
	IDW	5.12	5.46	6.85	7.39	7.40	9.86	9.91	9.32	9.39	11.87	15.14
	LSK	4.07	3.76	4.89	5.39	5.37	8.74	8.89	8.77	9.50	11.34	15.02
	SK	4.13	3.77	4.93	5.42	5.46	8.79	8.88	8.71	9.28	11.62	15.31
	OK	4.11	3.78	4.93	5.42	5.43	8.82	8.88	8.74	9.19	11.25	15.32
	MRSM	5.62	4.92	6.62	6.89	7.09	9.65	9.52	9.18	10.29	12.97	15.50
	MURS	3.98	3.78	5.43	6.06	6.12	9.44	9.36	9.25	10.28	12.39	15.32
3GLS	FA	19.94	20.39	22.55	22.71	24.17	26.45	25.52	24.32	23.47	24.37	26.91
	TS	12.45	13.35	15.15	16.42	16.82	19.46	18.30	16.16	15.03	15.42	19.24
	NN	7.45	5.90	7.46	7.72	8.26	11.36	10.90	10.96	12.38	18.05	16.73
	IDW	5.49	5.97	7.58	8.05	8.35	11.62	11.28	10.16	9.83	11.43	17.80
	LSK	4.10	3.79	4.90	5.36	5.33	8.79	8.88	8.63	9.32	11.21	18.87
	SK	4.16	3.81	4.96	5.40	5.41	8.82	8.88	8.61	9.05	10.59	18.35
	OK	4.14	3.81	4.96	5.40	5.41	8.82	8.87	8.61	9.00	10.49	18.45
	MRSM	5.52	4.95	6.77	6.85	6.96	9.30	9.67	9.61	10.60	13.28	19.07
	MURS	3.92	3.80	5.32	5.85	5.86	9.41	9.41	9.19	10.28	11.08	18.68
SM	FA	19.94	20.39	22.55	22.71	24.17	26.45	25.52	24.32	23.47	24.37	26.91
	TS	19.94	20.39	22.55	22.71	24.17	26.45	25.52	24.32	23.47	24.37	26.91
	NN	7.48	5.95	7.50	7.80	8.33	11.45	11.03	11.15	12.88	19.13	17.62
	IDW	6.25	6.74	8.24	8.66	9.19	12.68	12.28	11.05	10.43	11.67	20.57
	LSK	4.10	3.79	4.91	5.37	5.35	8.80	8.87	8.62	9.25	11.04	21.51
	SK	4.16	3.82	4.96	5.41	5.44	8.82	8.90	8.56	8.93	10.35	20.06
	OK	4.16	3.82	4.96	5.41	5.44	8.82	8.89	8.56	9.02	10.11	20.55
	MRSM	5.52	5.05	6.74	6.99	7.11	9.22	9.77	9.90	11.13	14.36	25.52
	MURS	3.95	3.83	5.35	5.85	5.78	9.28	9.38	9.04	9.88	11.32	23.47

Table A.28: CT RR, MAPE grouped by detrending method.

		Percentage Data Removed										
		19.26	30.88	41.33	50.98	60.21	70.12	77.44	85.67	93.24	96.26	98.46
1GLS	FA	3.17	3.12	3.21	3.17	3.22	3.18	3.13	3.10	3.16	2.93	2.96
	TS	2.86	2.84	2.96	2.90	2.94	3.02	2.97	2.98	2.98	3.03	3.05
	NN	1.20	1.17	1.29	1.33	1.42	1.58	1.60	1.69	1.94	2.36	2.26
	IDW	1.65	1.65	1.74	1.76	1.82	1.91	1.88	1.86	1.99	1.93	2.40
	LSK	0.92	0.90	1.00	1.08	1.13	1.32	1.36	1.45	1.68	1.99	2.68
	SK	0.93	0.91	1.00	1.08	1.13	1.32	1.36	1.44	1.64	1.79	2.47
	OK	0.93	0.91	1.01	1.08	1.13	1.32	1.36	1.45	1.67	1.82	2.41
	MRSM	1.22	1.18	1.32	1.36	1.44	1.56	1.63	1.72	1.95	2.14	2.75
	MURS	1.03	1.02	1.13	1.20	1.27	1.47	1.49	1.58	1.88	1.96	2.65
3ATPS	FA	3.17	3.12	3.21	3.17	3.22	3.18	3.13	3.10	3.16	2.93	2.96
	TS	1.52	1.53	1.62	1.61	1.62	1.70	1.65	1.80	2.15	2.55	2.25
	NN	1.22	1.18	1.30	1.34	1.41	1.55	1.55	1.70	2.06	2.54	2.21
	IDW	1.28	1.26	1.36	1.38	1.39	1.48	1.47	1.60	1.87	2.45	2.19
	LSK	0.93	0.92	1.01	1.10	1.17	1.35	1.36	1.53	1.79	2.42	2.23
	SK	0.94	0.92	1.02	1.09	1.16	1.34	1.37	1.53	1.91	2.40	2.22
	OK	0.93	0.92	1.02	1.09	1.15	1.34	1.37	1.54	1.85	2.39	2.21
	MRSM	1.23	1.19	1.31	1.33	1.42	1.52	1.53	1.68	2.16	2.51	2.25
	MURS	1.05	1.05	1.16	1.23	1.30	1.46	1.47	1.63	2.01	2.50	2.23
3FRS	FA	3.17	3.12	3.21	3.17	3.22	3.18	3.13	3.10	3.16	2.93	2.96
	TS	1.89	1.93	2.02	2.03	2.01	2.21	2.02	2.07	2.14	2.43	2.33
	NN	1.23	1.20	1.31	1.35	1.45	1.60	1.62	1.73	1.96	2.33	2.28
	IDW	1.43	1.42	1.53	1.58	1.59	1.69	1.69	1.76	1.83	2.15	2.25
	LSK	0.93	0.92	1.01	1.10	1.16	1.35	1.41	1.58	1.81	1.98	2.27
	SK	0.93	0.92	1.01	1.09	1.17	1.35	1.40	1.54	1.76	2.05	2.28
	OK	0.93	0.92	1.01	1.10	1.15	1.35	1.40	1.54	1.73	2.00	2.34
	MRSM	1.25	1.21	1.35	1.41	1.49	1.63	1.66	1.76	2.02	2.23	2.31
	MURS	1.06	1.05	1.22	1.30	1.37	1.58	1.62	1.75	2.02	2.25	2.29
3GLS	FA	3.17	3.12	3.21	3.17	3.22	3.18	3.13	3.10	3.16	2.93	2.96
	TS	2.36	2.36	2.49	2.52	2.53	2.59	2.54	2.42	2.43	2.57	2.33
	NN	1.20	1.17	1.29	1.33	1.42	1.58	1.60	1.70	1.93	2.34	2.22
	IDW	1.49	1.48	1.59	1.62	1.66	1.76	1.74	1.74	1.86	2.05	2.15
	LSK	0.92	0.90	1.00	1.08	1.13	1.32	1.36	1.47	1.71	1.98	2.25
	SK	0.93	0.91	1.00	1.08	1.13	1.32	1.36	1.46	1.69	1.94	2.19
	OK	0.93	0.91	1.00	1.08	1.13	1.32	1.36	1.46	1.68	1.92	2.20
	MRSM	1.23	1.18	1.31	1.34	1.43	1.56	1.63	1.72	2.00	2.19	2.27
	MURS	1.05	1.01	1.14	1.21	1.29	1.49	1.51	1.62	1.96	2.03	2.22
SM	FA	3.17	3.12	3.21	3.17	3.22	3.18	3.13	3.10	3.16	2.93	2.96
	TS	3.17	3.12	3.21	3.17	3.22	3.18	3.13	3.10	3.16	2.93	2.96
	NN	1.20	1.17	1.29	1.33	1.42	1.58	1.60	1.69	1.94	2.35	2.25
	IDW	1.67	1.66	1.76	1.78	1.85	1.94	1.90	1.89	1.97	1.91	2.30
	LSK	0.92	0.90	1.00	1.08	1.13	1.32	1.36	1.48	1.72	1.86	2.37
	SK	0.93	0.91	1.01	1.08	1.14	1.33	1.37	1.45	1.66	1.80	2.27
	OK	0.93	0.91	1.01	1.08	1.14	1.33	1.36	1.45	1.69	1.78	2.31
	MRSM	1.22	1.19	1.31	1.36	1.45	1.57	1.64	1.75	1.97	2.09	2.63
	MURS	1.04	1.02	1.15	1.22	1.28	1.48	1.50	1.60	1.89	1.93	2.51

Table A.29: CT RR, time grouped by detrending method.

		Percentage Data Removed										
		19.26	30.88	41.33	50.98	60.21	70.12	77.44	85.67	93.24	96.26	98.46
1GLS	FA	551.80	491.50	464.90	433.90	420.20	392.30	404.00	365.90	310.20	205.90	72.50
	TS	538.40	500.10	451.90	433.00	405.00	390.60	381.90	360.70	321.00	211.70	73.50
	NN	529.00	496.40	465.50	430.00	418.00	392.90	388.70	367.40	308.90	210.30	74.00
	IDW	538.20	497.70	447.70	434.40	417.20	397.80	384.50	370.20	320.30	211.30	71.00
	LSK	1033.20	959.80	920.50	847.60	864.80	791.50	769.80	733.90	615.00	421.00	141.10
	SK	1215.10	1145.60	1090.90	1016.90	948.60	854.00	816.40	751.10	615.80	411.90	140.10
	OK	1241.30	1220.00	1128.90	1025.20	954.40	878.50	805.70	755.30	629.20	412.80	139.80
	MRS	677.40	603.90	571.90	541.70	529.20	511.90	485.70	476.70	421.80	317.20	182.80
MURS	647.40	611.30	567.70	541.10	553.70	540.80	506.50	502.10	452.50	336.70	186.30	
3ATPS	FA	517.80	472.70	449.10	418.40	418.60	384.00	375.50	374.80	321.80	211.20	70.50
	TS	500.40	458.50	456.30	438.30	433.40	412.00	402.10	373.40	313.10	205.20	74.20
	NN	517.10	492.20	445.60	430.50	407.80	391.80	371.30	363.30	318.70	207.90	73.20
	IDW	511.00	468.30	454.10	417.80	404.20	398.20	379.90	371.30	311.00	212.00	71.40
	LSK	999.50	954.60	905.90	855.90	829.30	800.70	782.70	756.50	621.10	424.60	142.30
	SK	1214.20	1184.50	1106.30	1038.40	970.70	893.60	857.00	767.20	623.90	418.70	139.60
	OK	1208.80	1176.60	1112.70	1051.60	954.70	884.90	824.90	763.90	628.10	419.80	141.10
	MRS	615.50	564.80	531.30	525.50	507.20	485.40	472.10	467.90	404.00	307.50	179.00
MURS	589.70	564.80	546.70	525.00	510.40	484.20	477.90	463.30	401.90	307.60	179.50	
3FRS	FA	3887.00	2606.50	1822.00	1213.30	858.80	570.20	498.90	399.00	314.60	221.00	80.60
	TS	3916.10	2587.70	1742.00	1198.50	818.30	566.00	462.90	398.20	303.20	204.30	69.10
	NN	3848.70	2586.30	1738.20	1183.20	819.80	559.40	464.20	379.60	315.10	206.40	71.40
	IDW	3868.30	2582.50	1735.80	1179.30	827.80	568.70	454.30	388.20	312.60	203.30	70.70
	LSK	4368.60	3063.30	2189.90	1614.70	1226.60	953.40	859.40	764.10	627.40	415.80	138.60
	SK	4589.20	3273.70	2405.40	1793.80	1365.90	1051.00	895.40	786.40	621.80	423.30	142.20
	OK	4564.50	3295.80	2380.80	1778.90	1442.80	1054.50	903.50	794.60	630.30	416.60	138.80
	MRS	3970.90	2707.10	1866.30	1288.10	926.30	682.90	572.00	497.50	414.10	316.80	179.40
MURS	3968.20	2690.70	1859.40	1301.40	935.80	670.20	571.10	499.30	410.20	321.50	182.80	
3GLS	FA	570.20	492.40	468.50	445.00	423.30	405.10	403.00	379.80	313.40	223.90	72.60
	TS	539.60	504.20	459.00	437.50	428.70	402.70	394.70	385.70	326.80	216.80	72.80
	NN	548.20	507.10	466.20	437.40	416.20	394.40	387.20	386.00	320.90	213.70	71.40
	IDW	599.50	502.40	471.10	442.20	421.50	420.30	396.90	390.10	321.70	217.60	74.70
	LSK	1049.40	972.10	925.30	842.70	839.90	784.10	774.70	732.90	633.70	434.60	143.50
	SK	1284.40	1244.40	1109.50	1008.60	958.10	890.60	829.90	777.00	648.20	432.90	141.90
	OK	1261.80	1188.10	1090.80	1022.30	950.30	881.30	818.60	781.80	633.80	428.90	140.20
	MRS	663.60	611.60	580.20	538.60	549.00	515.80	513.90	490.50	432.50	325.50	183.00
MURS	771.40	618.90	589.80	551.00	527.40	522.10	503.80	490.30	432.10	318.00	182.60	
SM	FA	9.90	9.80	10.40	10.30	9.60	8.50	8.70	8.60	8.10	8.40	8.50
	TS	8.40	8.60	8.40	8.60	8.50	8.80	8.30	8.00	7.50	6.90	7.20
	NN	7.90	8.50	8.80	9.20	9.20	9.00	9.30	8.30	8.30	7.90	7.40
	IDW	9.20	9.30	10.10	10.10	9.50	9.60	9.50	9.20	7.40	5.80	5.90
	LSK	523.80	483.40	442.50	432.80	418.90	404.40	388.30	375.80	315.30	212.80	73.40
	SK	727.60	726.20	666.90	615.50	542.50	477.80	450.30	399.10	323.40	220.90	72.20
	OK	714.70	708.70	662.80	596.80	556.00	483.80	430.60	398.60	318.70	214.80	70.90
	MRS	120.40	119.50	121.00	116.50	117.60	118.70	117.40	117.30	114.10	113.90	115.90
MURS	122.40	118.90	119.30	118.00	120.90	118.90	117.60	116.10	118.50	115.10	116.40	

Table A.30: MO RR, MSPE grouped by detrending method.

		Percentage Data Removed										
		19.53	26.20	33.79	41.77	50.24	60.91	68.48	79.59	90.26	94.90	97.44
1GLS	FA	192.96	180.62	184.53	190.36	192.95	200.39	202.35	201.05	200.74	202.65	200.29
	TS	105.28	96.83	99.27	105.23	108.43	116.13	117.34	116.40	120.05	116.16	116.96
	NN	17.02	21.56	21.30	30.49	28.59	30.70	28.45	31.78	41.29	56.81	82.67
	IDW	29.07	27.59	27.73	31.75	32.84	36.06	36.88	36.60	42.00	45.41	56.56
	LSK	11.66	9.06	9.24	11.99	16.81	28.39	16.12	22.57	29.69	39.67	83.78
	SK	6.85	7.87	8.80	13.28	13.14	14.68	17.69	21.41	32.24	52.75	70.29
	OK	6.69	8.19	9.11	12.90	11.75	14.51	17.09	20.68	30.57	43.85	76.72
	MRSM	15.94	16.34	18.42	24.41	29.14	41.86	54.39	65.92	92.62	102.09	111.11
	MURS	13.23	13.26	16.53	18.42	22.84	31.78	45.23	55.68	84.88	99.67	108.70
3ATPS	FA	192.96	180.62	184.53	190.36	192.95	200.39	202.35	201.05	200.74	202.65	200.29
	TS	32.67	30.67	31.11	34.60	36.57	37.54	37.25	40.30	42.16	50.43	58.48
	NN	15.95	19.86	20.15	29.33	27.77	29.49	26.79	29.88	38.00	56.91	76.26
	IDW	21.97	21.11	20.95	23.88	25.20	26.70	26.62	27.22	30.60	44.06	52.10
	LSK	14.88	16.65	16.87	16.52	24.59	31.05	23.22	31.64	30.53	44.24	58.02
	SK	10.73	11.84	11.84	17.49	17.35	19.95	20.26	26.35	30.77	40.32	56.29
	OK	12.28	11.98	13.03	14.92	16.14	22.53	20.06	23.69	29.49	47.54	56.57
	MRSM	1.99	2.05	2.12	2.37	2.45	2.70	2.86	3.05	3.58	4.02	4.48
	MURS	1.70	1.75	1.91	2.12	2.21	2.43	2.52	2.82	3.35	3.92	4.43
3FRS	FA	192.96	180.62	184.53	190.36	192.95	200.39	202.35	201.05	200.74	202.65	200.29
	TS	75.25	73.34	78.39	83.52	86.07	84.53	84.63	85.10	85.98	93.94	97.81
	NN	17.05	21.42	21.11	30.35	28.34	30.61	28.27	31.44	41.22	57.14	81.65
	IDW	27.91	26.62	26.86	31.00	31.89	34.14	34.57	34.67	38.73	43.22	53.65
	LSK	7.59	8.51	12.60	12.54	28.12	17.38	18.26	20.87	31.13	52.64	73.36
	SK	8.78	8.37	8.97	15.27	11.91	15.17	15.90	26.94	37.69	40.71	70.24
	OK	9.39	8.24	9.84	12.33	11.86	17.89	19.96	23.03	37.35	47.81	63.65
	MRSM	16.40	16.10	19.20	26.01	29.28	39.22	47.20	55.91	74.10	85.64	93.43
	MURS	12.92	12.58	15.06	19.36	21.25	31.13	37.81	45.55	64.70	79.43	89.51
3GLS	FA	192.96	180.62	184.53	190.36	192.95	200.39	202.35	201.05	200.74	202.65	200.29
	TS	55.84	72.26	63.13	65.11	65.90	66.18	66.73	66.29	75.73	79.98	76.11
	NN	17.06	21.26	20.91	30.23	28.11	30.49	28.11	31.37	40.70	56.44	80.41
	IDW	26.10	25.68	25.48	29.47	30.64	33.04	32.63	32.95	37.53	41.48	51.78
	LSK	10.10	8.33	12.63	12.47	21.54	26.99	21.38	34.86	29.31	59.14	69.71
	SK	7.00	11.31	9.32	13.72	12.23	17.86	17.28	22.58	34.79	46.37	60.70
	OK	7.55	9.02	10.46	14.65	14.71	21.34	22.12	28.76	35.64	52.45	62.73
	MRSM	14.71	15.14	16.18	23.34	25.85	34.37	39.64	46.89	61.46	69.40	70.22
	MURS	11.24	12.20	13.16	16.90	20.62	25.72	31.59	40.08	51.59	65.08	68.82
SM	FA	192.96	180.62	184.53	190.36	192.95	200.39	202.35	201.05	200.74	202.65	200.29
	TS	192.96	180.62	184.53	190.36	192.95	200.39	202.35	201.05	200.74	202.65	200.29
	NN	17.42	21.91	21.74	30.75	28.85	30.89	28.66	31.91	41.60	57.46	82.51
	IDW	31.60	29.89	30.14	34.15	35.36	38.70	39.46	39.59	46.06	49.08	58.23
	LSK	6.94	8.66	9.77	12.68	13.12	28.13	16.28	33.92	34.03	65.41	82.51
	SK	7.47	8.57	8.80	11.40	12.06	15.82	19.88	27.99	33.33	65.55	67.09
	OK	6.71	8.14	9.02	11.65	11.74	15.14	20.98	21.12	43.68	51.24	62.31
	MRSM	14.72	15.90	17.71	23.40	25.57	33.79	42.02	47.56	78.20	105.29	99.88
	MURS	12.17	12.29	13.70	16.89	19.02	24.86	29.73	33.35	66.85	96.84	91.13

Table A.31: MO RR, MAPE grouped by detrending method.

		Percentage Data Removed										
		19.53	26.20	33.79	41.77	50.24	60.91	68.48	79.59	90.26	94.90	97.44
1GLS	FA	10.78	10.60	10.65	10.77	10.91	11.00	11.11	11.02	11.01	11.49	11.12
	TS	6.99	6.70	6.86	7.13	7.24	7.47	7.52	7.45	7.33	7.46	7.53
	NN	2.19	2.44	2.47	2.78	2.70	2.84	2.82	3.03	3.50	4.13	5.10
	IDW	3.23	3.25	3.32	3.50	3.55	3.70	3.83	3.80	4.01	4.37	4.82
	LSK	1.65	1.53	1.58	1.76	2.08	2.91	2.11	2.62	3.01	3.84	6.20
	SK	1.25	1.40	1.52	1.92	1.89	1.96	2.26	2.56	3.21	4.63	5.54
	OK	1.22	1.44	1.57	1.88	1.71	1.93	2.18	2.47	3.12	4.12	5.89
	MRSMS	2.20	2.23	2.44	2.85	3.24	3.79	4.47	5.10	6.10	6.80	7.35
MURS	2.04	2.05	2.41	2.53	2.93	3.46	4.30	4.91	5.98	6.72	7.23	
3ATPS	FA	10.78	10.60	10.65	10.77	10.91	11.00	11.11	11.02	11.01	11.49	11.12
	TS	3.11	3.14	3.23	3.43	3.47	3.50	3.50	3.60	3.87	4.26	4.53
	NN	2.13	2.33	2.38	2.70	2.63	2.75	2.71	2.93	3.34	4.23	4.90
	IDW	2.50	2.57	2.61	2.77	2.79	2.84	2.87	2.94	3.20	3.87	4.25
	LSK	1.97	2.18	2.27	2.14	2.69	3.08	2.57	3.09	3.18	3.91	4.50
	SK	1.59	1.77	1.83	2.26	2.19	2.35	2.38	2.79	3.12	3.72	4.43
	OK	1.72	1.80	1.96	2.04	2.09	2.54	2.37	2.65	3.04	4.08	4.44
	MRSMS	1.99	2.05	2.12	2.37	2.45	2.70	2.86	3.05	3.58	4.02	4.48
MURS	1.70	1.75	1.91	2.12	2.21	2.43	2.52	2.82	3.35	3.92	4.43	
3FRS	FA	10.78	10.60	10.65	10.77	10.91	11.00	11.11	11.02	11.01	11.49	11.12
	TS	6.07	6.16	6.29	6.57	6.53	6.57	6.65	6.61	6.59	7.02	6.88
	NN	2.24	2.47	2.50	2.79	2.72	2.85	2.82	3.03	3.51	4.20	5.08
	IDW	3.20	3.26	3.32	3.51	3.54	3.62	3.72	3.74	3.98	4.43	4.76
	LSK	1.33	1.47	1.87	1.84	3.07	2.23	2.36	2.56	3.35	4.99	5.75
	SK	1.49	1.47	1.55	2.15	1.73	2.02	2.08	2.97	3.65	4.22	5.70
	OK	1.55	1.45	1.69	1.82	1.72	2.25	2.55	2.76	3.84	4.63	5.35
	MRSMS	2.32	2.29	2.71	3.09	3.26	3.69	4.27	4.78	5.77	6.56	6.64
MURS	2.00	2.05	2.43	2.70	2.90	3.56	4.01	4.59	5.57	6.43	6.55	
3GLS	FA	10.78	10.60	10.65	10.77	10.91	11.00	11.11	11.02	11.01	11.49	11.12
	TS	4.60	5.66	5.17	5.15	5.19	5.28	5.34	5.39	5.76	6.11	5.90
	NN	2.21	2.44	2.45	2.75	2.68	2.83	2.81	3.03	3.48	4.20	5.09
	IDW	2.96	3.04	3.07	3.25	3.31	3.41	3.44	3.52	3.73	4.13	4.51
	LSK	1.50	1.43	1.84	1.81	2.50	2.87	2.52	3.49	3.01	5.05	5.58
	SK	1.25	1.71	1.60	1.94	1.76	2.27	2.20	2.68	3.52	4.40	5.11
	OK	1.32	1.54	1.73	2.00	1.99	2.53	2.61	3.08	3.56	4.74	5.24
	MRSMS	2.10	2.11	2.27	2.59	2.76	3.30	3.62	4.26	4.97	5.56	5.59
MURS	1.74	1.96	2.11	2.34	2.67	2.96	3.47	4.18	4.64	5.46	5.56	
SM	FA	10.78	10.60	10.65	10.77	10.91	11.00	11.11	11.02	11.01	11.49	11.12
	TS	10.78	10.60	10.65	10.77	10.91	11.00	11.11	11.02	11.01	11.49	11.12
	NN	2.18	2.44	2.48	2.78	2.70	2.83	2.81	3.03	3.48	4.10	5.03
	IDW	3.55	3.58	3.66	3.81	3.89	4.03	4.15	4.17	4.48	4.95	5.23
	LSK	1.25	1.49	1.66	1.85	1.85	2.84	2.12	3.18	3.30	5.42	6.31
	SK	1.34	1.50	1.52	1.69	1.75	2.10	2.53	3.26	3.43	5.79	5.48
	OK	1.23	1.43	1.56	1.73	1.70	2.01	2.54	2.57	4.03	4.68	5.09
	MRSMS	2.13	2.20	2.40	2.72	2.96	3.31	4.03	4.44	6.14	7.82	7.29
MURS	1.86	1.92	2.17	2.39	2.65	3.07	3.53	3.84	5.82	7.68	7.10	

Table A.32: MO RR, time grouped by detrending method.

		Percentage Data Removed										
		19.53	26.20	33.79	41.77	50.24	60.91	68.48	79.59	90.26	94.90	97.44
1GLS	FA	202.90	165.50	151.90	147.20	132.90	126.30	126.50	123.80	116.70	137.40	84.40
	TS	193.90	154.40	148.80	144.40	135.30	127.70	125.70	128.80	114.50	110.70	90.00
	NN	175.40	158.10	149.80	142.40	136.60	132.00	133.20	123.20	116.60	107.90	88.60
	IDW	173.90	158.80	149.60	146.70	141.40	133.00	129.40	123.70	115.50	108.10	89.60
	LSK	304.10	293.10	284.80	313.50	347.80	247.10	248.30	244.90	240.40	221.30	179.00
	SK	641.20	640.90	713.40	610.00	555.10	469.20	385.80	325.40	270.80	218.20	180.50
	OK	679.50	675.40	674.80	622.70	621.50	462.50	376.10	327.30	245.00	221.20	180.80
	MRSM	298.70	283.40	265.20	253.40	257.00	251.50	240.00	240.60	228.20	218.60	197.60
	MURS	291.80	276.40	271.00	256.70	248.50	245.40	245.50	273.40	200.80	185.90	157.50
3ATPS	FA	149.80	122.50	141.80	117.10	113.70	125.60	108.80	105.70	101.90	99.60	81.30
	TS	131.40	128.90	154.00	118.50	172.70	117.10	106.30	129.20	98.90	97.00	79.00
	NN	130.50	128.90	125.00	139.60	116.90	142.00	121.90	106.90	107.90	103.40	84.80
	IDW	169.00	146.50	132.20	147.10	126.20	122.40	119.80	119.30	113.30	104.30	85.50
	LSK	277.60	315.80	298.00	267.40	316.40	242.20	235.60	238.70	231.90	220.20	186.00
	SK	550.80	506.70	496.60	430.60	447.30	385.50	352.30	273.50	231.90	208.70	175.80
	OK	448.00	483.30	430.80	432.60	398.80	304.50	288.40	233.90	189.20	173.30	145.30
	MRSM	215.70	195.00	190.00	186.50	178.20	178.30	172.70	190.50	166.30	162.80	150.80
	MURS	199.50	191.10	188.40	185.10	176.40	170.10	192.20	169.30	162.70	158.40	145.10
3FRS	FA	3260.60	2481.20	1901.10	1275.20	848.20	464.10	331.50	168.00	106.10	92.90	83.00
	TS	3219.60	2484.50	1827.00	1275.50	858.00	508.20	425.90	160.60	117.50	98.20	84.50
	NN	3213.40	2485.70	1826.00	1286.40	833.40	460.30	300.90	165.60	113.70	99.20	81.80
	IDW	3216.90	2483.90	1827.10	1275.60	834.00	483.20	299.90	168.40	115.10	100.00	86.10
	LSK	3326.60	2611.00	1949.00	1389.10	943.10	569.10	417.10	316.20	229.40	209.70	165.20
	SK	3649.40	2924.70	2269.80	1649.80	1232.00	804.90	551.60	337.70	214.90	194.40	161.20
	OK	3568.40	2872.10	2186.20	1624.10	1193.90	790.00	577.30	347.70	225.70	197.90	161.80
	MRSM	3346.90	2566.20	1911.10	1368.70	930.30	595.70	411.60	270.80	207.60	193.40	175.10
	MURS	3309.70	2564.20	1902.20	1360.50	947.70	583.80	398.10	253.50	185.20	171.60	157.50
3GLS	FA	144.60	135.90	122.40	114.60	113.00	106.70	104.40	128.20	96.90	90.80	71.30
	TS	156.00	131.70	122.80	118.10	111.80	110.40	105.90	102.10	99.10	91.40	73.50
	NN	150.20	140.20	151.80	138.10	107.50	126.30	102.40	100.00	97.10	93.10	74.80
	IDW	151.50	139.00	125.50	121.60	116.40	110.10	105.70	104.10	99.40	91.30	72.80
	LSK	258.30	242.10	248.10	224.40	240.50	210.80	207.40	210.00	197.30	184.00	149.80
	SK	600.80	583.40	612.70	562.20	515.80	396.20	339.90	262.10	206.10	183.10	151.50
	OK	589.20	569.80	574.00	526.60	482.60	370.60	325.60	273.20	202.80	202.90	151.10
	MRSM	239.30	226.20	263.30	225.50	218.80	193.30	193.10	193.00	185.80	172.70	160.60
	MURS	239.60	246.60	214.20	210.90	205.60	196.20	192.40	187.70	168.40	160.00	146.60
SM	FA	4.70	4.40	4.00	3.60	3.60	3.00	2.50	2.00	1.60	0.60	0.80
	TS	4.60	4.50	4.10	3.70	3.40	3.00	2.70	2.00	1.30	0.80	0.50
	NN	5.30	5.10	4.90	5.00	4.50	4.10	3.80	3.00	1.70	1.30	1.20
	IDW	6.40	6.60	6.50	6.40	6.10	5.80	4.60	3.70	2.30	1.60	1.20
	LSK	131.80	132.50	131.60	133.70	177.60	122.60	122.00	119.70	115.50	109.10	91.40
	SK	486.40	563.70	566.70	510.00	480.90	373.50	307.60	206.10	131.60	112.70	90.70
	OK	585.60	530.40	541.10	624.70	441.80	353.50	269.40	190.80	128.10	112.80	93.00
	MRSM	145.40	147.20	148.90	145.40	135.30	137.30	138.00	142.20	141.90	140.30	137.20
	MURS	145.80	141.50	145.20	147.50	136.50	133.60	123.90	125.40	116.40	110.70	108.00

Table A.33: CT MM, MSPE grouped by detrending method.

		Percentage Data Removed										
		54.30	62.21	69.21	74.27	79.27	85.11	88.57	93.26	96.75	98.27	99.24
1GLS	FA	21.72	22.00	24.07	25.01	25.64	29.58	30.04	28.52	27.22	31.17	34.89
	IDW	9.99	9.83	10.37	10.80	10.67	16.34	16.73	15.77	14.83	19.28	33.61
	LSK	10.49	9.25	10.09	9.38	9.85	12.82	13.85	13.14	14.91	21.08	34.70
	MRSMS	15.52	15.36	15.22	15.65	14.36	17.38	17.10	16.70	17.15	20.75	34.70
	MURS	10.38	9.98	10.52	10.77	10.41	13.60	14.35	14.29	14.91	19.81	34.72
	NN	21.52	19.54	23.15	19.56	22.65	24.57	25.65	16.93	17.87	34.95	31.68
	OK	9.44	8.26	8.88	9.23	9.50	12.40	13.04	12.67	12.65	16.62	34.44
	SK	9.25	8.81	8.76	8.97	9.48	12.37	13.13	12.71	13.67	17.09	34.49
	TS	26.24	25.26	26.50	27.24	26.69	30.39	29.34	27.25	25.88	26.31	34.86
3ATPS	FA	21.72	22.00	24.07	25.01	25.64	29.58	30.04	28.52	27.22	31.17	34.89
	IDW	17.30	16.79	15.35	13.19	13.15	15.16	16.99	17.70	15.30	22.21	24.60
	LSK	12.76	13.24	11.55	11.68	10.82	13.62	14.63	12.73	14.50	17.11	22.60
	MRSMS	15.53	15.49	15.64	15.97	14.70	17.38	17.16	16.72	17.23	20.65	32.59
	MURS	9.60	9.23	9.73	9.97	9.65	12.63	13.32	13.30	13.99	18.42	32.40
	NN	16.20	15.47	17.13	15.25	17.50	19.25	21.01	18.54	15.53	23.53	24.56
	OK	9.20	8.67	10.32	10.07	11.38	13.11	13.32	12.86	13.12	17.10	32.27
	SK	9.08	8.78	10.20	10.15	11.45	13.28	14.51	13.58	14.86	18.46	23.67
	TS	15.98	18.66	16.16	15.13	15.15	16.14	16.98	447.69	15.93	24.64	24.74
3FRS	FA	21.72	22.00	24.07	25.01	25.64	29.58	30.04	28.52	27.22	31.17	34.89
	IDW	17.32	16.70	17.62	17.69	17.29	16.49	15.95	15.87	18.73	71.00	156.97
	LSK	13.19	13.77	14.03	14.26	16.08	15.02	15.98	14.68	27.86	73.65	138.47
	MRSMS	18.08	17.48	18.99	18.94	17.36	17.77	17.90	18.67	31.85	74.15	250.22
	MURS	15.92	15.32	16.53	16.58	16.53	15.65	15.77	15.79	27.19	68.87	181.84
	NN	18.88	18.02	22.08	19.16	23.29	22.77	23.46	16.70	33.02	71.84	166.98
	OK	12.14	11.56	13.62	13.60	14.75	14.93	15.69	14.45	24.51	64.17	245.83
	SK	13.21	12.02	13.39	13.37	14.43	15.04	15.65	14.41	22.82	55.78	233.74
	TS	19.62	19.92	20.98	22.04	21.32	19.21	18.73	18.57	28.48	75.76	168.74
3GLS	FA	21.72	22.00	24.07	25.01	25.64	29.58	30.04	28.52	27.22	31.17	34.89
	IDW	11.20	11.33	11.80	11.92	11.94	14.11	14.82	14.93	16.00	18.28	23.69
	LSK	9.52	8.87	10.92	10.35	11.05	13.34	14.89	13.67	15.56	18.20	23.61
	MRSMS	16.23	16.36	16.91	16.93	15.68	17.27	17.46	16.87	17.91	19.83	23.56
	MURS	11.81	11.33	12.42	12.42	12.30	13.64	14.42	14.47	16.09	19.11	23.73
	NN	20.79	18.82	22.45	18.98	22.03	23.33	24.09	16.70	18.17	32.28	23.79
	OK	9.20	8.67	10.32	10.07	11.34	13.15	14.43	13.64	14.96	17.92	23.57
	SK	9.08	8.78	10.20	10.15	11.45	13.28	14.51	13.58	14.86	18.46	23.67
	TS	15.84	16.53	17.84	18.32	19.00	19.65	19.84	19.50	19.56	22.13	23.67
SM	FA	21.72	22.00	24.07	25.01	25.64	29.58	30.04	28.52	27.22	31.17	34.89
	IDW	10.02	9.86	10.43	10.82	10.69	16.19	16.70	15.71	14.57	20.02	32.06
	LSK	9.26	8.67	9.26	9.37	9.69	13.33	13.85	13.82	15.56	21.97	34.60
	MRSMS	16.05	15.75	16.04	16.11	14.52	17.50	17.25	16.76	16.98	21.56	34.66
	MURS	10.67	10.20	10.86	11.17	10.56	13.63	14.40	14.20	14.37	20.56	34.67
	NN	21.90	19.76	23.43	19.89	22.81	24.91	26.11	17.13	18.09	36.41	29.84
	OK	8.96	8.16	8.89	8.99	9.44	12.47	13.06	12.78	13.07	17.73	34.23
	SK	8.84	8.12	8.85	8.99	9.53	12.50	13.08	12.64	14.27	19.06	34.21
	TS	21.72	22.00	24.07	25.01	25.64	29.58	30.04	28.52	27.22	31.17	34.89

Table A.34: CT MM, MAPE grouped by detrending method.

		Percentage Data Removed										
		54.30	62.21	69.21	74.27	79.27	85.11	88.57	93.26	96.75	98.27	99.24
1GLS	FA	2.95	2.98	3.08	3.09	3.09	3.06	3.04	3.01	3.03	3.01	3.34
	IDW	2.00	1.95	1.98	2.00	1.98	2.15	2.14	2.16	2.21	2.45	3.07
	LSK	1.94	1.74	1.78	1.75	1.83	1.90	1.95	1.97	2.17	2.59	3.22
	MRSM	2.45	2.36	2.30	2.33	2.26	2.27	2.21	2.20	2.29	2.56	3.23
	MURS	2.00	1.89	1.92	1.94	1.94	1.99	2.00	2.09	2.25	2.51	3.23
	NN	2.71	2.49	2.64	2.47	2.71	2.66	2.74	2.31	2.42	3.32	3.06
	OK	1.80	1.64	1.71	1.70	1.83	1.85	1.90	1.95	2.00	2.31	3.17
	SK	1.79	1.68	1.69	1.70	1.82	1.83	1.89	1.96	2.07	2.34	3.18
	TS	3.07	2.95	3.02	3.02	3.02	3.11	3.06	2.98	3.04	3.07	3.27
3ATPS	FA	2.95	2.98	3.08	3.09	3.09	3.06	3.04	3.01	3.03	3.01	3.34
	IDW	2.75	2.69	2.45	2.27	2.28	2.26	2.39	2.61	2.45	3.00	2.72
	LSK	2.20	2.17	1.99	2.00	1.95	2.02	2.09	2.04	2.38	2.72	2.83
	MRSM	2.46	2.39	2.35	2.37	2.30	2.29	2.24	2.24	2.36	2.67	3.15
	MURS	1.87	1.78	1.81	1.84	1.84	1.89	1.91	2.00	2.19	2.43	3.14
	NN	2.36	2.23	2.33	2.24	2.43	2.41	2.54	2.55	2.33	3.04	2.72
	OK	1.88	1.79	1.93	1.91	2.06	1.94	1.94	1.99	2.08	2.44	3.12
	SK	1.88	1.78	1.92	1.91	2.09	1.99	2.12	2.14	2.39	2.90	2.92
	TS	2.68	2.88	2.56	2.45	2.51	2.38	2.41	9.52	2.48	3.23	2.73
3FRS	FA	2.95	2.98	3.08	3.09	3.09	3.06	3.04	3.01	3.03	3.01	3.34
	IDW	2.84	2.72	2.80	2.79	2.72	2.38	2.33	2.40	2.64	4.82	6.46
	LSK	2.34	2.31	2.29	2.32	2.50	2.16	2.24	2.23	2.98	4.92	6.62
	MRSM	2.85	2.72	2.75	2.78	2.72	2.48	2.48	2.57	3.29	4.77	8.91
	MURS	2.71	2.55	2.60	2.61	2.63	2.31	2.29	2.38	3.05	4.72	7.30
	NN	2.52	2.39	2.61	2.48	2.78	2.56	2.58	2.32	3.30	4.74	6.81
	OK	2.24	2.10	2.27	2.27	2.39	2.17	2.24	2.21	2.96	4.73	8.69
	SK	2.35	2.13	2.24	2.25	2.36	2.19	2.24	2.21	2.81	4.42	8.62
	TS	3.11	3.13	3.18	3.29	3.20	2.76	2.70	2.74	3.25	4.97	7.03
3GLS	FA	2.95	2.98	3.08	3.09	3.09	3.06	3.04	3.01	3.03	3.01	3.34
	IDW	2.29	2.24	2.24	2.22	2.25	2.12	2.15	2.33	2.55	2.90	2.91
	LSK	9.52	8.87	10.92	10.35	11.05	13.34	14.89	13.67	15.56	18.20	23.61
	MRSM	16.23	16.36	16.91	16.93	15.68	17.27	17.46	16.87	17.91	19.83	23.56
	MURS	11.81	11.33	12.42	12.42	12.30	13.64	14.42	14.47	16.09	19.11	23.73
	NN	2.58	2.39	2.55	2.41	2.65	2.59	2.63	2.30	2.58	3.53	2.92
	OK	9.20	8.67	10.32	10.07	11.34	13.15	14.43	13.64	14.96	17.92	23.57
	SK	9.08	8.78	10.20	10.15	11.45	13.28	14.51	13.58	14.86	18.46	23.67
	TS	2.73	2.74	2.86	2.87	3.00	2.83	2.87	2.86	2.88	3.43	2.91
SM	FA	2.95	2.98	3.08	3.09	3.09	3.06	3.04	3.01	3.03	3.01	3.34
	IDW	1.99	1.94	1.97	1.99	1.98	2.14	2.13	2.15	2.17	2.49	2.96
	LSK	1.83	1.69	1.74	1.74	1.83	1.91	1.96	2.02	2.22	2.55	3.24
	MRSM	2.47	2.37	2.35	2.36	2.27	2.28	2.23	2.22	2.29	2.52	3.25
	MURS	2.03	1.91	1.95	1.98	1.96	1.99	2.01	2.08	2.20	2.49	3.27
	NN	2.75	2.51	2.66	2.50	2.72	2.69	2.77	2.33	2.44	3.38	3.00
	OK	1.79	1.65	1.72	1.72	1.81	1.85	1.91	1.95	2.03	2.31	3.17
	SK	1.76	1.64	1.71	1.72	1.84	1.87	1.91	1.96	2.12	2.37	3.16
	TS	2.95	2.98	3.08	3.09	3.09	3.06	3.04	3.01	3.03	3.01	3.34

Table A.35: MO MM, MSPE grouped by detrending method.

		Percentage Data Removed										
		48.97	53.13	58.06	63.28	68.80	75.68	80.54	87.21	93.95	96.97	98.51
1GLS	FA	229.99	221.72	213.38	209.75	204.41	203.58	203.99	204.56	202.96	200.09	201.37
	TS	115.77	115.96	114.01	114.52	113.59	116.95	119.09	121.08	124.37	121.89	126.10
	NN	111.88	94.53	79.78	83.87	84.37	77.08	79.00	84.47	92.03	72.14	82.29
	IDW	86.23	79.83	73.54	68.68	62.73	58.94	57.59	59.39	63.50	63.30	75.26
	LSK	91.79	82.45	75.18	67.96	57.39	60.40	67.14	69.49	79.58	82.80	104.86
	SK	85.17	79.21	70.42	63.64	60.24	55.28	53.19	60.20	61.17	72.08	89.18
	OK	85.85	77.72	71.81	62.06	55.90	51.86	51.85	62.68	58.96	73.02	94.19
	MRSM	97.16	91.70	86.24	79.61	74.36	75.37	79.22	89.49	99.28	112.77	122.84
	MURS	96.64	90.37	84.14	78.02	71.52	71.94	73.95	83.81	95.51	109.21	120.68
3ATPS	FA	229.99	221.72	213.38	209.75	204.41	203.58	203.99	204.56	202.96	200.09	201.37
	TS	92.76	85.67	73.44	76.09	67.82	63.34	58.73	66.65	64.45	98.95	85.14
	NN	102.04	84.88	74.18	77.35	76.25	70.86	71.38	88.02	88.33	79.68	90.73
	IDW	89.11	80.25	69.89	67.14	64.92	57.12	54.39	59.57	61.77	81.72	80.47
	LSK	89.98	79.43	72.04	69.83	67.97	61.29	56.87	60.00	60.64	86.47	87.52
	SK	88.62	78.14	68.67	68.91	60.99	56.30	59.90	52.86	57.20	83.84	85.91
	OK	89.77	77.92	69.49	68.13	64.59	56.01	52.72	57.65	56.60	85.91	86.58
	MRSM	89.89	80.63	73.65	70.60	65.12	59.42	60.76	55.23	66.39	92.52	86.58
	MURS	88.71	81.20	70.67	69.68	63.27	57.88	60.14	53.80	56.14	90.94	85.65
3FRS	FA	229.99	221.72	213.38	209.75	204.41	203.58	203.99	204.56	202.96	200.09	201.37
	TS	105.76	100.49	96.05	94.90	89.94	89.16	89.52	95.46	92.70	97.73	111.12
	NN	108.12	91.89	77.71	82.94	81.88	75.24	75.95	88.22	94.60	73.14	83.49
	IDW	87.02	80.00	72.69	67.49	61.99	57.99	56.94	59.11	59.71	61.29	74.40
	LSK	84.47	79.52	69.94	63.13	61.13	58.47	52.35	62.53	57.98	82.85	83.88
	SK	84.38	76.85	71.11	67.22	56.50	51.97	51.95	56.49	62.06	63.92	83.38
	OK	84.52	78.47	68.81	60.06	57.30	52.77	52.37	64.29	58.42	66.50	86.00
	MRSM	94.39	88.83	80.00	74.67	70.23	68.84	70.07	76.95	80.58	99.97	105.03
	MURS	92.46	85.27	79.46	72.20	66.29	62.78	65.37	72.49	77.37	86.35	101.44
3GLS	FA	229.99	221.72	213.38	209.75	204.41	203.58	203.99	204.56	202.96	200.09	201.37
	TS	102.93	95.59	92.47	99.14	81.12	77.33	76.39	73.89	74.85	80.35	81.90
	NN	110.41	93.30	77.83	83.83	84.01	77.41	79.41	87.56	92.74	71.37	85.63
	IDW	94.23	85.30	76.01	68.10	65.79	61.96	61.79	58.00	54.42	59.27	73.79
	LSK	90.39	79.82	76.97	67.71	62.33	56.19	56.06	55.99	57.73	72.59	79.15
	SK	88.17	81.58	69.12	62.95	60.43	54.23	54.65	55.16	52.88	64.96	80.79
	OK	91.03	81.65	70.56	64.28	59.36	55.51	60.45	54.74	57.12	62.44	78.13
	MRSM	99.03	84.93	75.84	73.76	71.15	66.30	66.13	66.72	72.68	77.37	83.12
	MURS	101.45	84.21	76.18	70.03	65.99	61.29	61.68	62.34	68.21	73.27	83.35
SM	FA	229.99	221.72	213.38	209.75	204.41	203.58	203.99	204.56	202.96	200.09	201.37
	TS	229.99	221.72	213.38	209.75	204.41	203.58	203.99	204.56	202.96	200.09	201.37
	NN	112.70	95.42	80.67	84.78	85.14	78.08	79.43	86.53	95.23	73.96	82.47
	IDW	108.54	99.12	90.97	83.97	76.06	70.75	68.89	71.12	74.77	75.41	88.66
	LSK	159.49	121.53	78.25	108.86	102.91	75.11	76.95	92.27	98.34	132.04	161.96
	SK	113.43	118.70	87.66	57.37	62.79	75.90	56.13	70.97	68.15	84.59	123.43
	OK	126.64	99.92	69.15	69.55	91.24	73.93	54.41	86.13	85.41	97.45	136.92
	MRSM	158.99	147.40	133.28	121.94	113.58	106.10	104.87	120.22	113.90	165.71	186.47
	MURS	161.75	142.11	134.28	125.41	112.61	106.99	101.51	115.33	110.16	156.06	184.78

Table A.36: MO MM, MAPE grouped by detrending method.

		Percentage Data Removed										
		48.97	53.13	58.06	63.28	68.80	75.68	80.54	87.21	93.95	96.97	98.51
1GLS	FA	11.15	11.03	10.89	10.83	10.85	10.84	10.89	10.72	10.63	10.83	10.41
	TS	6.61	6.65	6.69	6.80	6.91	7.06	7.16	7.19	7.17	7.38	7.52
	NN	6.45	5.68	5.11	5.20	5.05	4.78	4.80	4.82	4.99	4.71	5.16
	IDW	5.45	5.18	4.89	4.70	4.50	4.39	4.39	4.37	4.53	4.72	5.07
	LSK	5.37	4.87	4.52	4.27	3.87	4.07	4.53	4.60	5.01	5.55	6.53
	SK	5.18	4.85	4.43	4.08	3.99	3.78	3.79	4.01	4.13	5.03	5.73
	OK	5.18	4.78	4.46	4.07	3.82	3.67	3.71	4.15	4.03	5.13	5.99
	MRSM	5.66	5.33	5.10	4.90	4.81	4.95	5.19	5.72	6.07	6.93	7.32
	MURS	5.64	5.31	5.04	4.84	4.69	4.93	5.11	5.63	6.01	6.90	7.28
3ATPS	FA	11.15	11.03	10.89	10.83	10.85	10.84	10.89	10.72	10.63	10.83	10.41
	TS	5.95	5.60	5.14	5.15	4.83	4.61	4.42	4.67	4.72	6.16	5.20
	NN	6.13	5.36	4.93	4.89	4.69	4.49	4.49	4.70	4.80	5.44	5.42
	IDW	5.79	5.36	4.92	4.75	4.60	4.25	4.09	4.35	4.46	5.62	5.05
	LSK	5.79	5.27	4.95	4.82	4.73	4.47	4.28	4.19	4.36	5.74	5.21
	SK	5.66	5.19	4.76	4.64	4.29	4.12	4.18	4.00	4.26	5.60	5.23
	OK	5.76	5.18	4.79	4.62	4.41	4.16	4.01	4.13	4.25	5.73	5.16
	MRSM	5.74	5.33	4.93	4.77	4.50	4.26	4.25	4.14	4.65	5.92	5.24
	MURS	5.68	5.31	4.86	4.66	4.41	4.18	4.12	4.06	4.37	5.86	5.24
3FRS	FA	11.15	11.03	10.89	10.83	10.85	10.84	10.89	10.72	10.63	10.83	10.41
	TS	6.54	6.53	6.49	6.46	6.48	6.43	6.53	6.44	6.48	6.79	6.93
	NN	6.61	5.85	5.24	5.37	5.13	4.85	4.85	4.97	5.10	4.85	5.26
	IDW	5.53	5.28	4.99	4.81	4.57	4.44	4.38	4.38	4.48	4.81	4.98
	LSK	5.27	5.13	4.65	4.29	4.34	4.32	3.83	4.30	4.07	5.77	5.49
	SK	5.27	5.04	4.53	4.64	4.14	3.83	3.96	3.90	4.53	4.78	5.49
	OK	5.32	5.11	4.59	4.11	4.12	3.95	4.01	4.56	4.20	5.08	5.59
	MRSM	5.91	5.49	5.24	5.00	4.97	4.91	5.17	5.38	5.68	6.64	6.59
	MURS	5.81	5.46	5.19	4.98	4.90	4.79	5.07	5.23	5.62	6.36	6.45
3GLS	FA	11.15	11.03	10.89	10.83	10.85	10.84	10.89	10.72	10.63	10.83	10.41
	TS	6.78	6.57	6.43	6.70	5.90	5.78	5.77	5.63	5.77	6.16	5.51
	NN	6.45	5.63	5.07	5.10	5.00	4.72	4.79	4.86	4.98	4.96	5.30
	IDW	6.19	5.80	5.43	5.05	4.93	4.83	4.84	4.62	4.53	5.02	5.00
	LSK	6.05	5.51	5.41	4.85	4.55	4.31	4.38	4.32	4.47	5.73	5.31
	SK	5.97	5.49	4.86	4.59	4.46	4.17	4.27	4.25	4.30	5.37	5.41
	OK	5.84	5.51	5.06	4.68	4.37	4.31	4.68	4.34	4.63	5.21	5.24
	MRSM	6.38	5.85	5.41	5.24	5.13	5.02	5.04	5.18	5.55	5.96	5.51
	MURS	6.54	5.81	5.40	5.10	4.94	4.81	4.88	4.99	5.39	5.81	5.52
SM	FA	11.15	11.03	10.89	10.83	10.85	10.84	10.89	10.72	10.63	10.83	10.41
	TS	11.15	11.03	10.89	10.83	10.85	10.84	10.89	10.72	10.63	10.83	10.41
	NN	6.45	5.71	5.14	5.23	5.07	4.82	4.82	4.89	5.09	4.76	5.20
	IDW	6.55	6.21	5.88	5.61	5.39	5.22	5.20	5.13	5.30	5.65	5.76
	LSK	8.31	6.78	5.03	6.26	6.00	4.91	5.02	5.57	6.00	8.06	8.84
	SK	6.60	6.76	5.39	4.05	4.29	4.97	4.03	4.48	4.50	5.87	7.28
	OK	7.09	5.94	4.55	4.58	5.66	4.93	3.96	5.34	5.44	6.52	7.85
	MRSM	8.39	7.93	7.37	6.94	6.73	6.60	6.71	7.32	7.16	9.60	9.83
	MURS	8.64	7.85	7.48	7.19	6.82	6.71	6.63	7.21	7.06	9.27	9.81

## Appendix B

# List of Socioeconomic Variables Used for Inventory Prediction

Taken from the provided WDI metadata, WDI code and basic explanation is listed (see [49]).

### B.1 Regular Variables

**EN.ATM.CO2E.KD.GD** CO2 emissions (kg per 2000 US\$ of GDP)

**EN.ATM.CO2E.KT** CO2 emissions (kt)

**EN.ATM.CO2E.PP.GD** CO2 emissions (kg per PPP \$ of GDP)

**EN.ATM.CO2E.PP.GD.KD** CO2 emissions (kg per 2005 PPP \$ of GDP)

**EN.ATM.PM10.MC.M3** PM10, country level (micrograms per cubic meter)

**IS.ROD.TOTL.KM** Roads, total network (km)

**IT.CEL.SETS** Mobile cellular subscriptions

**IT.MLT.MAIN** Telephone lines

**IT.NET.USER** Internet users

**NY.GDP.MKTP.KD** GDP (constant 2000 US\$)

**NY.GDP.MKTP.KD.ZG** GDP growth (annual %)

**NY.GDS.TOTL.CD** Gross domestic savings (current US\$)

**NY.GDS.TOTL.ZS** Gross domestic savings (% of GDP)

**NY.GNP.MKTP.CD** GNI (current US\$)

**NY.GNP.MKTP.PP.CD** GNI, PPP (current international \$)

**PA.NUS.ATLS** DEC alternative conversion factor (LCU per US\$)

**PA.NUS.PPPC.RF** PPP conversion factor (GDP) to market exchange rate ratio

**SL.TLF.TOTL.IN** Labor force, total

**SP.DYN.LE00.IN** Life expectancy at birth, total (years)

**SP.POP.GROW** Population growth (annual %)

**SP.RUR.TOTL.ZG** Rural population growth (annual %)

**SP.URB.GROW** Urban population growth (annual %)

## B.2 Per Capita Variables

**EN.ATM.CO2E.PC** CO2 emissions (metric tons per capita)

**ER.H2O.INTR.PC** Renewable internal freshwater resources per capita (cubic meters)

**IT.CEL.SETS.P2** Mobile cellular subscriptions (per 100 people)

**IT.MLT.MAIN.P2** Telephone lines (per 100 people)

**IT.NET.BBND.P2** Fixed broadband Internet subscribers (per 100 people)

**IT.NET.SECR.P6** Secure Internet servers (per 1 million people)

**IT.NET.USER.P2** Internet users (per 100 people)

**NE.CON.PRVT.PC.KD** Household final consumption expenditure per capita (constant 2000 US\$)

**NY.GDP.PCAP.KD** GDP per capita (constant 2000 US\$)

**NY.GDP.PCAP.KD.ZG** GDP per capita growth (annual %)

**NY.GDP.PCAP.PP.CD** GDP per capita, PPP (current international \$)

**NY.GDP.PCAP.PP.KD** GDP per capita, PPP (constant 2005 international \$)

**SH.XPD.PCAP** Health expenditure per capita (current US\$)

**SH.XPD.PCAP.PP.KD** Health expenditure per capita, PPP (constant 2005 international \$)

**SP.DYN.CBRT.IN** Birth rate, crude (per 1,000 people)

**SP.DYN.CDRT.IN** Death rate, crude (per 1,000 people)

**VC.HOM.ITEN.P5.HE** Intentional homicide rate (per 100,000 people, CTS and national sources)

**SH.MED.BEDS.ZS** Hospital beds (per 1,000 people)

**SH.MED.NUMW.P3** Nurses and midwives (per 1,000 people)

**SH.MED.PHYS.ZS** Physicians (per 1,000 people)

**SN.ITK.DPTH** Depth of hunger (kilocalories per person per day)

**SP.POP.0014.TO.ZS** Population ages 0-14 (% of total)

**SP.POP.1564.TO.ZS** Population ages 15-64 (% of total)

**SP.POP.65UP.TO.ZS** Population ages 65 and above (% of total)

**SN.ITK.DEFC.ZS** Prevalence of undernourishment (% of population)  
**SL.TLF.CACT.ZS** Labor participation rate, total (% of total population ages 15+)  
**SH.H2O.SAFE.ZS** Improved water source (% of population with access)  
**SH.STA.ACSN** Improved sanitation facilities (% of population with access)  
**IC.REG.COST.PC.ZS** Cost of business start-up procedures (% of GNI per capita)

# Appendix C

## Inventory Prediction Data Tables

Table C.1: Summary statistics for reported data used with RF prediction.

Gas and Sector	Min	1st Qu.	Median	Mean	3rd Qu.	Max
CH <sub>4</sub> Agr	0.000E+000	0.000E+000	0.000E+000	8.342E-006	0.000E+000	1.014E-002
CH <sub>4</sub> Energy	0.000E+000	0.000E+000	0.000E+000	4.539E-008	0.000E+000	7.046E-004
CH <sub>4</sub> Livestock	0.000E+000	0.000E+000	0.000E+000	7.548E-006	0.000E+000	6.653E-002
CH <sub>4</sub> OilGasProd	0.000E+000	0.000E+000	0.000E+000	3.870E-006	0.000E+000	9.019E-002
CH <sub>4</sub> Residential	0.000E+000	0.000E+000	0.000E+000	1.033E-006	0.000E+000	5.545E-003
CH <sub>4</sub> RoadTrans	0.000E+000	0.000E+000	0.000E+000	6.471E-008	0.000E+000	9.320E-004
CO <sub>2</sub> Agr	0.000E+000	0.000E+000	0.000E+000	9.601E-006	0.000E+000	1.065E-002
CO <sub>2</sub> Energy	0.000E+000	0.000E+000	0.000E+000	1.693E-003	0.000E+000	3.238E+001
CO <sub>2</sub> OilGasProd	0.000E+000	0.000E+000	0.000E+000	5.476E-005	0.000E+000	2.513E+000
CO <sub>2</sub> Residential	0.000E+000	0.000E+000	0.000E+000	3.553E-004	0.000E+000	1.938E+000
CO <sub>2</sub> RoadTrans	0.000E+000	0.000E+000	0.000E+000	3.666E-004	0.000E+000	3.272E+000
N <sub>2</sub> OAgr	0.000E+000	0.000E+000	0.000E+000	3.621E-007	0.000E+000	1.019E-003
N <sub>2</sub> OEnergy	0.000E+000	0.000E+000	0.000E+000	2.536E-008	0.000E+000	4.715E-004
N <sub>2</sub> OLivestock	0.000E+000	0.000E+000	0.000E+000	3.913E-008	0.000E+000	6.133E-004
N <sub>2</sub> OOilGasProd	0.000E+000	0.000E+000	0.000E+000	2.830E-010	0.000E+000	1.192E-005
N <sub>2</sub> OResidential	0.000E+000	0.000E+000	0.000E+000	1.677E-008	0.000E+000	6.244E-005
N <sub>2</sub> ORoadTrans	0.000E+000	0.000E+000	0.000E+000	1.361E-008	0.000E+000	2.094E-004

Table C.2: Summary statistics for reported data used with ELM prediction.

Gas and Sector	Min	1st Qu.	Median	Mean	3rd Qu.	Max
CH <sub>4</sub> Agr	0.000E+000	0.000E+000	0.000E+000	8.015E-006	0.000E+000	1.014E-002
CH <sub>4</sub> Energy	0.000E+000	0.000E+000	0.000E+000	4.592E-008	0.000E+000	7.046E-004
CH <sub>4</sub> Livestock	0.000E+000	0.000E+000	0.000E+000	7.505E-006	0.000E+000	6.653E-002
CH <sub>4</sub> OilGasProd	0.000E+000	0.000E+000	0.000E+000	3.952E-006	0.000E+000	9.019E-002
CH <sub>4</sub> Residential	0.000E+000	0.000E+000	0.000E+000	1.018E-006	0.000E+000	5.545E-003
CH <sub>4</sub> RoadTrans	0.000E+000	0.000E+000	0.000E+000	6.535E-008	0.000E+000	9.320E-004
CO <sub>2</sub> Agr	0.000E+000	0.000E+000	0.000E+000	9.433E-006	0.000E+000	1.065E-002
CO <sub>2</sub> Energy	0.000E+000	0.000E+000	0.000E+000	1.731E-003	0.000E+000	3.238E+001
CO <sub>2</sub> OilGasProd	0.000E+000	0.000E+000	0.000E+000	5.611E-005	0.000E+000	2.513E+000
CO <sub>2</sub> Residential	0.000E+000	0.000E+000	0.000E+000	3.629E-004	0.000E+000	1.938E+000
CO <sub>2</sub> RoadTrans	0.000E+000	0.000E+000	0.000E+000	3.705E-004	0.000E+000	3.272E+000
N <sub>2</sub> OAgr	0.000E+000	0.000E+000	0.000E+000	3.568E-007	0.000E+000	1.019E-003
N <sub>2</sub> OEnergy	0.000E+000	0.000E+000	0.000E+000	2.525E-008	0.000E+000	4.715E-004
N <sub>2</sub> OLivestock	0.000E+000	0.000E+000	0.000E+000	3.791E-008	0.000E+000	6.133E-004
N <sub>2</sub> OOilGasProd	0.000E+000	0.000E+000	0.000E+000	2.892E-010	0.000E+000	1.192E-005
N <sub>2</sub> OResidential	0.000E+000	0.000E+000	0.000E+000	1.664E-008	0.000E+000	6.244E-005
N <sub>2</sub> ORoadTrans	0.000E+000	0.000E+000	0.000E+000	1.387E-008	0.000E+000	2.094E-004

Table C.3: Summary statistics for predictions made with RF.

Gas and Sector	Min	1st Qu.	Median	Mean	3rd Qu.	Max
CH <sub>4</sub> Agr	0.000E+000	0.000E+000	0.000E+000	8.061E-006	0.000E+000	2.408E-003
CH <sub>4</sub> Energy	0.000E+000	0.000E+000	0.000E+000	2.291E-008	0.000E+000	3.349E-005
CH <sub>4</sub> Livestock	0.000E+000	0.000E+000	0.000E+000	7.505E-006	0.000E+000	1.295E-003
CH <sub>4</sub> OilGasProd	0.000E+000	0.000E+000	0.000E+000	2.173E-006	1.049E-008	1.677E-003
CH <sub>4</sub> Residential	0.000E+000	0.000E+000	0.000E+000	1.019E-006	0.000E+000	3.548E-004
CH <sub>4</sub> RoadTrans	0.000E+000	0.000E+000	0.000E+000	3.572E-008	0.000E+000	1.585E-005
CO <sub>2</sub> Agr	0.000E+000	0.000E+000	0.000E+000	9.539E-006	0.000E+000	2.755E-003
CO <sub>2</sub> Energy	0.000E+000	0.000E+000	0.000E+000	9.946E-004	0.000E+000	2.190E+000
CO <sub>2</sub> OilGasProd	0.000E+000	0.000E+000	0.000E+000	1.970E-004	0.000E+000	1.222E+000
CO <sub>2</sub> Residential	0.000E+000	0.000E+000	0.000E+000	3.114E-004	0.000E+000	1.877E-001
CO <sub>2</sub> RoadTrans	0.000E+000	0.000E+000	0.000E+000	2.359E-004	0.000E+000	1.520E-001
N <sub>2</sub> OAgr	0.000E+000	0.000E+000	0.000E+000	3.606E-007	0.000E+000	4.076E-005
N <sub>2</sub> OEnergy	0.000E+000	0.000E+000	0.000E+000	1.427E-008	0.000E+000	3.263E-005
N <sub>2</sub> OLivestock	0.000E+000	0.000E+000	0.000E+000	3.784E-008	0.000E+000	8.438E-006
N <sub>2</sub> OOilGasProd	0.000E+000	0.000E+000	0.000E+000	6.866E-010	0.000E+000	3.940E-006
N <sub>2</sub> OResidential	0.000E+000	0.000E+000	0.000E+000	1.591E-008	0.000E+000	4.557E-006
N <sub>2</sub> ORoadTrans	0.000E+000	0.000E+000	0.000E+000	8.193E-009	0.000E+000	8.252E-006

Table C.4: Summary statistics for predictions made with ELM.

Gas and Sector	Min	1st Qu.	Median	Mean	3rd Qu.	Max
CH <sub>4</sub> Agr	-5.702E-004	2.368E-017	3.112E-008	7.346E-006	5.936E-007	8.821E-004
CH <sub>4</sub> Energy	-1.226E-006	-3.365E-020	1.345E-011	4.365E-008	3.031E-009	1.464E-006
CH <sub>4</sub> Livestock	-1.296E-004	6.977E-018	1.233E-017	7.154E-006	8.542E-006	2.036E-004
CH <sub>4</sub> OilGasProd	-1.419E-004	-4.164E-018	1.401E-009	3.288E-006	5.890E-007	9.985E-005
CH <sub>4</sub> Residential	-4.448E-005	2.538E-018	5.636E-018	1.042E-006	1.325E-007	9.023E-005
CH <sub>4</sub> RoadTrans	-2.923E-006	-1.057E-019	3.538E-020	8.844E-008	1.354E-008	2.894E-006
CO <sub>2</sub> Agr	-2.486E-004	7.593E-018	2.153E-017	8.330E-006	1.131E-006	3.166E-004
CO <sub>2</sub> Energy	-2.212E-002	4.041E-016	1.083E-006	1.179E-003	1.048E-004	3.297E-002
CO <sub>2</sub> OilGasProd	-1.227E-003	-6.592E-017	6.127E-013	9.402E-005	8.295E-008	1.010E-003
CO <sub>2</sub> Residential	-5.766E-003	5.195E-016	2.212E-008	3.811E-004	1.016E-004	1.120E-002
CO <sub>2</sub> RoadTrans	-7.363E-003	-3.590E-016	1.226E-016	4.145E-004	1.271E-004	8.238E-003
N <sub>2</sub> OAgr	-7.664E-006	3.293E-019	7.022E-019	3.346E-007	2.899E-007	1.165E-005
N <sub>2</sub> OEnergy	-6.409E-007	6.783E-021	1.593E-011	1.934E-008	7.731E-010	7.660E-007
N <sub>2</sub> OLivestock	-1.459E-006	9.293E-020	1.961E-019	3.463E-008	9.816E-009	2.176E-006
N <sub>2</sub> OOilGasProd	-6.793E-009	-4.249E-022	8.947E-018	4.218E-010	1.324E-012	5.319E-009
N <sub>2</sub> OResidential	-9.952E-007	4.505E-020	7.803E-020	1.756E-008	2.361E-009	1.503E-006
N <sub>2</sub> ORoadTrans	-1.645E-007	-1.131E-020	-2.282E-021	1.412E-008	3.726E-009	1.655E-007

Table C.5: Summary statistics for absolute error from RF predictions.

Gas and Sector	Min	1st Qu.	Median	Mean	3rd Qu.	Max
CH <sub>4</sub> Agr	0.000E+000	0.000E+000	0.000E+000	2.811E-006	0.000E+000	8.657E-003
CH <sub>4</sub> Energy	0.000E+000	0.000E+000	0.000E+000	2.937E-008	0.000E+000	6.765E-004
CH <sub>4</sub> Livestock	0.000E+000	0.000E+000	0.000E+000	1.317E-006	0.000E+000	6.558E-002
CH <sub>4</sub> OilGasProd	0.000E+000	0.000E+000	0.000E+000	2.280E-006	3.637E-009	8.945E-002
CH <sub>4</sub> Residential	0.000E+000	0.000E+000	0.000E+000	2.004E-007	0.000E+000	5.297E-003
CH <sub>4</sub> RoadTrans	0.000E+000	0.000E+000	0.000E+000	3.765E-008	0.000E+000	9.197E-004
CO <sub>2</sub> Agr	0.000E+000	0.000E+000	0.000E+000	2.673E-006	0.000E+000	8.292E-003
CO <sub>2</sub> Energy	0.000E+000	0.000E+000	0.000E+000	1.052E-003	0.000E+000	3.066E+001
CO <sub>2</sub> OilGasProd	0.000E+000	0.000E+000	0.000E+000	2.088E-004	0.000E+000	1.844E+000
CO <sub>2</sub> Residential	0.000E+000	0.000E+000	0.000E+000	1.167E-004	0.000E+000	1.771E+000
CO <sub>2</sub> RoadTrans	0.000E+000	0.000E+000	0.000E+000	1.737E-004	0.000E+000	3.151E+000
N <sub>2</sub> OAgr	0.000E+000	0.000E+000	0.000E+000	4.284E-008	0.000E+000	9.941E-004
N <sub>2</sub> OEnergy	0.000E+000	0.000E+000	0.000E+000	1.582E-008	0.000E+000	4.445E-004
N <sub>2</sub> OLivestock	0.000E+000	0.000E+000	0.000E+000	7.949E-009	0.000E+000	6.059E-004
N <sub>2</sub> OOilGasProd	0.000E+000	0.000E+000	0.000E+000	6.931E-010	0.000E+000	8.977E-006
N <sub>2</sub> OResidential	0.000E+000	0.000E+000	0.000E+000	3.212E-009	0.000E+000	5.931E-005
N <sub>2</sub> ORoadTrans	0.000E+000	0.000E+000	0.000E+000	7.415E-009	0.000E+000	2.019E-004

Table C.6: Summary statistics for absolute error from ELM predictions.

Gas and Sector	Min	1st Qu.	Median	Mean	3rd Qu.	Max
CH <sub>4</sub> Agr	7.469E-019	2.392E-017	3.112E-008	1.446E-005	5.936E-007	1.009E-002
CH <sub>4</sub> Energy	1.422E-021	4.122E-020	1.345E-011	8.693E-008	3.031E-009	7.044E-004
CH <sub>4</sub> Livestock	3.653E-021	9.327E-018	1.310E-009	1.117E-005	8.542E-006	6.651E-002
CH <sub>4</sub> OilGasProd	9.540E-020	6.380E-018	1.401E-009	6.214E-006	5.890E-007	9.017E-002
CH <sub>4</sub> Residential	5.577E-020	3.840E-018	5.153E-010	1.767E-006	1.325E-007	5.527E-003
CH <sub>4</sub> RoadTrans	5.561E-021	1.015E-019	8.514E-012	1.450E-007	1.354E-008	9.316E-004
CO <sub>2</sub> Agr	4.743E-019	1.086E-017	2.709E-009	1.375E-005	1.131E-006	1.061E-002
CO <sub>2</sub> Energy	1.320E-017	1.010E-015	1.083E-006	2.744E-003	1.048E-004	3.237E+001
CO <sub>2</sub> OilGasProd	4.754E-019	7.678E-017	6.127E-013	1.490E-004	8.295E-008	2.512E+000
CO <sub>2</sub> Residential	3.793E-018	5.195E-016	2.212E-008	6.256E-004	1.016E-004	1.935E+000
CO <sub>2</sub> RoadTrans	1.513E-017	3.449E-016	7.427E-009	7.293E-004	1.271E-004	3.270E+000
N <sub>2</sub> OAgr	2.343E-020	4.623E-019	1.198E-010	4.672E-007	2.899E-007	1.018E-003
N <sub>2</sub> OEnergy	4.177E-022	1.233E-020	1.593E-011	4.297E-008	7.731E-010	4.714E-004
N <sub>2</sub> OLivestock	6.859E-022	1.281E-019	1.523E-011	5.806E-008	9.816E-009	6.131E-004
N <sub>2</sub> OOilGasProd	1.411E-023	4.397E-022	8.947E-018	6.941E-010	1.324E-012	1.192E-005
N <sub>2</sub> OResidential	3.694E-021	5.618E-020	5.081E-012	2.876E-008	2.361E-009	6.222E-005
N <sub>2</sub> ORoadTrans	5.496E-023	8.765E-021	2.754E-013	2.643E-008	3.726E-009	2.093E-004

Table C.7: Summary statistics for RF percentage error.

Gas and Sector	Min	1st Qu.	Median	Mean	3rd Qu.	Max
CH <sub>4</sub> Energy	1.235E-005	1.127E+000	7.036E+000	4.076E+003	3.424E+001	8.861E+007
CH <sub>4</sub> Agr	6.463E-004	1.010E+001	2.319E+001	1.485E+002	5.035E+001	8.153E+004
CH <sub>4</sub> Livestock	3.152E-004	5.567E+000	1.356E+001	4.956E+003	4.093E+001	3.163E+007
CH <sub>4</sub> OilGasProd	1.335E-004	1.997E+000	5.482E+000	4.137E+003	1.579E+001	1.051E+008
CH <sub>4</sub> Residential	3.640E-007	1.614E+000	6.476E+000	7.834E+002	2.516E+001	1.066E+007
CH <sub>4</sub> RoadTrans	6.715E-005	4.544E+000	1.243E+001	6.102E+001	3.228E+001	5.528E+005
CO <sub>2</sub> Agr	1.140E-005	4.470E+000	1.682E+001	7.194E+002	8.201E+001	1.036E+006
CO <sub>2</sub> Energy	1.971E-007	1.254E+000	5.579E+000	6.431E+003	2.253E+001	3.601E+008
CO <sub>2</sub> OilGasProd	1.652E-004	6.649E+000	9.600E+001	1.040E+008	3.360E+004	1.249E+012
CO <sub>2</sub> Residential	1.633E-005	1.159E+000	5.140E+000	1.175E+002	1.991E+001	2.235E+006
CO <sub>2</sub> RoadTrans	3.715E-004	3.691E+000	1.154E+001	7.443E+001	3.246E+001	1.488E+006
N <sub>2</sub> OAgr	4.832E-005	2.005E+000	5.984E+000	2.266E+001	1.538E+001	6.642E+003
N <sub>2</sub> OEnergy	6.969E-006	1.571E+000	8.905E+000	9.326E+003	3.868E+001	2.807E+008
N <sub>2</sub> OLivestock	4.943E-004	8.942E+000	2.606E+001	4.739E+003	1.909E+002	8.839E+007
N <sub>2</sub> OOilGasProd	1.844E-004	3.363E+000	1.002E+001	7.035E+002	3.584E+001	2.158E+006
N <sub>2</sub> OResidential	5.822E-006	1.416E+000	5.967E+000	2.832E+002	1.873E+001	5.690E+006
N <sub>2</sub> ORoadTrans	3.857E-006	3.757E+000	1.193E+001	8.198E+001	3.516E+001	1.362E+006

Table C.8: Summary statistics for ELM percentage error.

Gas and Sector	Min	1st Qu.	Median	Mean	3rd Qu.	Max
CH <sub>4</sub> Energy	4.517E-008	1.146E+002	1.283E+003	2.066E+006	6.020E+003	7.176E+010
CH <sub>4</sub> Agr	8.388E-002	7.085E+001	9.106E+001	3.492E+002	9.780E+001	1.841E+005
CH <sub>4</sub> Livestock	1.635E-010	6.361E+001	9.254E+001	2.188E+004	4.807E+002	3.955E+007
CH <sub>4</sub> OilGasProd	1.781E-009	5.430E+001	1.173E+002	5.830E+005	6.419E+002	1.469E+010
CH <sub>4</sub> Residential	2.123E-008	8.226E+001	2.886E+002	1.468E+005	1.955E+003	4.303E+009
CH <sub>4</sub> RoadTrans	3.894E-003	5.088E+001	7.854E+001	8.962E+003	1.375E+002	1.926E+008
CO <sub>2</sub> Agr	6.620E-011	7.240E+001	8.663E+001	4.430E+003	3.393E+002	6.211E+006
CO <sub>2</sub> Energy	4.224E-008	9.950E+001	1.479E+003	1.002E+006	6.262E+003	2.508E+010
CO <sub>2</sub> OilGasProd	7.389E-002	2.510E+002	7.942E+003	7.519E+007	5.779E+005	7.378E+011
CO <sub>2</sub> Residential	1.970E-009	5.463E+001	1.009E+002	3.069E+005	7.206E+002	1.243E+010
CO <sub>2</sub> RoadTrans	1.100E-002	4.755E+001	7.699E+001	7.654E+003	1.363E+002	2.528E+008
N <sub>2</sub> OAgr	3.824E-011	5.374E+001	8.531E+001	1.827E+002	1.223E+002	2.508E+005
N <sub>2</sub> OEnergy	3.735E-008	1.308E+002	2.401E+003	2.667E+006	1.192E+004	5.857E+010
N <sub>2</sub> OLivestock	1.040E-002	6.313E+001	9.715E+001	3.000E+004	3.444E+003	1.783E+007
N <sub>2</sub> OOilGasProd	3.063E-002	7.061E+001	9.917E+001	4.579E+005	1.349E+003	3.994E+009
N <sub>2</sub> OResidential	2.024E-008	7.829E+001	2.438E+002	8.294E+004	1.418E+003	1.364E+009
N <sub>2</sub> ORoadTrans	4.265E-003	4.666E+001	8.240E+001	7.649E+003	2.764E+002	2.305E+008